EVALUATING THE IMPACT OF LIME ON PAVEMENT PERFORMANCE

NATIONAL LIME ASSOCIATION
Suite 800
200 N. Glebe Rd
Arlington, VA 22203
www.lime.org
703 243-5463

Final Report
June 9, 2010

UNIVERSITY OF NEVADA RENO

Pavements/Materials Program

Department of Civil and Environmental Engineering
College of Engineering
University of Nevada
Reno, Nevada 89557

EVALUATING THE IMPACT OF LIME ON PAVEMENT PERFORMANCE

Peter E. Sebaaly, Ph.D., P.E.
University of Nevada, Reno

Elie Hajj, Ph.D.
University of Nevada, Reno

Dallas Little, Ph.D., P.E.
Texas A&M University

Sivakulan Shivakolunthar, Graduate Assistant
University of Nevada, Reno

Thileepan Sathanathan, Graduate Assistant
University of Nevada, Reno

Kamilla Vasconcelos
Texas A&M University

June 9, 2010

TECHNICAL ADVISORY PANEL

Tim Aschenbrener, Colorado DOT
Hussain Bahia, University of Wisconsin, Madison
John Bukowski, Federal Highway Administration
James Eason, Georgia DOT
Jon Epps, Granite Construction
Milt Fletcher, S. Carolina DOT
Adam Hand, Granite Construction
Rita Leahy, Asphalt Pavement Association of California
Randy Mountcastle, Alabama DOT
Joe Peterson, California DOT
Dale Rand, Texas DOT
Dean Weitzel, Formerly, Nevada DOT
Randy West, National Center for Asphalt Technology
Tom Zehr, Illinois DOT

The University of Nevada, Reno, Texas A&M University, and members of the Technical Advisory Panel do not endorse products or manufacturers. The views expressed in this report represent the views of the research team and supported by members of the Technical Advisory Panel but do not constitute the views of the agencies represented on the Technical Advisory Panel.

TABLE OF CONTENTS

LIST OF TABLES

LIST OF FIGURES

EXECUTIVE SUMMARY

This study represents the largest of its kind to evaluate the multifunctional impact of lime and liquid additives on hot mix asphalt (HMA) pavements. Typically, lime and liquid are used as additives to combat moisture damage, and therefore, their impact is only evaluated with respect to their influence on the moisture sensitivity of the HMA mixture. This study extended the evaluation to cover the impact of lime and liquid additives on the structural performance of the HMA mixtures and their impact on the long term performance of typical HMA pavements.

Aggregates and binders were obtained from five different sources: Alabama, California, Illinois, South Carolina, and Texas to produce HMA mixtures that were evaluated in this study. Three mix designs were conducted for each material source: un-treated, liquid-treated, and lime-treated mixtures. All mix designs were conducted following the Superpave Volumetric Mix Design Method. The types of liquid additive were selected by each participating state agency (i.e. mix source) and were added at the rate of 0.5% by weight of binder. A single lime source was used for all five sources at the rate of 1% by dry weight of aggregates.

A binder aging study was conducted to evaluate the impact of liquid and lime additives on the long term aging of the various asphalt binders.

The following performance properties were evaluated for all 15 mixtures:

- Resistance to moisture damage: relationship between dynamic modulus and multiple freeze-thaw (F-T) cycles.
- Resistance to permanent deformation: relationship between permanent strain in the HMA mix and number of load repetitions under triaxial testing conditions at the un-conditioned and moisture-conditioned stages.
- Resistance to fatigue cracking: relationship between bending strain in the HMA mix and number of load repetitions to failure under beam fatigue testing conditions at the un-conditioned and moisture-conditioned stages.
- Resistance to thermal cracking: fracture temperature and fracture stress under the restrained specimen testing conditions at the un-conditioned and moisture-conditioned stages.

The measured performance properties of the mixtures were used in the AASHTO Mechanistic-Empirical Pavement Design Guide (MEPDG) to conduct 20 years structural designs for actual projects selected from the five sources of mixtures. For each project, a total of three structural designs were established by changing the type of mix used in the HMA layer e.g. un-treated, liquid-treated, and lime-treated.

The MEPDG structural designs were used with typical cost figures for the three types of mixtures to estimate the costs of the three types of structural designs for each project. The percent cost savings/additional costs were estimated relative to the cost of the HMA pavement with the un-treated HMA mixtures.

Based on the extensive data generated from this research and the analyses of these data, the following findings are warranted.

- The use of both liquid and lime additives improved the moisture sensitivity of the HMA mixtures as measured by the tensile strength ratio (TSR) following AASHTO T283 method. However, as the mixtures were subjected to further moisture damage induced through multiple freeze-thaw (F-T) cycling, the un-treated and liquid-treated mixtures had significantly reduced their strength properties (i.e. E*). On the other hand, the lime-treated mixtures maintained higher strength properties for the entire 15 F-T cycles for all five sources.
- Lime either maintained or improved the rutting resistance of the HMA mixtures from all five sources. The impact of liquid on the rutting resistance of the HMA mixtures was source dependent; for the non-moisture sensitive mixtures from AL and IL, the liquid additives reduced their resistance to rutting as compare to the un-treated mixtures.
- Lime either maintained or improved the fatigue resistance of four out of the five sources of HMA mixtures. On the other hand, the impact of the liquid additive on the fatigue resistance of the HMA mixtures was source dependent and very inconsistent.
- In the case of thermal cracking, both the lime and liquid additives improved the fracture temperature of the HMA mixtures from all five sources. However, the lime-treated mixtures showed significantly higher fracture stresses for all sources.
- The life cycle cost data for new constructions revealed the following:
    - The use of lime additives in HMA mixtures resulted in significant savings, in some cases more than 45%.
    - The use of liquid anti-strip additives in HMA mixtures may result in additional cost, in some cases as high as 50%.
    - The data generated on the four mixtures from Alabama, California, Illinois, and S. Carolina show that lime is highly compatible with the use of neat asphalt binders and will always results in savings on the order of 13-34%.
    - The data generated on the mixtures from Texas show that the lime is highly compatible with the use of polymer-modified binders and will result in savings on the order of 40-45% which is significantly higher than the savings that could be realized with the use of the liquid anti-strip.
    - This data show that the use of lime additives will always improve the performance of the HMA pavement to a magnitude that always far outweighs its cost. On the other hand, the use of liquid anti-strip additives will not always improve the pavement performance to the magnitude that it will offset its cost.
    - The life cycle cost data showed that the use of lime in HMA mixtures that do not require improvement in their mix design TSR will still result in significant savings such as the case of the mixtures from Alabama and Illinois. On the other hand, the use of liquid in HMA mixtures that do not require improvement in their mix design TSR will result in significant cost increases such as the case of the mixtures from Alabama and Illinois.
    - The life cycle cost data showed that the use of lime in HMA mixtures that require improvement in their mix design TSR will still result in significantly higher savings such as the case of the mixtures from California, S. Carolina, and Texas. On the other hand, the use of liquid in HMA mixtures that require improvement in their TSR will result in

mediocre cost savings such as the case of the mixtures from California, S. Carolina, and Texas.

- Adding the savings realized by the use of lime-treated mixtures from the MEPDG structural designs to the savings realized from the lower thermal cracks per mile resulted in very significant overall cost savings to the highway industry and time savings for the road users.

- The life cycle cost data for rehabilitated pavements revealed the following:
  - The use of lime additive in HMA mixtures resulted in significant savings, in some cases more than 68%.
  - The use of liquid anti-strip additive in HMA mixtures may result in additional cost, in some cases as high as 45%.
  - This data show that the use of lime additive will always improve the performance of the HMA overlay to a magnitude that always far outweighs its cost. On the other hand, the use of liquid anti-strip additives will not always improve the performance of the overlay to the magnitude that it will offset its cost.
  - The life cycle cost data showed that the use of lime in HMA mixtures that do not require improvement in their mix design TSR will still result in significant savings such as the case of the mixtures from Alabama and Illinois. On the other hand, the use of liquid in HMA mixtures that do not require improvement in their mix design TSR will result in significant cost increases such as the case of the mixtures from Alabama.
  - The life cycle cost data showed that the use of lime in HMA mixtures that require improvement in their mix design TSR will still result in significantly higher savings such as the case of the mixtures from S. Carolina and Texas. On the other hand, the use of liquid in HMA mixtures that require improvement in their TSR will result in mediocre cost savings such as the case of the mixtures from S. Carolina and Texas.
  - Adding the savings realized by the use of lime-treated mixtures from the RPA overlay designs to the savings realized from the lower thermal cracks per mile resulted in very significant overall cost savings to the highway industry and time savings for the road users.

I. INTRODUCTION

The purpose of this project is to quantify expected changes in pavement life from adding lime to hot mix asphalt (HMA) based on an extensive laboratory testing program and advanced mechanistic analyses. This research differs from previous studies in several respects. First, because lime is used in HMA primarily for anti-stripping benefits, previous studies rarely quantified lime's other performance benefits. Second, because testing is typically performed on only the HMA mix being considered for a project, and only as necessary to satisfy specifications, typical studies do not capture the full range of failure modes and environmental stresses. Furthermore, once specifications are met, test results are rarely translated into pavement performance characteristics. This research, by contrast, evaluated fifteen HMA mixtures with the most widely accepted laboratory tests for the following modes of pavement failure:

- oxidative aging of binders
- moisture damage
- fatigue cracking
- permanent deformation
- thermal cracking

With these tests, the impact of lime and liquid additives on the mechanical properties and performance of HMA mixtures were estimated, in terms of changes in pavement life. Changes in pavement life and performance were then translated into changes in the life cycle cost of HMA pavements.

II. MATERIALS AND MIX DESIGNS

A total of five material sources were evaluated in this effort. Materials were obtained from the following sources: Alabama, California, Illinois, South Carolina, and Texas. Each mixture source has three types of mix designs: un-treated, lime-treated, and liquid-treated. Table 1 summarizes the fifteen HMA mixtures that were evaluated in this research.

Appendix A shows the locations of the aggregate sources on the geological maps of the five participating states. The Alabama aggregates consisted of light-dark gray thick bedded sedimentary stone from the Nevada limestone formation. This aggregate has a history of good performance on Alabama's asphalt pavements without any indications of moisture sensitivity. The California aggregate originated in the Sierra Nevada geological province. Hydraulic mining washed these alluvial gravels approximately 50 miles down the Yuba River to the Yuba Gold Fields. Much of the transported material is in excess of 100 feet thick. The aggregates are silica based, and when used in conjunction with lime and a good bitumen, produce a quality hot mix asphalt. The Illinois aggregate came from the Racine formation in the Niagaran series of the Silurian system which underlies most of Illinois. The Racine rock is exceptionally pure dolomite, medium grain and light-white gray. This aggregate performed well on Illinois asphalt pavements without any indication of moisture sensitivity. The South Carolina aggregates came from the region between the Coastal Plain and the Piedmont. The aggregates were produced from igneous or metamorphic rocks and are granite or granitic gneisses. This aggregates performed well on S. Carolina's asphalt pavements. However, some sources within the region have shown to be susceptible to moisture damage. The Texas aggregates came from a siliceous crushed river gravel quarry located in Corpus Christi, TX. This source of siliceous gravel is considered to have

high frictional and durability properties. HMA mixtures produced with this siliceous gravel, generally including an anti-stripping additive, have performed very well under a variety of conditions.

All mix designs were conducted at the University of Nevada laboratory following the Superpave volumetric mix design method with a minimum dry tensile strength of 70 psi at 77^{o}F and minimum retained tensile strength ratio (TSR) for the treated mixtures of 80%.

The lime was added to the mixtures in the form of dry hydrated lime on wet aggregate (3% moisture above the saturated surface dry condition) at the rate of 1% by dry weight of aggregate. The liquid anti-strip additives were selected by the source state and were blended into the asphalt binder in the laboratory at the rate of 0.5% by weight of binder. The Superpave Performance Grades (PG) of the binders were validated on the blended binders samples.

III. EXPERIMENTAL PROGRAM

III.1. Impact of Additives on the Long-Term Aging of the Asphalt Binders

The objective of this task was to evaluate the impact of lime and liquid anti-strip on the long-term aging of the five asphalt binders that were used in this study. This task evaluated the intermediate and low temperature rheological properties of the five binders with no additive, blended with hydrated lime, and blended with liquid anti-strip. The rheological properties of the binders were evaluated at the original and long-term aged stages. The long-term aging of the binders was achieved in the Pressure Aging Vessel (PAV) at 140^{o}F (60^{o}C) for 100, 400, and 800 hours.

III.2. Impact of Additives on the Performance of HMA Mixtures

Table 2 shows the experimental program for this effort. The program builds on the basis of testing laboratory prepared HMA mixtures as they are subjected to moisture conditioning. The moisture conditioning consisted of subjecting the samples to multiple freeze-thaw (F-T) cycling. The actual number of freeze-thaw cycles to be applied for the various tests were determined based on the results of the dynamic modulus (E*) versus multiple freeze-thaw (F-T) cycles testing.

Some of the properties were evaluated at both the unaged and aged stages while others were only evaluated at a single stage. For example, in the case of resistance to permanent deformation, the HMA mixtures were evaluated at the unaged stage because permanent deformation is a short-term distress mode. On the other hand, the fatigue resistances of the HMA mixtures were evaluated at the aged stage because fatigue cracking is a long-term distress mode. The mechanical properties of the HMA mixtures, namely the dynamic modulus were evaluated under both the unaged and aged stages to cover the entire life span of the HMA pavement. The aging of the mixtures followed the Superpave recommendation for long term aging of HMA mixtures which consisted of subjecting the compacted samples to 185^{o}F (85^{o}C) temperatures for 5 days in a forced draft laboratory oven.

III.3. Impact of Additives on the Life Cycle Cost of HMA Pavements

Life cycle cost analysis (LCCA) is a fundamental process of comparing the overall cost of various design alternatives to achieve a fixed performance period. In the context of this research,

the compared design alternatives include: pavements with un-treated HMA layer, pavements with liquid-treated HMA layer, and pavements with lime-treated HMA layer.

The measured engineering properties and performance characteristics of the three types of HMA pavements were used in the AASHTO Mechanistic-Empirical Pavement Design Guide (MEPDG) to estimate the performance of the three types of pavements over a performance period of 20 years (NCHRP, 2004). In other words, using the properties and performance characteristics of the three pavement types, the AASHTO MEPDG was used to develop their fatigue and rutting performances over a 20 years period. The pavement type that shows thinner pavement structure will definitely cost less and provide higher benefit to the owner and road users. The LCCA incorporated the additional cost of using lime and liquid anti-strip in the HMA layer as compared with the un-treated HMA layer. However, the LCCA did not incorporate the cost of maintenance activities over the design life of the pavement. In order for the additives (i.e. lime or liquid) to be effective their additional cost will have to be balanced by the savings realized from the reduced thickness of the HMA due to the improved performance.

In summary, this effort used the measured engineering properties and performance characteristics of the un-treated, lime-treated, and liquid-treated HMA mixtures in the AASHTO MEPDG to predict their relative long term performances. The predicted performances were then coupled with the cost figures produced by the LCCA to identify the most effective design alternative.

IV. DESCRIPTION OF LABORATORY TESTS

IV.1. Resistance of the HMA Mixtures to Moisture Damage

The resistances of the various HMA mixtures to moisture damage were evaluated in terms of measuring the dynamic modulus of the mixtures under multiple freeze-thaw (F-T) cycling. The multiple F-T cycling followed the procedure outlined in AASHTO T-283: Standard Method of Test for Resistance of Compacted Hot Mix Asphalt (HMA) to Moisture-Induced Damage, at multiple stages. A total of three samples from each mix were evaluated following the procedure outlined below:

- Measure the unconditioned E* master curve (i.e., 0 F-T cycles).
- Subject the samples to 75% saturation.
- Subject the saturated samples to multiple freeze-thaw cycling wherein one freeze-thaw cycle consists of freezing at 0^{o}F for 16 hours followed by 24 hours thawing at 140^{o}F and 2 hours at 77^{o}F.
- Subject each sample to the required number of freeze-thaw cycles.
- Conduct E* testing after cycles: 1, 3, 6, 9, 12, and15.
- Take pictures of the samples at various freeze-thaw cycles.

The AASHTO Mechanistic-Empirical Pavement Design Guide (MEPDG) uses the dynamic modulus (E*) master curve to evaluate the structural response of the HMA pavement under various combinations of traffic loads, speed, and environmental conditions (NCHRP, 2004). The E* property of the various HMA mixtures is evaluated under various combinations of loading frequency and temperature. The AASHTO TP62-07: “Determining Dynamic Modulus of Hot Mix Asphalt” and PP62-09: “Developing Dynamic Modulus Master Curves for Hot Mix

Asphalt" were followed. The test is conducted at frequencies of: 25, 10, 5, 0.5, 0.1 Hz and at temperatures of: 40, 70, 100, and 130°F for a total of 270 tests. Using the visco-elastic behavior of an HMA mixture (i.e. interchangeability of the effect of loading rate and temperature) the master curve can be used to identify the appropriate E* for any combination of pavement temperature and traffic speed. Figure 1 shows the components and testing conditions of the complex modulus test along with a typical master curve for HMA mixtures. Figure 2 shows the sequence used for the preparation and testing of the E* samples at various F-T cycles.

The E* property provides an indication on the general quality of the HMA mixtures. The relationship between E* and the number of F-T cycles gives an excellent indication on the moisture resistance of the HMA mixture. The E* master curves will also be used in the mechanistic analyses of the various sections.

In addition to the mixture testing described above, the impact of hydrated lime and liquid additive on the fine aggregate and mastic portion of the mixture was assessed using Dynamic Mechanical Analysis (DMA). The DMA testing and results are presented in Appendix B.

IV.2. Resistance of the HMA Mixtures to Permanent Deformation

The resistances of the various HMA mixtures to permanent deformation were evaluated under the repeated load triaxial (RLT) test. The RLT test consists of testing 4 inches x 6 inches cylindrical sample under triaxial state of stress. Under a given confining pressure, a repeated haversine deviator stress is applied for 0.1 second followed by a 0.6 second rest period while keeping the confining pressure constant. Figure 3 shows the components of the RLT test and a typical response. Figure 4 shows the sequence used for the preparation and testing of the RLT samples at various F-T cycles. The axial deformation of the sample is measured over the middle 4.0 inches of the sample by two linear variable differential transformers (LVDTs) placed 180 degrees apart. The LVDTs measure both the resilient and permanent deformations. The axial permanent strain is calculated as the ratio of the permanent deformation over the 4.0 inches gauge length times 100. The RLT tests for all mixtures were conducted at temperatures of 86, 104, and 125°F. The following model will be used to characterize the permanent deformation behavior of the HMA mixtures:

$$\frac{\varepsilon_p}{\varepsilon_r} = a(N_r)^b(T)^c \qquad (1)$$

Where: ε_p is the permanent axial strain in in/in, ε_r is the resilient axial strain in in/in, N_r is the number of load repetitions, T is the temperature of the HMA mix in (°F), and a, b, and c are experimentally determined coefficients.

IV.3. Resistance of the HMA Mixtures to Fatigue Cracking

The resistances of the various HMA mixtures to fatigue cracking were evaluated using the flexural beam fatigue test "AASHTO T321-07: Determining the Fatigue Life of Compacted Hot-Mix Asphalt Subjected to Repeated Flexural Bending". The 2.5×2.0×15" beam specimen is subjected to a 4-point bending with free rotation and horizontal translation at all load and reaction points. This produces a constant bending moment over the center portion of the specimen. In this research, constant strain tests were conducted at different strain levels; using a repeated haversine load at a frequency of 10 Hz. The beam fatigue tests for all mixtures were

conducted at temperatures of 55, 70, and 85°F except for the California mixtures which were tested at temperatures of 70, 85, and 95°F. Initial flexural stiffness was measured at the 50th load cycle. Fatigue life or failure was defined as the number of cycles corresponding to a 50% reduction in the initial stiffness. The following model will be used to characterize the fatigue behavior of the HMA mixtures:

$$N_f = k_1 \left(\frac{1}{\varepsilon_t}\right)^{k_2} \left(\frac{1}{E}\right)^{k_3} \quad (2)$$

Where: N_f is the fatigue life (number of load repetitions to fatigue damage), ε_t is the applied tensile strain in in/in, E is the stiffness of the HMA mix in psi, and k_1 - k_2 are experimentally determined coefficients. Figure 5 shows the schematics of flexural beam fatigue and typical fatigue curve for HMA mixtures. Figure 6 shows the sequence used for the preparation and testing of the fatigue samples at various F-T cycles.

Another way of assessing the resistance of HMA mixtures to fatigue cracking is by measuring their ability to dissipate energy through deformation. These properties of the mixtures were evaluated using DMA and the results are discussed in Appendix B.

IV.4. Resistance of the HMA Mixtures to Thermal Cracking

The Thermal Stress Restrained Specimen Test (TSRST) (AASHTO TP10-93) was used to determine the low-temperature cracking resistance of the various HMA mixtures. The test cools down a 2"x2"x10" beam specimen at a rate of 10°C/hour while restraining it from contracting. While the beam is being cooled down, tensile stresses are generated due to the ends being restrained. The HMA mixture would fracture as the internally generated stress exceeds its tensile strength. The temperature and stress at which fracture occurs is referred to as "fracture temperature" and "fracture stress", respectively, and represents the field temperature under which the pavement will experience thermal cracking. Figure 7 shows the schematics of the TSRST and a typical stress versus temperature relationship for HMA mixtures. Figure 8 shows the sequence used for the preparation and testing of the TSRST samples at various F-T cycles.

V. ANALYSIS OF THE LABORATORY EVALUATIONS DATA

This section of the report presents the analyses of the data that were generated from the various laboratory evaluations of the fifteen HMA mixtures. The DMA testing and data analyses are presented in Appendix B. Table 3 summarizes the characteristics of the HMA mixtures that were recommended by the participating DOTs. The PG67-22 recommended by the Alabama DOT is not a standard PG grade but it is the most commonly used in Alabama.

V.1. Impact of Additives on Binders Aging

The objective of this evaluation was to assess the impact of the liquid anti-strip and hydrated lime additives on the long-term aging of the five binders that were evaluated in this study. The long-term aging of the binders was achieved in the Pressure Aging Vessel (PAV) at 140°F for 100, 400, and 800 hours. The liquid anti-strip was added to the binders at the rate of 0.5% by weight and the hydrated lime was added at the rate of 20% by weight of binder (i.e. ~ 1% by weight of dry weight aggregate).

The first part of this effort evaluated the Superpave PG of the five binders without and with the additives. The Superpave PG system is summarized in Figure 9. In summary the PG system identifies a grade for the asphalt binder based on three critical temperatures: maximum, intermediate, and minimum. For example, a binder with a grade of PG64-22 will have a maximum temperature of 64^{o}C, an intermediate temperature of 25^{o}C, and a minimum temperature of -22^{o}C. In addition, the identified temperatures indicate that this binder will perform well in an environment where the maximum, intermediate, and low temperatures of the pavement are: 64^{o}C, 25^{o}C, and -22^{o}C, respectively. In practice, the PG64-22 binder is suppose to resist rutting in an environment where the maximum pavement temperature reaches 64^{o}C, resist fatigue cracking in an environment where the average intermediate pavement temperature is around 25^{o}C and resist thermal cracking in an environment where the low pavement temperature reaches -22^{o}C.

Table 4 summarizes the PG grading of the five binders without and with the addition of lime and liquid anti-strips. The data in Table 4 indicate that all binders except the California one met the supplier's specified grade with no additives. The California binder graded as a PG64-22 while its supplier's grade was a PG64-16. This is an acceptable shift since a PG64-22 is supposed to perform excellent in a 64-16 environment.

The data in Table 4 can be used to assess the impact of the additives on the PG of the various binders. In the case of the liquid anti-strip, the addition of 0.5% by weight of binder did not change any of the grades of the binders except for the California binder which was shifted from a PG64-22 to a PG64-16 which coincided with the supplier's grade for this binder. In the case of the lime, the addition of 20% by weight of binder had different impacts on the high temperature and low temperature grades. In the case of high temperature, the addition of lime increased the high temperature grade of the binders by 6^{o}C except for the Alabama binder where the increase was only 3^{o}C and for the California binder which showed no impact. In the case of low temperature, the addition of lime did not impact the low temperature grades of the binders from Alabama, Texas, and South Carolina, and reduced the low temperature grade by 6^{o}C for the binders from Illinois and California.

In summary, the variations due to the addition of the liquid and lime additives on the PG of the binders all fell within the expected influences, where the addition of the liquid is not anticipated to alter the PG while the addition of lime is expected to stiffen the binder. In other words, the increase of one grade on the high end and a decrease of one grade at the low end due to the addition of lime are highly expected due to the filler effect of the hydrated lime.

The second part of this effort evaluated the aging characteristics of the binders without and with the additives. Since long-term aging adversely impacts the binders ability to resist fatigue and thermal cracking, the binders properties were evaluated at the intermediate and low temperatures only. In the case of fatigue resistance, the G*sinδ is the rheological property that is used to measure the binder's ability to resist fatigue. The Superpave PG system hypothesizes that the higher the G*sinδ, the lower the binder's ability to resist fatigue cracking. In the case of thermal cracking, the S(t) and m-value are the two rheological properties that are used to measure the binder's ability to resist thermal cracking. The higher the S(t) and the lower the m-value, the

lower the binder's ability to resist thermal cracking. The hydrated lime was extracted from the aged binders prior to testing the lime-treated binders.

Figures 10 – 14 compare the impact of liquid and lime additives on the long-term aging of the binders at 100, 400, and 800 hrs in the PAV at 60°C (140°F). Tables 5 – 9 summarize the rheological properties of the aged binders. An aging index was calculated as the percent change in a give property relative to the 100 hours aging. The aging index was calculated for all the un-treated and treated binders at the 400 and 800 hours aging periods. Evaluating the measured properties and the calculated aging indexes presented in Figures 10 – 14 and Tables 5 – 9, the following observations can be made:

- Hydrated lime increases the values of the G*sinδ and S(t) and decreases the m-value for all binders at the three aging periods.

However

- Hydrated lime does not significantly change the aging index of all the binders.

The above observations indicate that hydrated lime stiffens the binders but it does not negatively impact their long-term aging characteristics. Therefore, lime-treated binders are expected to be stiffer than un-treated and liquid-treated binders in their early life which increases their resistance to rutting but not too brittle in their later life to negatively impact their resistance to fatigue and thermal cracking.

V.2. Mix Designs

All mixtures were designed following the Superpave volumetric mix design method with a medium traffic level that is equivalent to 3–10 millions equivalent single axle loads (ESAL). The corresponding values of N_{ini}, N_{des}, and N_{max} are 8, 100, and 160, respectively. This level of design is representative for the majority of HMA mixtures around the country. Designing all mixtures to the same level would allow comparisons across the entire matrix.

Each source is evaluated at three mix designs: un-treated, lime-treated, and liquid-treated. The liquid anti-strip additive was selected to represent a commonly used liquid additive in the region where the aggregate source is located. The states were asked to select a liquid additive that is commonly used and not one that is specially fabricated for this application.

Figures 15 – 29 summarize the mix design information for the mixtures from all five sources. Each figure summarizes pertinent mix design data and information on aggregate specific gravities and gradation. The mix design data include the number of gyrations at the initial, design, and maximum compaction stages. It should be noted that these levels are constant (i.e. 8, 100, and 160 gyrations) for all mixtures since all mixtures were designed to a constant traffic level of 3-10 millions ESALs.

The moisture sensitivity of the mixtures were evaluated using the unconditioned and conditioned tensile strengths (TS) along with the tensile strength ratio (TSR). It should be noted that the mix designs for the fifteen mixtures were conducted using the 6" diameter Superpave Gyratory Compactor (SGC) samples while the TS and TSR properties were evaluated on 4" diameter SGC samples. This change in the size of the SGC samples for the TS and TSR properties was implemented since the majority of the moisture sensitivity specifications are based on 4"

diameter samples. The data in Figures 15 – 29 indicate that all mixtures met the minimum dry tensile strength criterion of 70 psi at 77°F. In addition, all mixtures met the Superpave criterion of 80% TSR except the California, South Carolina, and Texas mixtures which failed the 80% criterion when un-treated.

In summary, the mix designs showed that the mixtures from California, South Carolina, and Texas required additives to pass the Superpave moisture sensitivity criterion of 80% TSR while the mixtures from Alabama and Illinois did not require any additive. The following TSR values were measured on the un-treated mixtures: Alabama – 81, California – 72, Illinois – 82, South Carolina – 61, and Texas – 61. The TSR data showed that the experiment includes two mixtures that can be classified as highly moisture sensitive (SC and TX), one mix that is moderately moisture sensitive (CA), and two mixtures that are not moisture sensitive (AL and IL). This provided a wide range of mixtures to be evaluated in the study. Figures 30 – 34 show the TS and TSR values for the five sources along with the ranges of the TS values of each mix. The data in these figures show that the addition of lime increased both the unconditioned, except for the California mix, and conditioned TS, and therefore, generating stronger and more durable mixtures. Figure 31 shows the addition of lime to the California mix reduced its unconditioned TS value at 77°F from 214 to 164 psi. Even-though this behavior is not typical of lime-treated mixtures, the California lime-treated mix still exhibited a relatively high unconditioned TS value relative to the other treated mixtures that were evaluated in this study. Therefore, the strength reduction in the unconditioned TS value of the California lime-treated mix should not be a source of concern. The impact of adding the liquid anti-strip was inconsistent among the five mixtures. When looking at the TSR data, it can be seen that the addition of both liquid and lime improved the TSR values regardless of the TSR values of the un-treated mixtures. In other words, the addition of liquid and lime benefitted both the moisture sensitive mixtures and non-sensitive mixtures.

V.3. Resistance of the HMA Mixtures to Moisture Damage

The resistance of the various HMA mixtures to moisture damage was evaluated in terms of measuring the dynamic modulus master curves of the mixtures under multiple F-T cycling.

The multiple freeze-thaw cycling follows the procedure outlined in AASHTO T-283 at multiple stages and as described in Section IV.1 of this report. For every mixture, the dynamic modulus master curve was measured at the unconditioned stage and after multiple F-T cycles of 1, 3, 6, 9, 12, and 15. The E* master curves were used in the AASHTO MEPDG to conduct the structural designs and life cycle cost portion of this research. The E* master curve provides the modulus property of the HMA mix at any combination of loading rate and temperature. Such data are used to assess the response of HMA pavement under all possible combinations of loading speed and environment. Since the E* is the fundamental engineering property of the mixtures that will be used in the MEPDG to evaluate the performance of HMA pavements, the E* master curves were measured on the unaged and aged mixtures to simulate short and long term behavior of the various mixtures.

Figures 35 – 44 show the E* masters curves for the various mixtures at the 0, 6, and 15 F-T cycles. There are two sets of figures for each mix. The first figure shows the E* master curves at the unaged stage and 125°F temperature to represent the curves that are applicable to the

permanent deformation analysis. The second figure shows the E* master curves at the aged stage and 70°F temperature to represent the curves that are applicable to the fatigue analysis. The temperatures and aging conditions of the E* master curves presented in Figures 35 – 44 were selected to represent the critical conditions for permanent deformation of high temperature/unaged and for fatigue cracking of intermediate temperature/aged.

Examining the E* master curves in Figures 35 – 44 leads to the observation that the E* master curves become lower as the mixtures are subjected to multiple freeze thaw cycles at both the aged and unaged stages. However, the lime-treated mixtures show smaller downward shift of the master curves as a function of freeze thaw cycling as is clearly shown in Figures 36, 37, 38, 40, 42, 43, and 44. The E* master curve data is basically indicating that the impact of the multiple F-T cycling on the mixtures varies depending on the type of additive and the aging stage of the mix.

The next step of the moisture damage analysis was to identify a representative number of multiple F-T cycles that can be used to moisture condition the various mixes prior to testing for permanent deformation, fatigue, and thermal cracking. For this analysis, the E* master curves at a loading frequency of 10 Hz were selected to be consistent with the loading conditions in the permanent deformation and beam fatigue testing. Figures 45 – 49 show the E* properties of the various mixtures as a function of multiple F-T cycling. The top portion of each figure shows the E* property at 104^{o}F of the unaged mixtures to represent the condition for permanent deformation and the bottom portion of the figure shows the E* property at 70^{o}F of the aged mixtures to represent the condition for fatigue.

The data in Figures 45 – 49 show a significant reduction in the E* property as a function of multiple F-T cycling. Figure 46, 48, and 49 show that the un-treated mixtures from California, South Carolina, and Texas could not withstand the entire set of 15 F-T cycles. This data coincide very well with the mix design data that showed the same three mixtures having low TSR. Examining the data in Figures 45 – 49 leads to the following observations:

- The E* property of the various mixtures is significantly impacted by the temperature of the test and the aging condition of the mix. This becomes very clear when the E* values at the top portion of each figure are compared with the E* values at the bottom portion of the figure.
- As the various mixtures are subjected to multiple F-T cycling, the lime-treated mixtures of all five sources hold their E* properties significantly better than the un-treated and liquid-treated mixtures.
- The sixth F-T cycle seems to indicate the point after which most of the mixtures hold a steady value of E*. This indicates that the sixth F-T represents an effective moisture conditioning stage for the various mixtures. Therefore, it was recommended to subject the permanent deformation, fatigue, and thermal cracking samples to 6 F-T cycles to represent their moisture conditioning stage. It should be noted that the use of multiple F-T cycles is not meant to mimic the actual field conditioning process but to accelerate the moisture damage in a manner that can be measured under laboratory conditions.

Table 10 summarizes the E* property of the various mixtures at the unconditioned stage (0 F-T) and after 6 F-T cycles. The unaged E* at 104^{o}F is selected to represent permanent deformation behavior and the aged E* at 70^{o}F is selected to represent fatigue behavior. The data in Table 10 clearly show the significant difference between the E* properties of the lime-treated mixtures and the other mixtures. For example, the Texas mix shows a higher unconditioned E* (i.e. 0 F-T) for the un-treated than the treated mixtures, however, the E* property of the un-treated mix significantly dropped after the 6 F-T cycles for both the unaged and aged stages. The ratio of the conditioned E* over the conditioned E* is also shown in Table 10 which indicates that the lime-treated mixtures from all five sources maintained a higher ratio than the un-treated and liquid-treated mixtures at both unaged and aged stages. In summary, the data in Table 10 shows that the lime-treated mixtures maintained a significantly higher E* property after moisture damage in terms of magnitude and retained ratio for all mixtures and at both the unaged and aged stages.

It should be noted that even-though the higher E* property of the lime-treated mixtures that is shown throughout the moisture damage analysis indicate more stable mixtures, its combined effect on the permanent deformation and fatigue performance will have to be carefully examined prior to understanding the full impact of the lime treatment of the various mixtures. This analysis will be fully covered under the LCCA portion of this study.

V.4. Resistance of the HMA Mixtures to Permanent Deformation

The resistances of the various HMA mixtures to permanent deformation were evaluated using the repeated load triaxial (RLT) test as described in section IV.2 of this report. The testing matrix in Table 2 indicates that the resistance of the unaged mixtures to permanent deformation will be measured at the unconditioned and moisture conditioned stages. The moisture conditioning was accomplished by subjecting the RLT samples to 6 F-T cycles prior to testing.

Figures 50-54 show the RLT data for the mixtures from Alabama, California, Illinois, South Carolina, and Texas at the three testing temperatures for the 0 and 6 F-T cycles. Each curve in the figures represents the average of three replicate tests. In general, the lower the RLT curve the higher the resistance of the mixture to permanent deformation. The data in Figures 50 – 54 show that the resistance of the mixtures to permanent deformation increase as the temperature of the test decreases. The RLT data at the three testing temperatures were used to develop the generalized permanent deformation model for each mixture as presented in Equation 1. Table 11 summarizes the generalized permanent deformation models for all fifteen mixtures after 0 and 6 F-T cycles. The generalized permanent deformation models will be used in the AASHTO MEPDG to conduct the structural designs and life cycle cost of HMA pavements constructed with the various HMA mixtures.

The next step of this analysis is shown in Figures 55 – 59 which compare the permanent deformation of the various mixtures at a constant temperature of 104^{o}F representing hot weather where permanent deformation is expected to be a problem. It should be noted that the rutting curves shown in Figure 55 – 59 are based on the generalized models summarized in Table 11. The top portion of each figure represents the rutting curves for the unconditioned mixtures and the bottom portion represents the RLT data for the mixtures after 6 F-T cycles. The results of the RLT test are expressed in the form of Equation 1 at a constant temperature which relates the ratio of the permanent strain in the HMA mix over the resilient strain to the number of load cycles.

While describing the impact of the additives on the rutting behavior of the mixtures, the following two concepts must be fully understood:

1. The lower the rutting curve, the higher the resistance of the mixture to rutting.

But

2. The higher the resistance of the mixture to rutting does not necessarily lead to better rutting performance of the HMA pavement.

The above two concepts may seem to be contradicting each other because of the interaction between the E* property of the mix and the rutting curve of the HMA mix. For example, in a given HMA pavement structure, the magnitude of the E* property controls the magnitude of the generated strain at the middle of the HMA layer which is then used in the rutting model of the HMA mix to estimate the rutting life for the HMA pavement. Therefore, an HMA mix with a lower rutting curve may still produce a lower estimated rutting life of the HMA pavement if its E* property is low enough to generate a significantly higher vertical strain at the middle of the HMA layer.

Based on the above discussion, the data in Figures 55 – 59 can only be evaluated in terms of the impact of the additives on the resistance of the HMA mixtures to rutting but not in terms of their impact on the rutting performance of the HMA pavement. The impact of the additives on the rutting performance of the HMA pavement can only be evaluated through a mechanistic analysis using the AASHTO MEPDG which combines the contributions of both the E* property and the rutting characteristics of the HMA mix. Such analyses will be presented in the later part of this report.

- For the Alabama source (Figure 55):
    - The liquid significantly decreased the rutting resistance of the unconditioned mixture (i.e. 0 F-T)
    - The liquid-treated and lime-treated mixtures showed lower rutting resistance than the un-treated mix at the conditioned stage (i.e. 6 F-T).

- For the California source (Figures 56):
    - The liquid slightly increased the rutting resistance of the unconditioned mixture (i.e. 0 F-T).
    - All three mixtures showed similar rutting resistance at the conditioned stage (i.e. 6 F-T).

- For the Illinois source (Figures 57):
    - The liquid significantly decreased the rutting resistance of the unconditioned mixture (i.e. 0 F-T)
    - All three mixtures showed similar rutting resistance at the conditioned stage (i.e. 6 F-T).

- For the South Carolina source (Figures 58):
    - The liquid significantly decreased the rutting resistance of the unconditioned mixture (i.e. 0 F-T)

- All three mixtures showed similar rutting resistance at the conditioned stage (i.e. 6 F-T).

- For the Texas source (Figures 68):
  - All three mixtures showed similar rutting resistance at the unconditioned stage (i.e. 0 F-T)
  - The lime significantly increased the rutting resistance of the conditioned mixture (i.e. 6 F-T).

V.5. Resistance of the HMA Mixtures to Fatigue

The resistances of the various HMA mixtures to fatigue cracking were evaluated using the flexural beam fatigue test as described in section IV.3 of this report. The testing matrix in Table 2 indicates that the resistance of the mixtures to fatigue cracking will be measured at the aged, unconditioned, and moisture conditioned stages. The moisture conditioning was accomplished by subjecting the beam samples to 6 F-T cycles prior to testing.

Figures 60 – 64 summarize the fatigue characteristics of the various mixtures in terms of the relationship between the flexural strain and the number of load repetitions to failure at the three testing temperatures. In general the higher the fatigue curve the higher the resistance of the mixture to fatigue cracking. The data in Figures 60 – 64 show the fatigue resistance of the various mixtures increases as the testing temperature decreases. The beam fatigue data at the three testing temperatures were used to develop the generalized fatigue model for each mixture as presented in Equation 2. Table 12 summarizes the generalized fatigue models for all fifteen mixtures after 0 and 6 F-T cycles. The generalized models will be used in the AASHTO MEPDG to conduct the structural designs and life cycle cost of HMA pavements constructed with the various HMA mixtures.

The next step of this analysis is shown in Figures 65 – 69 which compare the fatigue characteristics of the various mixtures at a constant temperature of 70^{o}F representing an intermediate weather where fatigue cracking is expected to be a problem. It should be noted that the fatigue curves shown in Figure 65 – 69 are based on the generalized models summarized in Table 12. The top portion of each figure represents the fatigue curves for the unconditioned mixtures and the bottom portion represents the fatigue data for the mixtures after 6 F-T cycles.

While describing the impact of the additives on the fatigue behavior of the mixtures, the following two concepts must be fully understood:

1. The higher the fatigue curve, the higher the resistance of the mixture to fatigue cracking.

But

2. The higher the resistance of the mixture to fatigue cracking does not necessarily lead to better fatigue performance of the HMA pavement.

The above two concepts may seem to be contradicting each other because of the interaction between the E* property of the mix and the fatigue curve of the HMA mix. For example, in a given HMA pavement structure, the magnitude of the E* property controls the magnitude of the

generated strain at the bottom of the HMA layer which is then used in the fatigue curve of the HMA mix to estimate the fatigue life for the HMA pavement. Therefore, an HMA mix with a higher fatigue curve may still produce a lower estimated fatigue life of the HMA pavement if its E* property is low enough to generate a significantly higher tensile strain at the bottom of the HMA layer.

Based on the above discussion, the data in Figures 65 – 69 can only be evaluated in terms of the impact of the additives on the resistance of the HMA mixtures to fatigue cracking but not in terms of their impact on the fatigue performance of the HMA pavement. The impact of the additives on the fatigue performance of the HMA pavement can only be evaluated through a mechanistic analysis using the AASHTO MEPDG which combines the contributions of both the E* property and the fatigue characteristics of the HMA mix. Such analyses will be presented in the later part of this report.

- For the Alabama source (Figure 65):
    - All three mixtures showed similar fatigue resistance of the unconditioned mixtures (i.e. 0 F-T)
    - The liquid additive created a significant change in the slope of the fatigue curve after 6 F-T cycles as compared to the un-treated and lime-treated mixtures (bottom portion of Figure 65). Such behavior leads to differing fatigue resistance of the mixtures under high strains versus low strains which makes it very complicated to assess the potential performance of the mixtures under mixed traffic. On the other hand, Figure 65 shows no change in the slope of the fatigue curve for the lime-treated mixture after 6 F-T cycles which makes it easier to predict the behavior of such mixtures under mixed traffic.

- For the California source (Figures 66):
    - The lime slightly increased the fatigue resistance of the unconditioned mixture (i.e. 0 F-T).
    - The liquid and lime significantly increased the fatigue resistance of the conditioned mixtures (i.e. 6 F-T).

- For the Illinois source (Figures 67):
    - The liquid and lime significantly increased the fatigue resistance of the unconditioned mixtures (i.e. 0 F-T) with the liquid showing slightly more improvement than the lime.
    - The lime significantly increased the fatigue resistance of the conditioned mixture (i.e. 6 F-T) while the liquid slightly increased the fatigue resistance of the conditioned mixture (i.e. 6 F-T).

- For the South Carolina source (Figures 68):
    - The lime additive caused a decrease in the fatigue resistance of the unconditioned mix while the liquid additive did not cause any changes.
    - The un-treated and liquid-treated mixtures exhibited significant changes in the slope of their fatigue relationship after moisture conditioning (i.e.

comparing the curves at 0 and 6 F-T) while the lime-treated mix exhibited a minor reduction in its resistance to fatigue cracking.

- For the Texas source (Figures 69):
  - The liquid and lime additives did not change the fatigue characteristics of the unconditioned mixtures (i.e. 0 F-T)
  - Both the liquid and lime additives caused a significant increase in the fatigue resistance of the conditioned mixtures (i.e. 6 F-T).

V.6. Resistance of the HMA Mixtures to Thermal Cracking

The resistances of the mixtures to thermal cracking were measured using the TSRST as described in Section IV.4 of this report. The TSRST measures the fracture temperature and fracture stress of HMA mixtures. The fracture temperature represents the temperature at which the HMA mix will crack due to thermal stresses and the fracture stress represents the magnitude of the stress caused by the thermal contraction of the HMA mix.

Table 13 summarizes the fracture stresses and fracture temperatures of the various mixtures at 0 and 6 F-T cycles. All the TSRST samples were aged following the procedure described earlier to simulate the long-term properties of the mixtures in the field when thermal cracking becomes critical. The fracture temperature represents the temperature at which the HMA pavement will develop a transverse crack due to thermal stresses. The fracture stress controls the spacing of the thermal cracks once they occur. It is believed that a higher fracture stress in the TSRST would indicate a longer spacing of the transverse cracks in the field.

The data in Table 13 indicate that the majority of the un-treated, liquid-treated, and lime-treated mixtures have similar fracture temperatures at both the 0 and 6 F-T cycles. However, the lime-treated mixtures showed significantly higher fracture stresses which would indicate that, once thermal cracking occurs, HMA pavements with lime-treated mixtures would experience fewer cracks per mile than the un-treated and liquid-treated mixtures. The fewer number of thermal cracks per mile would directly translate into lower maintenance cost for the lime-treated pavements as compared to the un-treated and liquid-treated pavements. However, there are couple exceptions to the above stated observation; 1) the California and South Carolina sources showed the liquid-treated mix having colder fracture temperature than the lime-treated mix at the conditioned stage and 2) the Illinois source showed the lime-treated mix having a colder fracture temperature than the liquid-treated mix at the unconditioned stage. On the other hand, the observation of higher fracture stresses for the lime-treated mixtures had no exceptions.

VI. IMPACT OF ADDITIVES ON THE LIFE CYCLE COST OF NEW HMA PAVEMENTS

The objective of this analysis is to evaluate the impact of liquid and lime additives on the life cycle cost of HMA pavements. This analysis used the AASHTO MEPDG to conduct structural designs of HMA pavements that use un-treated, liquid-treated, and lime-treated HMA mixtures in the surface layer. The basic concept behind this analysis is to assess if the use of liquid-treated and lime-treated HMA mixtures resulted in a reduction in the required thickness of the HMA. If this is true then the use of liquid and lime additives results in savings in the life cycle cost of the

HMA pavement once the reduction in the HMA thickness offsets the additional cost of the liquid and lime additives.
The MEDPG requires the following information to conduct structural designs of HMA pavements:

- Traffic
- Climate
- Materials Properties
- Performance Models

In general, the MEPDG conducts HMA pavement designs based on their performance in resisting: rutting, bottom-up fatigue, top-down fatigue, thermal cracking, roughness, and reflective cracking. However, because this study only evaluated the rutting and bottom-up fatigue characteristics of the HMA mixtures, the structural designs was only be based on those two distresses. In the case of thermal cracking, the TSRST data provided direct assessment of the effectiveness of the additives on this mode of distress, and therefore, the MEPDG analysis did not include thermal cracking.

Using the information from traffic, climate, and materials properties, the MEPDG calculates the mechanistic responses of the HMA pavement in terms of tensile strain at the bottom of the HMA layer and vertical resilient strain throughout the HMA layer. The calculated strains are then input into the performance models of the HMA layer that were developed in this study to estimate the rutting and fatigue performance of the HMA pavement.

Each participating state was asked to identify two project locations where the evaluated mixtures will most likely be used. The state of Illinois provided only one project that is applicable to the source of aggregate that was used in this study. Figure 70 shows the locations of the recommended projects along with the locations of the aggregate sources from all five participating states. The MEPDG was used to conduct a 20 years structural design for HMA pavements at each location using all three types of HMA layers: un-treated, liquid-treated, and lime-treated. The structural designs were conducted based on un-damaged and moisture-damaged conditions of the HMA layer. The dynamic modulus properties at 0 F-T cycles were used to represent the un-damaged conditions and the dynamic modulus properties at 6 F-T cycles were used to represent the moisture-damaged conditions of the HMA layer.

VI.1. Traffic

The traffic data required for the MEPDG software consist of the following:

- General traffic information
- Average daily truck traffic (ADTT) distributions by vehicle class
- The hourly truck traffic distributions

If the above data are not available, the MEPDG software provides default values depending on the functional classifications of the road being designed.

Each participating state was asked to provide traffic information for the recommended project locations. Table 14 summarizes the general traffic information that were supplied by the states and were used as an input into the MEPDG software. Table 15 summarizes the average daily truck traffic (ADTT) distributions for the various vehicle classes. Only South Carolina provided

project specific ADTT distributions while the MEPDG default ADTT distributions were used for the other four states. The default values provided by the MEPDG software were used for the hourly truck traffic distributions for all five states.

VI.2. Climate

The MEPDG considers the effects of climatic variables on pavement responses and pavement performance. Moisture and temperature profiles are predicted through the Enhanced Integrated Climatic Model (EICM) module incorporated into the MEPDG software. The climate module in the MEPDG software requires the user to specify a climate file. Table 16 shows the location of the climatic stations that were assigned to the various projects.

VI.3. Materials Properties

Asphalt Layer

The MEPDG software requires the dynamic modulus (E*) master curve for the HMA layer. The dynamic modulus master curves that were measured for the un-treated, liquid-treated, and lime-treated mixtures as shown in Figures 35-44 were used in the MEPDG software to represent the three types of mixtures from each of the five states. As mentioned earlier, the E* master curves at 0 F-T cycles were used to represent the un-damaged conditions and the E* master curves at 6 F-T cycles were used to represent the moisture-damaged conditions of the HMA layer.

Base Layer

A typical crushed aggregate dense graded base (CAB) was used with a resilient modulus (Mr) of 30,000 psi for all projects in the five participating states. This value is a representative Mr value for crushed aggregate at optimum density and moisture content. The Enhanced Integrated Climatic Model (EICM) is used to modify the representative Mr for the seasonal effect of climate.

Native Subgrade

A Level 3 analysis was used for the subgrade which means that a representative resilient modulus is assigned by the MEPDG software based on the AASHTO classification of the subgrade material. A relatively lower modulus value was assigned to the subgrade at the Illinois site because of its historically low California Bearing Ratio (CBR). Table 17 summarizes the modulus values assigned to the subgrades for the various projects.

VI.4. Performance Models

The rutting and fatigue performance models that were developed in this study for the three mixtures from every state were used in the MEPDG to estimate the rutting and fatigue performance of the HMA pavements. The performance models at the 0 F-T cycles were used to conduct the design at the un-damaged condition and the 6 F-T cycles were used to conduct the designs at the moisture-damaged condition. The models used in the MEPDG designs are shown in Figures 50-69 and Tables 11 and 12.

VI.5. MEPDG Structural Designs

The MEPDG structural design was conducted for each project location within the five participating state, only one location was designed for Illinois based on the recommendation of the state representative. In total the following structural designs were conducted:

(5 states)(2 locations)(2 damage conditions)(3 HMA mixtures) = 60 - 6 (one location in IL) = 54
At each location, the following process was followed:

- The design life was set at 20 years for all projects.
- The rutting failure criterion was set at 0.25" rut depth in the HMA layer.
- The fatigue failure criterion was set at 25% fatigue of the pavement surface.
- Conduct structural designs for the un-damaged condition using the 0 F-T cycles properties and performance models for each of the three HMA mixtures: un-treated, liquid-treated, and lime-treated.
- Conduct structural designs for the moisture-damaged condition using the 6 F-T cycles properties and performance models for each of the three HMA mixtures: un-treated, liquid-treated, and lime-treated.
- In each case of the un-damaged and moisture-damaged conditions, select the structural design that satisfy both the rutting and fatigue criteria.

A structural design based on the 1993 AASHTO Pavement Design Guide was conducted for the un-treated mix at the un-damaged condition for all five sources (AASHTO, 1993). The 1993 AASHTO designs were used to check the reasonableness of the MEPDG designs. Table 18 summarizes the 54 MEPDG structural designs. The basic concept of the structural design process was to keep the thickness of the base layer constant for each project location while changing the thickness of the HMA layer to achieve a 20 years design. The "Control Distress" column indicates the distress mode that controlled the structural section for the 20 years design. As indicated earlier, the MEPDG structural design was only based on the rutting in the HMA and bottom-up fatigue cracking. A minimum HMA thickness of 6.00 inches was implemented for all projects to ensure that adequate base and subgrade protection is provided through all the designs. Therefore, a "Neither" entry in the "Control Distress" indicates that the minimum HMA thickness was reached without exceeding the set criteria of rutting in the HMA layer nor the bottom-up fatigue cracking. A maximum HMA thickness of 16.00 inches was implemented for all projects to ensure realistic structural designs. The maximum HMA thickness was only invoked in one project (i.e. S. Carolina SC12).

In the case of the California project on Interstate Route 80 (PLA80) under the moisture-damaged condition a satisfactory 20 years structural design was not achievable. Due to the extremely high traffic volume on this project the rutting in the HMA layer was not controllable by simply increasing the thickness of the HMA layer. Further increase in the thickness of the HMA layer resulted in an increase in the rutting in the HMA layer. The MEPDG structural design for this project identified two issues: a) the extremely high traffic volume grossly violated the Superpave mix design criterion of 3 -10 million ESALs that was used in this research to design the mixtures (i.e. section V.2) and b) the excessive rutting in the HMA would require the use of a polymer-modified HMA mix in the top lift of the HMA which is un-available in this research. Due to the difficulties encountered in the MEDPG designs for the California PLA80 project, this project was excluded from the life cycle cost analysis.

In the case of the South Carolina project on SC12, the MEDPG was unable to recommend a structural design for the un-treated mix at the moisture-damaged condition due to extremely low dynamic modulus property of the un-treated mix after moisture conditioning (i.e. Figure 48).

The next step of the analysis was to identify the mix condition that controlled the structural design for each project that controls the 20 years performance life. For this step, the thicker structural design between the un-damaged and moisture-damaged conditions was selected for each project. Since the thickness of the base layer was kept constant within each project, the thicker structural designs were simply the ones having the thicker HMA layer. Table 19 summarizes the structural designs that controlled the 20 years performance life for all projects along with an indication on the condition that controlled the final design, e.g. un-damaged or moisture-damaged.

It should be noted again that the MEPDG analysis that was conducted in this research considered only fatigue cracking and rutting performance of the HMA pavements based on the strength properties and performance models that were measured on all of the evaluated mixtures. In practice the structural design maybe further adjusted to account for other factors such as safety and project geometrics. For example, the data in Tables 18 and 19 show a reduction in the thickness of the HMA close to 50% for the Texas project on FM396 (7.00 inches for lime-treated vs. 13.75 inches for un-treated) which indicates that from a pure mechanistic point of view, the lime-treated pavement can be constructed with a 7.00 inches HMA layer. However, it should be recognized that the strength properties and performance models that were developed in this research were based on the materials sampled for this research without considering potential materials and construction variability. Therefore, the data presented in Tables 18 and 19 should only be used for comparative purposes and the final recommended structural designs should be adjusted to account for other factors that include safety, project geometrics, and variabilities associated with materials production and construction techniques.

Figures 71 – 75 show the 20 years design performance of the designed projects from all states in terms of fatigue cracking and rutting in the HMA layer. The pavement structures corresponding to the performances shown in Figures 71 -75 are the final designs identified in Table 19. The control distresses identified in Table 18 are based on the performances shown in Figures 71 – 75. For example the Alabama project on US31 showed the failures of the un-treated (un-damaged) and lime-treated (moisture-damaged) to be in rutting while the failure of the liquid-treated (moisture-damaged) to be in fatigue. In the same time Figure 71 shows the rutting performance of the un-treated and lime-treated pavements are worse than the liquid-treated pavement while the fatigue performance of the liquid-treated pavement is worse than the un-treated and lime-treated pavements.

VI.6. Simplified Mechanistic-Empirical Design

The MEPDG uses the full E* master curve along with the full distribution of traffic loads over the entire design period to conduct the structural design of the HMA pavement. Therefore, it is very difficult to independently explain the various steps that are involved in the overall mechanistic-empirical process that is incorporated in the MEPDG.

This section presents a simplified mechanistic analysis for fatigue cracking to explain the step by step process that is involved in the mechanistic design process. The following conditions were selected for this analysis.

- Select the California project on PLA28 with un-treated, liquid-treated, and lime-treated mixtures at the moisture-damaged condition.

- Design axle: single axle/dual tires loaded to 18,000 lb.
- Tire inflation pressure of 100 psi.

The following steps were followed to conduct the simplified mechanistic analysis for fatigue cracking at 70°F on the CA PLA28 project.

1. The moisture-damaged structures (Table 19):
    a. For the un-treated mix
        HMA = 9.5 inches
        CAB = 8.0 inches
    b. For the liquid-treated mix
        HMA = 8.0 inches
        CAB = 8.0 inches
    c. For the lime-treated mix
        HMA = 6.0 inches
        CAB = 8.0 inches
2. Select the aged E* property after 6 F-T cycles at 70°F for fatigue analysis:
    a. For the un-treated mix, E*= 622,000 psi
    b. For the liquid-treated mix, E* = 1,116,00 psi
    c. For the lime-treated mix, E* = 1,717,000 psi
3. Resilient modulus of the CAB layer is 30,000 psi for all structures.
4. Resilient modulus of the subgrade layer is 13,000 psi (Table 17) for all structures.
5. Run the multilayer elastic analysis to calculate the tensile strain at the bottom of the HMA layer.
    a. For the un-treated mix, $\varepsilon = 83 \times 10^{-6}$ in/in
    b. For the liquid-treated mix, $\varepsilon = 71 \times 10^{-6}$ in/in
    c. For the lime-treated mix, $\varepsilon = 77 \times 10^{-6}$ in/in
6. Select the fatigue models after 6 F-T cycles from Table 12.
    a. For the un-treated mix:

$$N_f = 1.893 \times 10^{18} \left(\frac{1}{\varepsilon}\right)^{5.146} \left(\frac{1}{E}\right)^{5.551}$$

    b. For the liquid-treated mix:

$$N_f = 2.043 \times 10^{7} \left(\frac{1}{\varepsilon}\right)^{3.654} \left(\frac{1}{E}\right)^{2.590}$$

    c. For the lime-treated mix:

$$N_f = 1.342 \times 10^{12} \left(\frac{1}{\varepsilon}\right)^{5.502} \left(\frac{1}{E}\right)^{4.308}$$

7. Plugging the E* and ε values in the appropriate fatigue models and calculating the number of load repetitions to failure in fatigue cracking N_f, showed that the lime-treated pavement will have 6 and 13 times better fatigue performance than the un-treated and liquid-treated pavements, respectively.
8. The simplified mechanistic analysis for fatigue cracking showed that under a single axle type with 18,000 lb, the un-treated and liquid-treated pavements at the moisture–damaged condition will fail in fatigue cracking while the lime-treated pavement will

not fail in fatigue (i.e. 6 and 13 times better fatigue performance). This conclusion is consistent with the MEPDG structural designs for this project presented in Table 18.

It should be recognized that the MEPDG conducts similar analysis for every axle type, axle load, and everyday over the entire 20 years design period using the full E* master curve of the various HMA mixtures. Therefore, the N_f numbers calculated from the equations in item 6 above should be looked at in relative terms and not in absolute values.

VI.6 Life Cycle Cost

The concept of the life cycle cost used in this research is based on comparing the actual initial construction cost of the three types of pavements for each project: un-treated, liquid-treated, and lime-treated. Since the type and thickness of the base course layer were kept constant, the difference in the cost only comes from the difference in the type of treatment of the HMA mix. The additional cost for the liquid-treated mix included the added cost of the liquid while the additional cost for lime-treated mix included both the added cost of the lime and the cost of the necessary modifications of the HMA plant to produce lime-treated HMA mixtures. it should be noted that the LCCA calculations were limited to the initial construction cost of the HMA layer and did not incorporate any future costs for maintenance of the various pavements.

The following unit costs were identified based on the 2008 market for the production of HMA mixtures and the experience of the researchers:

- Unit cost of un-treated HMA mix: \$5.12 /yd^2-in (\$65.0/ton of HMA)
- Unit cost of liquid-treated HMA mix: \$5.16 /yd^2-in (\$65.4/ton of HMA)
- Unit cost of Lime-treated HMA mix: \$5.39 /yd^2-in (\$68.4/ton of HMA)

The above unit costs are based on the cost of asphalt binder of \$650 per ton at the hot mix plant and the cost of aggregate of \$15 per ton at the hot mix plant. The unit cost of the liquid-treated HMA mix was calculated based on the cost of the liquid additive of \$0.70/ton of HMA without any additional cost for the production of the liquid-treated HMA mix. The unit cost of the lime-treated HMA mix was calculated based on the cost of lime of \$1.25/ton of HMA and the additional costs of plant modifications and equipment of \$3.75/ton of HMA mix. It should be noted that the above cost figures are representative of 2008 prices and may vary depending on the regions of the U.S. and the cost of shipping and handling.

Using the above figures, the total cost of the HMA for a lane-mile were calculated by multiplying the unit cost times the thickness of the HMA layer in inches and by the factor of 7040 which converts the yd^2 into lane-mile ([5280 feet/mile x 12 feet/lane]/9 ft^2/yd^2). The total costs of the HMA mix for a lane-mile for each of the pavements shown in Table 19 were calculated and are summarized in Table 20. The percent saving was calculated as the ratio of the difference between the cost of HMA for a lane-mile of the treated mix and the cost of the un-treated mix divided by the cost of HMA for a lane-mile of the un-treated mix times 100. In the case of the South Carolina project on SC12, the maximum HMA thickness of 16.00 inches was used for the un-treated mix at the moisture-damaged stage due to the inability of the MEPDG to recommend a final design.

A negative percent savings in Table 20 indicates that the use of treated HMA mix resulted in a more expensive pavement structure than the use of the un-treated mix. Negative percent savings were calculated for the two projects in Alabama and the one project in Illinois when the liquid-treated mix was used in the HMA layer. It is very interesting to note that both the Alabama and Illinois mixtures were considered as not moisture sensitive. To further examine these findings, the AL project on US31 and the IL project in Chicago were selected for further analysis. Since the percent savings are based on comparing the treated pavement with the un-treated pavement and negative savings are limited to liquid-treated pavements, the analysis was limited to comparing the behavior of the un-treated mix with the liquid-treated mix. As discussed earlier, the performance of the pavement is based on the interaction between the E* property and the performance characteristics of the HMA mixture.

In the case of the AL project on US31, the data in Table 19 show that the controlling pavement structure is the un-damaged and the distress mode is rutting for both the un-treated and liquid-treated pavements. Therefore, the analysis looked at the rutting behaviors of the AL un-treated and liquid-treated mixtures. The data in Table 10 show that the unaged E* at 104^{o}F at the un-damaged stage (i.e. 0 F-T) are 226 and 216 ksi for the un-treated and liquid-treated mixtures, respectively. Next, the rutting curves for the AL un-treated and liquid-treated mixtures shown in Figure 55 were examined. Since the un-damaged condition controlled the design, the top portion of Figure 55 was examined. The rutting curves in the top portion of Figure 55 indicate that the liquid-treated mix has a significantly lower rutting resistance than the un-treated mix (i.e. higher curve). Therefore, it can be confirmed that the use of the liquid-treated mix on AL US31 with a slightly lower E* and significantly lower resistance to rutting would lead to additional cost (i.e. negative savings) to the agency.

In the case of the IL project in Chicago, the data in Table 19 show that the controlling pavement structure is the un-damaged and the distress mode is rutting for the un-treated and liquid-treated pavements. Therefore, the analysis looked at the rutting behaviors of the IL un-treated and liquid-treated mixtures. The data in Table 10 show that the unaged E* at 104^{o}F at the un-damaged stage (i.e. 0 F-T) are 235 and 362 ksi for the un-treated and liquid-treated mixtures, respectively. Next, the rutting curves for the AL un-treated and liquid-treated mixtures shown in Figure 57 were examined. Since the un-damaged condition controlled the design, the top portion of Figure 57 was examined. The rutting curves in the top portion of Figure 57 indicate that the liquid-treated mix has a significantly lower rutting resistance than the un-treated mix (i.e. higher curve). In this case the combination of the moderately higher E* of the liquid-treated mix coupled with its significantly lower rutting resistance than the un-treated still led to additional cost (i.e. negative savings) to the agency.

Comparing the cost savings figures in Table 20 for the AL projects with the IL project indicates that the AL projects will incur significantly higher additional cost by using the liquid-treated mixtures as compared to the IL project (i.e. -54/-51 vs. -27% cost savings). This matches perfectly with the observations presented above which indicates that using a liquid-treated mix with slightly lower E* and significantly lower rutting resistance (i.e. the AL liquid-treated mix) will result in higher additional cost to the agency then using a mix that has moderately higher E* and significantly lower rutting resistance (i.e. the IL liquid-treated mix).

In the case of the S. Carolina projects, the use of liquid- and lime-treated mixtures showed very close cost savings. On the other hand, the mix design data for the SC mixtures summarized in Figures 25 and 26 show optimum binder contents of 5.28 and 4.71 for the liquid-treated and lime-treated mixtures, respectively. The 0.57% reduction in the optimum binder content for the lime-treated mix will result in an increase of the cost savings associated with the use of lime-treated mixtures. Therefore, the final cost savings of the lime-treated pavements on the two SC projects will be moderately higher than the cost savings realized by the liquid-treated pavements.

In summary, the cost data in Table 20 show that the use of liquid additives in HMA mixtures may result in additional cost of the HMA pavements in the order of 25-50%. On the other hand, the use of lime in HMA mixtures always resulted in cost savings which could be as high as 46% in some cases.

VII. IMPACT OF ADDITIVES ON THE LIFE CYCLE COST OF REHABILITATED HMA PAVEMENTS

As a high percentage of road pavements in the U.S. have already been constructed, their maintenance and rehabilitation becomes a major part of road agencies program. The decision to apply maintenance or rehabilitation activities to a given HMA pavement is guided by the agencies pavement management system. If the HMA pavement is experiencing surface distresses such as bleeding and raveling, it will be subjected to maintenance activities. Most commonly used maintenance activities are: chip seal, slurry seal, and micro-surface. If the HMA pavement is experiencing structural distresses such as rutting and cracking or the combination of both, it will be subjected to rehabilitation activities. One of the most commonly used rehabilitation technique for HMA pavements is to apply HMA overlay over the existing pavement. The objective of the HMA overlay is to increase the structural capacity of the existing pavement and thereby extending the performance life of the pavement. Typically the same HMA mix is used for the construction of new pavement and the overlay. However, the expected long-term performance may differ between new constructions and overlays.

In the case of new constructions, the potential failure modes include: rutting, fatigue cracking, and thermal cracking. In the case of overlays, the potential failure modes depend on the condition of the existing pavement. Typically, HMA pavements that will be subjected to overlays may be experiencing one of the following failure modes: a) rutting alone, b) cracking alone, or c) combination of rutting and cracking. If the existing pavement is not experiencing surface cracking (i.e. category a), then the potential distress modes of the overlay are similar to the new construction. And the life cycle cost analysis already conducted for new constructions (Section VI) also applies for overlays over non-cracked HMA pavements. If the existing pavement is experiencing surface cracking (i.e. category b or c) then the three distress modes for new construction will also be prevalent for the overlay plus reflective cracking. The reflective cracking mode is added to overlays over cracked pavements since the cracks in the exiting HMA pavement are likely to reflect through the HMA overlay.

Figures 76 and 77 show two HMA pavements subjected to overlays. Prior to the overlay, the pavement in Figure 76 was experiencing rutting failure without any surface cracking while the pavement in Figure 77 was experiencing surface cracking only. The performance of the HMA

overlay over the pavement in Figure 76 will be similar to a newly constructed HMA pavement. The performance life of the entire pavement will be controlled by the ability of the HMA overlay to resist rutting, fatigue, and thermal cracking under the combined action of environment and traffic loads. Therefore analyzing the life cycle cost of the pavement in Figure 76 will follow the same procedure followed for newly constructed pavements as presented in Section VI.

As the pavement in Figure 77 is subjected to the combined action of environment and traffic loads, the cracks on the surface of the old HMA layer become stress concentration points. Figure 77 shows the concept of reflective cracking which is likely to occur in the pavement. Temperature changes create horizontal movements on the tip of the cracks in the old HMA layer while traffic loads create vertical movements at the same location as shown in Figure 77. In addition, traffic loads also generate horizontal and vertical movements at the bottom of the HMA overlay. Because of the full bond condition at the interface between the HMA overlay and the old HMA layer, the four components are transferred to the new HMA mix. Superimposing all four components of movements will greatly increase the potential of the cracks to reflect through the HMA overlay. Therefore, the performance life of the entire pavement in Figure77 will be controlled by the ability of the HMA overlay to resist rutting, fatigue, thermal, and reflective cracking.

Based on the above discussions, it is clear that evaluating the life cycle costs of un-treated, liquid-treated, and lime-treated HMA mixtures used in HMA overlays over cracked HMA pavements (i.e. Figure 77) requires an additional analysis. This additional analysis consists of evaluating the resistance of the three mixtures from each aggregate source to reflective cracking.

Currently there are three analytical techniques to evaluate the resistance of HMA mixtures to reflective cracking:

- Virginia Tech Simplified Overlay Design Model
- Rubber Pavements Association (RPA) Overlay Design Model
- The AASHTO MEPDG Model for Reflective Cracking

The Virginia Tech Simplified Overlay Design Model consists of a simple regression equation for predicting the number of cycles in ESALs (W_{t80}) to produce the crack reflection to the pavement surface as a function of: thickness and modulus of HMA overlay, thickness and modulus of existing HMA layer, thickness and modulus of base layer, and modulus of subgrade layer (Elseifi and Al-Qadi, 2003).

The Rubber Pavements Association Overlay Design Model consists of mechanistic relationships and statistically based equations for designing HMA overlays on top of cracked HMA pavements (Sousa et al, 2001).

The reflective cracking models incorporated in the new AASHTO Mechanistic-Empirical Pavement Design Guide are strictly based on empirical observations of field performance data (NCHRP, 2004).

Researchers at the University of Nevada, Reno recently completed an evaluation of the three analytical techniques listed above and concluded that the RPA Overlay Design Model is the most fundamental method for evaluating reflective cracking performance of HMA overlays (Hajj et al., 2008). Therefore, the RPA Overlay Design Model has been used to evaluate the resistance to reflective cracking of the un-treated, liquid-treated, and lime-treated mixtures from all five sources.

The RPA model utilizes the E* property and the fatigue characteristics of the various HMA mixtures to evaluate their long term performance as they are placed over cracked HMA pavements. The final result of the RPA model is the required thickness of the overlay for the design ESALs. The following input were used into the RPA model to design HMA overlays at the same project locations that were used for the design of new HMA pavements (section VI).

- Conditions of the old HMA pavements: moderately cracked (i.e. longitudinal cracks in the wheel-path) and severely cracked (i.e. alligator cracks in the wheel-path).
- An overlay design period of 10 years. The design ESALs were obtained from the traffic data provided for the project locations that were used for the design of new HMA pavements (Tables 14 and 15).
- A design criterion of 10% cracking at the end of the 10 years design life was used for all projects.
- The climatic conditions and the properties of base and subgrade layers were similar to the ones used for the project locations for the design of new HMA pavements (Tables 16 and 17).
- The thickness of base course was similar to the ones obtained for the new designs (Table 19).
- The measured dynamic modulus (E*) and fatigue relationships for the three types of mixtures (i.e. un-treated, liquid-treated, and lime-treated) were used in the design of overlays.
- Overlay designs were conducted for both the un-damaged and moisture-damaged conditions for each project location. The controlling design was identified as the one requiring thicker overlay.
- The life cycle cost analysis used the same cost figures that were used in the analysis of new designs (section VI.6).

Table 21 summarizes the overlay designs for all projects as determined by the RPA model. The required overlay thicknesses were rounded-up to the nearest 0.5 inch except where an overlay thickness less than one inch was required where the thickness was rounded-up to the nearest 0.25 inch. The general trend in the overlay designs indicates the following:

- The severe cracking condition requires thicker overlay than the moderate cracking condition. In some cases the rounding-up of the overlay thickness may not show this trend.
- The un-treated mix on the California and Illinois projects did not result in a practical overlay design. In such cases polymer-modified HMA mixes will be recommended.

Using the same cost figures that were used in the life cycle coast analysis for new construction (section VI.6), the total cost of the HMA for a lane-mile was calculated. However, due to the fact that the California and Illinois projects did result in overlay designs for the un-treated, the cost analysis for these two projects was conducted separately. The total costs of the HMA mix for a lane-mile for each of the pavements shown in Table 21 were calculated and are summarized in Tables 22 and 23. Table 22 summarizes the cost analyses for the projects that included overlay designs for the un-treated mix (i.e. Alabama, S. Carolina, and Texas). Table 22 summarizes the cost analyses for the projects that did not include overlay designs for the un-treated mix (i.e. California and Illinois).

In the case of projects with overlay design for the un-treated mix, the percent saving was calculated as the ratio of the difference between the cost of HMA for a lane-mile of the treated mix and the cost of the un-treated mix divided by the cost of HMA for a lane-mile of the un-treated mix times 100. A negative percent savings in Table 22 indicates that the use of treated HMA mix resulted in a more expensive overlay than the use of the un-treated mix. Negative percent savings were calculated for the two projects in Alabama when the liquid-treated mix was used in the HMA overlay.

In the case of projects without overlay design for the un-treated mix, the percent saving was calculated as the ratio of the difference between the cost of HMA for a lane-mile of the liquid-treated mix and the cost of the lime-treated mix divided by the cost of HMA for a lane-mile of the liquid-treated mix times 100.

In summary, the cost data in Table 22 show that the use of liquid additives in HMA mixtures may result in additional cost of the HMA overlay in the order of 30-45%. On the other hand, the use of lime in HMA mixtures always resulted in cost savings which could be as high as 68% in some cases. The cost data in Table 23 show that the use of lime in HMA mixtures resulted in cost savings of 22-48% relative to use of liquid additive.

VIII. FINDINGS

This research project conducted an extensive evaluation of the impact of additives on the performance of HMA pavements. The three types of HMA mixtures: un-treated, liquid-treated, and lime-treated, were all evaluated in the laboratory using the most advanced mechanical testing and mechanistic analyses. Based on the extensive data generated from this research and the analyses of these data, the following findings are warranted.

- The use of both liquid and lime additives improved the moisture sensitivity of the HMA mixtures as measured by the TSR following AASHTO T283 method. In the case of the California aggregate source, the use of lime reduced the dry tensile strength of the mix. This behavior is not very common in lime-treated mixtures and should be further investigated in a separate research study.
- As the mixtures were subjected to further moisture damage induced through multiple F-T cycling, the un-treated and liquid-treated mixtures had significantly reduced their strength properties (i.e. E*). On the other hand, the lime-treated mixtures maintained higher strength properties for the entire 15 F-T cycles for all five sources.

- Lime either maintained or improved the rutting resistance of the HMA mixtures from all five sources. The impact of liquid on the rutting resistance of the HMA mixtures was source dependent; for the non-moisture sensitive mixtures from Al and IL, the liquid additives reduced their resistance to rutting as compare to the un-treated mixtures.
- Lime either maintained or improved the fatigue resistance of four out of the five sources of HMA mixtures. On the other hand, the impact of the liquid additive on the fatigue resistance of the HMA mixtures was source dependent and very inconsistent. In most cases the liquid additive resulted in a significant change in the slope of the fatigue curve of the mix indicating an un-balanced impact on the low and high strains regions. This behavior contributed to the poor performance of the liquid-treated mixtures in the MEPDG fully mechanistic structural design.
- For some sources, the liquid anti-strip additive showed similar improvements in the fatigue and rutting resistances of the mixtures to the lime additive. However, further use of the rutting and fatigue characteristics of the mixtures in the MEPDG design showed that the lime-treated mixtures significantly out-performed both the un-treated and liquid-treated mixtures from all five sources. This observation is highly critical since it points out the problems associated with using a single performance indicator to make misleading conclusions on the overall performance of HMA pavements. It is highly critical that the impact of an additive be evaluated on multiple performance indicators and coupled with its influence on the strength property of the mix (E*) prior to making any judgment regarding its influence on the performance of the HMA pavement.
- In the case of thermal cracking, both the lime and liquid additives improved the fracture temperature of the HMA mixtures from all five sources. However, the lime-treated mixtures showed significantly higher fracture stresses for all sources. This indicates that if thermal cracking occurs, the lime-treated mixtures will have significantly less cracks per mile than the un-treated and liquid-treated mixtures. Fewer cracks per mile translate directly into lower maintenance cost and time for repair.
- The MEPDG structural designs showed that the use of lime-treated mixtures resulted in thinner pavement structures under all cases. In 3 out of 8 designs (Table 19) the lime-treated HMA layer was maintained at the minimum recommended thickness of 6.00 inches while the required thickness of the liquid-treated HMA layer for the same projects was in the order of 8.00 – 11.00 inches.
- The RPA overlay designs showed that the use of lime-treated mixtures resulted in thinner overlays under all cases. In 3 cases the lime-treated HMA overlay was maintained at the minimum recommended thickness of 0.75 inch.
- The life cycle cost data for new constructions revealed the following:
    - The use of lime additive in HMA mixtures resulted in significant savings, in some cases more than 45%.
    - The use of liquid anti-strip additive in HMA mixtures may result in additional cost, in some cases as high as 50%.
    - The data generated on the four mixtures from Alabama, California, Illinois, and S. Carolina show that the lime is highly compatible with the use of neat asphalt binders and will always results in savings in the order of 13-34%.
    - The data generated on the mixtures from Texas show that the lime is highly compatible with the use of polymer-modified binders and will

result in savings in the order of 40-45% which is significantly higher than the savings that could be realized with the use of the liquid anti-strip.

- This data show that the use of lime additive will always improve the performance of the HMA pavement to a magnitude that always far outweighs its cost. On the other hand, the use of liquid anti-strip additives will not always improve the pavement performance to the magnitude that it will offset its cost.
- The life cycle cost data showed that the use of lime in HMA mixtures that do not require improvement in their mix design TSR will still result in significant savings such as the case of the mixtures from Alabama and Illinois. On the other hand, the use of liquid in HMA mixtures that do not require improvement in their mix design TSR will result in significant cost increases such as the case of the mixtures from Alabama and Illinois.
- The life cycle cost data showed that the use of lime in HMA mixtures that require improvement in their mix design TSR will still result in significantly higher savings such as the case of the mixtures from California, S. Carolina, and Texas. On the other hand, the use of liquid in HMA mixtures that require improvement in their TSR will result in mediocre cost savings such as the case of the mixtures from California, S. Carolina, and Texas.
- Adding the savings realized by the use of lime-treated mixtures from the MEPDG structural designs to the savings realized from the lower thermal cracks per mile resulted in very significant overall cost savings to the highway industry and time savings for the road users.

- The life cycle cost data for rehabilitated pavements revealed the following:
  - The use of lime additive in HMA mixtures resulted in significant savings, in some cases more than 68%.
  - The use of liquid anti-strip additive in HMA mixtures may result in additional cost, in some cases as high as 44%.
  - This data show that the use of lime additive will always improve the performance of the HMA overlay to a magnitude that always far outweighs its cost. On the other hand, the use of liquid anti-strip additives will not always improve the performance of the overlay to the magnitude that it will offset its cost.
  - The life cycle cost data showed that the use of lime in HMA mixtures that do not require improvement in their mix design TSR will still result in significant savings such as the case of the mixtures from Alabama and Illinois. On the other hand, the use of liquid in HMA mixtures that do not require improvement in their mix design TSR will result in significant cost increases such as the case of the mixtures from Alabama.
  - The life cycle cost data showed that the use of lime in HMA mixtures that require improvement in their mix design TSR will still result in significantly higher savings such as the case of the mixtures from S. Carolina and Texas. On the other hand, the use of liquid in HMA mixtures that require improvement in their TSR will result in mediocre cost savings such as the case of the mixtures from S. Carolina and Texas.

- Adding the savings realized by the use of lime-treated mixtures from the RPA overlay designs to the savings realized from the lower thermal cracks per mile resulted in very significant overall cost savings to the highway industry and time savings for the road users.

- In this research, the results of the AASHTO T283 at the mix design stage of all fifteen mixtures were consistent with the mixtures behavior in all of the performance testing and structural designs. For example, the AASHTO T283 mix design data indicated that the S. Carolina un-treated mix has poor resistance to moisture damage (i.e. TSR of 61%). The behavior of the SC un-treated mixture under multiple F-T cycling, in rutting and fatigue, was consistent with the AASHTO T283 recommendation. In addition, the MEPDG was unable to recommend a structural design for the SC un-treated. If one follows the behavior of all the mixtures through the entire evaluation and structural design process, the same conclusion can be drawn for all five sources. This leads to the finding that if the AASHTO T283 test is precisely and carefully followed, its recommendations are highly reliable. However, in order to quantify the impact of the additive on the life cycle cost of the HMA pavement, the TSR value as conducted by the AASHTO T283 is not sufficient and additional testing is needed in terms of multiple F-T cycling and performance characteristics of the mixtures.

REFRENCES

American Association of State Highway and Transportation Officials (AASHTO) 1993. *Guide for the Structural Design of Pavements*. AASHTO, Washington, DC.

Elseifi, M., and Al-Qadi, I. 2003. *A Simplified Overlay Design Model Against Reflective Cracking Utilizing Service Life Prediction*, Paper No. 03-3285 presented at the TRB 82nd Annual Meeting, Washington, D.C.

Hajj, E.Y., Sebaaly P.E., and Loria L. 2008. *Reflective Cracking of Flexible Pavements, Phase II: Review of Analysis Models and Evaluation Tests*, Research Report # 13JF-1, Nevada Department of Transportation, Materials Division, Carson City, Nevada.

National Cooperative Highway Research Program (NCHRP) 2004. *Guide for Mechanistic-Empirical Design of New and Rehabilitated Structures.* Final Report for Project 1-37A, Transportation Research Board, National Research Council, Washington, DC.

Sousa, J., Pais, J., Saim, R., Way, G., and Stubstad, R. 2001. *Development of a Mechanistic Overlay Design Method Based on Reflective Cracking Concepts*, Final Report for Rubber Pavements Association, Consulpav International.

Table 1. Summary of the Mixtures to be evaluated in the Experimental Program.

Mixture Type	**Material Source**				
	Alabama	**California**	**Illinois**	**South Carolina**	**Texas**
Un-treated	X	X	X	X	X
Lime-Treated	X	X	X	X	X
Liquid-Treated	X	X	X	X	X

Table 2. Number of Samples/Tests Evaluated in the Experimental Program.

Property	**Mixture Type**					
	Un-treated		**Lime-treated**		**Liquid-treated**	
	Unaged	**aged**	**unaged**	**aged**	**unaged**	**Aged**
Resistance to Moisture Damage - E* vs. F-T cycles - DMA	3 @ 15 cycles 12	3 @ 15 cycles	3 @ 15 cycles 12	3 @ 15 cycles	3 @ 15 cycles 12	3 @ 15 cycles
Resistance to Permanent Deformation - Dry RLT - RLT after 6 F-T cycles	9 9		9 9		9 9	
Resistance to Fatigue - Dry Flexural Beam - Flexural Beam after 6 F-T cycles - DMA	12	10 10	12	10 10	12	10 10
Resistance to Thermal Cracking - Dry TSRST - TSRST after 6 F-T cycles		3 3		3 3		3 3

E*: Dynamic Modulus, DMA: Dynamic Mechanical Analysis,
RLT: Repeated Load Triaxial, TSRST: Thermal Stress Restrained Specimen Test.

Table 3. Properties of the Mixtures Recommended by the Participating DOTs.

Agency	**Type of Mix**	**Type of Aggregate**	**Asphalt Binder**			**Liquid Anti-strip**	**Lime**
			PG Grade	**Polymer-modified**	**Acid-Modified**		
Alabama	Dense	Limestone	PG67-22	No	No	Polyamine derived	Type "N" normal hydrate 95% CaO
California	Dense	Siliceous	PG64-16	No	No	Polyamine derived	
Illinois	Dense	Dolomite Limestone	PG64-22	No	No	Amidoamine derived	
South Carolina	Dense	Granite	PG64-22	No	No	Amidoamine derived	
Texas	Dense	Gravel	PG76-22	Yes-SBS	No	Amino acid based	

Table 4. Binders PG grading without and with the Addition of Lime and Liquid Anti-strips.

Material Source	Supplier Binder Grade	Additives	Mass Loss, %	Brookfield Viscosity at 135°C, Pa.s	Flash Point, °C	Specific Gravity at 25°C	Limiting Temperature, °C			Superpave PG Grade
							for T_{max}	for T_{int}	for T_{min}	
Alabama	PG67-22	None	0.11	0.556	315	1.035	69.4	17.0	-16.1	PG67-22
		0.5% Liquid Anti-strip*	0.08	0.555	315	1.035	68.0	19.5	-16.6	PG67-22
		20% Lime *	0.12	0.975	322	1.131	74.2	23.1	-14.0	PG70-22
California	PG64-16	None	0.45	0.313	294	1.017	65.3	24.4	-13.6	PG64-22
		0.5% Liquid Anti-strip	0.45	0.301	295	1.018	65.9	25.3	-13.1	PG64-16
		20% Lime	0.38	0.582	301	1.099	69.8	28.1	-10.9	PG64-10
Illinois	PG64-22	None	0.08	0.372	332	1.036	65.6	21.4	-13.5	PG64-22
		0.5% Liquid Anti-strip	0.24	0.361	314	1.036	65.2	22.9	-13.9	PG64-22
		20% Lime	0.15	0.612	340	1.141	70.6	28.3	-11.3	PG70-16
South Carolina	PG64-22	None	0.36	0.578	268	1.034	69.6	19.9	-17.1	PG64-22
		0.5% Liquid Anti-strip	0.43	0.537	262	1.034	69.5	20.5	-17.5	PG64-22
		20% Lime	0.37	1.06	284	1.111	75.3	24.2	-13.6	PG70-22
Texas	PG76-22	None	0.18	1.184	298	1.033	81.3	17.0	-14.7	PG76-22
		0.5% Liquid Anti-strip	0.42	1.489	307	1.032	79.1	18.2	-15.0	PG76-22
		20% Lime	0.15	1.957	332	1.116	86.6	22.4	-12.1	PG82-22

* Percentages of liquid anti-strip and lime are by weight of binder.

Table 5. Impact of Additives on Long-term Aged Properties of Alabama Binder

Property	Aging Time at 60°C	Analysis Temperature, °C	Additives		
			None	0.5% Liquid Anti-strip	20% Lime by Binder
G* sinδ, MPa	100 hour *(1)*	25	1.84	1.98	2.29
	400 hour *(2)*		2.44	3.18	3.04
	800 hour *(3)*		3.74	3.54	4.46
	Aging Index relative to 100 hours	400 hour *[(2)-(1)]/(1)*	32.7%	60.7%	33.0%
		800 hour *[(3)-(1)]/(1)*	103.0%	78.5%	95.1%
S(t), MPa	100	-12	111.0	114.0	124.5
	400		139.0	133.5	151.0
	800		148.1	152.0	166.5
	Aging Index relative to 100 hours	400 hour *[(2)-(1)]/(1)*	25.2%	17.1%	21.3%
		800 hour *[(3)-(1)]/(1)*	33.4%	33.3%	33.7%
m-value	100	-12	0.360	0.365	0.353
	400		0.326	0.336	0.320
	800		0.321	0.315	0.298
	Aging Index relative to 100 hours	400 hour *[(2)-(1)]/(1)*	-9.3%	-7.8%	-9.2%
		800 hour *[(3)-(1)]/(1)*	-10.7%	-13.6%	-15.6%

Table 6. Impact of Additives on Long-term Aged Properties of California Binder

Property	Aging Time at 60°C	Analysis Temperature, °C	Additives		
			None	0.5% Liquid Anti-strip	20% Lime by Binder
G* sinδ, MPa	100 hour *(1)*	25	2.25	2.65	2.78
	400 hour *(2)*		4.64	5.27	4.64
	800 hour *(3)*		6.30	5.48	6.42
	Aging Index relative to 100 hours	400 hour *[(2)-(1)]/(1)*	106.0%	98.9%	66.7%
		800 hour *[(3)-(1)]/(1)*	179.9%	106.8%	130.9%
S(t), MPa	100	-12	239.5	212.0	259.0
	400		257.5	262.5	275.5
	800		327.7	298.0	335.6
	Aging Index relative to 100 hours	400 hour *[(2)-(1)]/(1)*	7.5%	23.8%	6.4%
		800 hour *[(3)-(1)]/(1)*	36.8%	40.6%	29.6%
m-value	100	-12	0.318	0.329	0.321
	400		0.289	0.282	0.292
	800		0.263	0.271	0.260
	Aging Index relative to 100 hours	400 hour *[(2)-(1)]/(1)*	-9.1%	-14.3%	-9.2%
		800 hour *[(3)-(1)]/(1)*	-17.2%	-17.8%	-19.0%

Table 7. Impact of Additives on Long-term Aged Properties of Illinois Binder

Property	Aging Time at 60°C	Analysis Temperature, °C	Additives		
			None	0.5% Liquid Anti-strip	20% Lime by Binder
G* sinδ, MPa	100 hour *(1)*	25	2.80	2.99	3.36
	400 hour *(2)*		5.18	5.30	5.32
	800 hour *(3)*		8.00	7.86	7.74
	Aging Index relative to 100 hours	400 hour *[(2)-(1)]/(1)*	85.1%	77.1%	58.2%
		800 hour *[(3)-(1)]/(1)*	185.6%	162.7%	130.1%
S(t), MPa	100	-12	200.0	182.5	214.6
	400		252.5	232.0	256.5
	800		257.6	270.0	299.5
	Aging Index relative to 100 hours	400 hour *[(2)-(1)]/(1)*	26.3%	27.1%	19.5%
		800 hour *[(3)-(1)]/(1)*	28.8%	47.9%	39.6%
m-value	100	-12	0.332	0.344	0.328
	400		0.294	0.309	0.291
	800		0.280	0.282	0.270
	Aging Index relative to 100 hours	400 hour *[(2)-(1)]/(1)*	-11.5%	-10.0%	-11.1%
		800 hour *[(3)-(1)]/(1)*	-15.7%	-17.9%	-17.7%

Table 8. Impact of Additives on Long-term Aged Properties of South Carolina Binder

Property	Aging Time at 60°C	Analysis Temperature, °C	Additives		
			None	0.5% Liquid Anti-strip	20% Lime by Binder
G* sinδ, MPa	100 hour *(1)*	25	1.82	1.84	2.50
	400 hour *(2)*		3.15	3.46	3.61
	800 hour *(3)*		5.18	5.19	5.67
	Aging Index relative to 100 hours	400 hour *[(2)-(1)]/(1)*	73.2%	87.9%	44.5%
		800 hour *[(3)-(1)]/(1)*	184.6%	181.5%	126.8%
S(t), MPa	100	-12	114.0	118.0	154.5
	400		158.5	158.0	174.3
	800		213.0	202.3	226.2
	Aging Index relative to 100 hours	400 hour *[(2)-(1)]/(1)*	39.0%	33.9%	12.8%
		800 hour *[(3)-(1)]/(1)*	86.8%	71.4%	46.4%
m-value	100	-12	0.397	0.405	0.377
	400		0.356	0.361	0.345
	800		0.315	0.318	0.310
	Aging Index relative to 100 hours	400 hour *[(2)-(1)]/(1)*	-10.3%	-10.9%	-8.5%
		800 hour *[(3)-(1)]/(1)*	-20.7%	-21.5%	-17.8%

Table 9. Impact of Additives on Long-term Aged Properties of Texas Binder

Property	Aging Time at 60°C	Analysis Temperature, °C	Additives		
			None	0.5% Liquid Anti-strip	20% Lime by Binder
G* sinδ, MPa	100 hour *(1)*	25	0.93	0.94	1.07
	400 hour *(2)*		1.20	1.36	1.43
	800 hour *(3)*		1.62	1.64	1.66
	Aging Index relative to 100 hours	400 hour *[(2)-(1)]/(1)*	28.9%	44.1%	33.8%
		800 hour *[(3)-(1)]/(1)*	73.9%	73.8%	54.9%
S(t), MPa	100	-12	110.5	102.7	112.4
	400		133.5	125.5	139.8
	800		144.1	145.2	153.1
	Aging Index relative to 100 hours	400 hour *[(2)-(1)]/(1)*	20.8%	22.2%	24.4%
		800 hour *[(3)-(1)]/(1)*	30.4%	41.3%	36.2%
m-value	100	-12	0.333	0.345	0.328
	400		0.313	0.312	0.309
	800		0.295	0.306	0.278
	Aging Index relative to 100 hours	400 hour *[(2)-(1)]/(1)*	-6.2%	-9.4%	-5.9%
		800 hour *[(3)-(1)]/(1)*	-11.6%	-11.2%	-15.4%

Table 10. Dynamic Modulus of various Mixes at 10 Hz.

State	Mix	Unaged E^*, (ksi) at 104°F			Aged E^* (ksi) at 70°F		
		0 F-T	6 F-T	Ratio E_{6FT}/E_{0FT}	0 F-T	6 F-T	Ratio E_{6FT}/E_{0FT}
Alabama	Un-treated	226	167	74%	1,123	806	72%
	Liquid-treated	218	143	66%	1,113	813	73%
	Lime-treated	261	205	79%	1,236	1,043	84%
California	Un-treated	292	144	49%	1,479	622	42%
	Liquid-treated	407	207	51%	1,649	1,116	68%
	Lime-treated	324	296	91%	1,683	1,717	102%
Illinois	Un-treated	235	154	66%	1,648	826	50%
	Liquid-treated	362	203	56%	1,500	881	59%
	Lime-treated	456	200	44%	1,614	1,328	82%
South Carolina	Un-treated	243	56	23%	754	275	36%
	Liquid-treated	175	160	91%	749	560	75%
	Lime-treated	197	248	126%	1,037	958	92%
Texas	Un-treated	253	99	39%	870	508	58%
	Liquid-treated	207	149	72%	848	603	71%
	Lime-treated	194	174	90%	852	843	99%

Table 11. Generalized Permanent Deformation Models for all Mixtures.

Source	Treatment	Condition	Model*	R^2
Alabama	Un-treated	0 F-T	$\frac{\varepsilon_p}{\varepsilon_r} = 5.653 \times 10^{-8} N^{0.469} T^{3.491}$	0.979
		6 F-T	$\frac{\varepsilon_p}{\varepsilon_r} = 2.101 \times 10^{-9} N^{0.455} T^{4.191}$	0.971
	Liquid-treated	0 F-T	$\frac{\varepsilon_p}{\varepsilon_r} = 2.834 \times 10^{-4} N^{0.464} T^{1.747}$	0.991
		6 F-T	$\frac{\varepsilon_p}{\varepsilon_r} = 1.179 \times 10^{-8} N^{0.399} T^{3.955}$	0.969
	Lime-treated	0 F-T	$\frac{\varepsilon_p}{\varepsilon_r} = 6.398 \times 10^{-10} N^{0.408} T^{4.519}$	0.985
		6 F-T	$\frac{\varepsilon_p}{\varepsilon_r} = 8.175 \times 10^{-9} N^{0.412} T^{4.054}$	0.968
California	Un-treated	0 F-T	$\frac{\varepsilon_p}{\varepsilon_r} = 1.134 \times 10^{-8} N^{0.421} T^{3.914}$	0.915
		6 F-T	$\frac{\varepsilon_p}{\varepsilon_r} = 1.53 \times 10^{-7} N^{0.409} T^{3.413}$	0.969
	Liquid-treated	0 F-T	$\frac{\varepsilon_p}{\varepsilon_r} = 5.833 \times 10^{-11} N^{0.449} T^{4.950}$	0.997
		6 F-T	$\frac{\varepsilon_p}{\varepsilon_r} = 1.481 \times 10^{-6} N^{0.464} T^{2.851}$	0.993
	Lime-treated	0 F-T	$\frac{\varepsilon_p}{\varepsilon_r} = 1.178 \times 10^{-7} N^{0.401} T^{3.422}$	0.995
		6 F-T	$\frac{\varepsilon_p}{\varepsilon_r} = 9.699 \times 10^{-8} N^{0.503} T^{3.366}$	0.991
Illinois	Un-treated	0 F-T	$\frac{\varepsilon_p}{\varepsilon_r} = 3.148 \times 10^{-6} N^{0.464} T^{2.659}$	0.998
		6 F-T	$\frac{\varepsilon_p}{\varepsilon_r} = 8.913 \times 10^{-12} N^{0.390} T^{5.470}$	0.997
	Liquid-treated	0 F-T	$\frac{\varepsilon_p}{\varepsilon_r} = 2.355 \times 10^{-5} N^{0.493} T^{2.298}$	0.982
		6 F-T	$\frac{\varepsilon_p}{\varepsilon_r} = 1.849 \times 10^{-9} N^{0.483} T^{4.172}$	0.992
	Lime-treated	0 F-T	$\frac{\varepsilon_p}{\varepsilon_r} = 1.780 \times 10^{-10} N^{0.458} T^{4.793}$	0.948
		6 F-T	$\frac{\varepsilon_p}{\varepsilon_r} = 8.853 \times 10^{-9} N^{0.443} T^{3.927}$	0.949
South Carolina	Un-treated	0 F-T	$\frac{\varepsilon_p}{\varepsilon_r} = 2.074 \times 10^{-9} N^{0.400} T^{4.256}$	0.989
		6 F-T	$\frac{\varepsilon_p}{\varepsilon_r} = 5.524 \times 10^{-6} N^{0.362} T^{2.630}$	0.977
	Liquid-treated	0 F-T	$\frac{\varepsilon_p}{\varepsilon_r} = 1.314 \times 10^{-6} N^{0.412} T^{2.931}$	0.985
		6 F-T	$\frac{\varepsilon_p}{\varepsilon_r} = 8.904 \times 10^{-5} N^{0.407} T^{1.966}$	0.997
	Lime-treated	0 F-T	$\frac{\varepsilon_p}{\varepsilon_r} = 4.351 \times 10^{-6} N^{0.431} T^{2.577}$	0.992
		6 F-T	$\frac{\varepsilon_p}{\varepsilon_r} = 6.287 \times 10^{-6} N^{0.358} T^{2.572}$	0.965
Texas	Un-treated	0 F-T	$\frac{\varepsilon_p}{\varepsilon_r} = 5.871 \times 10^{-7} N^{0.392} T^{2.975}$	0.983
		6 F-T	$\frac{\varepsilon_p}{\varepsilon_r} = 7.296 \times 10^{-8} N^{0.413} T^{3.418}$	0.987
	Liquid-treated	0 F-T	$\frac{\varepsilon_p}{\varepsilon_r} = 3.295 \times 10^{-6} N^{0.395} T^{2.622}$	0.994
		6 F-T	$\frac{\varepsilon_p}{\varepsilon_r} = 2.554 \times 10^{-5} N^{0.363} T^{2.242}$	0.989
	Lime-treated	0 F-T	$\frac{\varepsilon_p}{\varepsilon_r} = 1.653 \times 10^{-5} N^{0.341} T^{2.304}$	0.940
		6 F-T	$\frac{\varepsilon_p}{\varepsilon_r} = 1.036 \times 10^{-8} N^{0.368} T^{3.803}$	0.981

* ε_p = Axial permanent strain in in/in, ε_r = Axial resilient strain in in/in, N = Number of load repetitions, T = Temperature in °F.

Table 12. Generalized Fatigue Models for all Mixtures.

Source	Treatment	Condition	Model*	R^2
Alabama	Un-treated	0 F-T	$N_f = 1.448 \times 10^7 \left(\frac{1}{\varepsilon}\right)^{3.700} \left(\frac{1}{E}\right)^{2.499}$	0.964
		6 F-T	$N_f = 1.948 \times 10^5 \left(\frac{1}{\varepsilon}\right)^{4.851} \left(\frac{1}{E}\right)^{2.944}$	0.949
	Liquid-treated	0 F-T	$N_f = 1.386 \times 10^4 \left(\frac{1}{\varepsilon}\right)^{4.878} \left(\frac{1}{E}\right)^{2.648}$	0.955
		6 F-T	$N_f = 2.421 \times 10^7 \left(\frac{1}{\varepsilon}\right)^{2.960} \left(\frac{1}{E}\right)^{2.190}$	0.979
	Lime-treated	0 F-T	$N_f = 2.328 \times 10^{11} \left(\frac{1}{\varepsilon}\right)^{4.542} \left(\frac{1}{E}\right)^{3.638}$	0.887
		6 F-T	$N_f = 9.187 \times 10^1 \left(\frac{1}{\varepsilon}\right)^{5.399} \left(\frac{1}{E}\right)^{2.636}$	0.964
California	Un-treated	0 F-T	$N_f = 6.087 \times 10^{12} \left(\frac{1}{\varepsilon}\right)^{3.702} \left(\frac{1}{E}\right)^{3.460}$	0.872
		6 F-T	$N_f = 1.893 \times 10^{18} \left(\frac{1}{\varepsilon}\right)^{5.146} \left(\frac{1}{E}\right)^{5.551}$	0.844
	Liquid-treated	0 F-T	$N_f = 2.635 \times 10^8 \left(\frac{1}{\varepsilon}\right)^{4.630} \left(\frac{1}{E}\right)^{3.238}$	0.972
		6 F-T	$N_f = 2.043 \times 10^7 \left(\frac{1}{\varepsilon}\right)^{3.654} \left(\frac{1}{E}\right)^{2.590}$	0.810
	Lime-treated	0 F-T	$N_f = 5.795 \times 10^{10} \left(\frac{1}{\varepsilon}\right)^{5.897} \left(\frac{1}{E}\right)^{4.280}$	0.942
		6 F-T	$N_f = 1.342 \times 10^{12} \left(\frac{1}{\varepsilon}\right)^{5.502} \left(\frac{1}{E}\right)^{4.308}$	0.885
Illinois	Un-treated	0 F-T	$N_f = 7.917 \times 10^{16} \left(\frac{1}{\varepsilon}\right)^{2.748} \left(\frac{1}{E}\right)^{3.537}$	0.828
		6 F-T	$N_f = 5.975 \times 10^5 \left(\frac{1}{\varepsilon}\right)^{5.393} \left(\frac{1}{E}\right)^{3.405}$	0.953
	Liquid-treated	0 F-T	$N_f = 2.378 \times 10^{13} \left(\frac{1}{\varepsilon}\right)^{4.732} \left(\frac{1}{E}\right)^{3.985}$	0.727
		6 F-T	$N_f = 4.250 \times 10^5 \left(\frac{1}{\varepsilon}\right)^{5.519} \left(\frac{1}{E}\right)^{3.402}$	0.935
	Lime-treated	0 F-T	$N_f = 8.291 \times 10^{26} \left(\frac{1}{\varepsilon}\right)^{5.238} \left(\frac{1}{E}\right)^{6.459}$	0.900
		6 F-T	$N_f = 6.925 \times 10^{-2} \left(\frac{1}{\varepsilon}\right)^{5.165} \left(\frac{1}{E}\right)^{1.946}$	0.974
South Carolina	Un-treated	0 F-T	$N_f = 1.082 \times 10^9 \left(\frac{1}{\varepsilon}\right)^{5.624} \left(\frac{1}{E}\right)^{3.930}$	0.793
		6 F-T	$N_f = 1.020 \times 10^{-7} \left(\frac{1}{\varepsilon}\right)^{10.934} \left(\frac{1}{E}\right)^{4.606}$	0.924
	Liquid-treated	0 F-T	$N_f = 3.168 \times 10^7 \left(\frac{1}{\varepsilon}\right)^{5.418} \left(\frac{1}{E}\right)^{3.549}$	0.923
		6 F-T	$N_f = 1.325 \times 10^5 \left(\frac{1}{\varepsilon}\right)^{4.270} \left(\frac{1}{E}\right)^{2.598}$	0.971
	Lime-treated	0 F-T	$N_f = 1.424 \times 10^1 \left(\frac{1}{\varepsilon}\right)^{5.072} \left(\frac{1}{E}\right)^{2.292}$	0.890
		6 F-T	$N_f = 1.224 \times 10^7 \left(\frac{1}{\varepsilon}\right)^{4.115} \left(\frac{1}{E}\right)^{2.784}$	0.926
Texas	Un-treated	0 F-T	$N_f = 3.968 \times 10^9 \left(\frac{1}{\varepsilon}\right)^{4.642} \left(\frac{1}{E}\right)^{3.327}$	0.993
		6 F-T	$N_f = 4.163 \times 10^{16} \left(\frac{1}{\varepsilon}\right)^{5.960} \left(\frac{1}{E}\right)^{5.585}$	0.911
	Liquid-treated	0 F-T	$N_f = 1.080 \times 10^{-1} \left(\frac{1}{\varepsilon}\right)^{5.260} \left(\frac{1}{E}\right)^{1.884}$	0.984
		6 F-T	$N_f = 7.972 \times 10^8 \left(\frac{1}{\varepsilon}\right)^{4.443} \left(\frac{1}{E}\right)^{3.214}$	0.938
	Lime-treated	0 F-T	$N_f = 9.210 \times 10^7 \left(\frac{1}{\varepsilon}\right)^{5.009} \left(\frac{1}{E}\right)^{3.283}$	0.863
		6 F-T	$N_f = 3.993 \times 10^6 \left(\frac{1}{\varepsilon}\right)^{5.257} \left(\frac{1}{E}\right)^{3.203}$	0.933

* N_f = Number of cycles to failure, ε = Tensile strain at the bottom of the HMA layer (in/in), E = Stiffness of HMA (psi).

Table 13. Thermal Cracking Characteristics of the Various Mixtures.

State	Mix	0 F-T		6 F-T	
		Fracture stress (psi)	Fracture temperature (°C)	Fracture stress (psi)	Fracture temperature (°C)
Alabama	Un-treated	368	-24	333	-24
	Liquid-treated	345	-26	304	-29
	Lime-treated	406	-24	424	-27
California	Un-treated	303	-10	210	-11
	Liquid-treated	329	-11	300	-17
	Lime-treated	404	-13	381	-13
Illinois	Un-treated	375	-13	232	-16
	Liquid-treated	275	-14	251	-16
	Lime-treated	426	-18	377	-16
South Carolina	Un-treated	292	-19	126	-25
	Liquid-treated	268	-17	229	-28
	Lime-treated	311	-17	198	-15
Texas	Un-treated	287	-19	210	-20
	Liquid-treated	277	-19	235	-20
	Lime-treated	353	-17	377	-18

Table 14. General Traffic Information.

Traffic Parameter	Alabama		California		Illinois	South Carolina		Texas	
	US31	SR7	PLA80	PLA28	Chicago	SC12	SC161	FM396	SH30
ADT*	28760	30300	41500	12000	35000	6200	29500	4000	10700
Total percent truck traffic (%)	5.0	3.0	14.45	3.0	3.0	35.0	8.0	21.8	7.7
ADTT[+]	1438	909	6000	360	1050	2170	2360	872	824
Growth factor (%)[#]	1.0	2.0	3.0	2.0	2.0	7.0	3.6	9.5	2.0
Lanes in design direction	2	2	2	1	2	2	2	2	2
Trucks in design direction (%)	50	50	50	50	50	50	50	50	50
Trucks in design lane (%)	80	70	70	100	80	60	90	90	90
Operational speed (mph)	50	50	60	50	40	35	50	55	60

* Initial two-way average daily traffic

[+] Initial two-way average daily truck traffic

[#] Annual truck volume compounded growth factor

Table 15. ADTT Distributions by Vehicle Class.

FHWA Vehicle Class	ADTT distributions by vehicle class in percentage								
	Alabama		California		Illinois	South Carolina		Texas	
	US31	SR7	PLA80	PLA28	Chicago	SC12	SC161	FM396	SH30
Class 4	2.4	2.4	1.3	2.8	2.8	3.0	2.0	1.8	1.8
Class 5	23.7	23.7	8.5	31.0	31.0	12.0	40.0	24.6	24.6
Class 6	6.7	6.7	2.8	7.3	7.3	3.0	7.0	7.6	7.6
Class 7	2.4	2.4	0.3	0.8	0.8	0.0	0.0	0.5	0.5
Class 8	9.1	9.1	7.6	9.3	9.3	4.0	6.0	5.0	5.0
Class 9	51.2	51.2	74.0	44.8	44.8	72.0	41.0	31.3	31.3
Class 10	1.7	1.7	1.2	2.3	2.3	2.5	1.0	9.8	9.8
Class 11	2.2	2.2	3.4	1.0	1.0	2.5	1.0	0.8	0.8
Class 12	0.2	0.2	0.6	0.4	0.4	0.5	1.0	3.3	3.3
Class 13	0.4	0.4	0.3	0.3	0.3	0.5	1.0	15.3	15.3
Total	100	100	100	100	100	100	100	100	100

Table 16. Locations of Climatic Stations.

State	Project ID	Climate Station Used in Analysis			
		Station	Elevation	Lat./Long.	Location
Alabama	US31	Birmingham, AL	639 ft	33.34/-86.45	Birmingham Intl Airport
	SR7	Birmingham, AL	639 ft	33.34/-86.45	Birmingham Intl Airport
California	PLA80	Sacramento, CA	41 ft	38.31/-121.29	Sacramento Executive Arpt
	PLA28	S. Lake Tahoe, CA	6316 ft	38.53/-119	Lake Tahoe Airport
Illinois	Chicago	Chicago, IL	658 ft	41.59/-87.55	O'Hare International Airport
South Carolina	SC12	Greenville, SC	1037 ft	34.51/-82.21	Greenville Downtown Arpt
	SC161	Charleston, SC	48 ft	32.54/-80.02	Charleston AFB/Intl Arpt
Texas	FM396	McAllen, TX	128 ft	26.11/-98.14	McAllen Miller Intl Airport
		Harlingen, TX	37 ft	26.14/-97.39	Valley International Airport
	SH30	Huntsville, TX	345 ft	30.45/-95.35	Huntsville Municipal Arpt

Table 17. Assigned Subgrade Resilient Modulus for the various Projects.

Subgrade	Alabama		California		Illinois	South Carolina		Texas	
	US31	SR7	PLA80	PLA28	Chicago	SC12	SC161	FM396	SH30
Type	A-7-5	A-7-5	A-7-5	A-7-5	A-7-5	A-7-5	A-2-4	A-7-6	A-6
Resilient Modulus*	13000	13000	13000	13000	8900	13000	20000	11500	14500

* Representative modulus at optimum density and moisture content

Table 18. MEPDG New Construction Designs for all Project Locations.

State	Location	Condition	HMA Mixture	Structural Design		Control Distress
				HMA (in)	Base (in)	
Alabama	US31 (4.6×10^6 ESALs, 1438 ADTT)	un-damaged (0F-T)	un-treated	8.50	11.00	Rutting
			liquid-treated	13.00	11.00	Rutting
			lime-treated	6.00	11.00	Neither
		moisture-damaged (6F-T)	un-treated	7.50	11.00	Rutting
			liquid-treated	11.00	11.00	Fatigue
			lime-treated	6.50	11.00	Rutting
	SR7 (2.8×10^6 ESALs, 909 ADTT)	un-damaged (0F-T)	un-treated	7.00	9.00	Rutting
			liquid-treated	--	9.00	No design[1]
			lime-treated	6.00	9.00	Neither
		moisture-damaged (6F-T)	un-treated	6.00	9.00	Neither
			liquid-treated	10.50	9.00	Rutting
			lime-treated	6.00	9.00	Rutting
California	PLA80 (31×10^6 ESALs, 6000 ADTT)	un-damaged (0F-T)	un-treated	10.5	12.0	Fatigue/Rutting
			liquid-treated	7.00	12.0	Fatigue/Rutting
			lime-treated	6.00	12.0	Neither
		moisture-damaged (6F-T)	un-treated	13.50	12.0	Rutting[2]
			liquid-treated	14.00	12.0	Rutting[2]
			lime-treated	14.00	12.0	Rutting[2]
	PLA28 (1.6×10^6 ESALs, 360 ADTT)	un-damaged (0F-T)	un-treated	7.00	8.00	Fatigue
			liquid-treated	6.00	8.00	Neither
			lime-treated	6.00	8.00	Neither
		moisture-damaged (6F-T)	un-treated	9.50	8.00	Fatigue
			liquid-treated	8.00	8.00	Fatigue
			lime-treated	6.00	8.00	Neither
Illinois	Chicago (3.7×10^6 ESALs, 1050 ADTT)	un-damaged (0F-T)	un-treated	8.50	10.00	Rutting/Fatigue
			liquid-treated	10.75	10.00	Rutting
			lime-treated	6.00	10.00	Neither
		moisture-damaged (6F-T)	un-treated	6.00	10.00	Fatigue
			liquid-treated	6.00	10.00	Neither
			lime-treated	6.00	10.00	Rutting
S. Carolina	SC12 (9.6×10^6 ESALs, 2170 ADTT)	un-damaged (0F-T)	un-treated	9.00	12.00	Rutting
			liquid-treated	13.75	12.00	Rutting
			lime-treated	13.00	12.00	Rutting
		moisture-damaged (6F-T)	un-treated	--	12.00	No-design[1]
			liquid-treated	13.00	12.00	Rutting
			lime-treated	6.00	12.00	Neither
	SC161 (7.1×10^6 ESALs, 2360 ADTT)	un-damaged (0F-T)	un-treated	6.50	10.00	Rutting
			liquid-treated	12.75	10.00	Rutting
			lime-treated	12.00	10.00	Rutting
		moisture-damaged (6F-T)	un-treated	15.50	10.00	Rutting
			liquid-treated	12.00	10.00	Rutting
			lime-treated	6.00	10.00	Neither

[1] a structural design could not be achieved. See discussion in text.
[2] does not represent a 20 year design. See discussion in text.

Table 18. MEPDG New Construction Designs for all Project Locations (Continued).

State	Location	Condition	HMA Mixture	Structural Design		Control Distress
				HMA (in)	Base (in)	
Texas	FM396 (7.8×10^6 ESALs, 872 ADTT)	un-damaged (0F-T)	un-treated	7.00	11.00	Fatigue
			liquid-treated	9.00	11.00	Rutting
			lime-treated	7.00	11.00	Fatigue
		moisture-damaged (6F-T)	un-treated	13.75	11.00	Rutting
			liquid-treated	9.25	11.00	Fatigue/Rutting
			lime-treated	6.25	11.00	Fatigue
	SH30 (3.3×10^6 ESALs, 824 ADTT)	un-damaged (0F-T)	un-treated	7.50	9.00	Fatigue
			liquid-treated	6.00	9.00	Neither
			lime-treated	7.25	9.00	Fatigue/Rutting
		moisture-damaged (6F-T)	un-treated	13.50	9.00	Rutting
			liquid-treated	9.75	9.00	Fatigue/Rutting
			lime-treated	7.00	9.00	Fatigue/Rutting

Table 19. MEPDG 20 Years New Construction Designs for all Project Locations.

State	Location	HMA Mixture	Structural Design		Control Condition/ Control Distress
			HMA (in)	Base (in)	
Alabama	US31 (4.6×10^6 ESALs, 1438 ADTT)	un-treated	8.50	11.00	un-damaged/rutting
		liquid-treated	13.00	11.00	un-damaged/rutting
		lime-treated	6.50	11.00	moisture-damaged/rutting
	SR7 (2.8×10^6 ESALs, 910 ADTT)	un-treated	7.00	9.00	un-damaged/rutting
		liquid-treated	10.50	9.00	moisture-damaged/rutting
		lime-treated	6.00	9.00	moisture-damaged/rutting
California	PLA28 (1.6×10^6 ESALs, 360 ADTT)	un-treated	9.50	8.00	moisture-damaged/fatigue
		liquid-treated	8.00	8.00	moisture-damaged/fatigue
		lime-treated	6.00	8.00	neither/neither
Illinois	Chicago (3.7×10^6 ESALs, 1050 ADTT)	un-treated	8.50	10.00	un-damaged/rutting & fatigue
		liquid-treated	10.75	10.00	un-damaged/rutting
		lime-treated	6.00	10.00	Moisture-damaged/rutting
S. Carolina	SC12 (9.6×10^6 ESALs, 2170 ADTT)	un-treated	*	12.00	moisture-damaged/rutting
		liquid-treated	13.75	12.00	un-damaged/rutting
		lime-treated	13.00	12.00	un-damaged/rutting
	SC161 (7.1×10^6 ESALs, 2360 ADTT)	un-treated	15.50	10.00	moisture-damaged/rutting
		liquid-treated	12.75	10.00	un-damaged/rutting
		lime-treated	12.00	10.00	un-damaged/rutting
Texas	FM396 (7.8×10^6 ESALs, 872 ADTT)	un-treated	13.75	11.00	moisture-damaged/rutting
		liquid-treated	9.25	11.00	moisture-damaged/rutting & fatigue
		lime-treated	7.00	11.00	un-damaged/rutting & fatigue
	SH30 (3.3×10^6 ESALs, 824 ADTT)	un-treated	13.50	9.00	moisture-damaged/rutting
		liquid-treated	9.75	9.00	moisture-damaged/rutting & fatigue
		lime-treated	7.25	9.00	un-damaged/rutting & fatigue

* a structural design could not be achieved.

Table 20. HMA Cost per Lane-mile and Percent Savings for New Constructions.

State	Location	HMA Mixture	HMA Thickness (in)	Total Cost of HMA ($ / lane-mile)	Percent Saving
Alabama	US31 (4.6×10^6 ESALs, 1438 ADTT)	un-treated	8.50	306,381	
		liquid-treated	13.00	472,243	-54%
		lime-treated	6.50	246,646	19%
	SR7 (2.8×10^6 ESALs, 910 ADTT)	un-treated	7.00	252,314	
		liquid-treated	10.50[1]	381,427	-51
		lime-treated	6.00	227,674	10%
California	PLA28 (1.6×10^6 ESALs, 360 ADTT)	un-treated	9.50	342,426	
		liquid-treated	8.00	290,611	15%
		lime-treated	6.00	227,674	34%
Illinois	Chicago (3.7×10^6 ESALs, 1050 ADTT)	un-treated	8.50	306,381	
		liquid-treated	10.75	390,509	-27%
		lime-treated	6.00	227,674	26%
S. Carolina	SC12 (9.6×10^6 ESALs, 2170 ADTT)	un-treated	16.00[2]	576,717	
		liquid-treated	13.75	499,488	13%
		lime-treated	13.00	493,293	14%
	SC161 (7.1×10^6 ESALs, 2360 ADTT)	un-treated	15.50	558,694	
		liquid-treated	12.75	463,162	17%
		lime-treated	12.00	455,347	18%
Texas	FM396 (7.8×10^6 ESALs, 872 ADTT)	un-treated	13.75	495,616	
		liquid-treated	9.25	336,019	32%
		lime-treated	7.00	265,619	46%
	SH30 (3.3×10^6 ESALs, 824 ADTT)	un-treated	13.50	486,605	
		liquid-treated	9.75	354,182	27%
		lime-treated	7.25	275,106	43%

[1] the moisture-damaged design was used due to unfeasible design at the un-damaged condition
[2] maximum HMA thickness of 16.00" was used due to un-feasible design.

Table 21. Rubber Pavement Association 10 Years Overlay Designs for all Project Locations.

State	Location	Cracking Condition of existing HMA	Mixture Type	Overlay Thickness (in)	Control Condition
Alabama	US31 ($2.2x10^6$ ESALs, 1438 ADTT)	Moderate	un-treated	3.50	Moisture-damaged
			liquid-treated	5.00	Moisture-damaged
			lime-treated	1.50	Moisture-damaged
		Severe	un-treated	4.00	Moisture-damaged
			liquid-treated	5.50	Moisture-damaged
			lime-treated	2.00	Moisture-damaged
	SR7 ($1.3x10^6$ ESALs, 910 ADTT)	Moderate	un-treated	3.00	Moisture-damaged
			liquid-treated	4.00	Moisture-damaged
			lime-treated	1.50	Moisture-damaged
		Severe	un-treated	3.50	Moisture-damaged
			liquid-treated	4.50	Moisture-damaged
			lime-treated	1.50	Moisture-damaged
California	PLA28 ($0.7x10^6$ ESALs, 360 ADTT)	Moderate	un-treated	---*	Moisture-damaged
			liquid-treated	2.00	Moisture-damaged
			lime-treated	1.50	Un-damaged
		Severe	un-treated	---*	Moisture-damaged
			liquid-treated	2.50	Moisture-damaged
			lime-treated	1.50	Un-damaged
Illinois	Chicago ($1.7x10^6$ESALs, 1050 ADTT)	Moderate	un-treated	---*	Moisture-damaged
			liquid-treated	3.00	Moisture-damaged
			lime-treated	1.50	Moisture-damaged
		Severe	un-treated	---*	Moisture-damaged
			liquid-treated	4.00	Moisture-damaged
			lime-treated	1.50	Moisture-damaged
S. Carolina	SC12 ($3.3x10^6$ ESALs, 2170 ADTT)	Moderate	un-treated	6.00	Moisture-damaged
			liquid-treated	4.50	Moisture-damaged
			lime-treated	2.50	Moisture-damaged
		Severe	un-treated	7.00	Moisture-damaged
			liquid-treated	5.00	Moisture-damaged
			lime-treated	3.00	Moisture-damaged
	SC161 ($2.9x10^6$ ESALs, 2360 ADTT)	Moderate	un-treated	5.00	Moisture-damaged
			liquid-treated	3.50	Moisture-damaged
			lime-treated	2.00	Moisture-damaged
		Severe	un-treated	5.50	Moisture-damaged
			liquid-treated	4.00	Moisture-damaged
			lime-treated	2.50	Moisture-damaged
Texas	FM396 ($2.2x10^6$ ESALs, 872 ADTT)	Moderate	un-treated	2.00	Moisture-damaged
			liquid-treated	1.00	Moisture-damaged
			lime-treated	0.75	Moisture-damaged
		Severe	un-treated	2.00	Moisture-damaged
			liquid-treated	1.50	Moisture-damaged
			lime-treated	1.00	Moisture-damaged
	SH30 ($1.5x10^6$ESALs, 824 ADTT)	Moderate	un-treated	4.00	Moisture-damaged
			liquid-treated	2.50	Moisture-damaged
			lime-treated	1.50	Moisture-damaged
		Severe	un-treated	5.00	Moisture-damaged
			liquid-treated	3.00	Moisture-damaged
			lime-treated	1.50	Moisture-damaged

*Overlay design for the un-treated mix was un-achievable.

Table 22. HMA Cost per Lane-mile and Percent Savings for Overlays with Un-treaded Designs.

State	Location	Cracking Condition of existing HMA	Mixture Type	Overlay Thickness (in)	Total Cost of HMA ($/lane-mile)	Percent Savings
Alabama	US31 ($2.2x10^6$ ESALs, 1438 ADTT)	Moderate	un-treated	3.50	126,157	
			liquid-treated	5.00	181,632	-44%
			lime-treated	1.50	56,918	55%
		Severe	un-treated	4.00	144,179	
			liquid-treated	5.50	199,795	-39%
			lime-treated	2.00	75,891	47%
	SR7 ($1.3x10^6$ ESALs, 910 ADTT)	Moderate	un-treated	3.00	108,134	
			liquid-treated	4.00	145,306	-34%
			lime-treated	1.50	56,918	47%
		Severe	un-treated	3.50	126,157	
			liquid-treated	4.50	163,469	-30%
			lime-treated	1.50	56,918	55%
S. Carolina	SC12 ($3.3x10^6$ ESALs, 2170 ADTT)	Moderate	un-treated	6.00	216,269	
			liquid-treated	4.50	163,469	24%
			lime-treated	2.50	94,864	56%
		Severe	un-treated	7.00	252,314	
			liquid-treated	5.00	181,632	28%
			lime-treated	3.00	113,837	55%
	SC161 ($2.9x10^6$ ESALs, 2360 ADTT)	Moderate	un-treated	5.00	180,224	
			liquid-treated	3.50	127,142	29%
			lime-treated	2.00	75,891	58%
		Severe	un-treated	5.50	198,246	
			liquid-treated	4.00	15,306	27%
			lime-treated	2.50	94,864	52%
Texas	FM396 ($2.2x10^6$ ESALs, 872 ADTT)	Moderate	un-treated	2.00	72,090	
			liquid-treated	1.00	36,326	50%
			lime-treated	0.75	28,459	61%
		Severe	un-treated	2.00	72,090	
			liquid-treated	1.50	54,490	24%
			lime-treated	1.00	37,946	47%
	SH30 ($1.5x10^6$ESALs, 824 ADTT)	Moderate	un-treated	4.00	144,179	
			liquid-treated	2.50	90,816	37%
			lime-treated	1.50	56,918	61%
		Severe	un-treated	5.00	180,224	
			liquid-treated	3.00	108,979	40%
			lime-treated	1.50	56,918	68%

Table 23. HMA Cost per Lane-mile and Percent Savings for Overlays without Un-treated Designs.

State	Location	Cracking Condition of existing HMA	Mixture Type	Overlay Thickness (in)	Total Cost of HMA ($/lane-mile)	Percent Savings
California	PLA28 ($0.7x10^6$ ESALs, 360 ADTT)	Moderate	liquid-treated	2.00	72,653	
			lime-treated	1.50	56,918	22%
		Severe	liquid-treated	2.50	90,816	
			lime-treated	1.50	56,918	37%
Illinois	Chicago ($1.7x10^6$ESALs, 1050 ADTT)	Moderate	liquid-treated	3.00	108,979	
			lime-treated	1.50	56,918	48%
		Severe	liquid-treated	4.00	145,306	
			lime-treated	2.00	75,891	48%

Dynamic Modulus Set-Up **Applied Stress & Measured Strain**

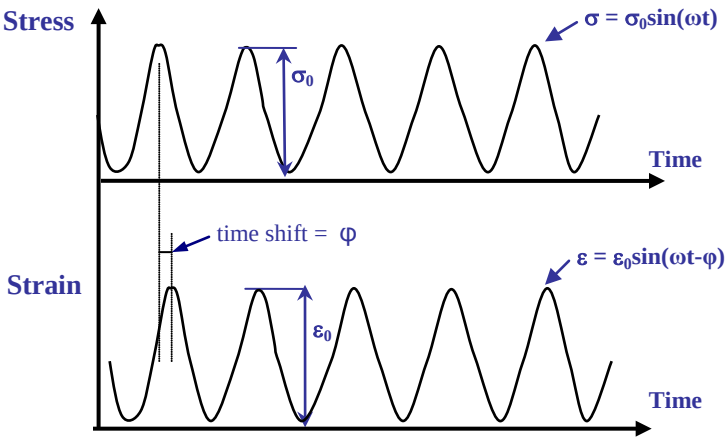

Dynamic Modulus $|E^*| = \frac{\sigma_0}{\varepsilon_0}$

Typical E* Master Curve

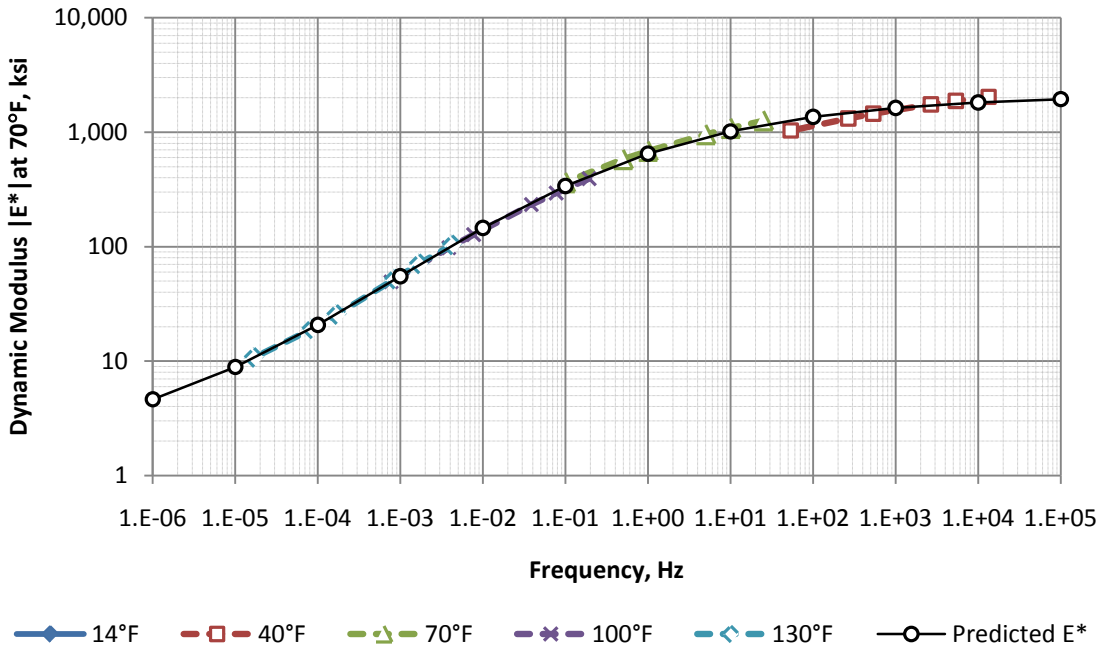

Figure 1. Components of the Dynamic Modulus Test and a Typical E* Master Curve for an HMA mix.

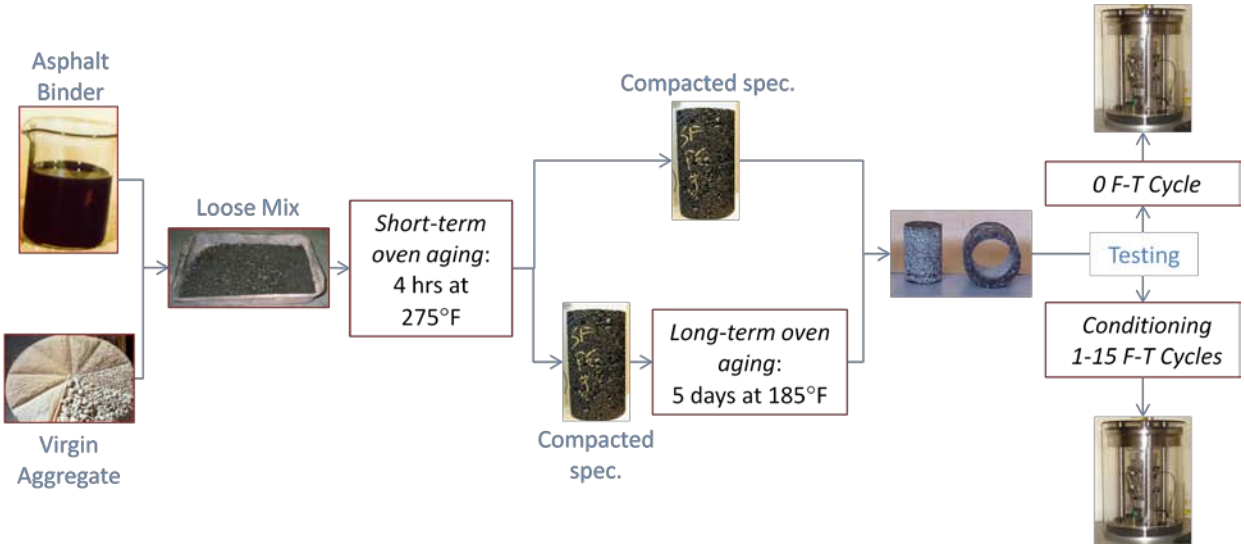

Figure 2. Dynamic Modulus Sample Preparation for Unaged and Aged Mixes.

Repeated Load Triaxial Set-Up **Loading and Response**

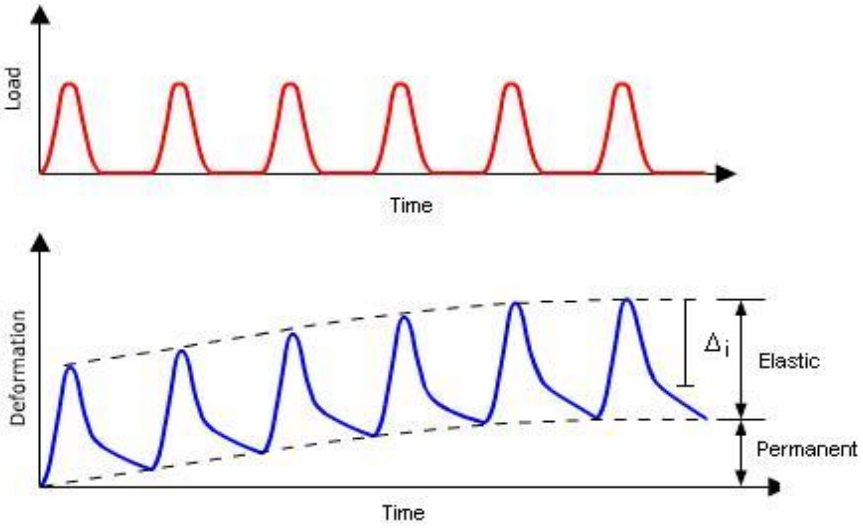

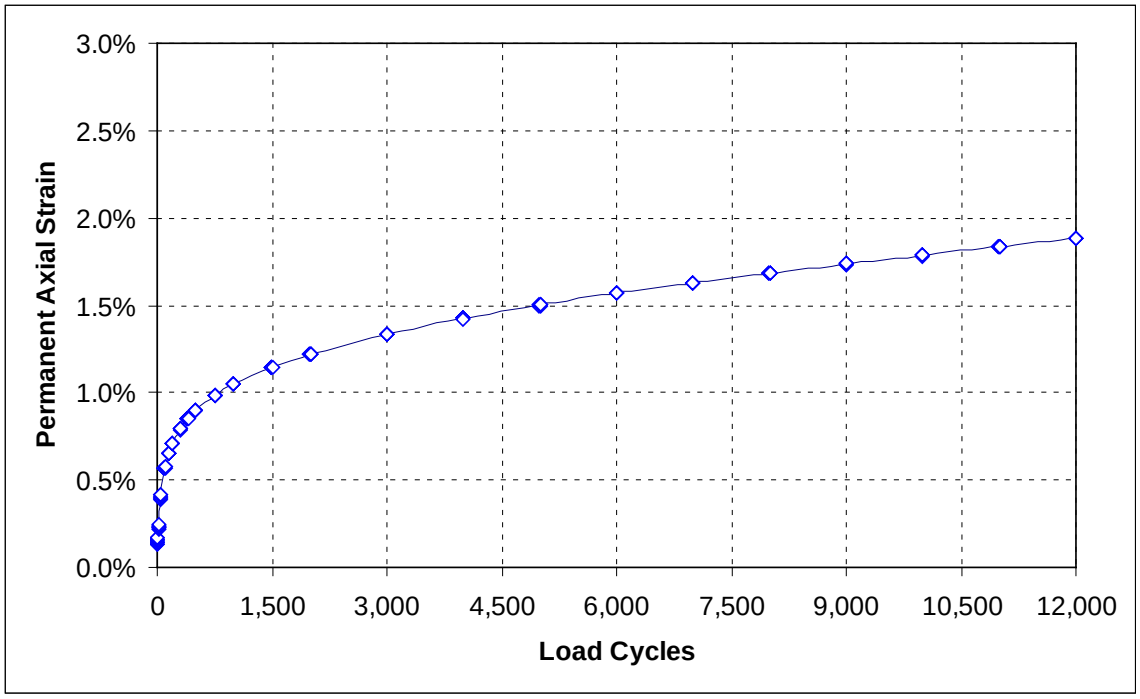

Figure 3. Components of the Repeated Load Triaxial Test and a Typical Permanent Deformation Curve for an HMA Mix.

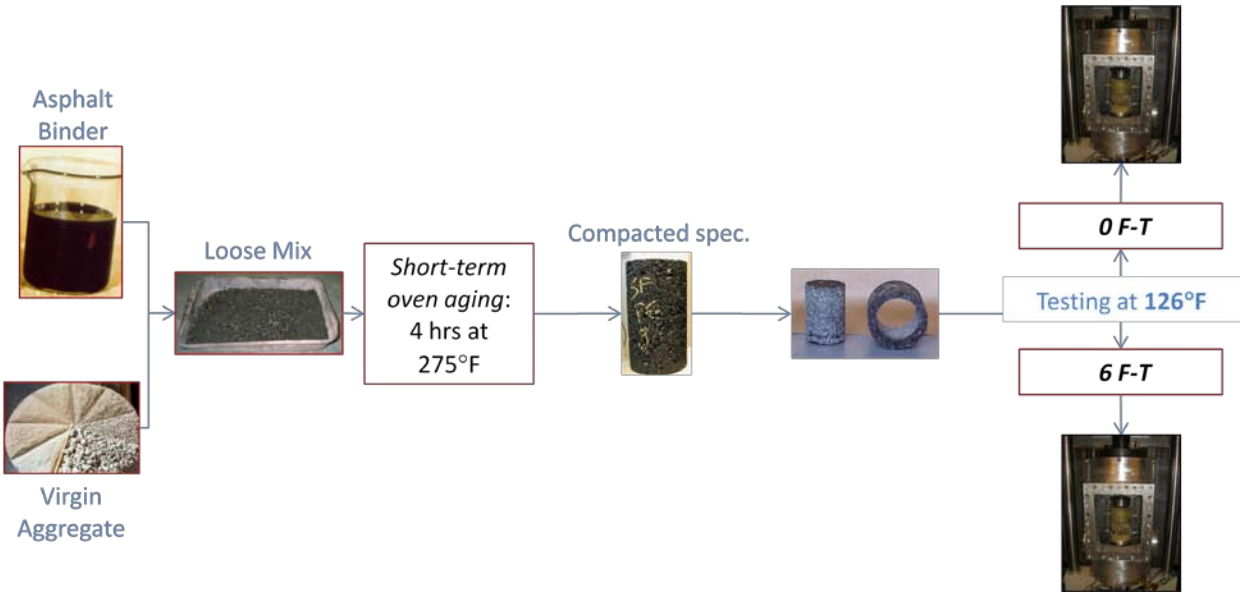

Figure 4. Repeated Load Triaxial Test Sample Preparation for Unaged Mixes.

Flexural Beam Fatigue Set-Up

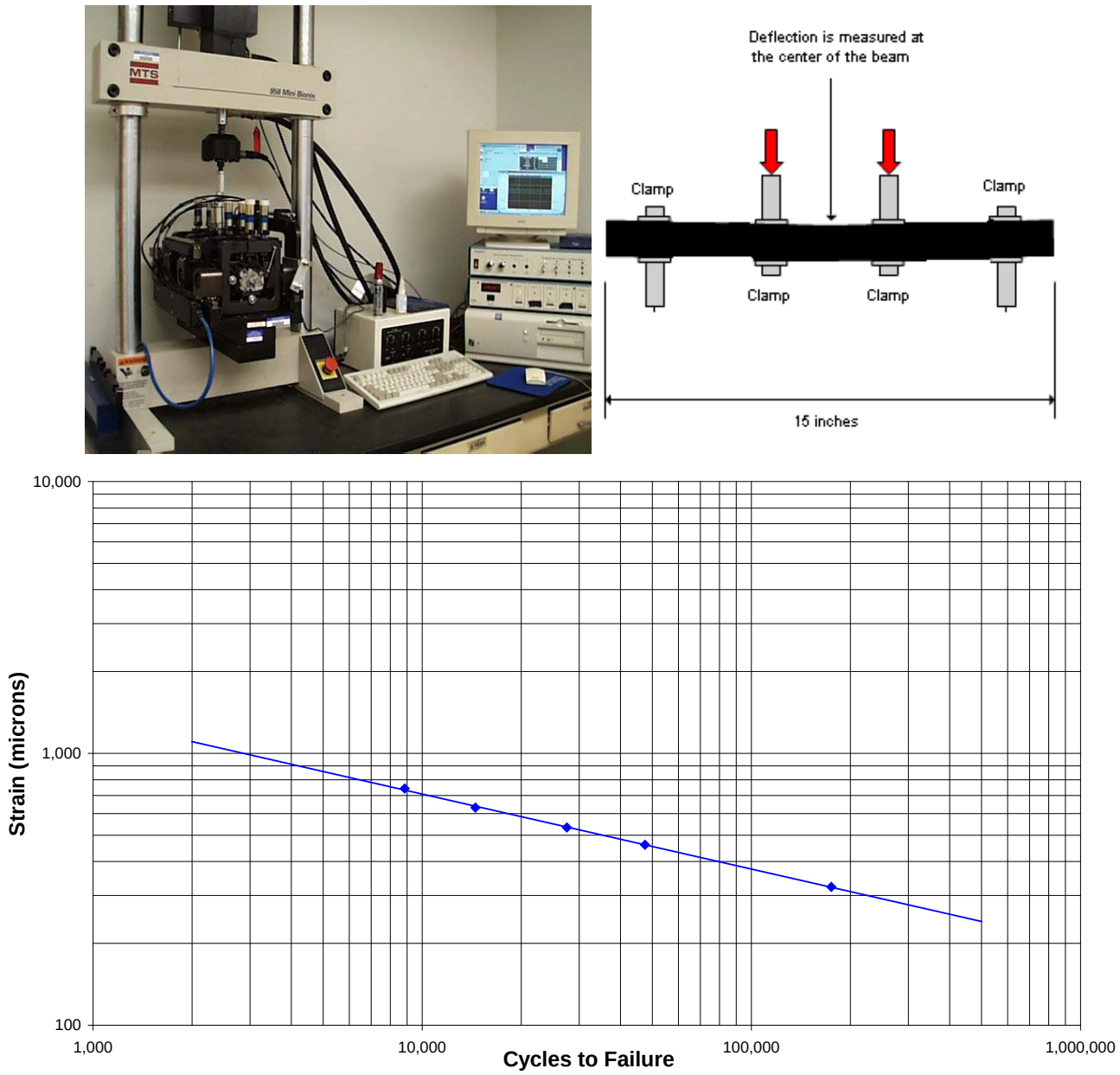

Figure 5. Components of the Beam Fatigue Test and a Typical Fatigue Curve for an HMA Mix.

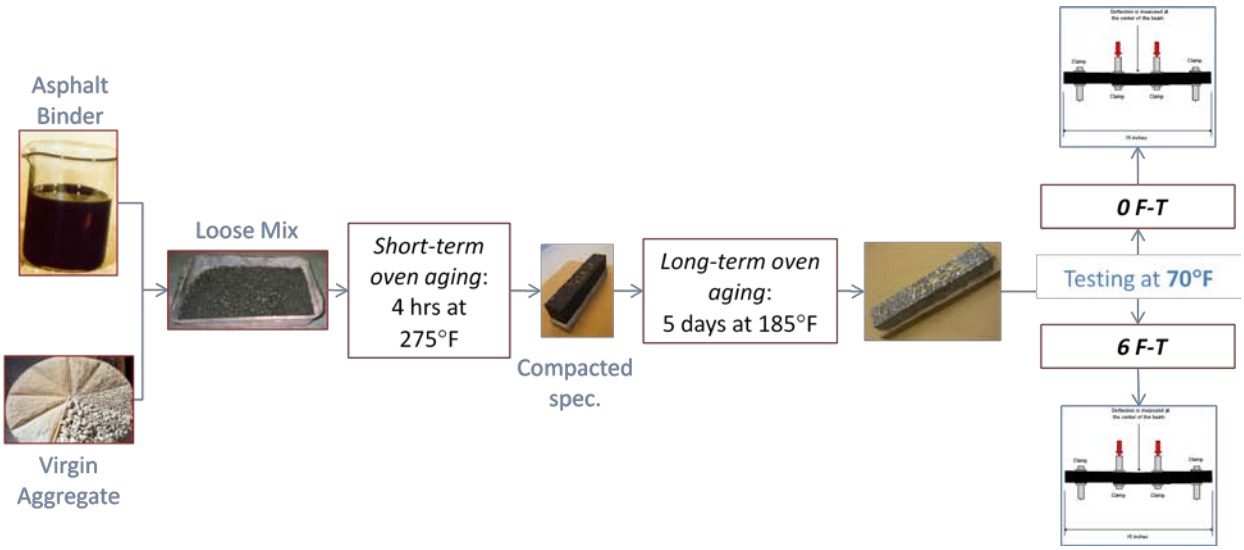

Figure 6. Beam Fatigue Test Sample Preparation for Aged Mixes.

TSRST Set-Up

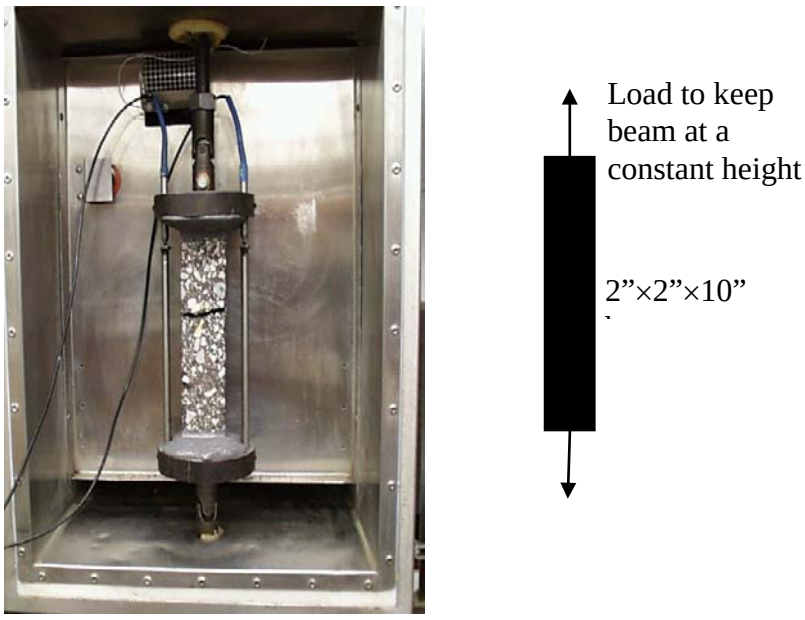

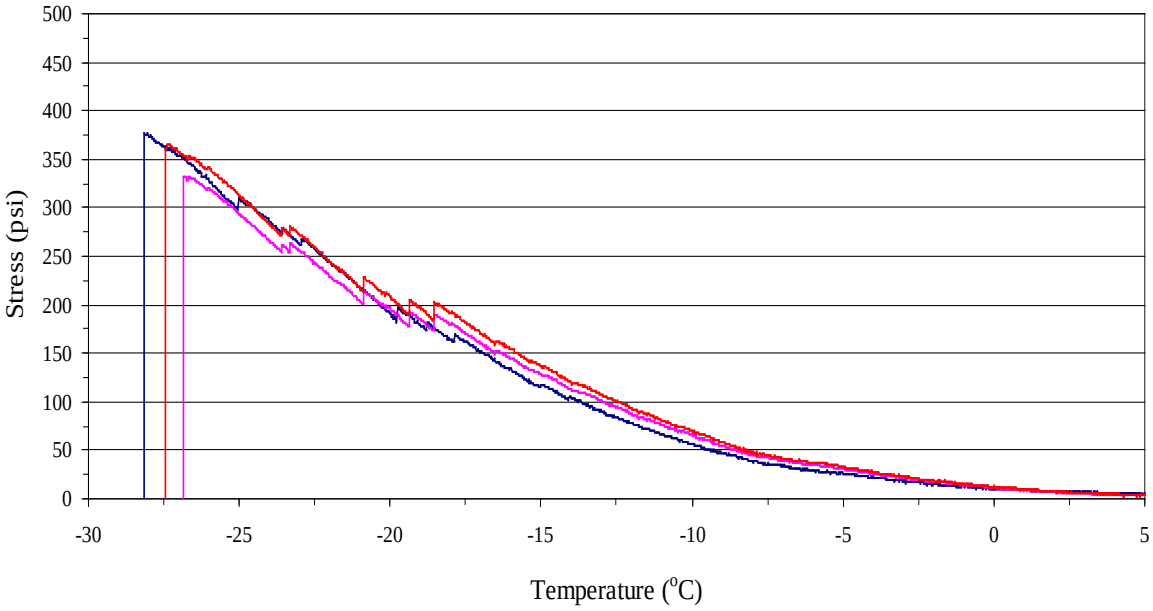

Figure 7. Components of the TSRST Test and Typical Stress-Temperature Curve for an HMA mix.

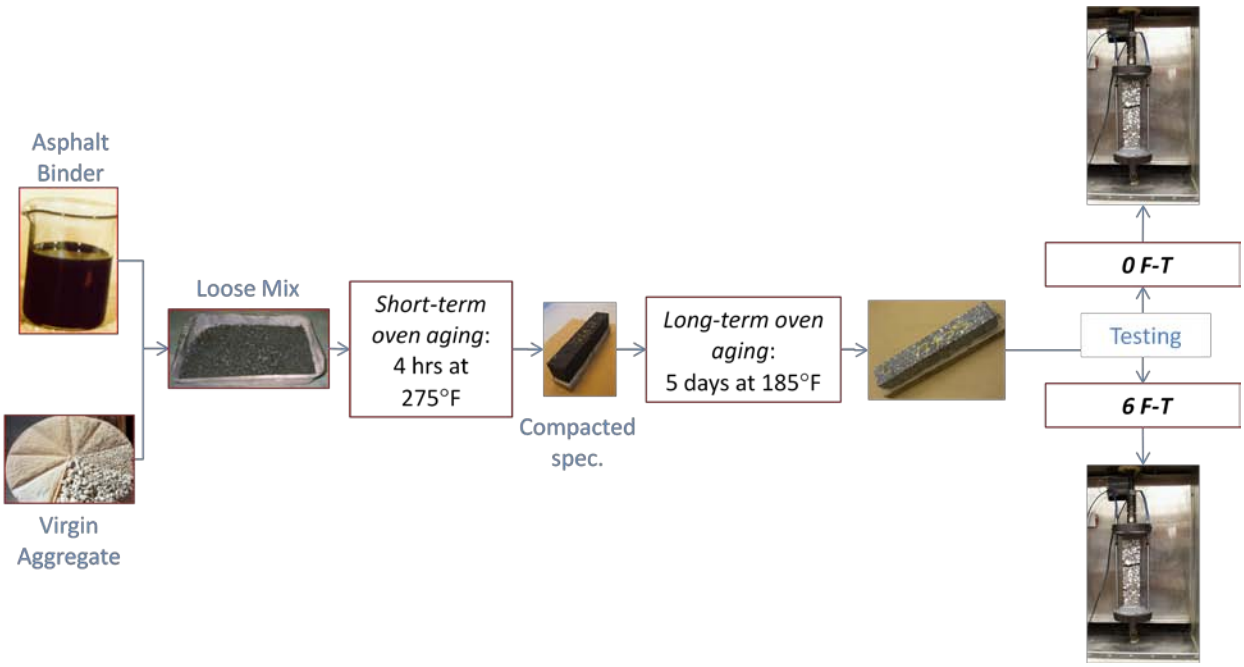

Figure 8. TSRST Sample Preparation for Aged Mixes.

PERFORMANCE GRADE	PG 46-			PG 52-							PG 58-					PG 64-						PG 70-						PG 76-					PG 82-				
	34	40	46	10	16	22	28	34	40	46	16	22	28	34	40	10	16	22	28	34	40	10	16	22	28	34	40	10	16	22	28	34	10	16	22	28	34
Average 7-day maximum pavement design temperature, °C	<46			<52							<58					<64						<70						<76					<82				
Minimum Pvement design temperature, °C	>-34	>-40	>-46	>-10	>-16	>-22	>-28	>-34	>-40	>-46	>-16	>-22	>-28	>-34	>-40	>-10	>-16	>-22	>-28	>-34	>-40	>-10	>-16	>-22	>-28	>-34	>-40	>-10	>-16	>-22	>-28	>-34	>-10	>-16	>-22	>-28	>-34
ORIGINAL BINDER																																					
Flash point temp, T 48, minimum, °C	230																																				
Viscosity, T 316: maximum 3 Pas, test temp, °C	135																																				
Dynamic shear, T 315: $G^*/\sin\delta$, minimum 1.00 kPa test temp @ 10 rad/s, °C	46			52							58					64						70						76					82				
ROLLING THIN-FILM OVEN RESIDUE (T 240)																																					
Mass Change, maximum, percent	1.00																																				
Dynamic shear, T 315: $G^*/\sin\delta$, minimum 2.20 kPa test temp @ 10 rad/s, °C	46			52							58					64						70						76					82				
PRESSURE AGING VESSEL (R 28)																																					
PAV aging temperature, °C	90			90							100					100						100						100					100				
Dynamic shear, T 315: $G^*/\sin\delta$, maximum 5000 kPa test temp @ 10 rad/s, °C	10	7	4	25	22	19	16	13	10	7	25	22	19	16	13	31	28	25	22	19	16	34	31	28	25	22	19	37	34	31	28	25	40	37	34	31	28
Creep stiffness, T 313: S, maximum 300 Mpa m-value, minimum 0.300 test temp @ 60s, °C	-24	-30	-36	0	-6	-12	-18	-24	-30	-36	-6	-12	-18	-24	-30	0	-6	-12	-18	-24	-30	0	-6	-12	-18	-24	-30	0	-6	-12	-18	-24	0	-6	-12	-18	-24
Direct tension, T 314: Failure strain, minimum 0.300 test temp @ 60s, °C	-24	-30	-36	0	-6	-12	-18	-24	-30	-36	-6	-12	-18	-24	-30	0	-6	-12	-18	-24	-30	0	-6	-12	-18	-24	-30	0	-6	-12	-18	-24	0	-6	-12	-18	-24

Figure 9. Performance Graded Asphalt Binder Specification.

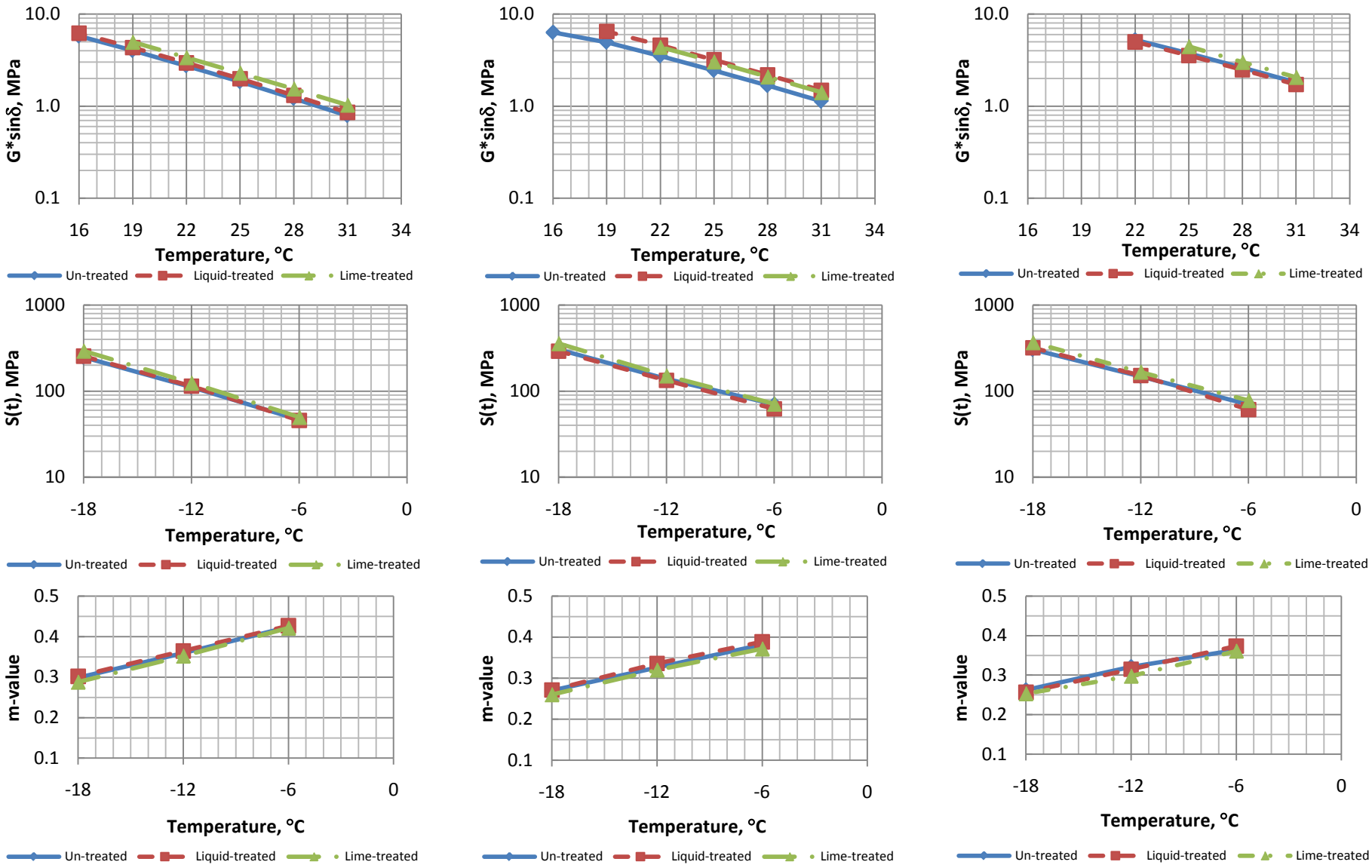

PAV aged for 100 hrs at 60°C

PAV aged for 400 hrs at 60°C

PAV aged for 800 hrs at 60°C

Figure 10. Impact of additives on the long-term aging of the Alabama binder at 100, 400, and 800 hrs in the PAV at 60°C.

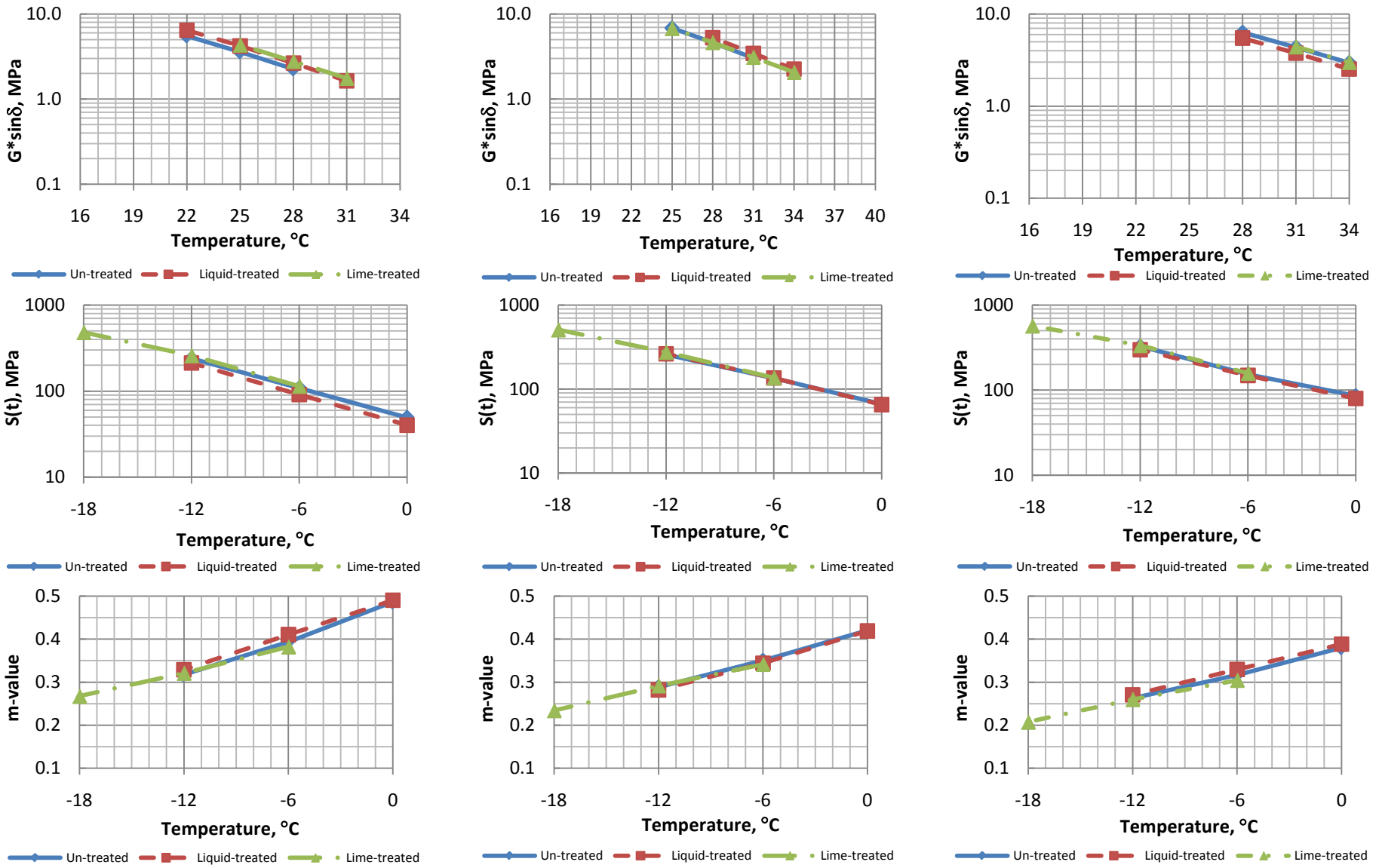

PAV aged for 100 hrs at 60°C

PAV aged for 400 hrs at 60°C

PAV aged for 800 hrs at 60°C

Figure 11. Impact of additives on the long-term aging of the California binder at 100, 400, and 800 hrs in the PAV at 60°C.

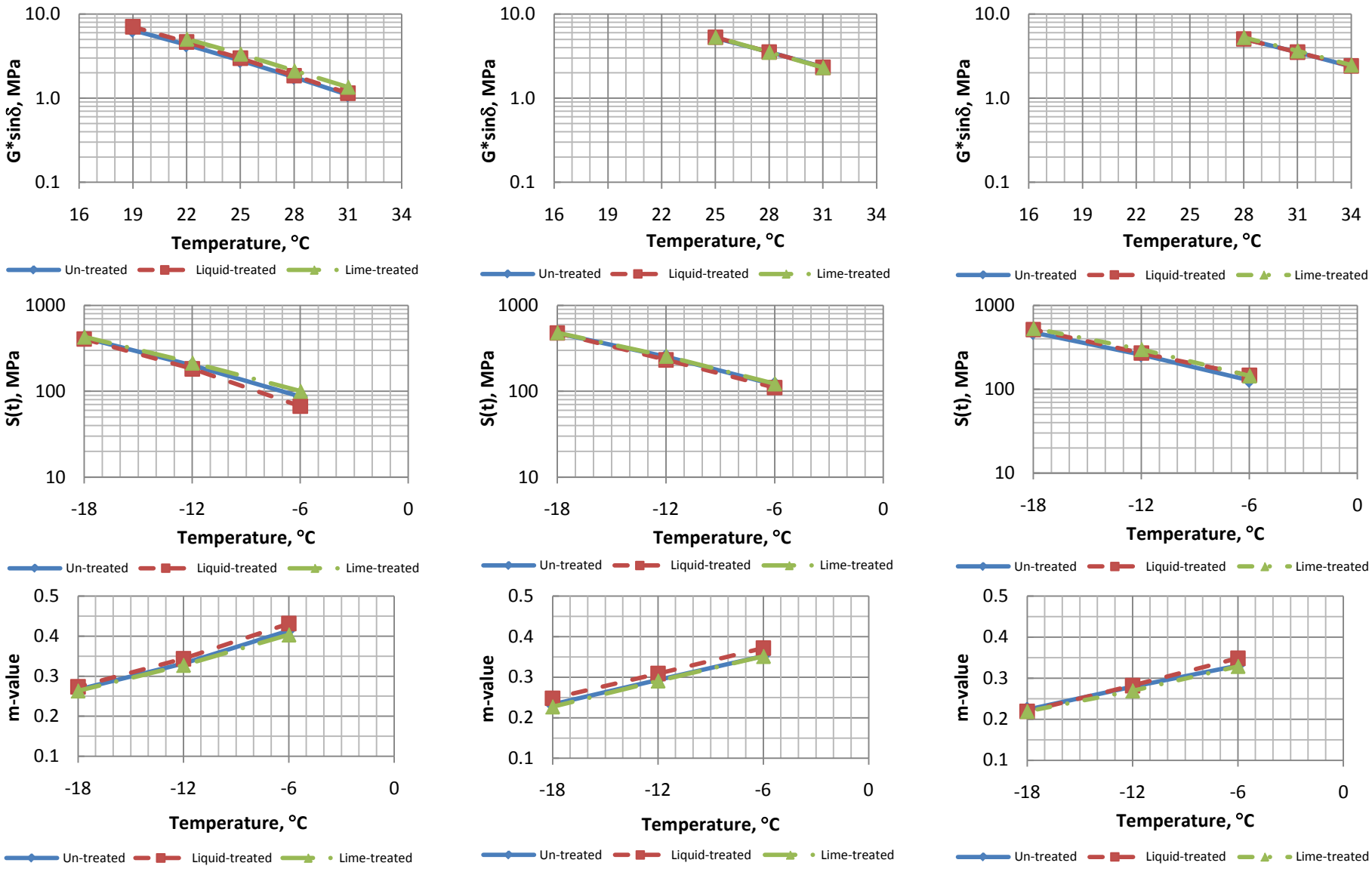

PAV aged for 100 hrs at 60°C

PAV aged for 400 hrs at 60°C

PAV aged for 800 hrs at 60°C

Figure 12. Impact of additives on the long-term aging of the Illinois binder at 100, 400, and 800 hrs in the PAV at 60°C.

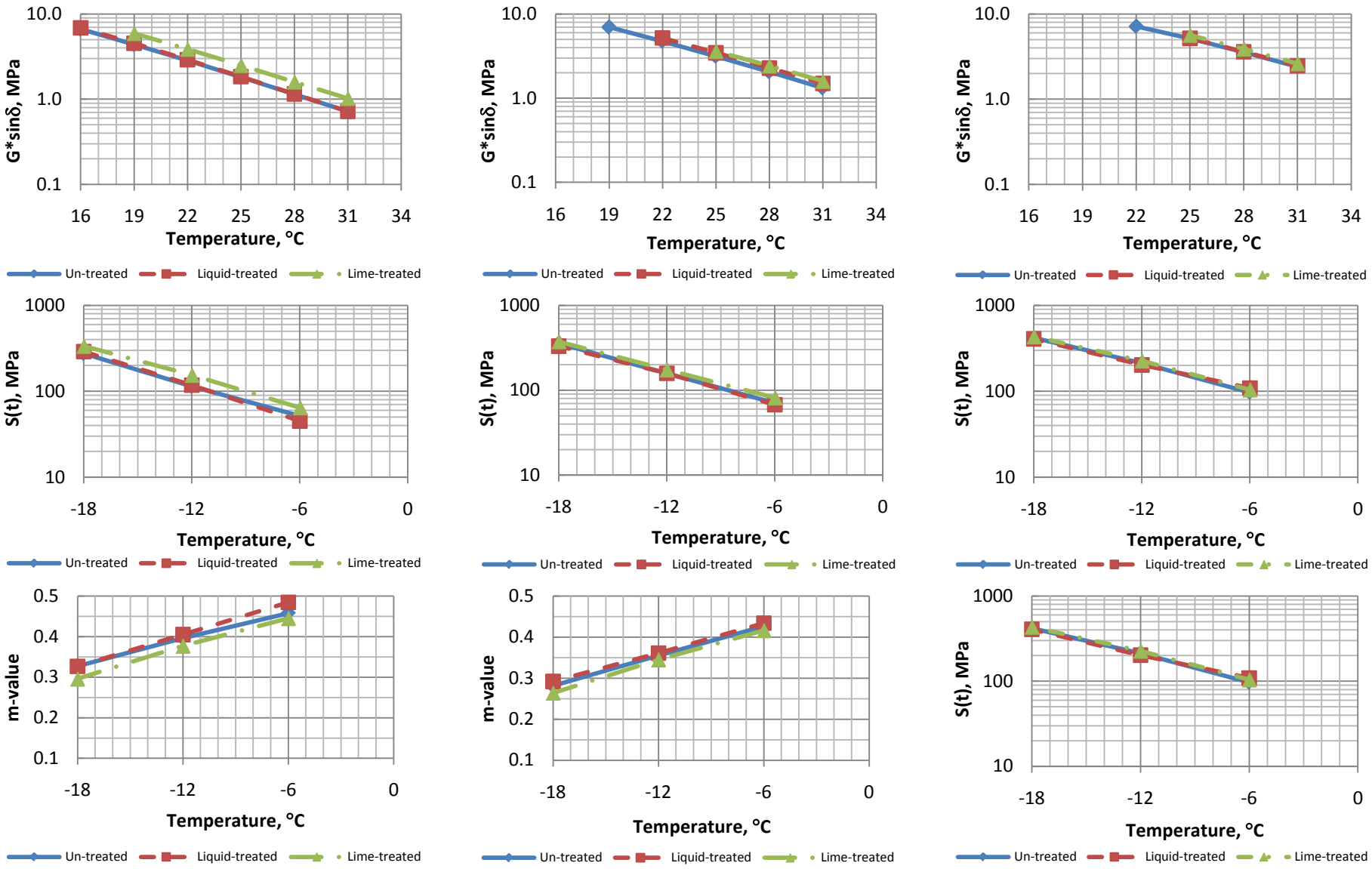

PAV aged for 100 hrs at 60°C

PAV aged for 400 hrs at 60°C

PAV aged for 800 hrs at 60°C

Figure 13. Impact of additives on the long-term aging of the South Carolina binder at 100, 400, and 800 hrs in the PAV at 60°C.

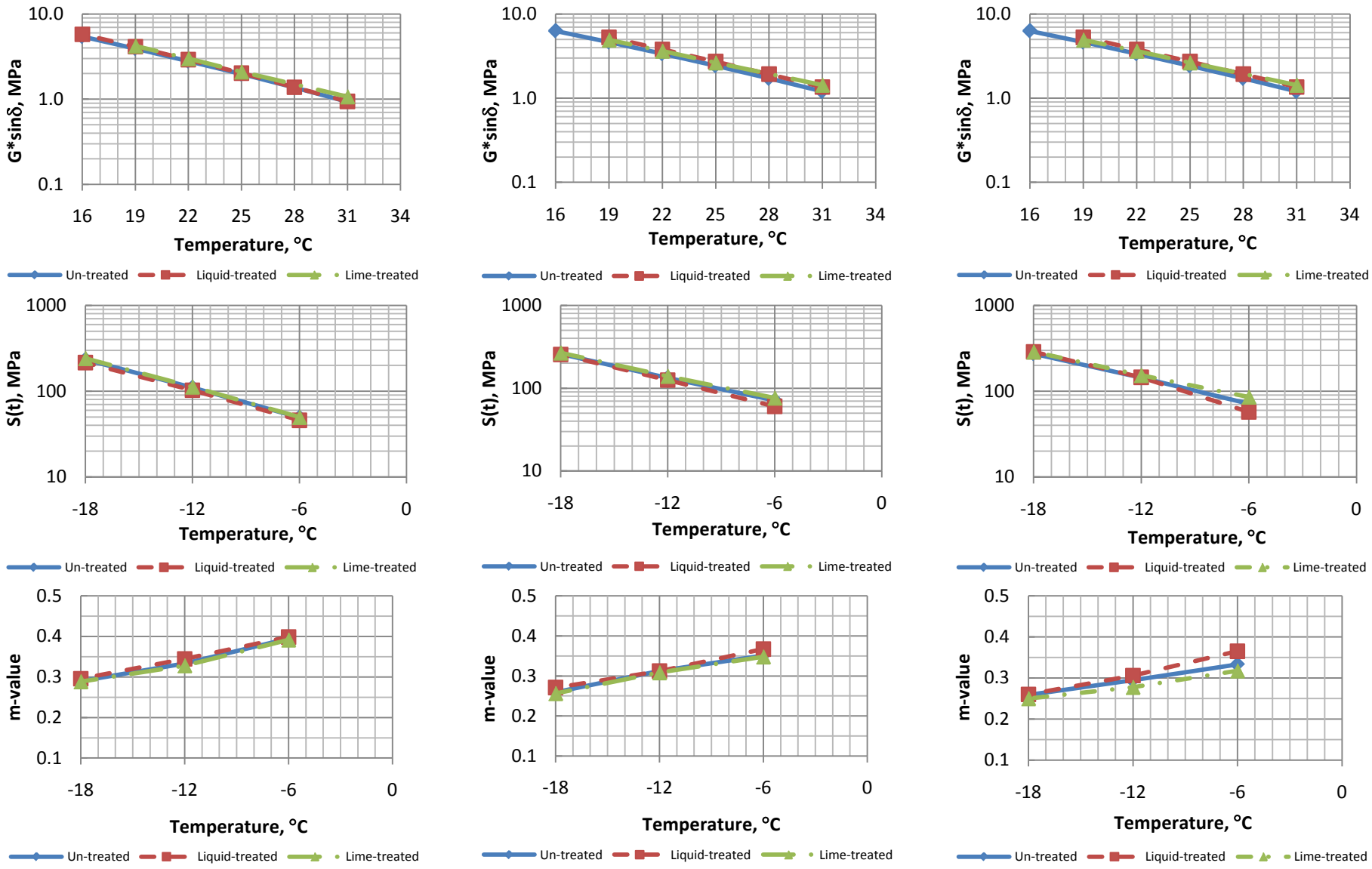

PAV aged for 100 hrs at 60°C

PAV aged for 400 hrs at 60°C

PAV aged for 800 hrs at 60°C

Figure 14. Impact of additives on the long-term aging of the Texas binder at 100, 400, and 800 hrs in the PAV at 60°C.

Mix Design		
Nominal Maximum Aggregate Size, mm		25.0
Property	**Value**	**Requirement**
Design ESALs, millions	6	--
N_{inital}	8	--
N_{design}	100	--
N_{max}	160	--
Optimum Binder Content, %	4.04	--
Hydrated Lime, %	None	--
Liquid Antistrip, %	None	--
Max theoretical specific gravity, G_{mm}	2.625	--
%Gmm at N_{ini}	85.1	≤ 89.0
%Gmm at N_{des}	96.0	96.0
%Gmm at N_{max}	96.4	≤ 98.0
VMA, %	12.1	12.0% Min.
VFA, %	67.0	65-75
Percent Effective Binder P_{be}, %	3.34	--
Dust Proportion, $P_{0.075}/P_{be}$	1.6	0.8-1.6
Unconditioned Tensile Strength on 4" Gyratory Samples @ 77°F, psi	113	--
Conditioned Tensile Strength on 4" Gyratory Samples @77°F, psi	92	--
Tensile Strength Ratio, %	81	80 Min.

Aggregate Properties			
Aggregate Bulk Specific Gravity, G_{sb}			2.752
Aggregate Effective Specific Gravity, G_{se}			2.806
Sieve Size	**%Passing**	**Control Points**	
		Min	**Max**
37.5 mm (1 1/2")	100.0	100	--
25.0 mm (1")	99.2	90	100
19.0 mm (3/4")	89.0	--	90
12.5 mm (1/2")	67.9	--	--
9.5 mm (3/8")	61.4	--	--
4.75 mm (No. 4)	35.6	--	--
2.36 mm (No. 8)	22.5	19	45
2.00 mm (No. 10)	20.0	--	--
1.18 mm (No. 16)	14.9	--	--
0.6 mm (No. 30)	10.6	--	--
0.425 mm (No. 40)	9.0	--	--
0.3 mm (No. 50)	7.9	--	--
0.15 mm (No. 100)	6.4	--	--
0.075 mm (No. 200)	5.26	1	7
Aggregates	**Description**		**Bin %**
Aggr. 1	#57 LS		32.0%
Aggr. 2	#67 LS		10.0%
Aggr. 3	#89 LS		24.0%
Aggr. 4	LS Scr		33.0%
Aggr. 5	BHF		1.0%

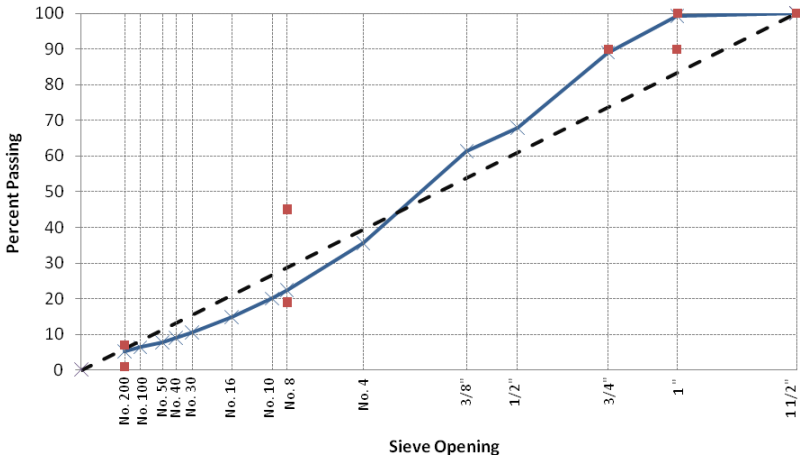

Figure 15. Alabama Un-treated Mix Design and Aggregate Properties.

Mix Design		
Nominal Maximum Aggregate Size, mm		25.0
Property	**Value**	**Requirement**
Design ESALs, millions	6	--
N_{inital}	8	--
N_{design}	100	--
N_{max}	160	--
Optimum Binder Content, %	3.92	--
Hydrated Lime, %	None	--
Liquid Antistrip, %	0.5% by binder	--
Max theoretical specific gravity, G_{mm}	2.625	--
%Gmm at N_{ini}	85.0	≤ 89.0
%Gmm at N_{des}	96.0	96.0
%Gmm at N_{max}	97.0	≤ 98.0
VMA, %	12.0	12.0% Min.
VFA, %	66.7	65-75
Percent Effective Binder P_{be}, %	3.30	--
Dust Proportion, $P_{0.075}/P_{be}$	1.6	0.8-1.6
Unconditioned Tensile Strength on 4" Gyratory Samples @ 77°F, psi	109	--
Conditioned Tensile Strength on 4" Gyratory Samples @77°F, psi	90	--
Tensile Strength Ratio, %	83	80 Min.

Aggregate Properties			
Aggregate Bulk Specific Gravity, G_{sb}			2.752
Aggregate Effective Specific Gravity, G_{se}			2.800
Sieve Size	**%Passing**	**Control Points**	
		Min	**Max**
37.5 mm (1 1/2")	100.0	100	--
25.0 mm (1")	99.2	90	100
19.0 mm (3/4")	89.0	--	90
12.5 mm (1/2")	67.9	--	--
9.5 mm (3/8")	61.4	--	--
4.75 mm (No. 4)	35.6	--	--
2.36 mm (No. 8)	22.5	19	45
2.00 mm (No. 10)	20.0	--	--
1.18 mm (No. 16)	14.9	--	--
0.6 mm (No. 30)	10.6	--	--
0.425 mm (No. 40)	9.0	--	--
0.3 mm (No. 50)	7.9	--	--
0.15 mm (No. 100)	6.4	--	--
0.075 mm (No. 200)	5.26	1	7
Aggregates	**Description**		**Bin %**
Aggr. 1	#57 LS		32.0%
Aggr. 2	#67 LS		10.0%
Aggr. 3	#89 LS		24.0%
Aggr. 4	LS Scr		33.0%
Aggr. 5	BHF		1.0%

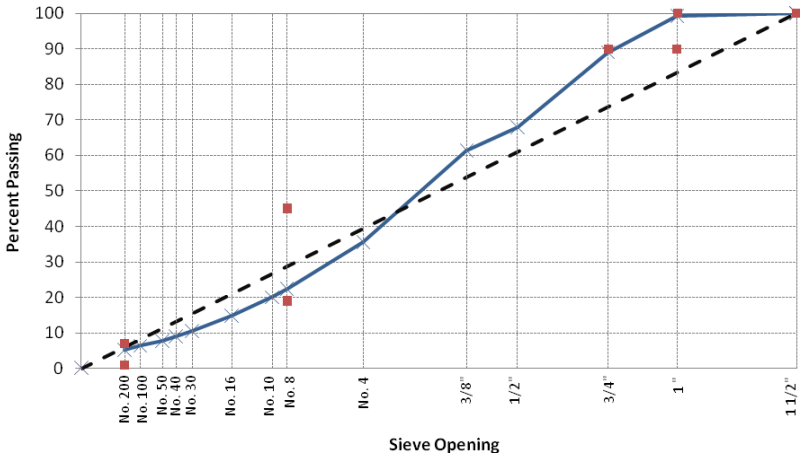

Figure 16. Alabama Liquid-Treated Mix Design and Aggregate Properties.

Mix Design		
Nominal Maximum Aggregate Size, mm		25.0
Property	**Value**	**Requirement**
Design ESALs, millions	6	--
N_{inital}	8	--
N_{design}	100	--
N_{max}	160	--
Optimum Binder Content, %	3.95	--
Hydrated Lime, %	1% Lime by DWA	--
Liquid Antistrip, %	None	--
Max theoretical specific gravity, G_{mm}	2.626	--
%Gmm at N_{ini}	85.8	≤ 89.0
%Gmm at N_{des}	96.0	96.0
%Gmm at N_{max}	98.0	≤ 98.0
VMA, %	12.0	12.0% Min.
VFA, %	66.6	65-75
Percent Effective Binder P_{be}, %	3.27	--
Dust Proportion, $P_{0.075}/P_{be}$	1.6	0.8-1.6
Unconditioned Tensile Strength on 4" Gyratory Samples @ 77°F, psi	120	--
Conditioned Tensile Strength on 4" Gyratory Samples @77°F, psi	109	--
Tensile Strength Ratio, %	90	80 Min.

Aggregate Properties			
Aggregate Bulk Specific Gravity, G_{sb}			2.750
Aggregate Effective Specific Gravity, G_{se}			2.803
Sieve Size	**%Passing**	**Control Points**	
		Min	**Max**
37.5 mm (1 1/2")	100.0	100	--
25.0 mm (1")	99.2	90	100
19.0 mm (3/4")	89.0	--	90
12.5 mm (1/2")	67.9	--	--
9.5 mm (3/8")	61.4	--	--
4.75 mm (No. 4)	35.6	--	--
2.36 mm (No. 8)	22.5	19	45
2.00 mm (No. 10)	20.0	--	--
1.18 mm (No. 16)	14.9	--	--
0.6 mm (No. 30)	10.6	--	--
0.425 mm (No. 40)	9.0	--	--
0.3 mm (No. 50)	7.9	--	--
0.15 mm (No. 100)	6.4	--	--
0.075 mm (No. 200)	5.28	1	7
Aggregates	**Description**		**Bin %**
Aggr. 1	#57 LS		32.0%
Aggr. 2	#67 LS		10.0%
Aggr. 3	#89 LS		24.0%
Aggr. 4	LS Scr		33.0%
Aggr. 5	Lime		1.0%

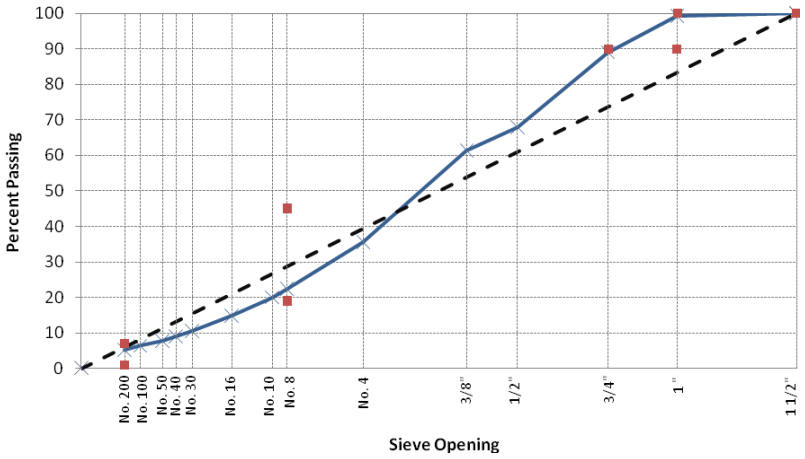

Figure 17. Alabama Lime-Treated Mix Design and Aggregate Properties.

Mix Design		
Nominal Maximum Aggregate Size, mm		19.0
Property	**Value**	**Requirement**
Design ESALs, millions	6	--
N_{inital}	8	--
N_{design}	100	--
N_{max}	160	--
Optimum Binder Content, %	4.47	--
Hydrated Lime, %	None	--
Liquid Antistrip, %	None	--
Max theoretical specific gravity, G_{mm}	2.608	--
%Gmm at N_{ini}	86.8	≤ 89.0
%Gmm at N_{des}	96.0	96.0
%Gmm at N_{max}	96.7	≤ 98.0
VMA, %	13.0	13.0% Min.
VFA, %	69.3	65-75
Percent Effective Binder P_{be}, %	3.66	--
Dust Proportion, $P_{0.075}/P_{be}$	1.2	0.8-1.6
Unconditioned Tensile Strength on 4" Gyratory Samples @ 77°F, psi	214	--
Conditioned Tensile Strength on 4" Gyratory Samples @77°F, psi	155	--
Tensile Strength Ratio, %	72	80 Min.

Aggregate Properties			
Aggregate Bulk Specific Gravity, G_{sb}			2.681
Aggregate Effective Specific Gravity, G_{se}			2.741
Sieve Size	**%Passing**	**Control Points**	
		Min	**Max**
37.5 mm (1 1/2")	100.0	--	--
25.0 mm (1")	100.0	100	--
19.0 mm (3/4")	98.4	90	100
12.5 mm (1/2")	81.4	--	90
9.5 mm (3/8")	72.4	--	--
4.75 mm (No. 4)	43.6	--	--
2.36 mm (No. 8)	29.9	23	49
2.00 mm (No. 10)	27.4	--	--
1.18 mm (No. 16)	21.8	--	--
0.6 mm (No. 30)	16.5	--	--
0.425 mm (No. 40)	13.6	--	--
0.3 mm (No. 50)	10.7	--	--
0.15 mm (No. 100)	6.4	--	--
0.075 mm (No. 200)	4.17	2	8
Aggregates	**Description**		**Bin %**
Aggr. 1	3/4 inch		6.0%
Aggr. 2	1/2 inch		20.0%
Aggr. 3	3/8 inch		35.0%
Aggr. 4	Crushed Dust		25.0%
Aggr. 5	Washed Sand		14.0%

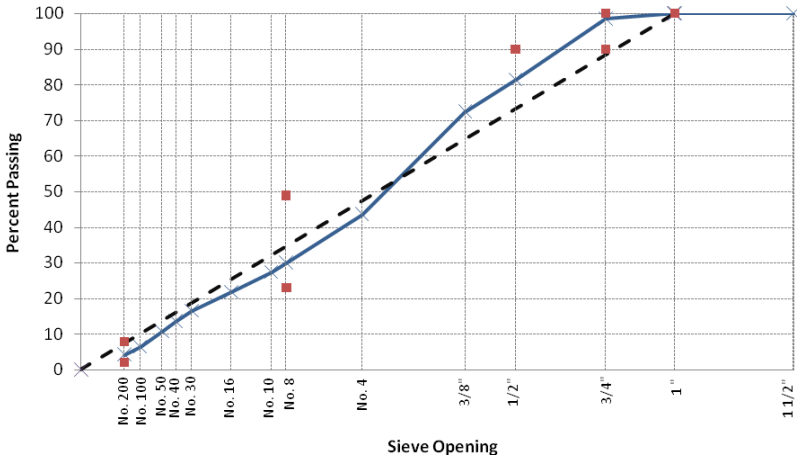

Figure 18. California Un-treated Mix Design and Aggregate Properties.

Mix Design		
Nominal Maximum Aggregate Size, mm		19.0
Property	**Value**	**Requirement**
Design ESALs, millions	6	--
N_{inital}	8	--
N_{design}	100	--
N_{max}	160	--
Optimum Binder Content, %	4.28	--
Hydrated Lime, %	None	--
Liquid Antistrip, %	0.5% by AC	--
Max theoretical specific gravity, G_{mm}	2.602	--
%Gmm at N_{ini}	86.7	≤ 89.0
%Gmm at N_{des}	96.0	96.0
%Gmm at N_{max}	97.8	≤ 98.0
VMA, %	13.0	13.0% Min.
VFA, %	69.2	65-75
Percent Effective Binder P_{be}, %	3.67	--
Dust Proportion, $P_{0.075}/P_{be}$	1.2	0.8-1.6
Unconditioned Tensile Strength on 4" Gyratory Samples @ 77°F, psi	180	--
Conditioned Tensile Strength on 4" Gyratory Samples @77°F, psi	164	--
Tensile Strength Ratio, %	91	80 Min.

Aggregate Properties			
Aggregate Bulk Specific Gravity, G_{sb}			2.681
Aggregate Effective Specific Gravity, G_{se}			2.741
Sieve Size	**%Passing**	**Control Points**	
		Min	**Max**
37.5 mm (1 1/2")	100.0	--	--
25.0 mm (1")	100.0	100	--
19.0 mm (3/4")	98.4	90	100
12.5 mm (1/2")	81.4	--	90
9.5 mm (3/8")	72.4	--	--
4.75 mm (No. 4)	43.6	--	--
2.36 mm (No. 8)	29.9	23	49
2.00 mm (No. 10)	27.4	--	--
1.18 mm (No. 16)	21.8	--	--
0.6 mm (No. 30)	16.5	--	--
0.425 mm (No. 40)	13.6	--	--
0.3 mm (No. 50)	10.7	--	--
0.15 mm (No. 100)	6.4	--	--
0.075 mm (No. 200)	4.17	2	8
Aggregates	**Description**		**Bin %**
Aggr. 1	3/4 inch		6.0%
Aggr. 2	1/2 inch		20.0%
Aggr. 3	3/8 inch		35.0%
Aggr. 4	Crushed Dust		25.0%
Aggr. 5	Washed Sand		14.0%

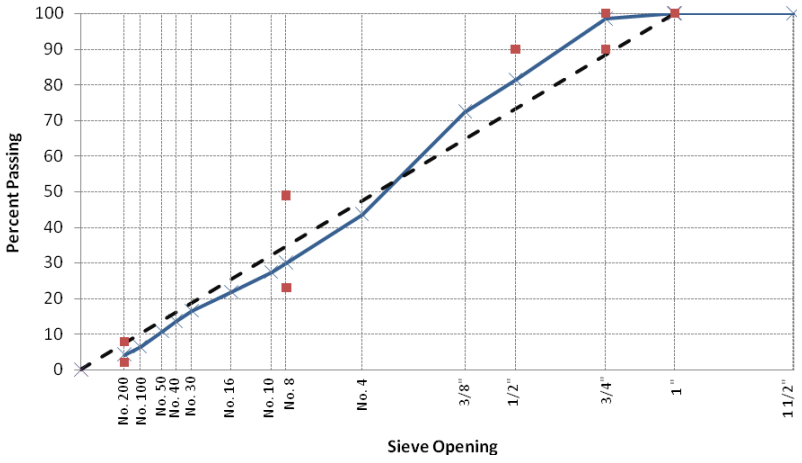

Figure 19. California Liquid-treated Mix Design and Aggregate Properties.

Mix Design		
Nominal Maximum Aggregate Size, mm		19.0
Property	**Value**	**Requirement**
Design ESALs, millions	6	--
N_{inital}	8	--
N_{design}	100	--
N_{max}	160	--
Optimum Binder Content, %	4.23	--
Hydrated Lime, %	1% Lime by DWA	--
Liquid Antistrip, %	None	--
Max theoretical specific gravity, G_{mm}	2.603	--
%Gmm at N_{ini}	85.5	≤ 89.0
%Gmm at N_{des}	96.0	96.0
%Gmm at N_{max}	97.3	≤ 98.0
VMA, %	13.0	13.0% Min.
VFA, %	69.1	65-75
Percent Effective Binder P_{be}, %	3.67	--
Dust Proportion, $P_{0.075}/P_{be}$	1.4	0.8-1.6
Unconditioned Tensile Strength on 4" Gyratory Samples @ 77°F, psi	164	--
Conditioned Tensile Strength on 4" Gyratory Samples @77°F, psi	155	--
Tensile Strength Ratio, %	95	80 Min.

Aggregate Properties			
Aggregate Bulk Specific Gravity, G_{sb}			2.681
Aggregate Effective Specific Gravity, G_{se}			2.741
Sieve Size	**%Passing**	**Control Points**	
		Min	**Max**
37.5 mm (1 1/2")	100.0	--	--
25.0 mm (1")	100.0	100	--
19.0 mm (3/4")	98.5	90	100
12.5 mm (1/2")	86.0	--	90
9.5 mm (3/8")	77.8	--	--
4.75 mm (No. 4)	40.2	--	--
2.36 mm (No. 8)	26.5	23	49
2.00 mm (No. 10)	24.3	--	--
1.18 mm (No. 16)	19.4	--	--
0.6 mm (No. 30)	14.9	--	--
0.425 mm (No. 40)	12.6	--	--
0.3 mm (No. 50)	10.3	--	--
0.15 mm (No. 100)	6.8	--	--
0.075 mm (No. 200)	4.95	2	8
Aggregates	**Description**		**Bin %**
Aggr. 1	3/4 inch		6.0%
Aggr. 2	1/2 inch		18.0%
Aggr. 3	3/8 inch		38.0%
Aggr. 4	Crushed Dust		23.0%
Aggr. 5	Washed Sand		14.0%

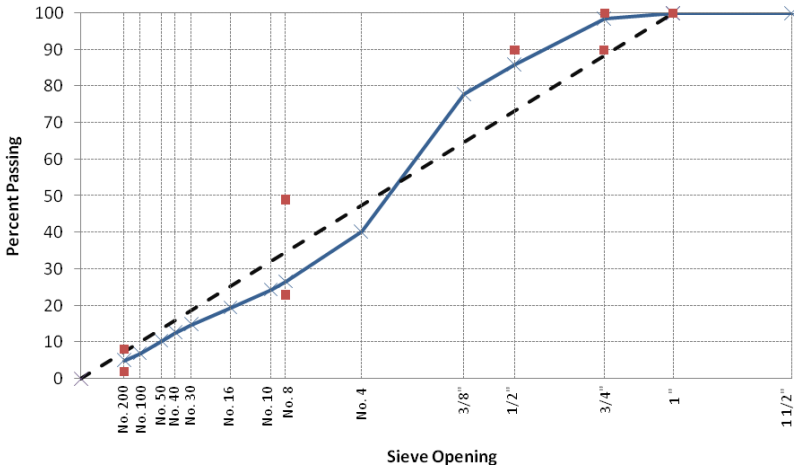

Figure 20. California Lime-treated Mix Design and Aggregate Properties.

Mix Design		
Nominal Maximum Aggregate Size, mm		19.0
Property	**Value**	**Requirement**
Design ESALs, millions	6	--
N_{inital}	8	--
N_{design}	100	--
N_{max}	160	--
Optimum Binder Content, %	4.61	--
Hydrated Lime, %	None	--
Liquid Antistrip, %	None	--
Max theoretical specific gravity, G_{mm}	2.547	--
%Gmm at N_{ini}	84.7	≤ 89.0
%Gmm at N_{des}	96.0	96.0
%Gmm at N_{max}	96.6	≤ 98.0
VMA, %	13.0	13.0% Min.
VFA, %	69.1	65-75
Percent Effective Binder P_{be}, %	3.81	--
Dust Proportion, $P_{0.075}/P_{be}$	1.3	0.8-1.6
Unconditioned Tensile Strength on 4" Gyratory Samples @ 77°F, psi	138	--
Conditioned Tensile Strength on 4" Gyratory Samples @77°F, psi	112	--
Tensile Strength Ratio, %	82	80 Min.

Aggregate Properties			
Aggregate Bulk Specific Gravity, G_{sb}			2.681
Aggregate Effective Specific Gravity, G_{se}			2.741
Sieve Size	**%Passing**	**Control Points**	
		Min	**Max**
37.5 mm (1 1/2")	100.0	--	--
25.0 mm (1")	100.0	100	--
19.0 mm (3/4")	95.8	90	100
12.5 mm (1/2")	78.1	--	90
9.5 mm (3/8")	68.9	--	--
4.75 mm (No. 4)	39.5	--	--
2.36 mm (No. 8)	25.5	23	49
2.00 mm (No. 10)	22.8	--	--
1.18 mm (No. 16)	16.4	--	--
0.6 mm (No. 30)	11.3	--	--
0.425 mm (No. 40)	9.5	--	--
0.3 mm (No. 50)	8.2	--	--
0.15 mm (No. 100)	6.6	--	--
0.075 mm (No. 200)	5.14	2	8
Aggregates	**Description**		**Bin %**
Aggr. 1	CCD		41.0%
Aggr. 2	CCDch		31.0%
Aggr. 3	CDS		26.0%
Aggr. 4	Mineral Filler		2.0%

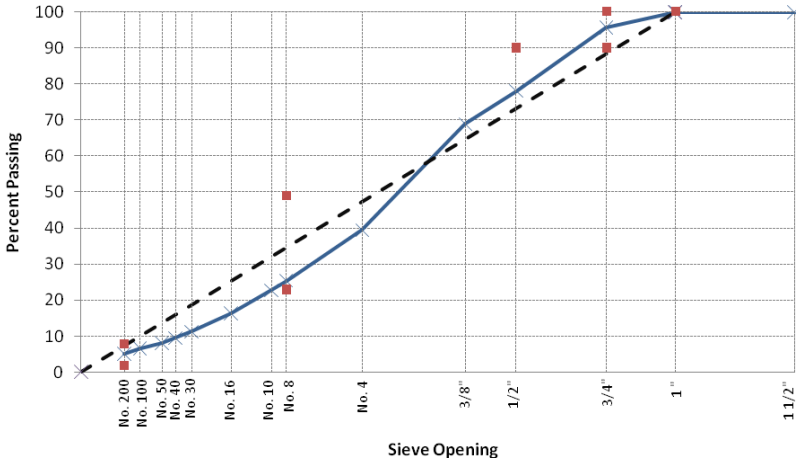

Figure 21. Illinois Un-treated Mix Design and Aggregate Properties.

Mix Design		
Nominal Maximum Aggregate Size, mm		19.0
Property	**Value**	**Requirement**
Design ESALs, millions	6	--
N_{inital}	8	--
N_{design}	100	--
N_{max}	160	--
Optimum Binder Content, %	4.92	--
Hydrated Lime, %	None	--
Liquid Antistrip, %	0.5% by AC	--
Max theoretical specific gravity, G_{mm}	2.540	--
%Gmm at N_{ini}	84.8	≤ 89.0
%Gmm at N_{des}	96.0	96.0
%Gmm at N_{max}	96.8	≤ 98.0
VMA, %	13.5	13.0% Min.
VFA, %	70.4	65-75
Percent Effective Binder P_{be}, %	4.05	--
Dust Proportion, $P_{0.075}/P_{be}$	1.3	0.8-1.6
Unconditioned Tensile Strength on 4" Gyratory Samples @ 77°F, psi	135	--
Conditioned Tensile Strength on 4" Gyratory Samples @77°F, psi	115	--
Tensile Strength Ratio, %	85	80 Min.

Aggregate Properties			
Aggregate Bulk Specific Gravity, G_{sb}			2.681
Aggregate Effective Specific Gravity, G_{se}			2.746
Sieve Size	**%Passing**	**Control Points**	
		Min	**Max**
37.5 mm (1 1/2")	100.0	--	--
25.0 mm (1")	100.0	100	--
19.0 mm (3/4")	95.8	90	100
12.5 mm (1/2")	78.1	--	90
9.5 mm (3/8")	68.9	--	--
4.75 mm (No. 4)	39.5	--	--
2.36 mm (No. 8)	25.5	23	49
2.00 mm (No. 10)	22.8	--	--
1.18 mm (No. 16)	16.4	--	--
0.6 mm (No. 30)	11.3	--	--
0.425 mm (No. 40)	9.5	--	--
0.3 mm (No. 50)	8.2	--	--
0.15 mm (No. 100)	6.6	--	--
0.075 mm (No. 200)	5.14	2	8
Aggregates	**Description**		**Bin %**
Aggr. 1	CCD		41.0%
Aggr. 2	CCDCh		31.0%
Aggr. 3	CDS		26.0%
Aggr. 4	Mineral Filler		2.0%

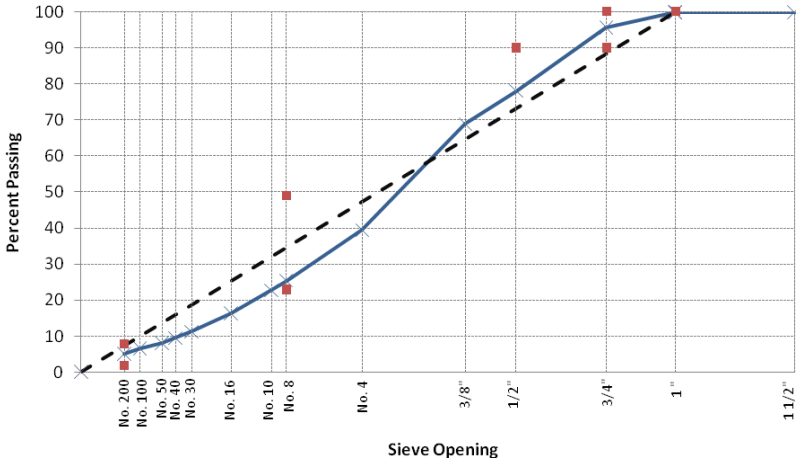

Figure 22. Illinois Liquid-Treated Mix Design and Aggregate Properties.

Mix Design		
Nominal Maximum Aggregate Size, mm		19.0
Property	**Value**	**Requirement**
Design ESALs, millions	6	--
N_{inital}	8	--
N_{design}	100	--
N_{max}	160	--
Optimum Binder Content, %	4.70	--
Hydrated Lime, %	1% Lime by DWA	--
Liquid Antistrip, %	None	--
Max theoretical specific gravity, G_{mm}	2.538	--
%Gmm at N_{ini}	84.6	≤ 89.0
%Gmm at N_{des}	96.0	96.0
%Gmm at N_{max}	97.7	≤ 98.0
VMA, %	13.0	13.0% Min.
VFA, %	69.1	65-75
Percent Effective Binder P_{be}, %	3.83	--
Dust Proportion, $P_{0.075}/P_{be}$	1.4	0.8-1.6
Unconditioned Tensile Strength on 4" Gyratory Samples @ 77°F, psi	149	--
Conditioned Tensile Strength on 4" Gyratory Samples @77°F, psi	129	--
Tensile Strength Ratio, %	87	80 Min.

Aggregate Properties			
Aggregate Bulk Specific Gravity, G_{sb}			2.669
Aggregate Effective Specific Gravity, G_{se}			2.733
Sieve Size	**%Passing**	**Control Points**	
		Min	**Max**
37.5 mm (1 1/2")	100.0	--	--
25.0 mm (1")	100.0	100	--
19.0 mm (3/4")	95.8	90	100
12.5 mm (1/2")	78.1	--	90
9.5 mm (3/8")	68.9	--	--
4.75 mm (No. 4)	39.5	--	--
2.36 mm (No. 8)	25.5	23	49
2.00 mm (No. 10)	22.8	--	--
1.18 mm (No. 16)	16.4	--	--
0.6 mm (No. 30)	11.3	--	--
0.425 mm (No. 40)	9.5	--	--
0.3 mm (No. 50)	8.2	--	--
0.15 mm (No. 100)	6.6	--	--
0.075 mm (No. 200)	5.24	2	8
Aggregates	**Description**		**Bin %**
Aggr. 1	CCD		41.0%
Aggr. 2	CCDch		31.0%
Aggr. 3	CDS		26.0%
Aggr. 4	Mineral Filler		1.0%
Aggr. 5	Lime		1.0%

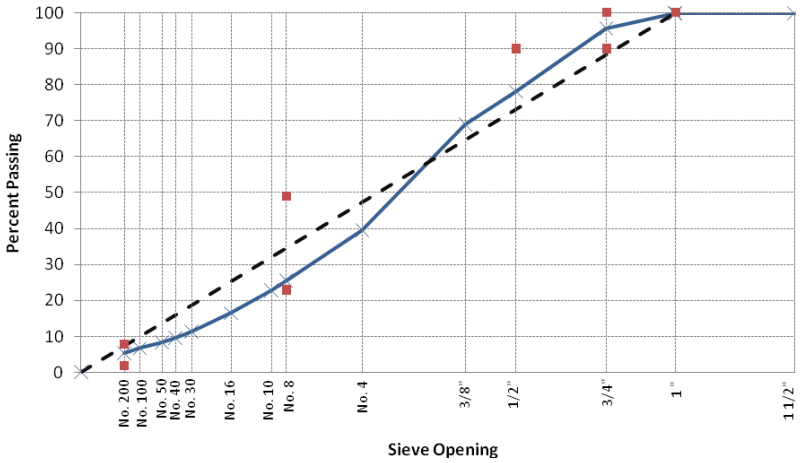

Figure 23. Illinois Lime-Treated Mix Design and Aggregate Properties.

Mix Design		
Nominal Maximum Aggregate Size, mm		12.5
Property	**Value**	**Requirement**
Design ESALs, millions	6	--
N_{inital}	8	--
N_{design}	100	--
N_{max}	160	--
Optimum Binder Content, %	5.33	--
Hydrated Lime, %	None	--
Liquid Antistrip, %	None	--
Max theoretical specific gravity, G_{mm}	2.564	--
%Gmm at N_{ini}	87.8	≤ 89.0
%Gmm at N_{des}	96.0	96.0
%Gmm at N_{max}	97.1	≤ 98.0
VMA, %	15.3	14.0% Min.
VFA, %	73.9	65-75
Percent Effective Binder P_{be}, %	4.77	--
Dust Proportion, $P_{0.075}/P_{be}$	0.7	0.6-1.2
Unconditioned Tensile Strength on 4" Gyratory Samples @ 77°F, psi	152	--
Conditioned Tensile Strength on 4" Gyratory Samples @77°F, psi	92	--
Tensile Strength Ratio, %	61	80 Min.

Aggregate Properties			
Aggregate Bulk Specific Gravity, G_{sb}			2.753
Aggregate Effective Specific Gravity, G_{se}			2.797
Sieve Size	**%Passing**	**Control Points**	
		Min	**Max**
37.5 mm (1 1/2")	100.0	--	--
25.0 mm (1")	99.8	--	--
19.0 mm (3/4")	98.1	100	--
12.5 mm (1/2")	95.2	90	100
9.5 mm (3/8")	88.6	--	90
4.75 mm (No. 4)	53.3	--	--
2.36 mm (No. 8)	30.4	28	58
2.00 mm (No. 10)	27.7	--	--
1.18 mm (No. 16)	22.9	--	--
0.6 mm (No. 30)	17.8	--	--
0.425 mm (No. 40)	14.8	--	--
0.3 mm (No. 50)	11.7	--	--
0.15 mm (No. 100)	6.3	--	--
0.075 mm (No. 200)	3.16	2	10
Aggregates	**Description**		**Bin %**
Aggr. 1	#57 Stone		6.0%
Aggr. 2	#789 Stone		73.0%
Aggr. 3	Washed Screenings		5.0%
Aggr. 4	Regular Screenings		16.0%

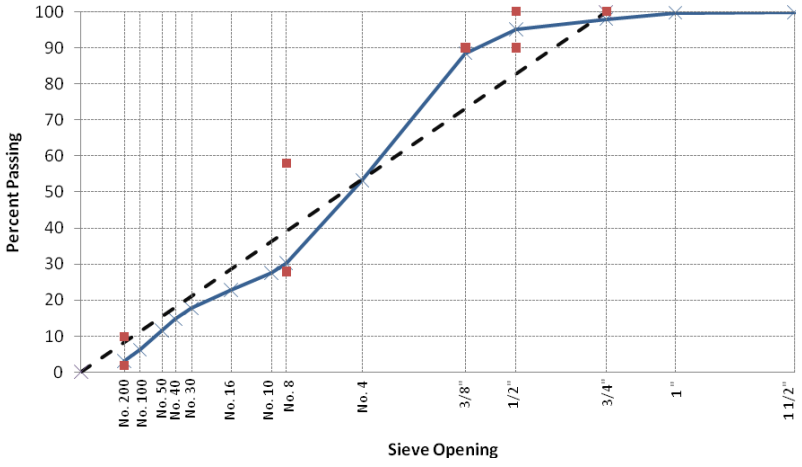

Figure 24. South Carolina Un-treated Mix Design and Aggregate Properties.

Mix Design		
Nominal Maximum Aggregate Size, mm		12.5
Property	**Value**	**Requirement**
Design ESALs, millions	6	--
N_{inital}	8	--
N_{design}	100	--
N_{max}	160	--
Optimum Binder Content, %	5.28	--
Hydrated Lime, %	None	--
Liquid Antistrip, %	0.5% by AC	--
Max theoretical specific gravity, G_{mm}	2.567	--
%Gmm at N_{ini}	86.8	≤ 89.0
%Gmm at N_{des}	96.0	96.0
%Gmm at N_{max}	97.5	≤ 98.0
VMA, %	15.2	14.0% Min.
VFA, %	73.8	65-75
Percent Effective Binder P_{be}, %	4.70	--
Dust Proportion, $P_{0.075}/P_{be}$	0.7	0.6-1.2
Unconditioned Tensile Strength on 4" Gyratory Samples @ 77°F, psi	154	--
Conditioned Tensile Strength on 4" Gyratory Samples @77°F, psi	125	--
Tensile Strength Ratio, %	82	80 Min.

Aggregate Properties			
Aggregate Bulk Specific Gravity, G_{sb}			2.753
Aggregate Effective Specific Gravity, G_{se}			2.798
Sieve Size	**%Passing**	**Control Points**	
		Min	**Max**
37.5 mm (1 1/2")	100.0	--	--
25.0 mm (1")	99.8	--	--
19.0 mm (3/4")	98.1	100	--
12.5 mm (1/2")	95.2	90	100
9.5 mm (3/8")	88.6	--	90
4.75 mm (No. 4)	53.3	--	--
2.36 mm (No. 8)	30.4	28	58
2.00 mm (No. 10)	27.7	--	--
1.18 mm (No. 16)	22.9	--	--
0.6 mm (No. 30)	17.8	--	--
0.425 mm (No. 40)	14.8	--	--
0.3 mm (No. 50)	11.7	--	--
0.15 mm (No. 100)	6.3	--	--
0.075 mm (No. 200)	3.16	2	10
Aggregates	**Description**		**Bin %**
Aggr. 1	#57 Stone		6.0%
Aggr. 2	#789 Stone		73.0%
Aggr. 3	Washed Screenings		5.0%
Aggr. 4	Regular Screenings		16.0%

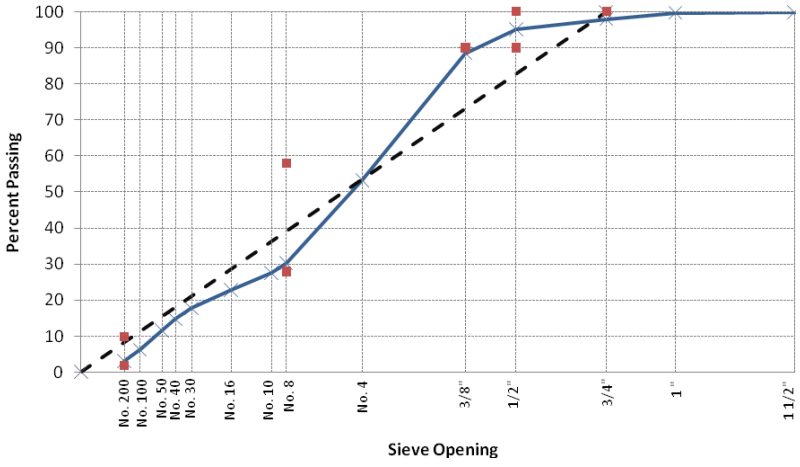

Figure 25. South Carolina Liquid-Treated Mix Design and Aggregate Properties.

Mix Design		
Nominal Maximum Aggregate Size, mm		12.5
Property	**Value**	**Requirement**
Design ESALs, millions	6	--
N_{inital}	8	--
N_{design}	100	--
N_{max}	160	--
Optimum Binder Content, %	4.71	--
Hydrated Lime, %	1% Lime by DWA	--
Liquid Antistrip, %	None	--
Max theoretical specific gravity, G_{mm}	2.581	--
%Gmm at N_{ini}	87.3	≤ 89.0
%Gmm at N_{des}	96.0	96.0
%Gmm at N_{max}	97.4	≤ 98.0
VMA, %	14.1	14.0% Min.
VFA, %	71.8	65-75
Percent Effective Binder P_{be}, %	4.21	--
Dust Proportion, $P_{0.075}/P_{be}$	0.9	0.6-1.2
Unconditioned Tensile Strength on 4" Gyratory Samples @ 77°F, psi	162	--
Conditioned Tensile Strength on 4" Gyratory Samples @77°F, psi	141	--
Tensile Strength Ratio, %	87	80 Min.

Aggregate Properties			
Aggregate Bulk Specific Gravity, G_{sb}			2.748
Aggregate Effective Specific Gravity, G_{se}			2.787
Sieve Size	**%Passing**	**Control Points**	
		Min	**Max**
37.5 mm (1 1/2")	100.0	--	--
25.0 mm (1")	99.8	--	--
19.0 mm (3/4")	98.1	100	--
12.5 mm (1/2")	95.2	90	100
9.5 mm (3/8")	88.6	--	90
4.75 mm (No. 4)	53.3	--	--
2.36 mm (No. 8)	30.6	28	58
2.00 mm (No. 10)	27.9	--	--
1.18 mm (No. 16)	23.2	--	--
0.6 mm (No. 30)	18.3	--	--
0.425 mm (No. 40)	15.3	--	--
0.3 mm (No. 50)	12.3	--	--
0.15 mm (No. 100)	7.1	--	--
0.075 mm (No. 200)	4.02	2	10
Aggregates	**Description**		**Bin %**
Aggr. 1	#57 Stone		6.0%
Aggr. 2	#789 Stone		73.0%
Aggr. 3	Washed Screenings		5.0%
Aggr. 4	Regular Screenings		15.0%
Aggr. 5	Lime		1.0%

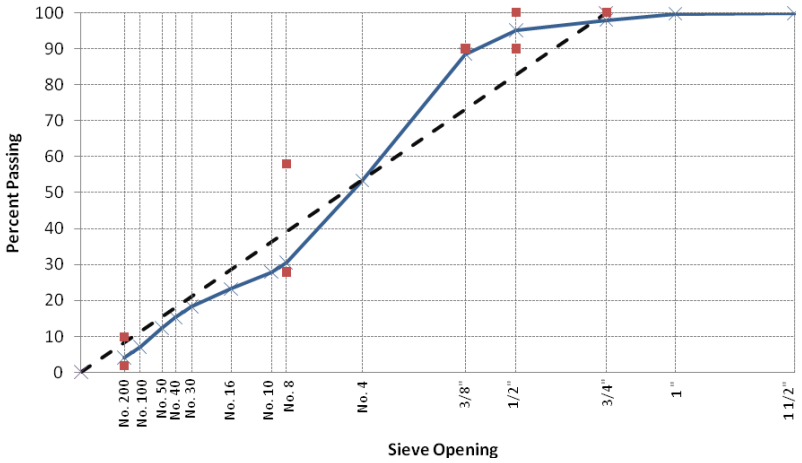

Figure 26. South Carolina Lime-Treated Mix Design and Aggregate Properties.

Mix Design		
Nominal Maximum Aggregate Size, mm		19.0
Property	**Value**	**Requirement**
Design ESALs, millions	6	--
N_{inital}	8	--
N_{design}	100	--
N_{max}	160	--
Optimum Binder Content, %	4.70	--
Hydrated Lime, %	None	--
Liquid Antistrip, %	None	--
Max theoretical specific gravity, G_{mm}	2.433	--
%Gmm at N_{ini}	88.1	≤ 89.0
%Gmm at N_{des}	96.0	96.0
%Gmm at N_{max}	96.4	≤ 98.0
VMA, %	13.7	13.0% Min.
VFA, %	70.8	65-75
Percent Effective Binder P_{be}, %	4.28	--
Dust Proportion, $P_{0.075}/P_{be}$	0.6	0.6-1.2
Unconditioned Tensile Strength on 4" Gyratory Samples @ 77°F, psi	159	--
Conditioned Tensile Strength on 4" Gyratory Samples @77°F, psi	98	--
Tensile Strength Ratio, %	61	80 Min.

Aggregate Properties			
Aggregate Bulk Specific Gravity, G_{sb}			2.578
Aggregate Effective Specific Gravity, G_{se}			2.607
Sieve Size	**%Passing**	**Control Points**	
		Min	**Max**
37.5 mm (1 1/2")	100.0	--	--
25.0 mm (1")	100.0	100	--
19.0 mm (3/4")	99.7	90	100
12.5 mm (1/2")	87.4	--	90
9.5 mm (3/8")	79.3	--	--
4.75 mm (No. 4)	55.1	--	--
2.36 mm (No. 8)	37.8	23	49
2.00 mm (No. 10)	34.4	--	--
1.18 mm (No. 16)	26.1	--	--
0.6 mm (No. 30)	17.8	--	--
0.425 mm (No. 40)	13.1	--	--
0.3 mm (No. 50)	8.8	--	--
0.15 mm (No. 100)	4.3	--	--
0.075 mm (No. 200)	2.74	2	8
Aggregates	**Description**		**Bin %**
Aggr. 1	3/4 - 1/2 inch		15.0%
Aggr. 2	1/2 - 1/4 inch		31.0%
Aggr. 3	1/4" - 2 mm		18.0%
Aggr. 4	2 mm - 0		13.0%
Aggr. 5	Man. Sand		13.0%
Aggr. 6	Conc. Sand		10.0%

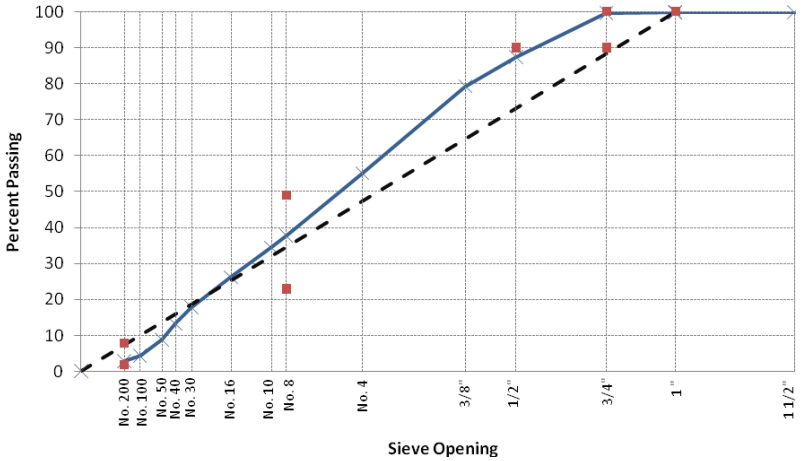

Figure 27. Texas Un-treated Mix Design and Aggregate Properties.

Mix Design		
Nominal Maximum Aggregate Size, mm		19.0
Property	**Value**	**Requirement**
Design ESALs, millions	6	--
N_{inital}	8	--
N_{design}	100	--
N_{max}	160	--
Optimum Binder Content, %	4.55	--
Hydrated Lime, %	None	--
Liquid Antistrip, %	0.5% by AC	--
Max theoretical specific gravity, G_{mm}	2.432	--
%Gmm at N_{ini}	88.7	≤ 89.0
%Gmm at N_{des}	96.0	96.0
%Gmm at N_{max}	96.7	≤ 98.0
VMA, %	13.6	13.0% Min.
VFA, %	70.4	65-75
Percent Effective Binder P_{be}, %	4.23	--
Dust Proportion, $P_{0.075}/P_{be}$	0.6	0.6-1.2
Unconditioned Tensile Strength on 4" Gyratory Samples @ 77°F, psi	112	--
Conditioned Tensile Strength on 4" Gyratory Samples @77°F, psi	112	--
Tensile Strength Ratio, %	100	80 Min.

Aggregate Properties			
Aggregate Bulk Specific Gravity, G_{sb}			2.578
Aggregate Effective Specific Gravity, G_{se}			2.600
Sieve Size	**%Passing**	**Control Points**	
		Min	**Max**
37.5 mm (1 1/2")	100.0	--	--
25.0 mm (1")	100.0	100	--
19.0 mm (3/4")	99.7	90	100
12.5 mm (1/2")	87.4	--	90
9.5 mm (3/8")	79.3	--	--
4.75 mm (No. 4)	55.1	--	--
2.36 mm (No. 8)	37.8	23	49
2.00 mm (No. 10)	34.4	--	--
1.18 mm (No. 16)	26.1	--	--
0.6 mm (No. 30)	17.8	--	--
0.425 mm (No. 40)	13.1	--	--
0.3 mm (No. 50)	8.8	--	--
0.15 mm (No. 100)	4.3	--	--
0.075 mm (No. 200)	2.74	2	8
Aggregates	**Description**		**Bin %**
Aggr. 1	3/4 - 1/2 inch		15.0%
Aggr. 2	1/2 - 1/4 inch		31.0%
Aggr. 3	1/4" - 2 mm		18.0%
Aggr. 4	2 mm - 0		13.0%
Aggr. 5	Man. Sand		13.0%
Aggr. 6	Conc. Sand		10.0%

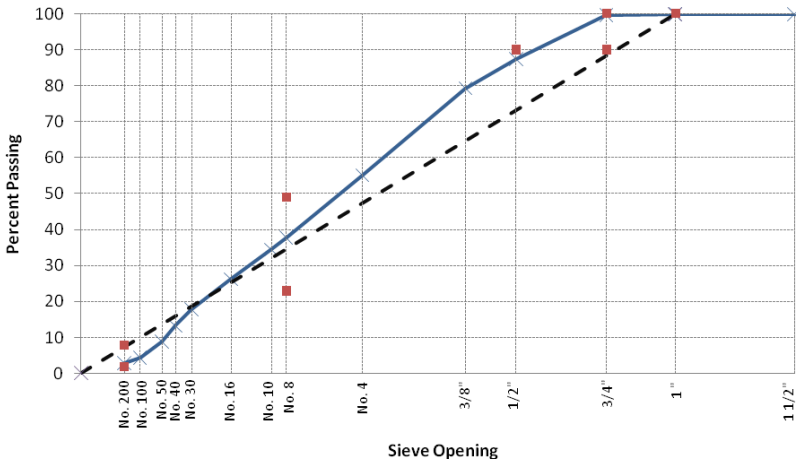

Figure 28. Texas Liquid-Treated Mix Design and Aggregate Properties.

Mix Design		
Nominal Maximum Aggregate Size, mm		19.0
Property	**Value**	**Requirement**
Design ESALs, millions	6	--
N_{inital}	8	--
N_{design}	100	--
N_{max}	160	--
Optimum Binder Content, %	4.78	--
Hydrated Lime, %	1% Lime by DWA	--
Liquid Antistrip, %	None	--
Max theoretical specific gravity, G_{mm}	2.431	--
%Gmm at N_{ini}	88.0	≤ 89.0
%Gmm at N_{des}	96.0	96.0
%Gmm at N_{max}	97.9	≤ 98.0
VMA, %	13.2	13.0% Min.
VFA, %	69.8	65-75
Percent Effective Binder P_{be}, %	4.08	--
Dust Proportion, $P_{0.075}/P_{be}$	0.9	0.6-1.2
Unconditioned Tensile Strength on 4" Gyratory Samples @ 77°F, psi	155	--
Conditioned Tensile Strength on 4" Gyratory Samples @77°F, psi	153	--
Tensile Strength Ratio, %	98	80 Min.

Aggregate Properties			
Aggregate Bulk Specific Gravity, G_{sb}			2.560
Aggregate Effective Specific Gravity, G_{se}			2.608
Sieve Size	**%Passing**	**Control Points**	
		Min	**Max**
37.5 mm (1 1/2")	100.0	--	--
25.0 mm (1")	100.0	100	--
19.0 mm (3/4")	99.7	90	100
12.5 mm (1/2")	87.4	--	90
9.5 mm (3/8")	79.3	--	--
4.75 mm (No. 4)	55.1	--	--
2.36 mm (No. 8)	37.9	23	49
2.00 mm (No. 10)	34.6	--	--
1.18 mm (No. 16)	26.4	--	--
0.6 mm (No. 30)	18.3	--	--
0.425 mm (No. 40)	13.8	--	--
0.3 mm (No. 50)	9.5	--	--
0.15 mm (No. 100)	5.1	--	--
0.075 mm (No. 200)	3.64	2	8
Aggregates	**Description**		**Bin %**
Aggr. 1	3/4 - 1/2 inch		15.0%
Aggr. 2	1/2 - 1/4 inch		31.0%
Aggr. 3	1/4" - 2 mm		18.0%
Aggr. 4	2 mm - 0		13.0%
Aggr. 5	Man. Sand		12.0%
Aggr. 6	Conc. Sand		10.0%
Aggr. 7	Lime		1.0%

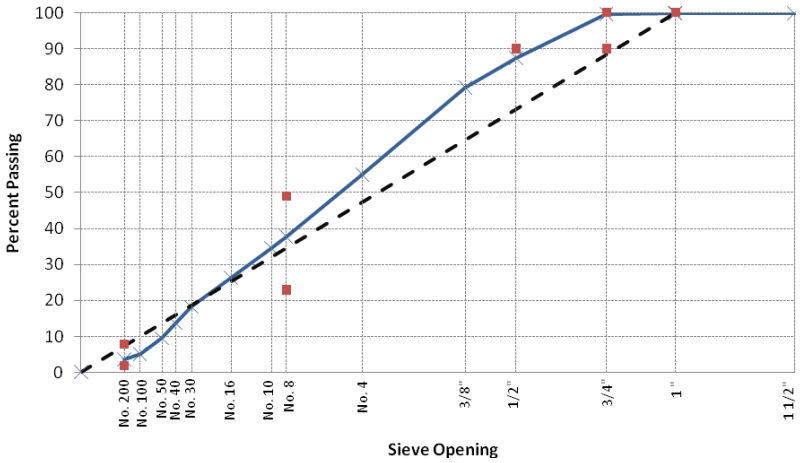

Figure 29. Texas Lime-Treated Mix Design and Aggregate Properties.

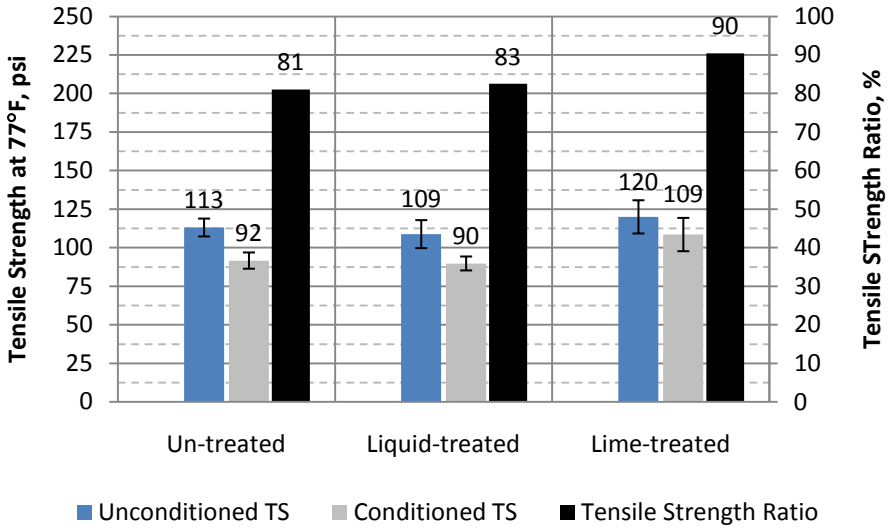

Figure 30. Tensile Strength Values at 77°F and TSR Values for the Alabama Mixtures. (Numbers above bars represent mean values and whiskers represent mean ± 1 STD)

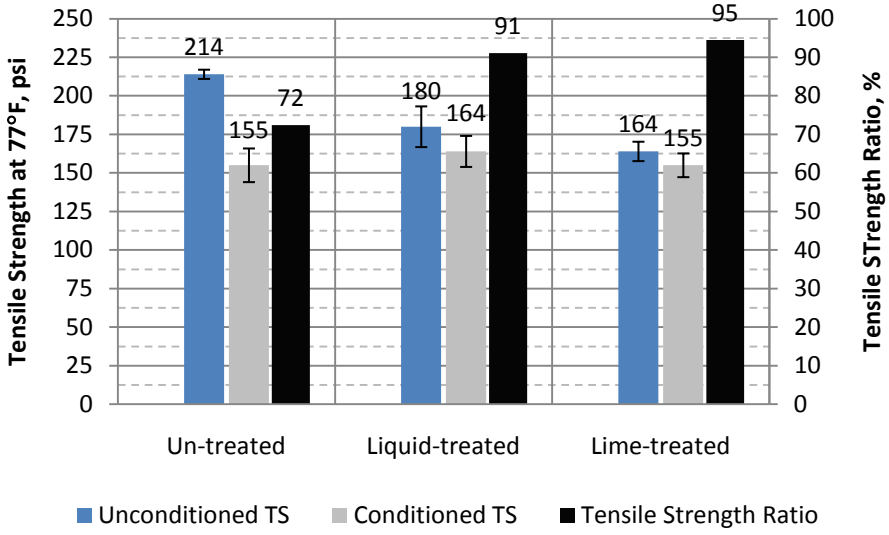

Figure 31. Tensile Strength Values at 77°F and TSR Values for the California Mixtures. (Numbers above bars represent mean values and whiskers represent mean ± 1 STD)

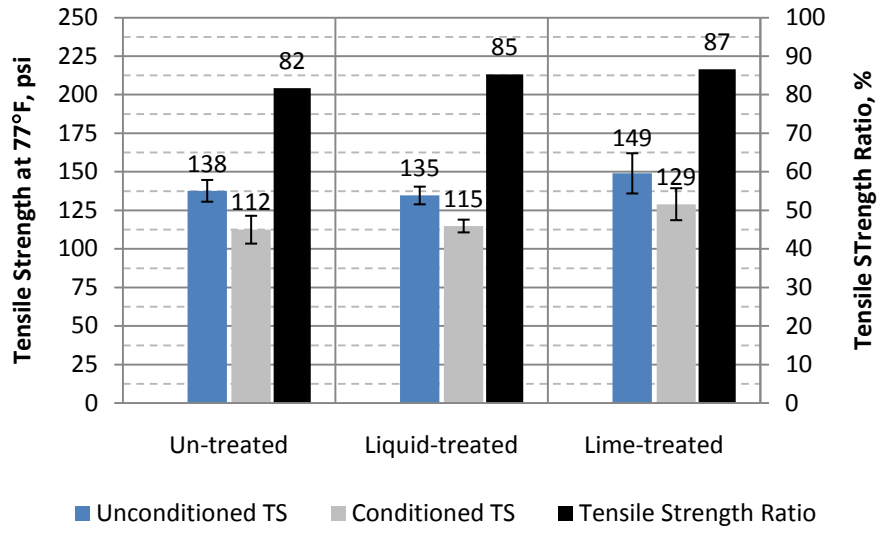

Figure 32. Tensile Strength Values at 77°F and TSR Values for the Illinois Mixtures. (Numbers above bars represent mean values and whiskers represent mean ± 1 STD)

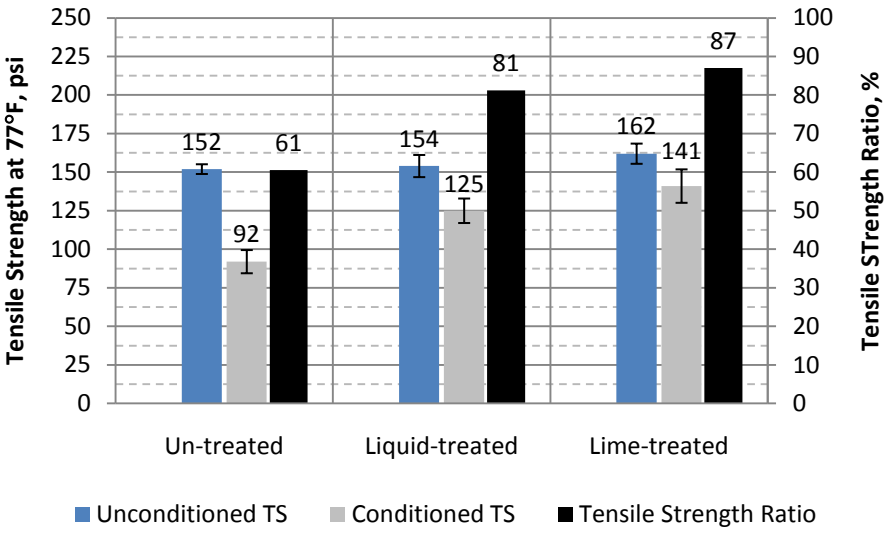

Figure 33. Tensile Strength Values at 77°F and TSR Values for the South Carolina Mixtures. (Numbers above bars represent mean values and whiskers represent mean ± 1 STD)

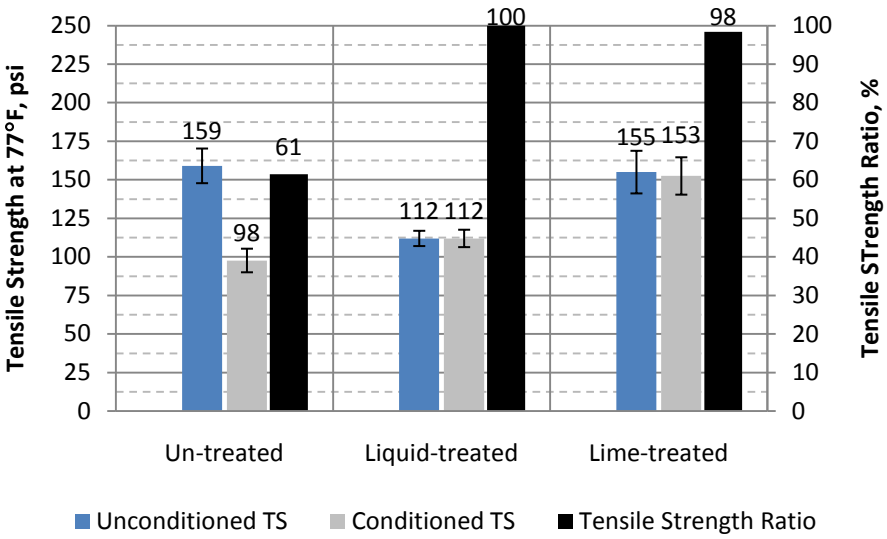

Figure 34. Tensile Strength Values at 77°F and TSR Values for the Texas Mixtures. (Numbers above bars represent mean values and whiskers represent mean ± 1 STD)

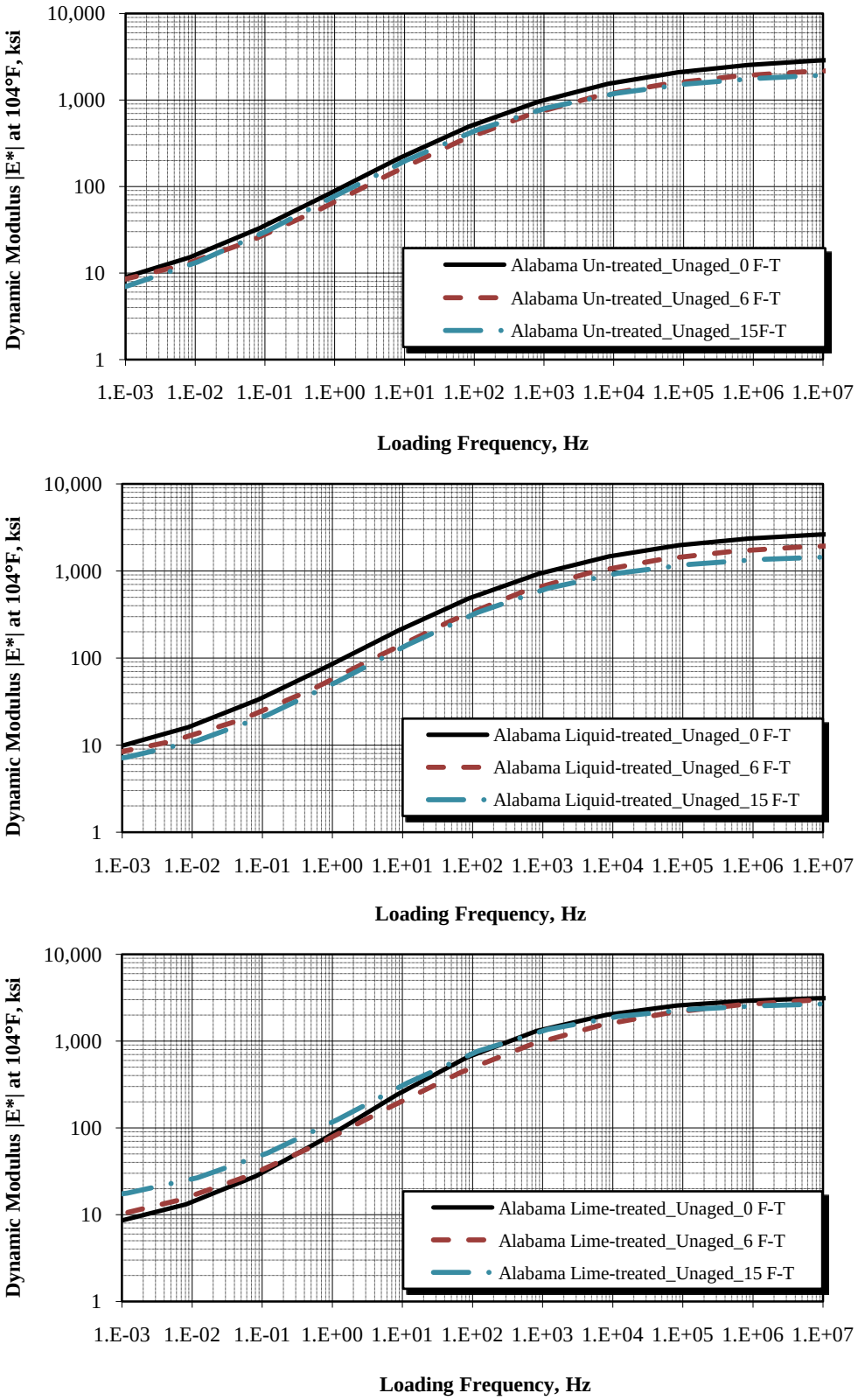

Figure 35. Dynamic Modulus Master Curve at 104°F for Unaged Alabama Mixes.

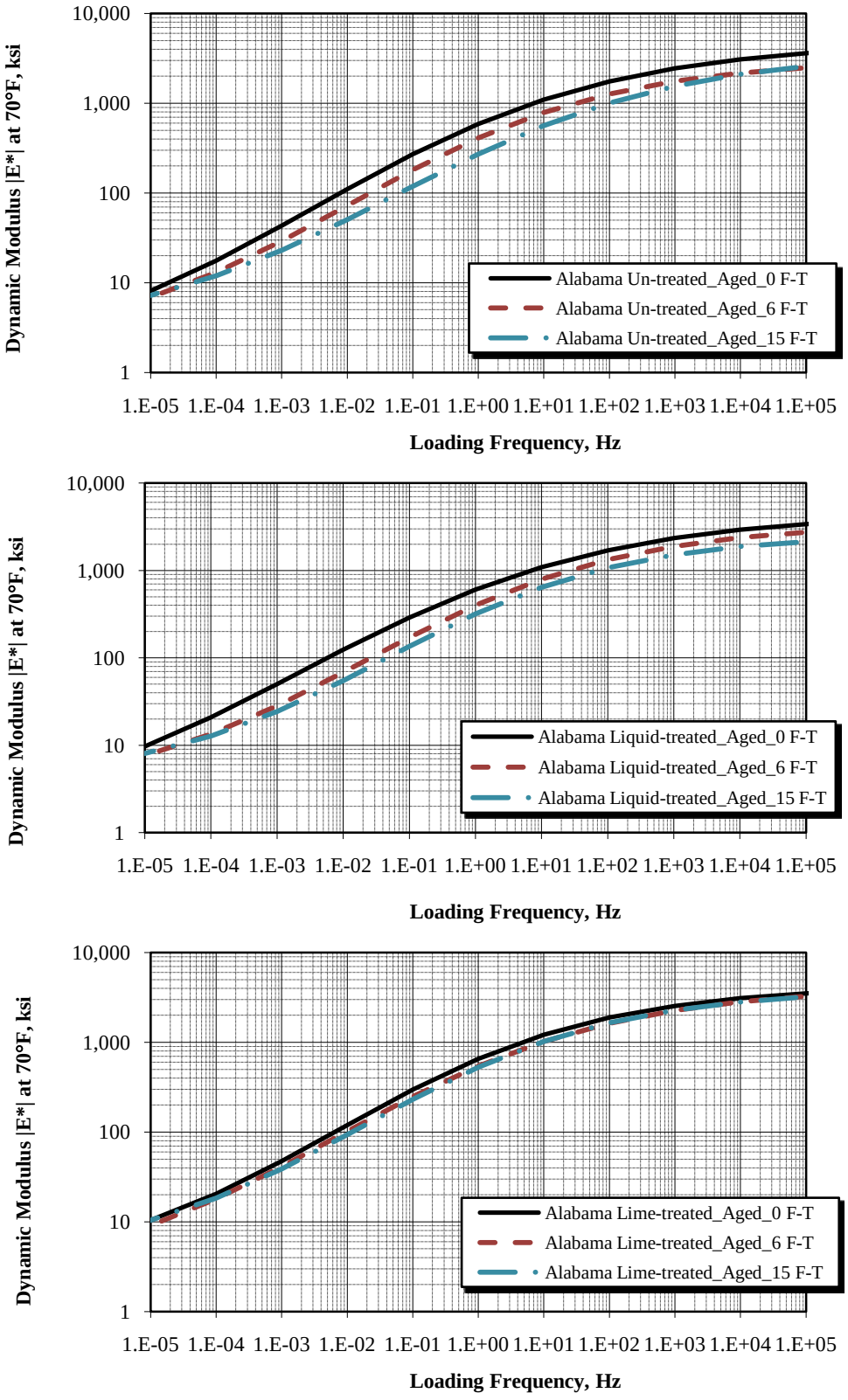

Figure 36. Dynamic Modulus Master Curve at 70°F for Aged Alabama Mixes.

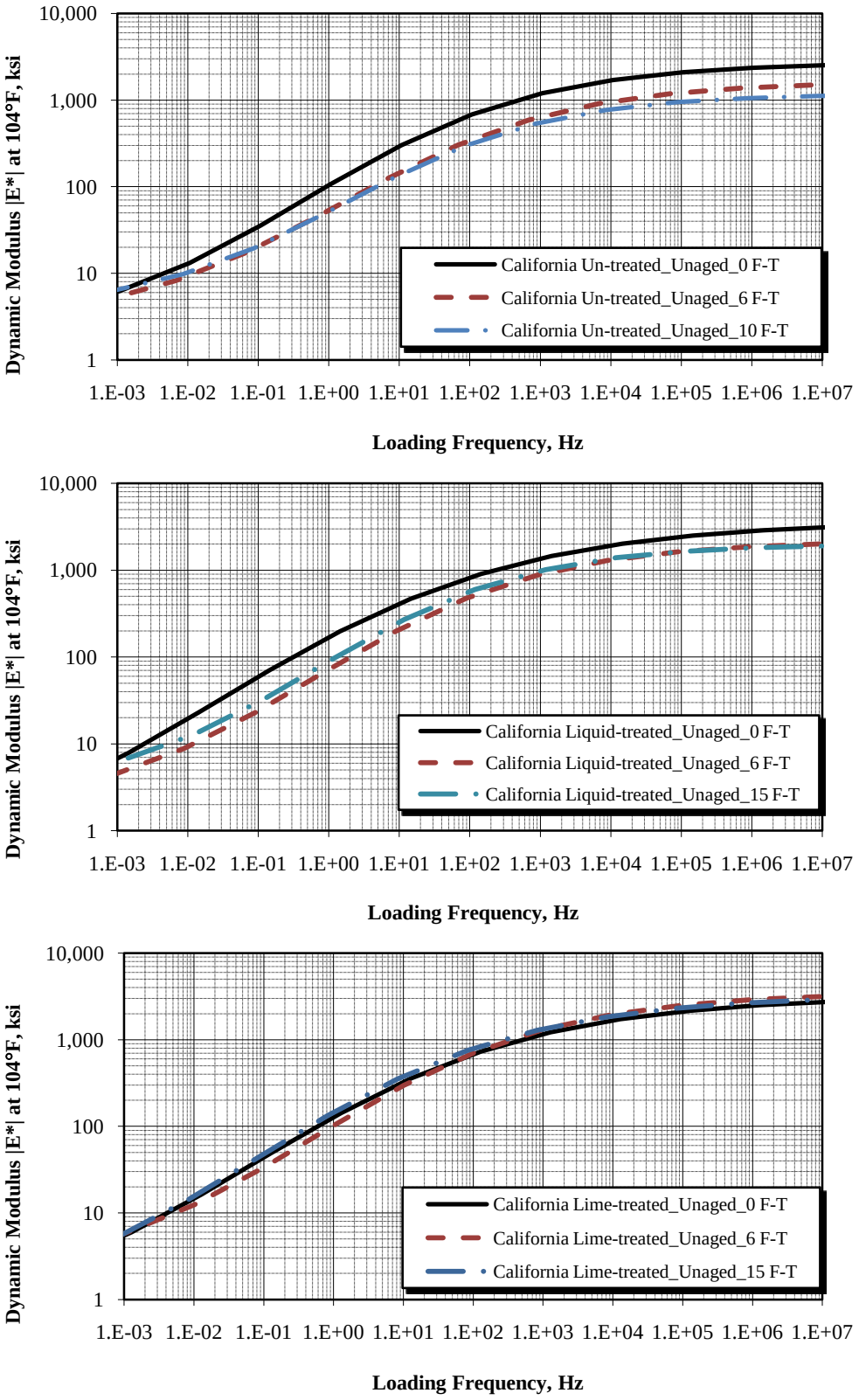

Figure 37. Dynamic Modulus Master Curve at 104°F for Unaged California Mixes.

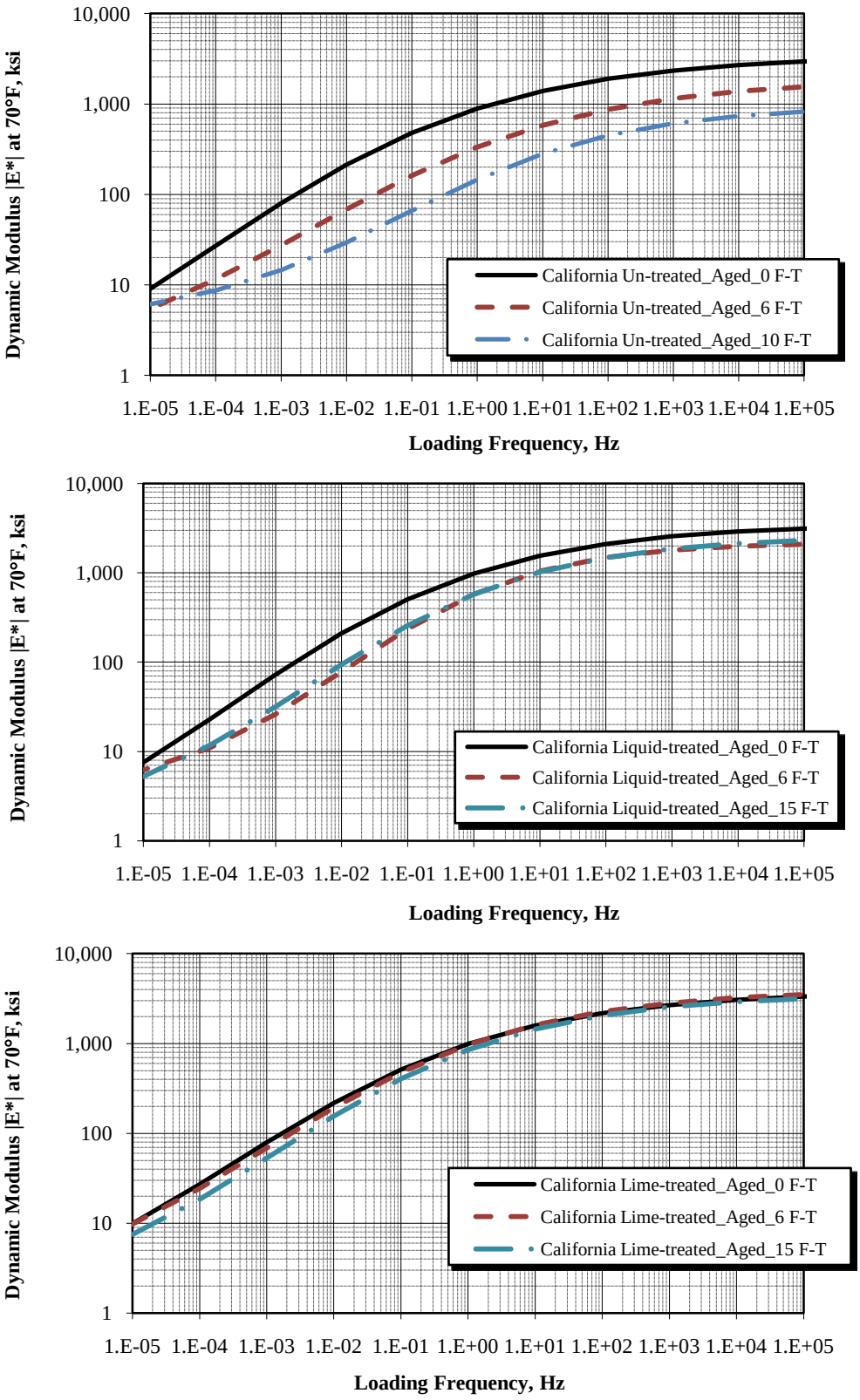

Figure 38. Dynamic Modulus Master Curve at 70°F for Aged California Mixes.

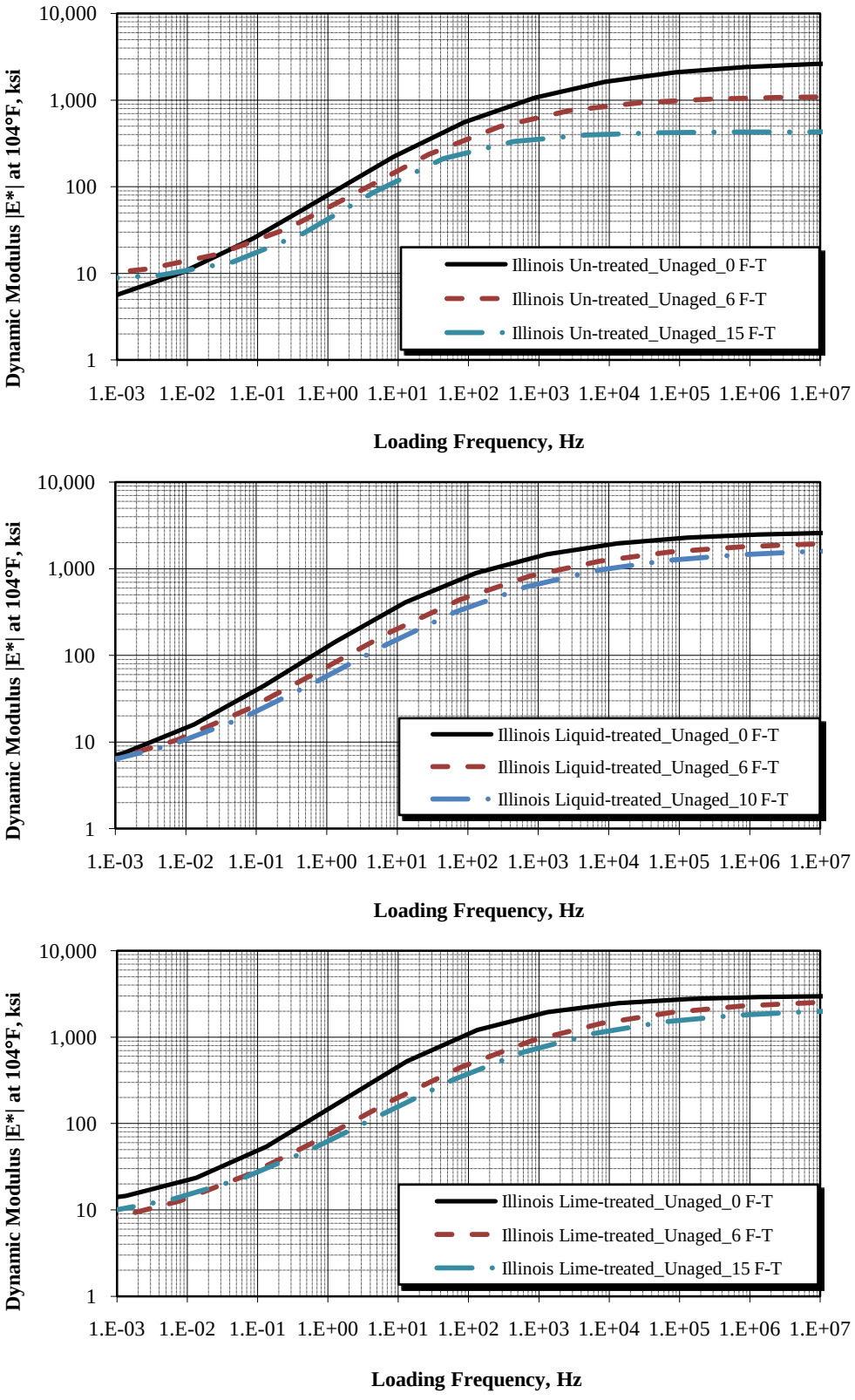

Figure 39. Dynamic Modulus Master Curve at 104°F for Unaged Illinois Mixes.

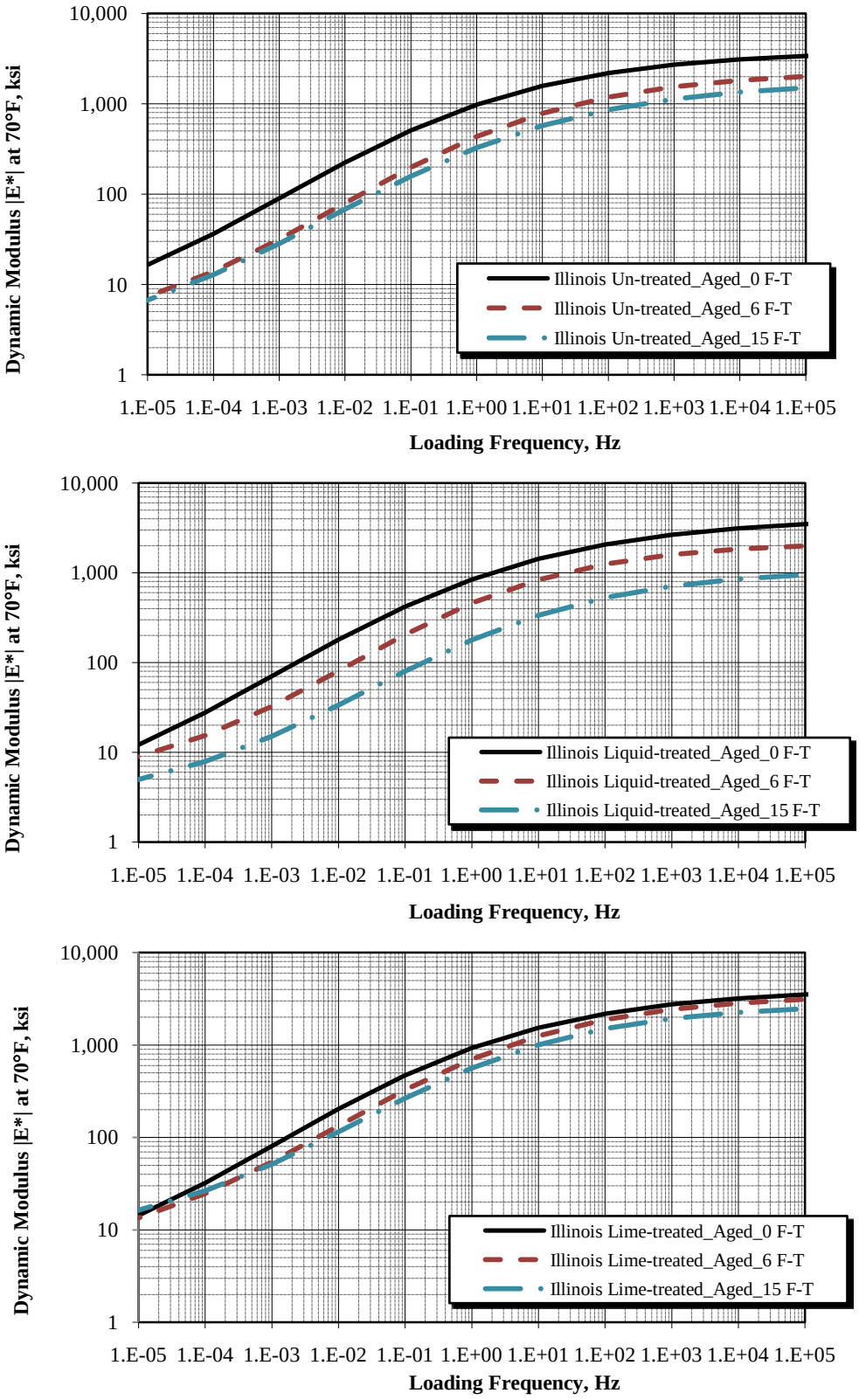

Figure 40. Dynamic Modulus Master Curve at 70°F for Aged Illinois Mixes.

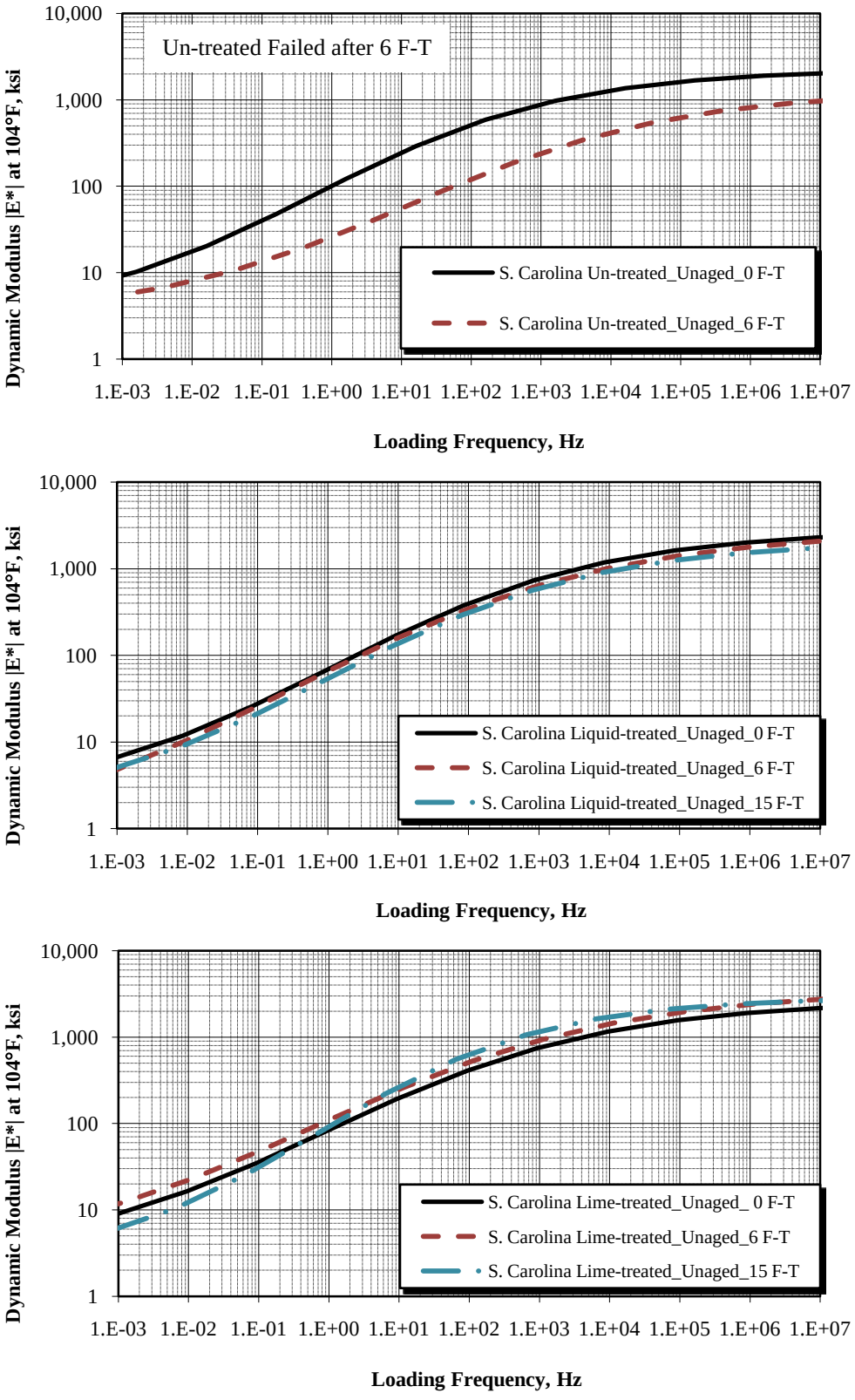

Figure 41. Dynamic Modulus Master Curve at 104°F for Unaged South Carolina Mixes.

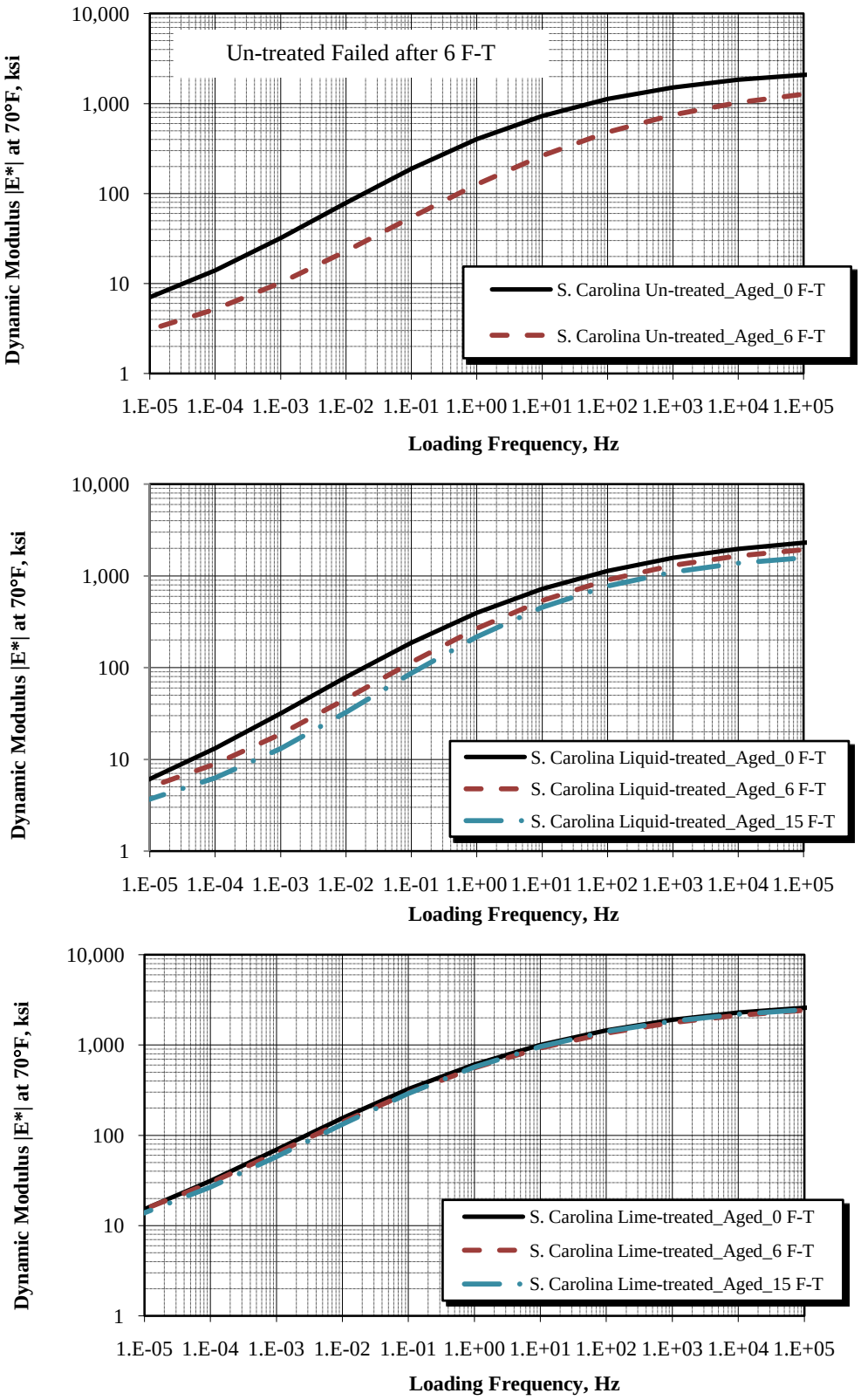

Figure 42. Dynamic Modulus Master Curve at 70°F for Aged South Carolina Mixes.

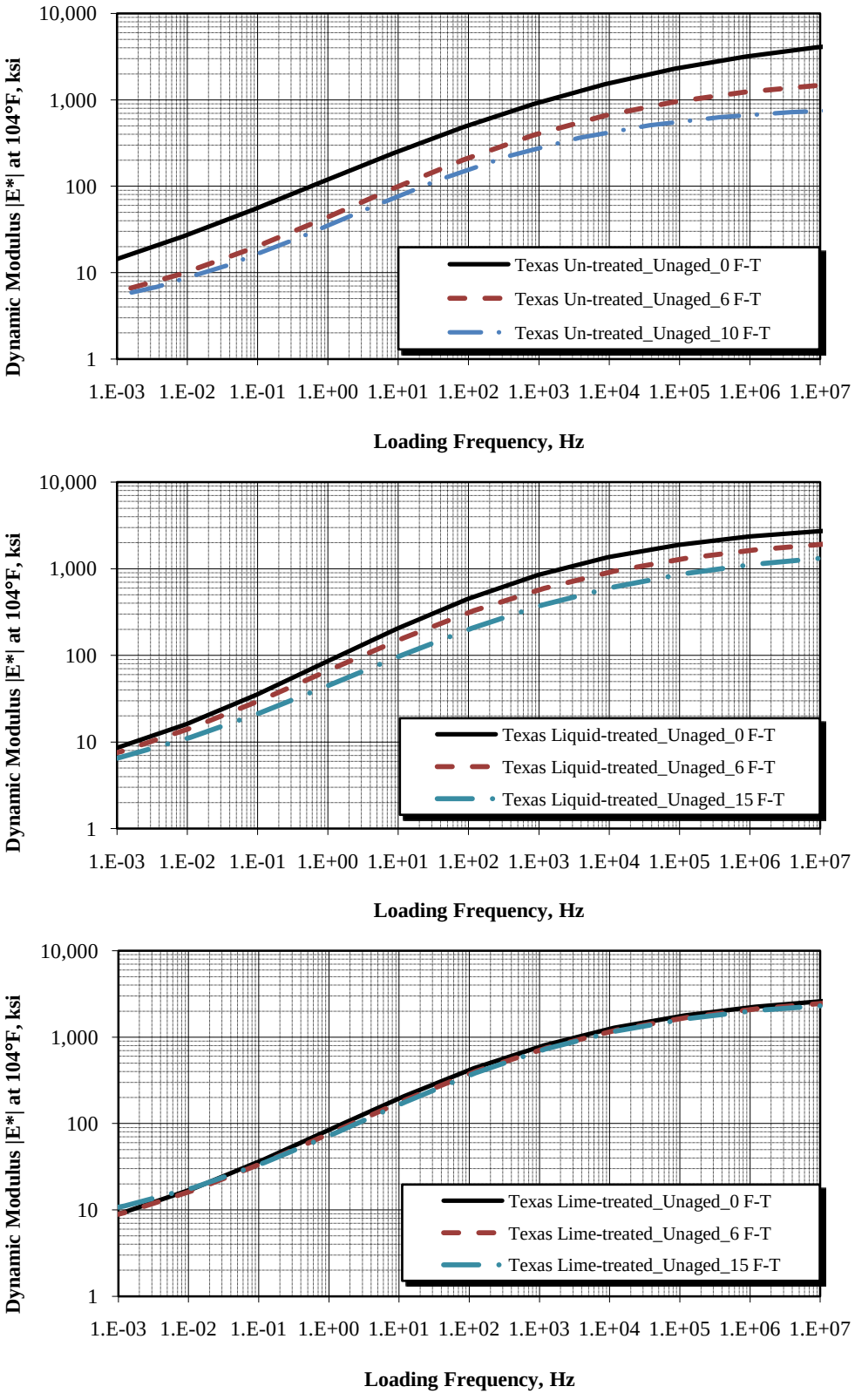

Figure 43. Dynamic Modulus Master Curve at 104°F for Unaged Texas Mixes.

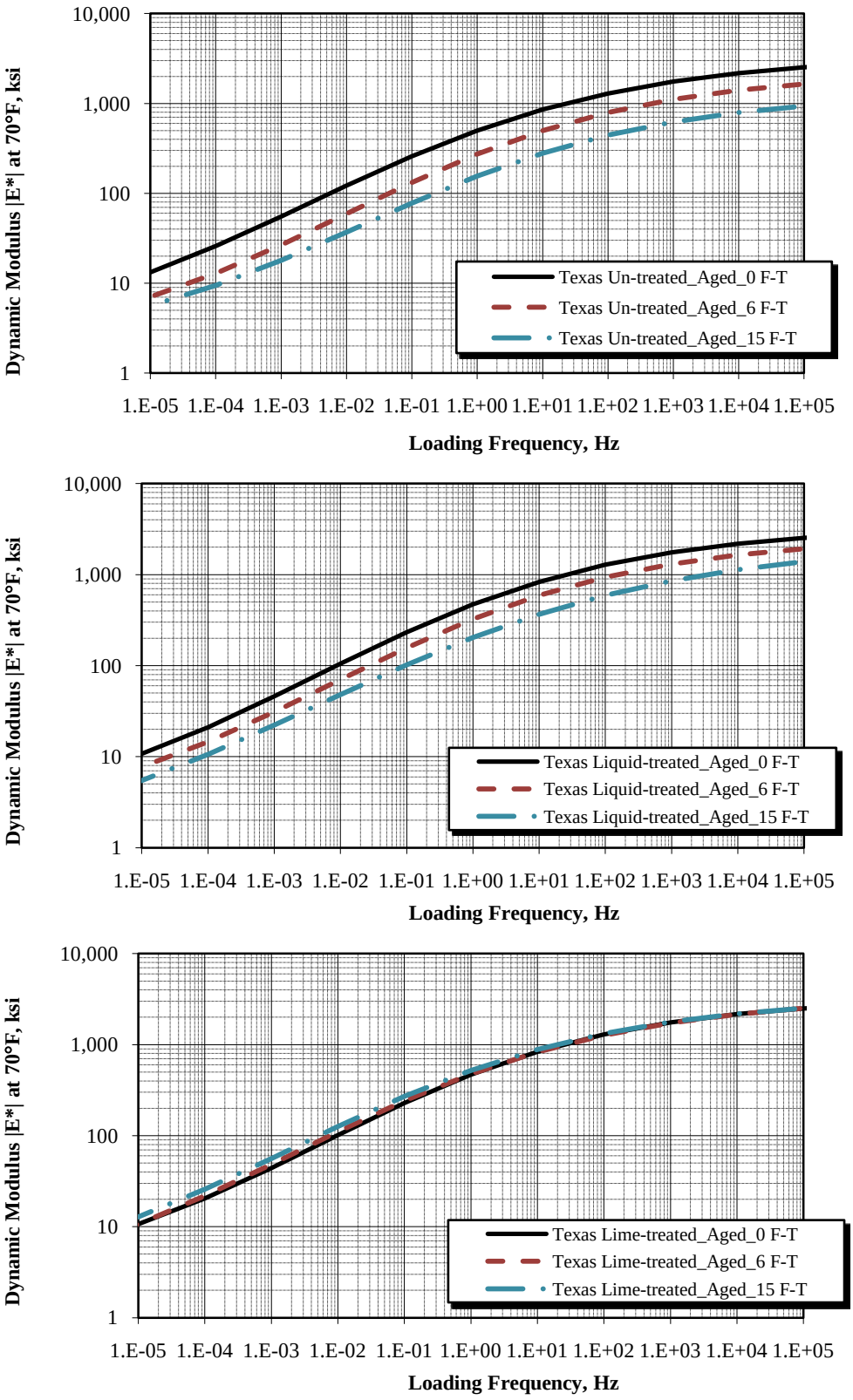

Figure 44. Dynamic Modulus Master Curve at 70°F for Aged Texas Mixes.

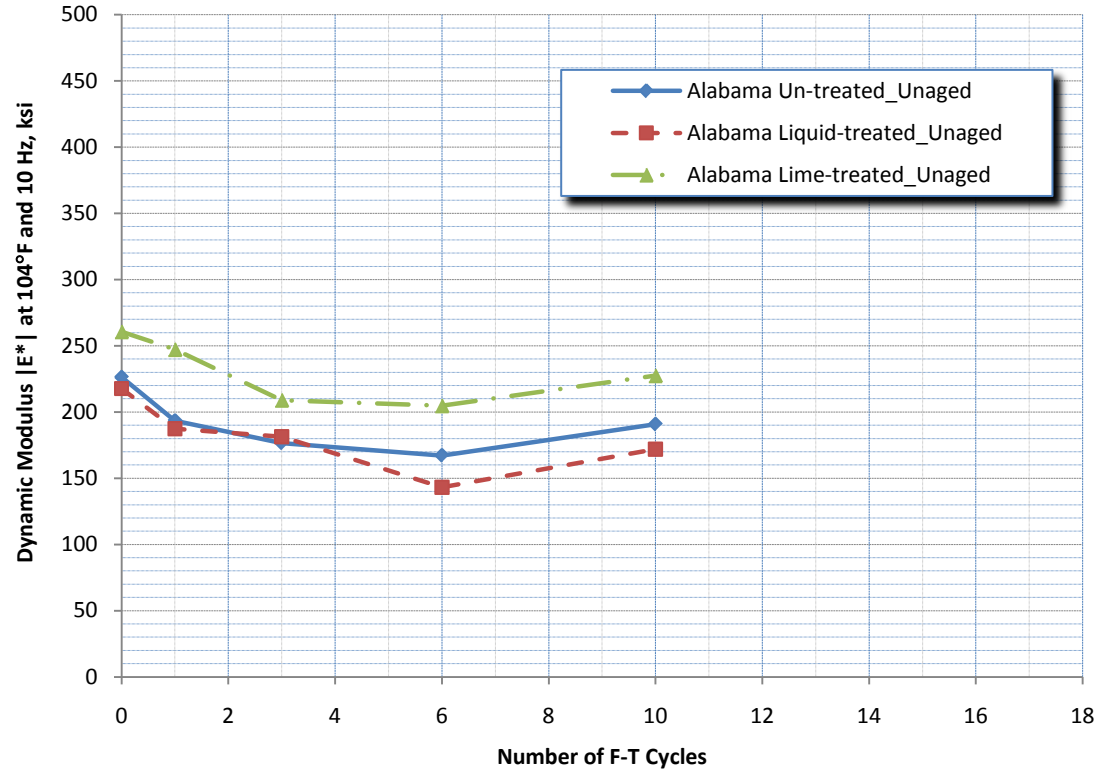

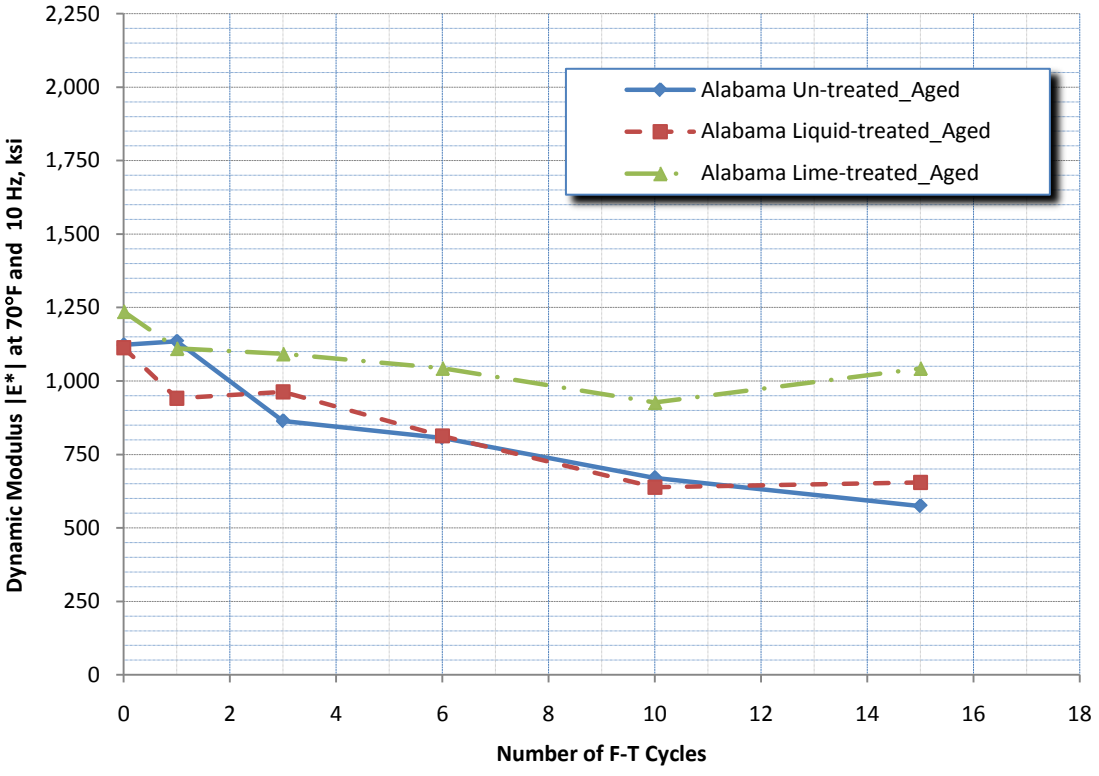

Figure 45. Dynamic Modulus at 104°F and 70°F for Alabama Mixes at Various F-T Cycles.

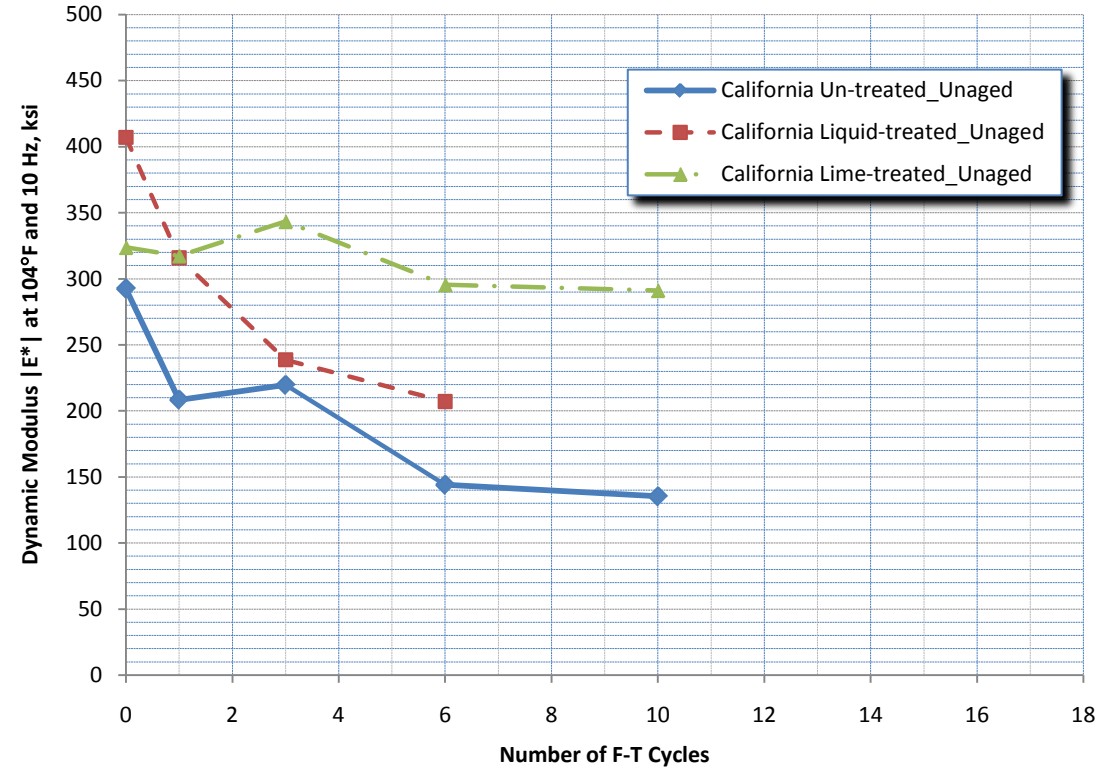

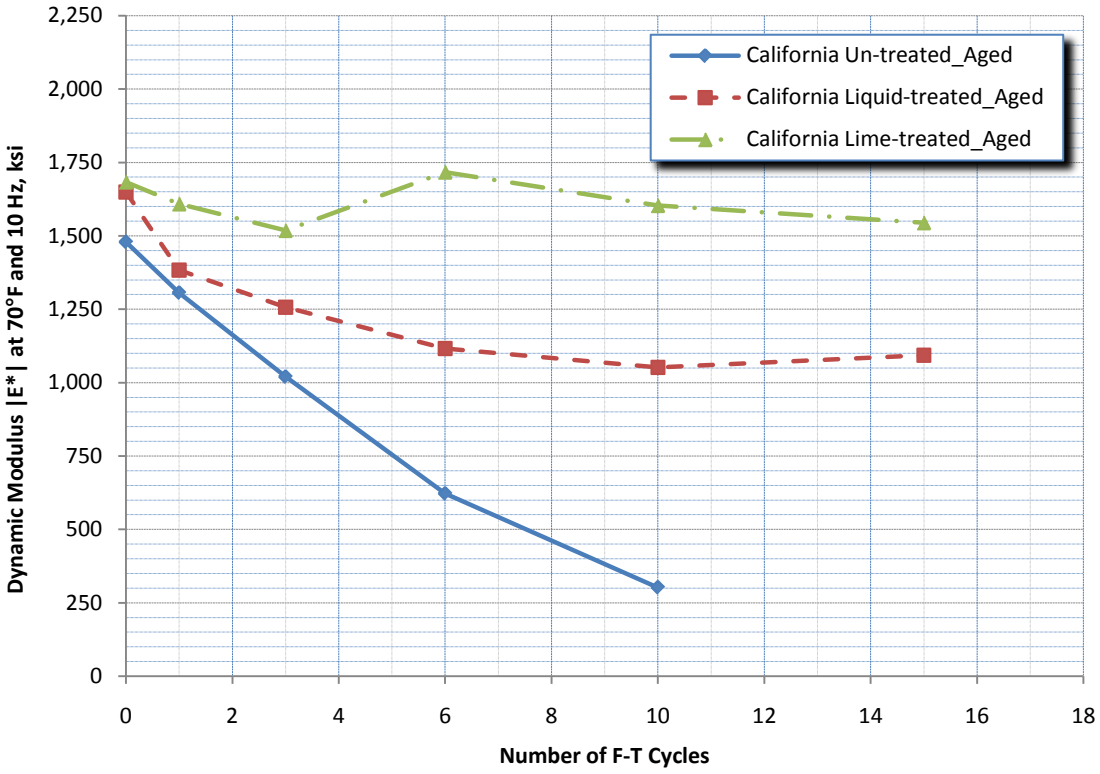

Figure 46. Dynamic Modulus at 104°F and 70°F for California Mixes at Various F-T Cycles.

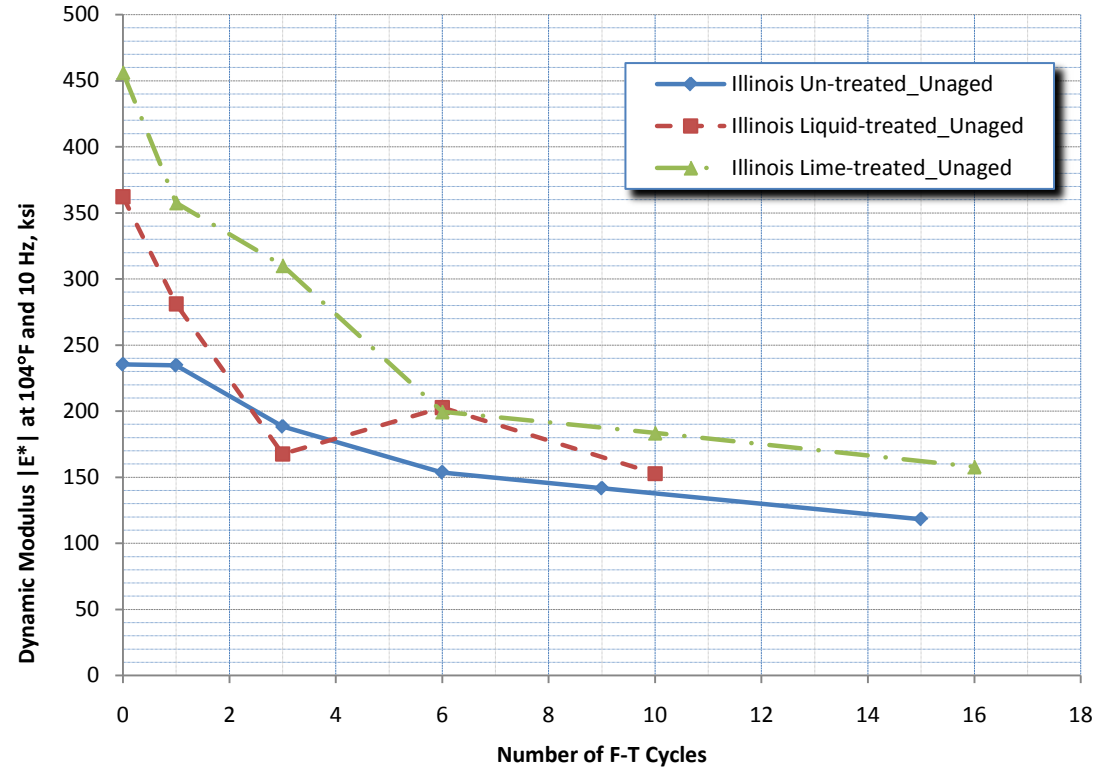

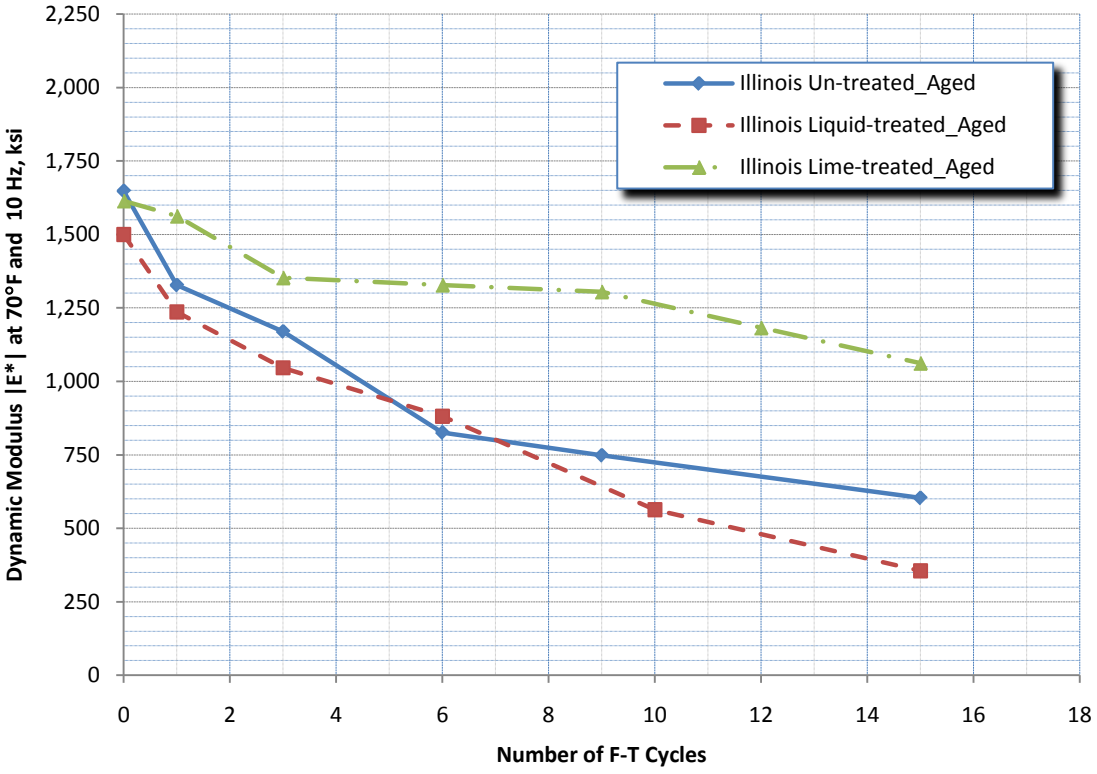

Figure 47. Dynamic Modulus at 104°F and 70°F for Illinois Mixes at Various F-T Cycles.

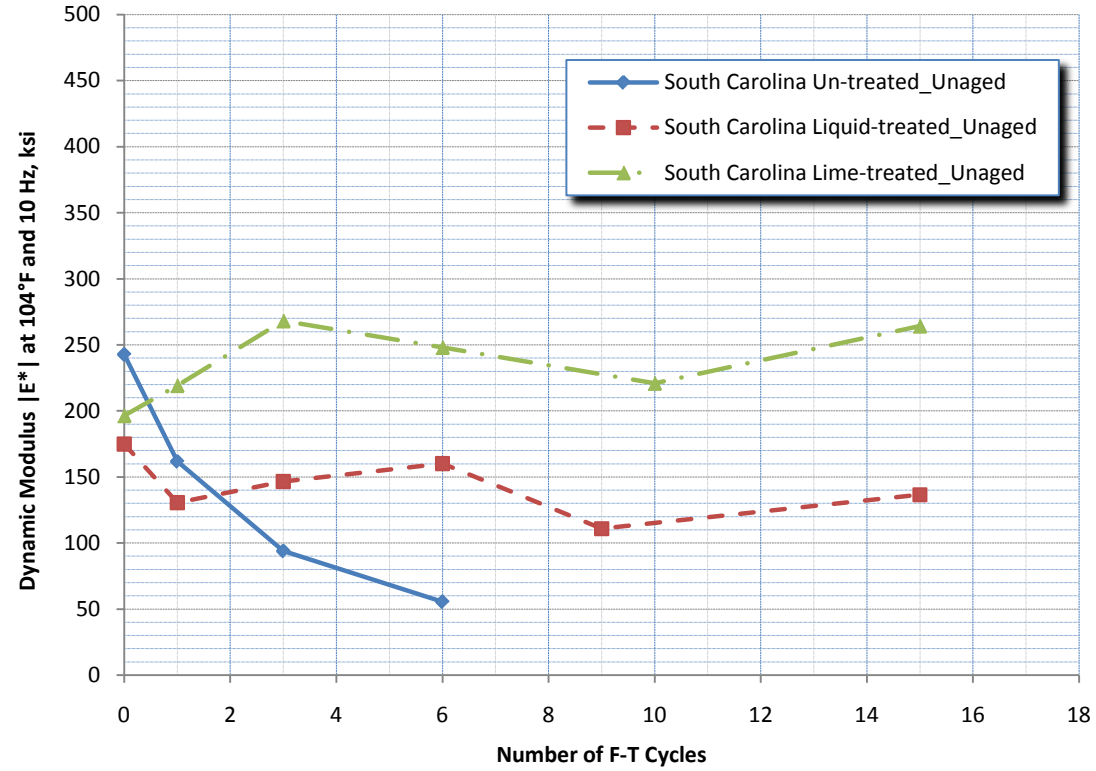

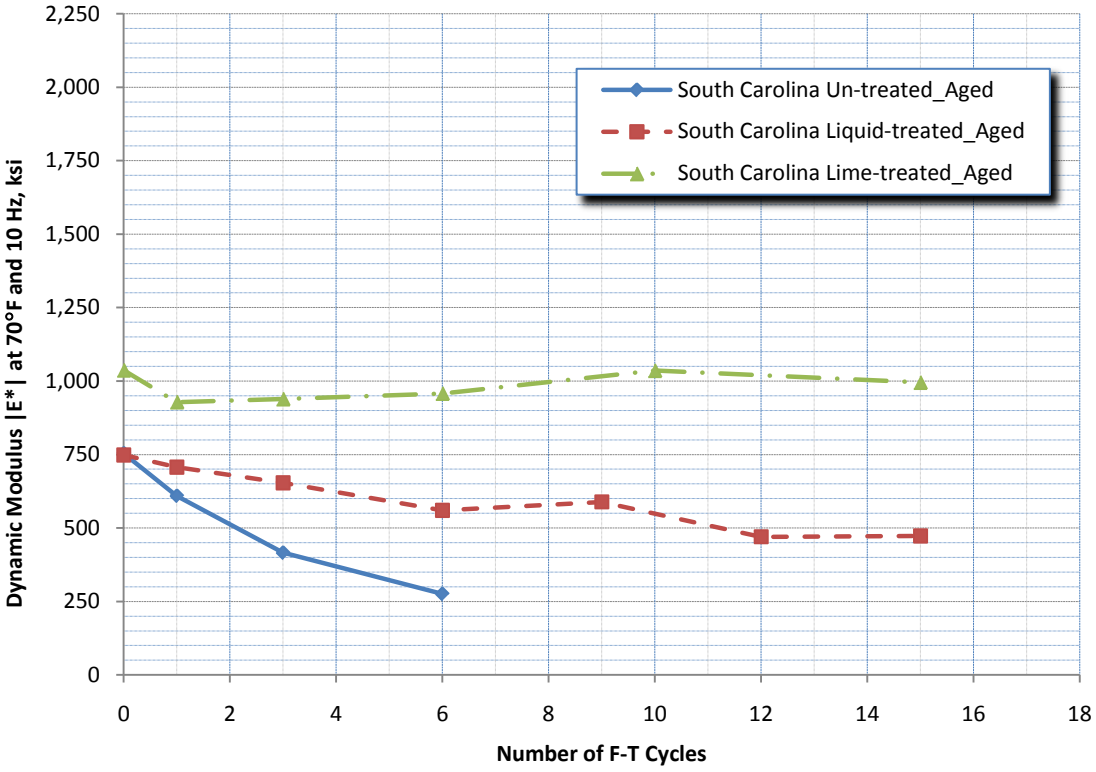

Figure 48. Dynamic Modulus at 104°F and 70°F for S. Carolina Mixes at Various F-T Cycles.

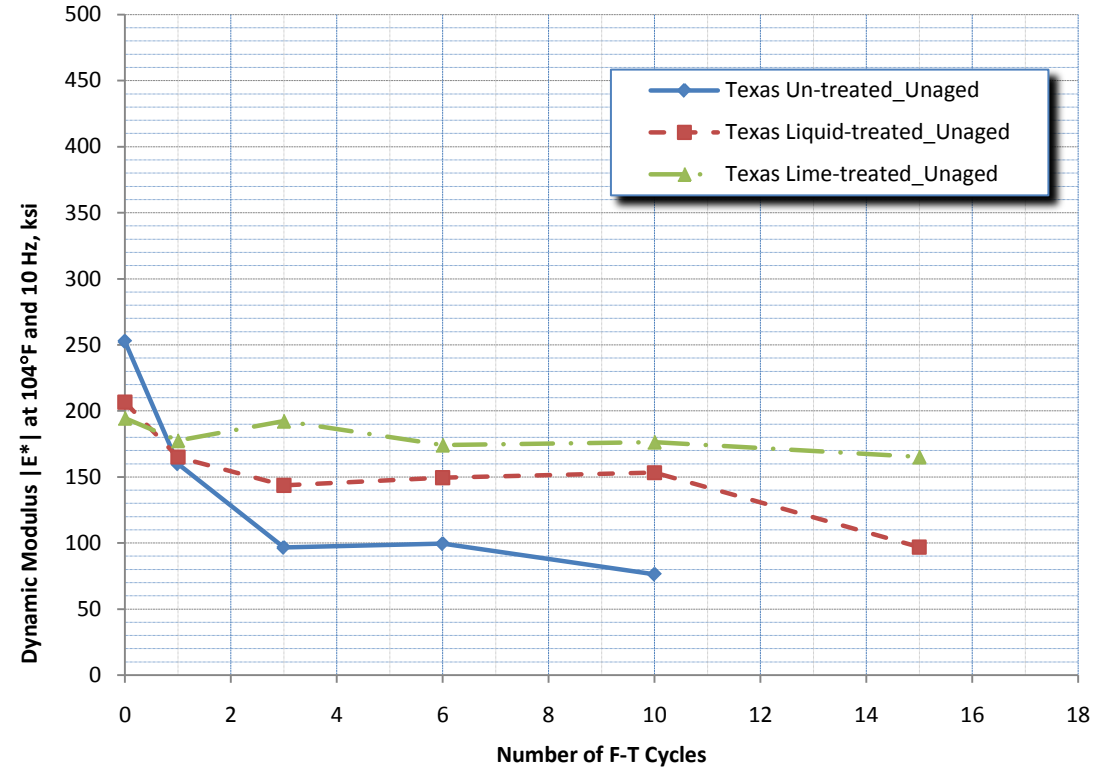

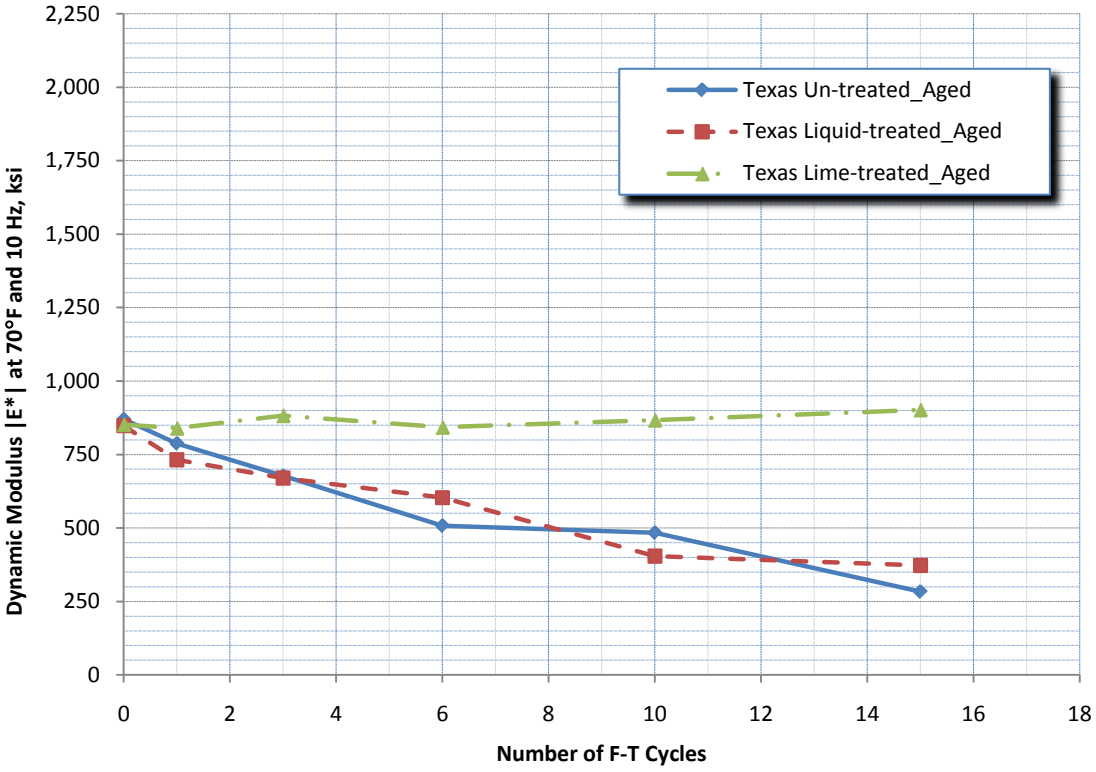

Figure 49. Dynamic Modulus at 104°F and 70°F for Texas Mixes at Various F-T Cycles.

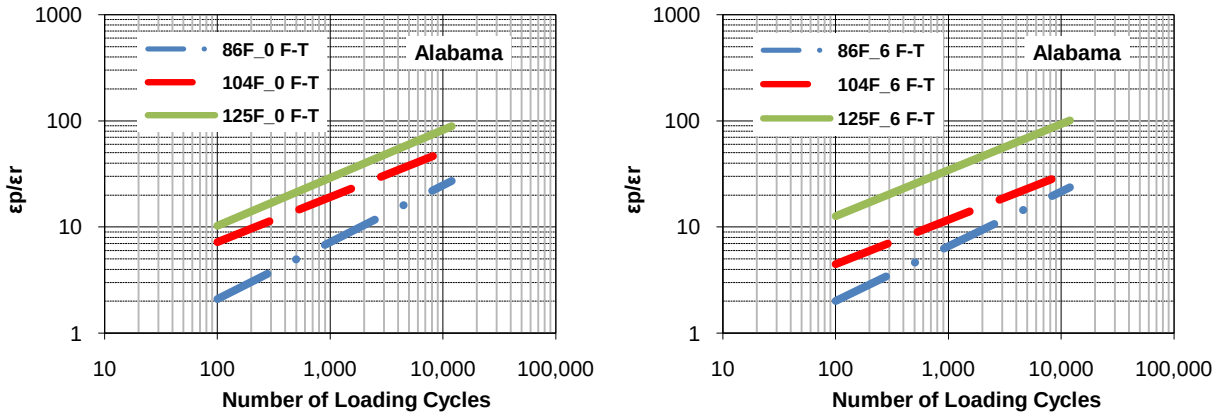

a. Alabama Un-treated Mixes at 0 and 6 F-T Cycles.

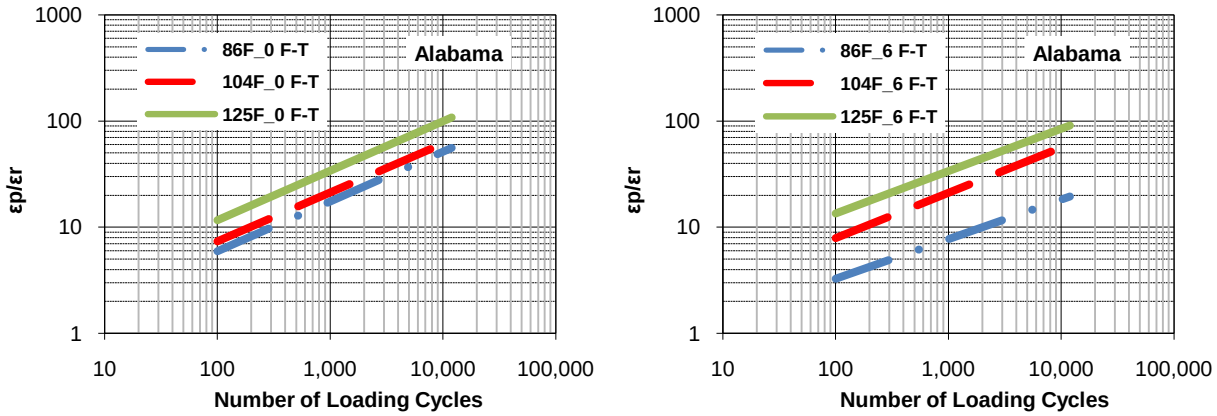

b. Alabama Liquid-treated Mixes at 0 and 6 F-T Cycles.

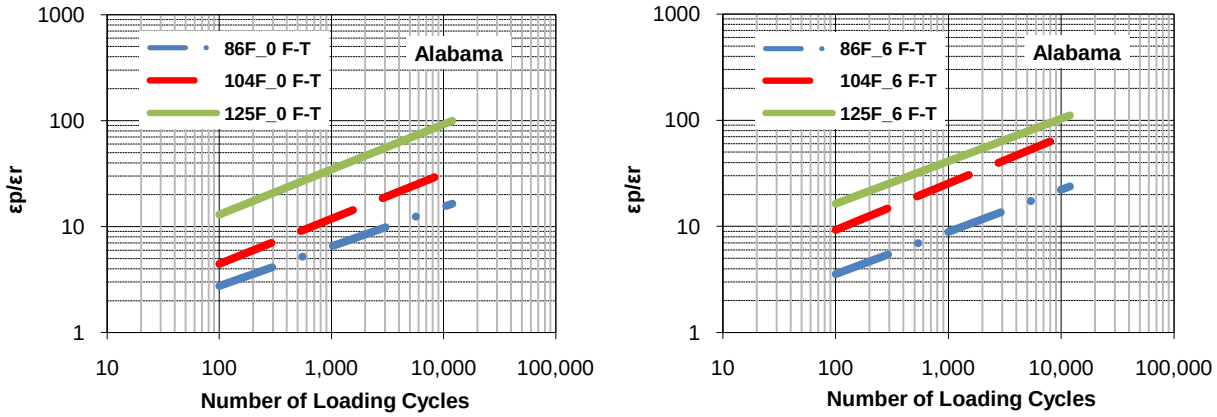

c. Alabama Lime-treated Mixes at 0 and 6 F-T Cycles.

Figure 50. Permanent Deformation Characteristics of the Alabama Mixtures.

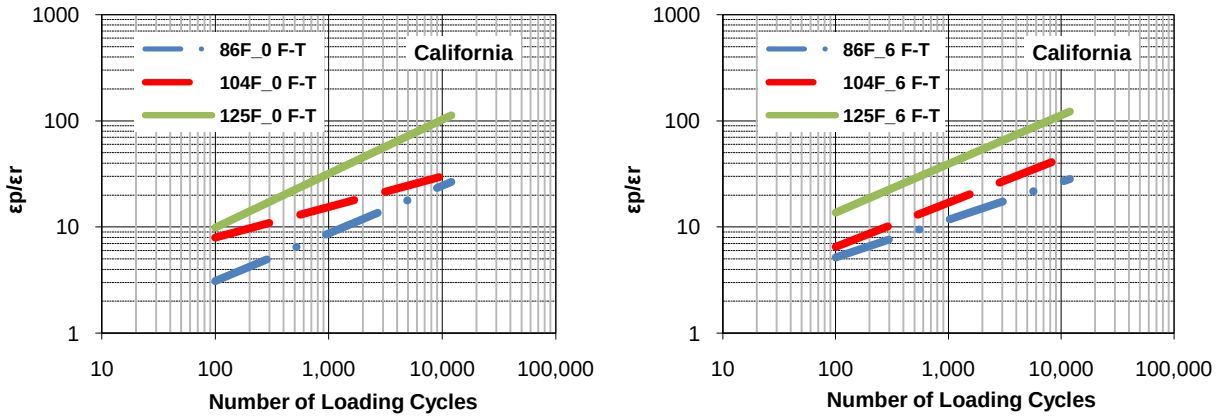

a. California Un-treated Mixes at 0 and 6 F-T Cycles.

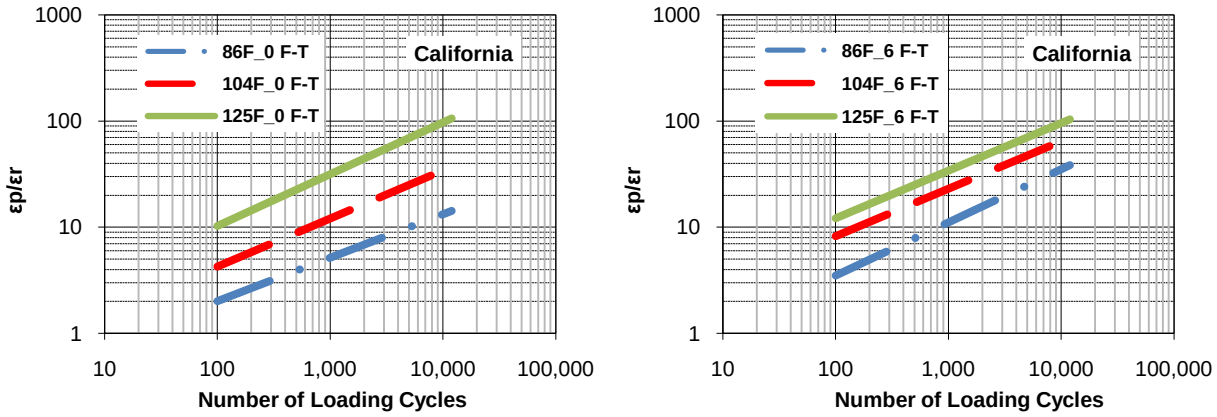

b. California Liquid-treated Mixes at 0 and 6 F-T Cycles.

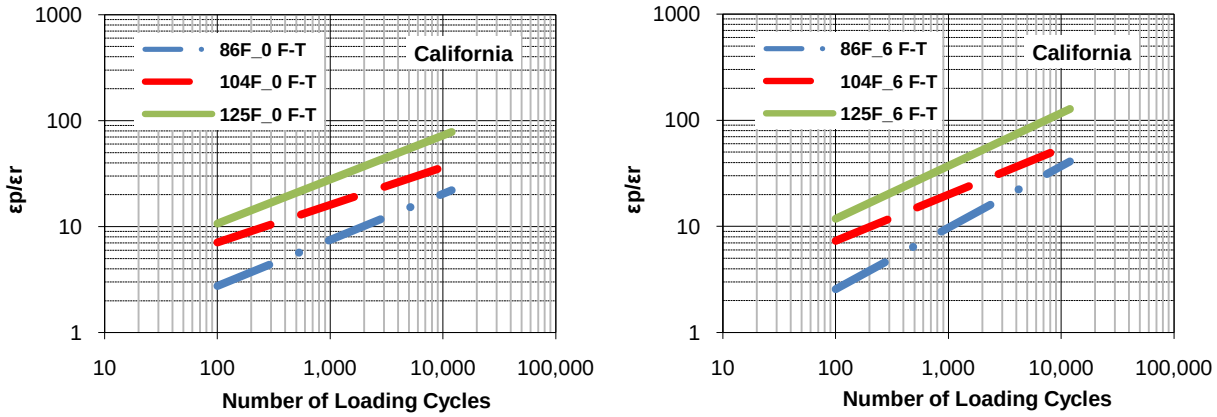

c. California Lime-treated Mixes at 0 and 6 F-T Cycles.

Figure 51. Permanent Deformation Characteristics of the California Mixtures.

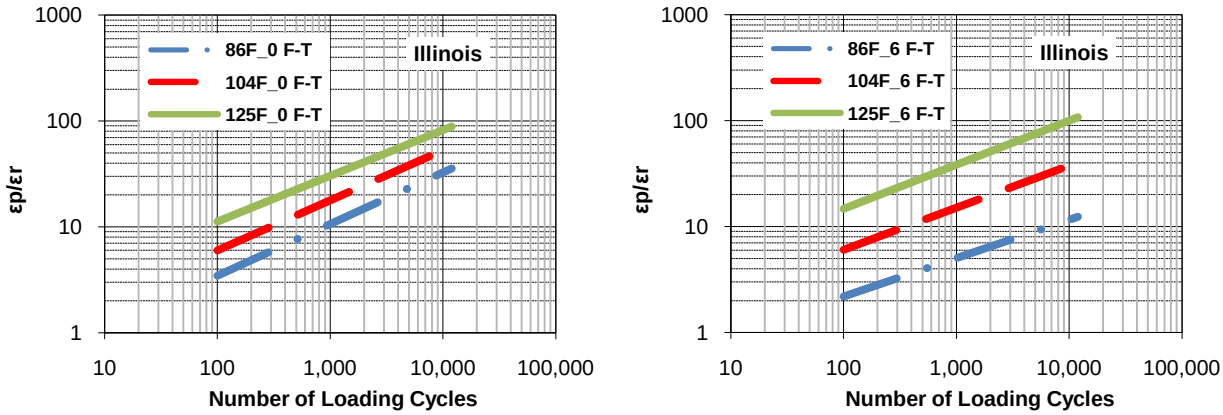

a. Illinois Un-treated Mixes at 0 and 6 F-T Cycles.

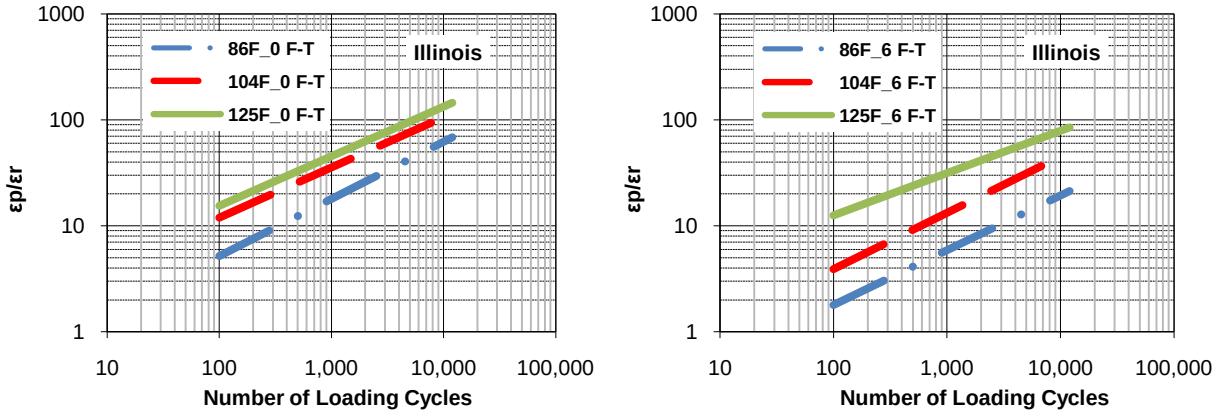

b. Illinois Liquid-treated Mixes at 0 and 6 F-T Cycles.

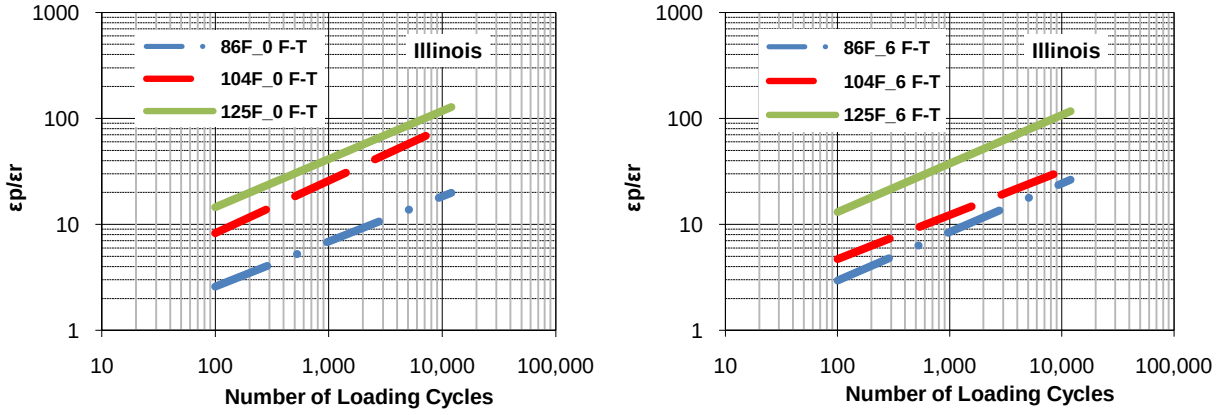

c. Illinois Lime-treated Mixes at 0 and 6 F-T Cycles.

Figure 52. Permanent Deformation Characteristics of the Illinois Mixtures.

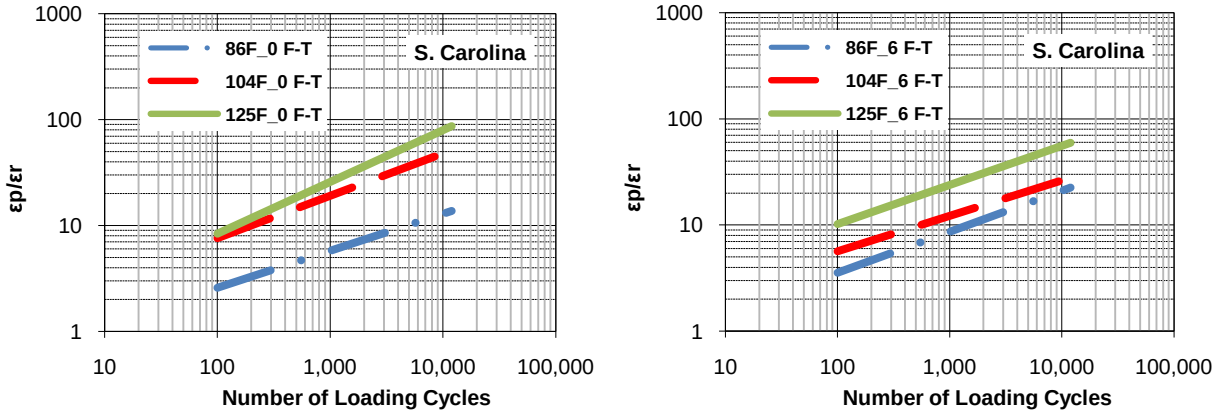

a. South Carolina Un-treated Mixes at 0 and 6 F-T Cycles.

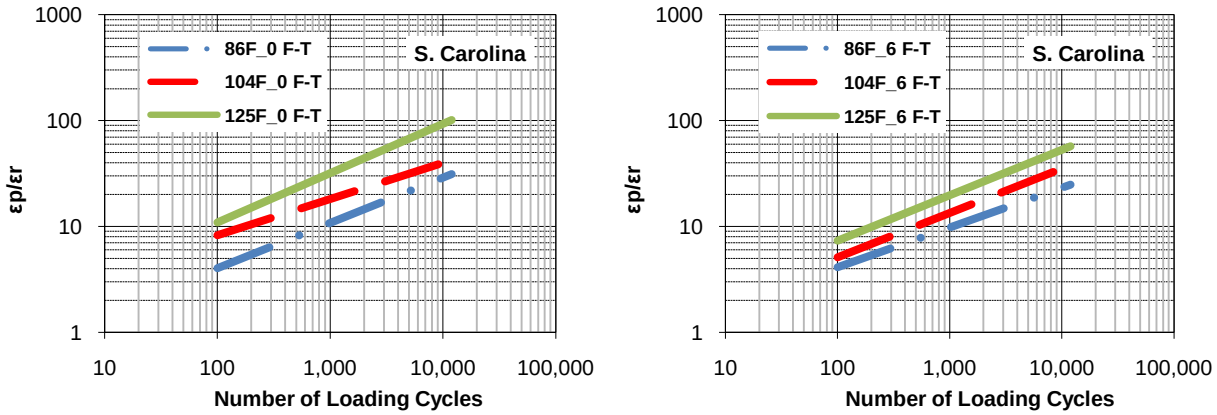

b. South Carolina Liquid-treated Mixes at 0 and 6 F-T Cycles.

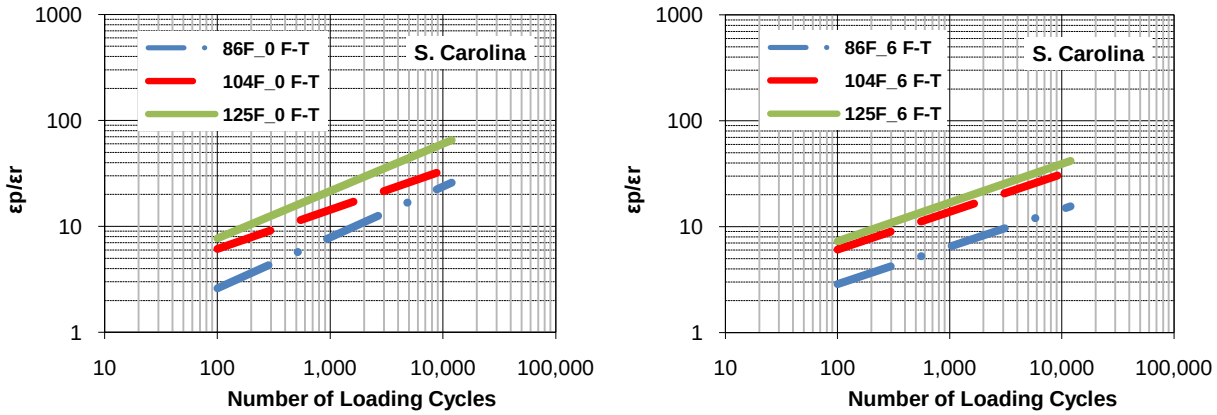

c. South Carolina Lime-treated Mixes at 0 and 6 F-T Cycles.

Figure 53. Permanent Deformation Characteristics of the South Carolina Mixtures.

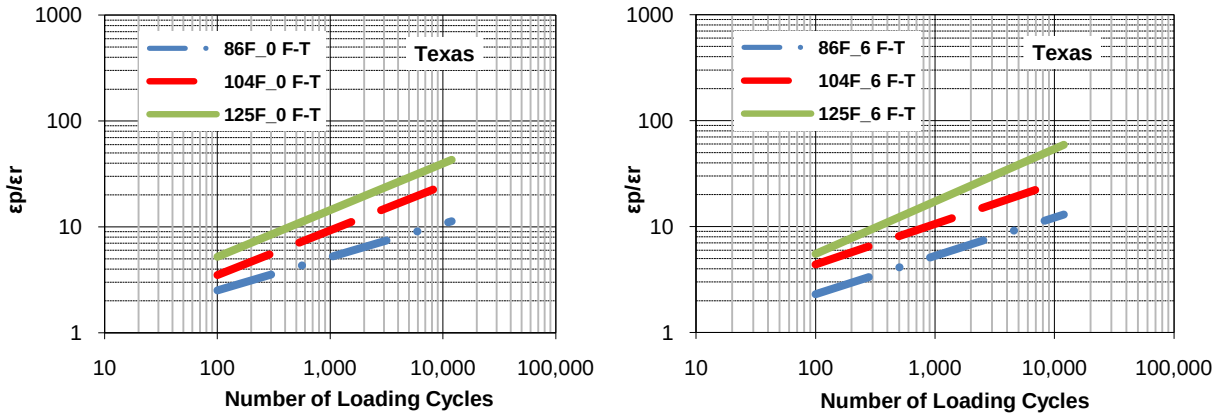

a. Texas Un-treated Mixes at 0 and 6 F-T Cycles.

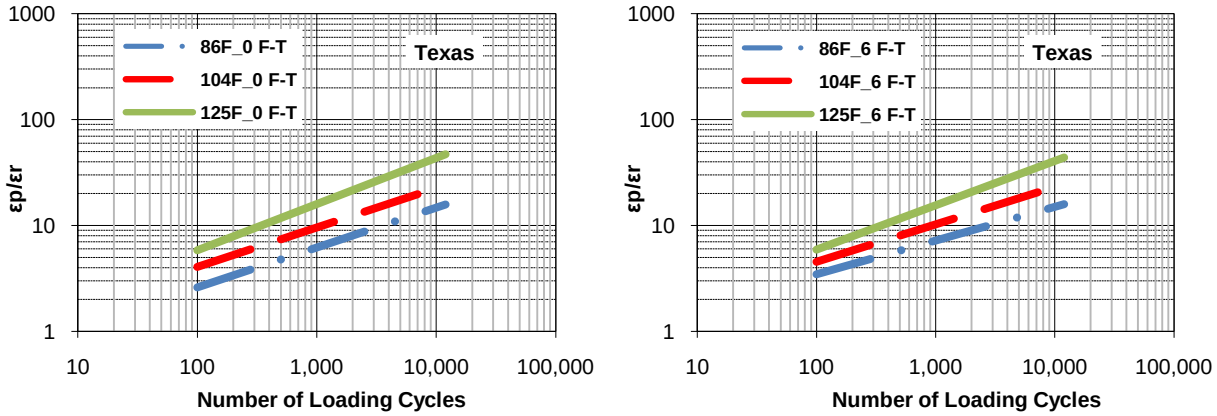

b. Texas Liquid-treated Mixes at 0 and 6 F-T Cycles.

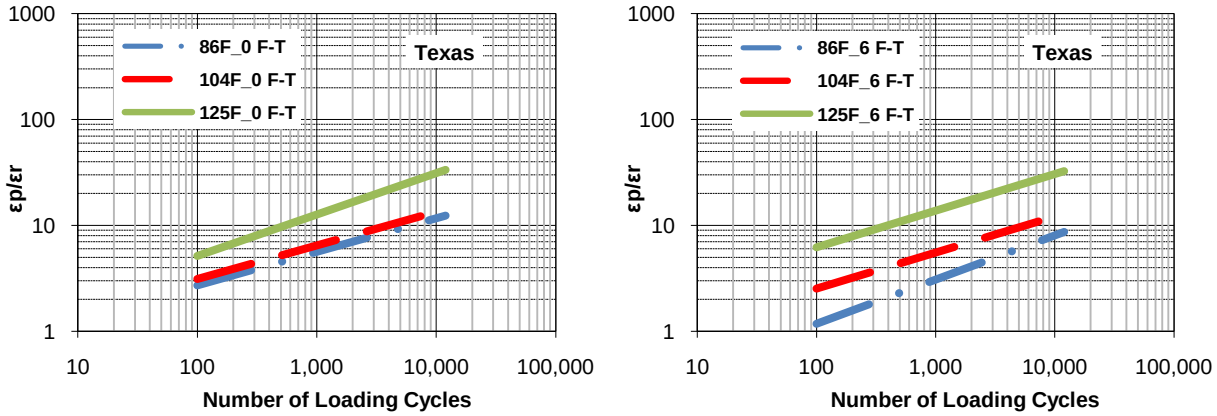

c. Texas Lime-treated Mixes at 0 and 6 F-T Cycles.

Figure 54. Permanent Deformation Characteristics of the Texas Mixtures.

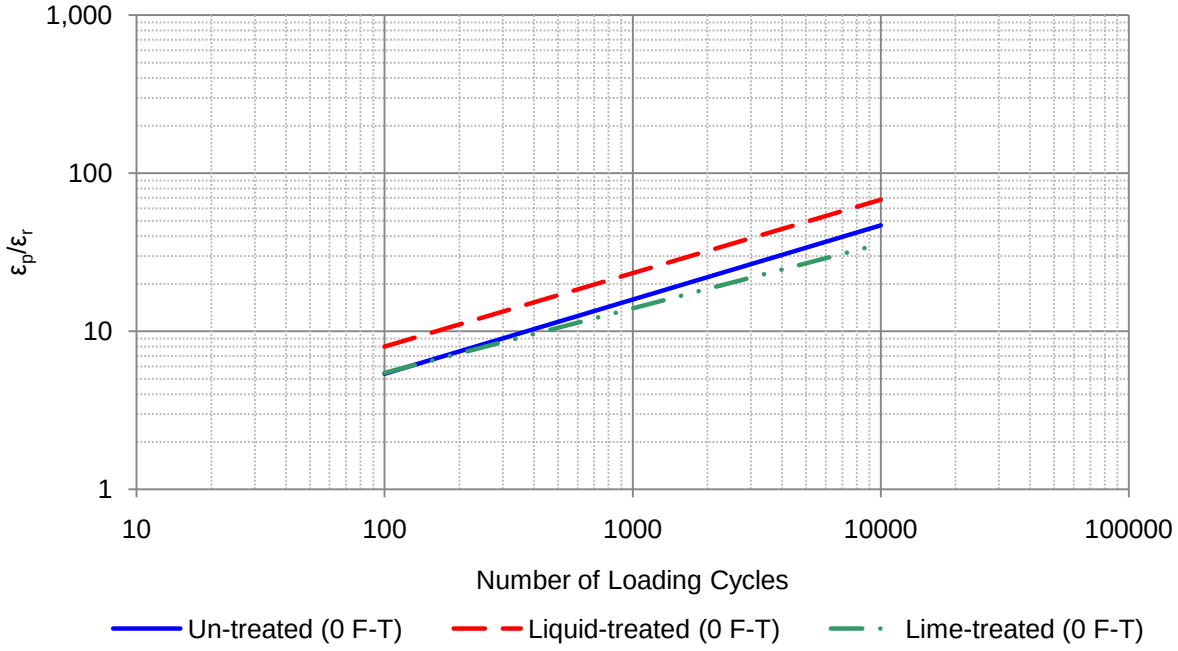

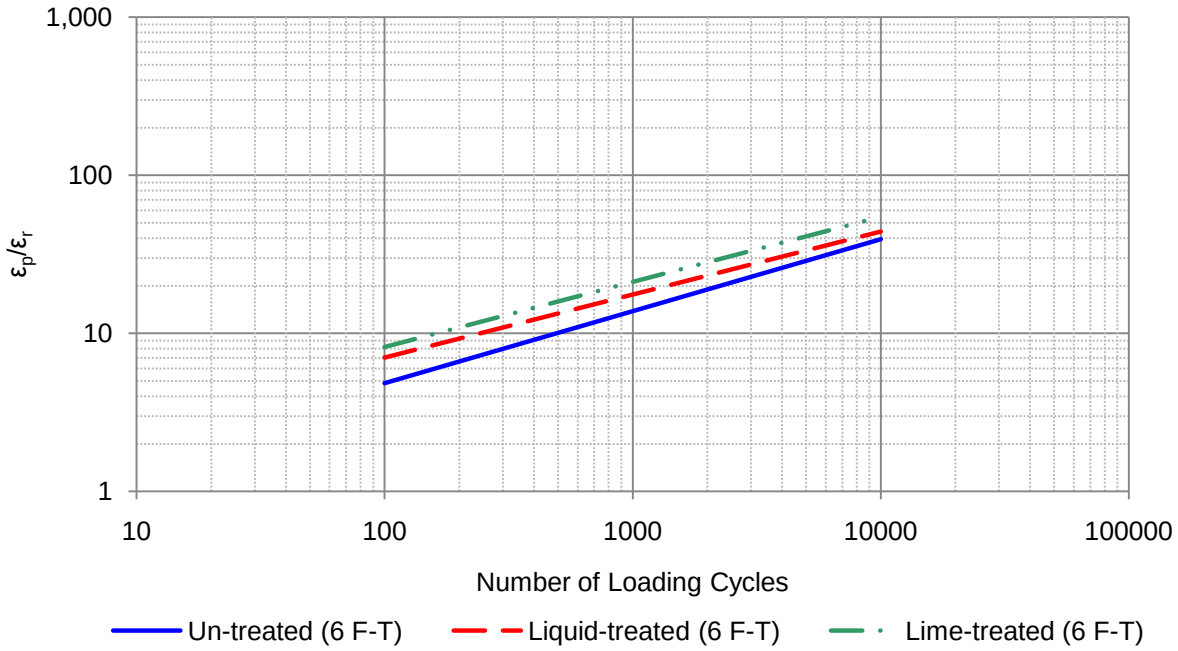

Figure 55. Permanent Deformation at 104°F for the Alabama Mixes at 0 and 6 F-T Cycles.

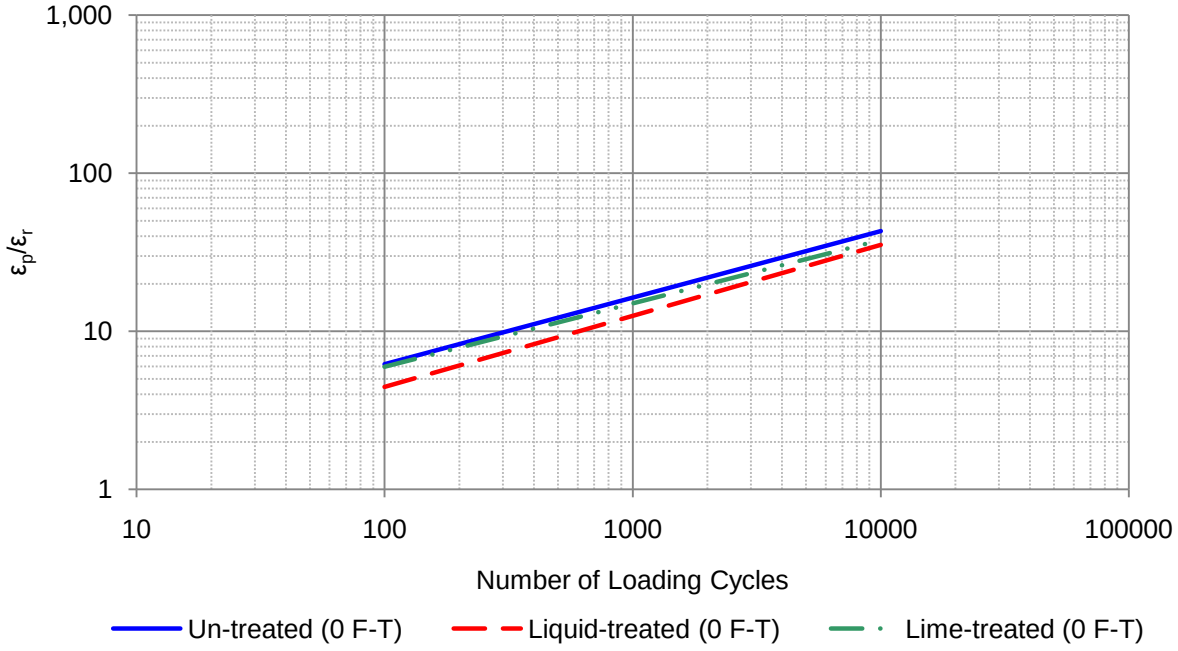

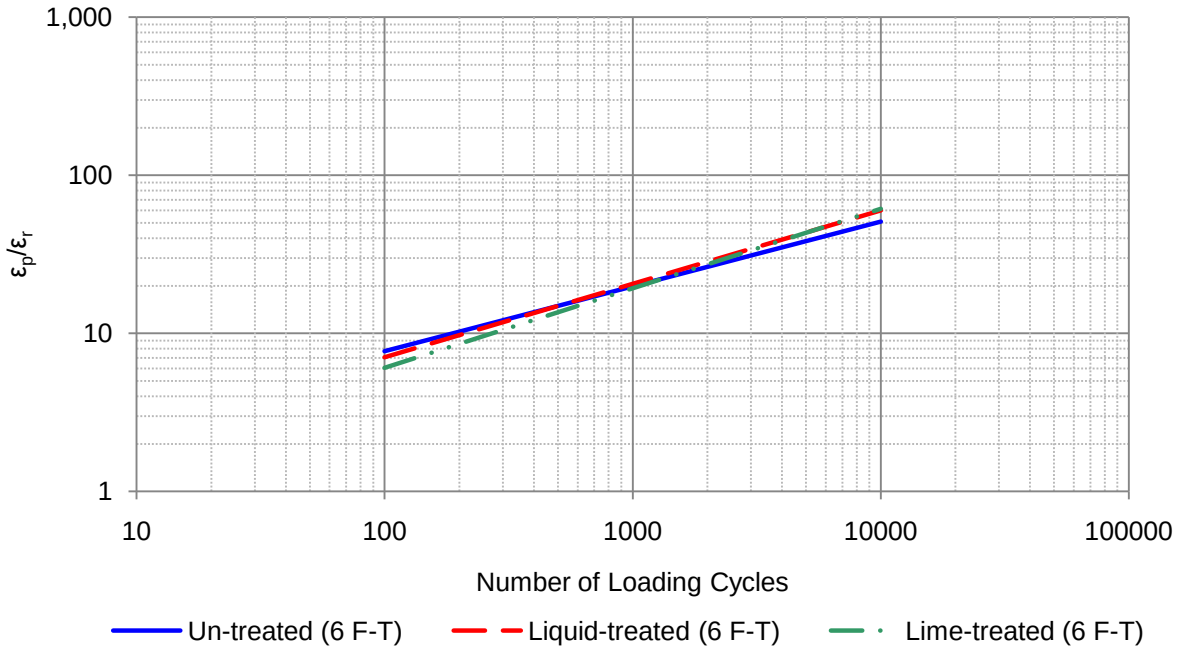

Figure 56. Permanent Deformation at 104°F for the California Mixes at 0 and 6 F-T Cycles.

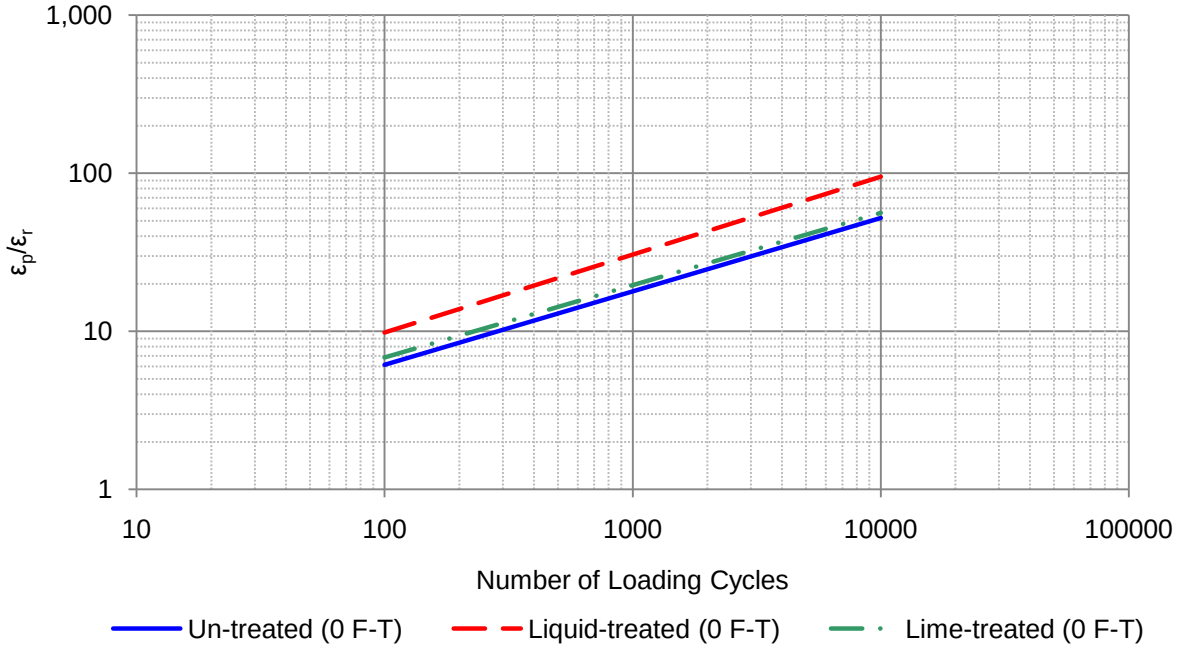

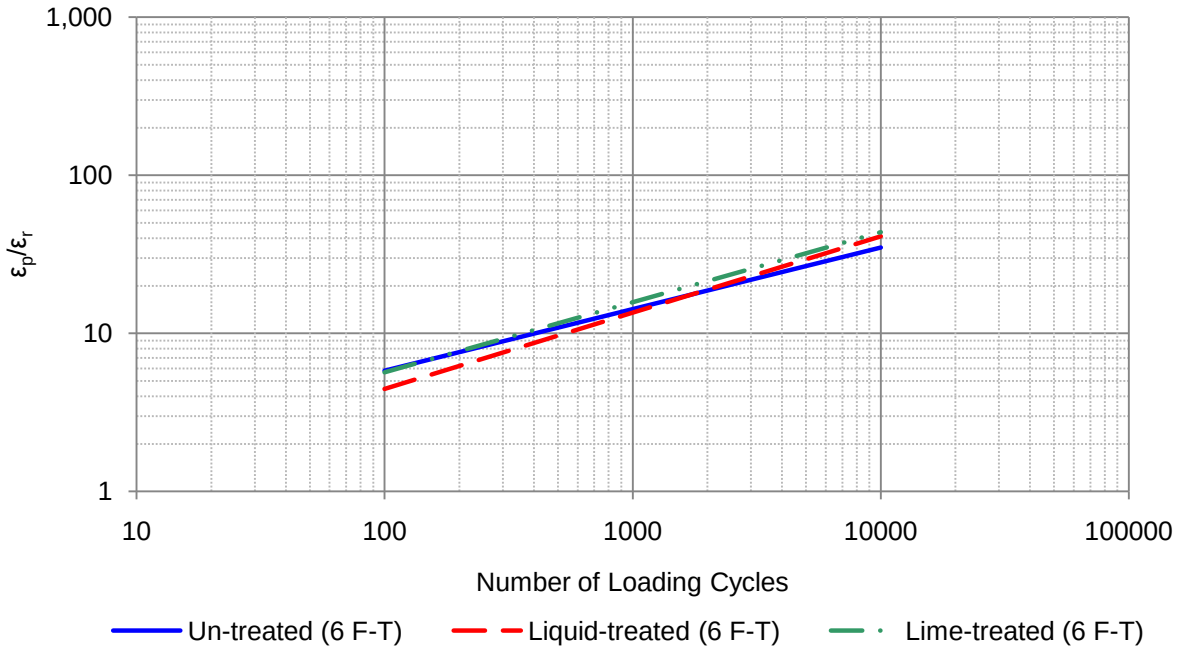

Figure 57. Permanent Deformation at 104°F for the Illinois Mixes at 0 and 6 F-T Cycles.

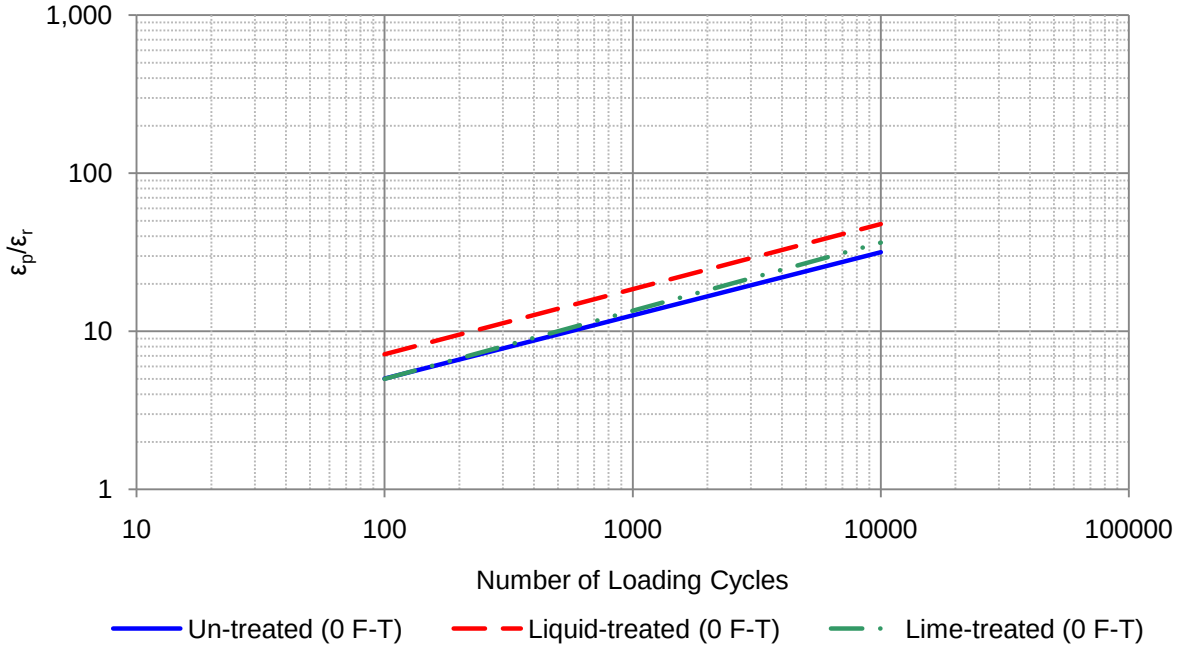

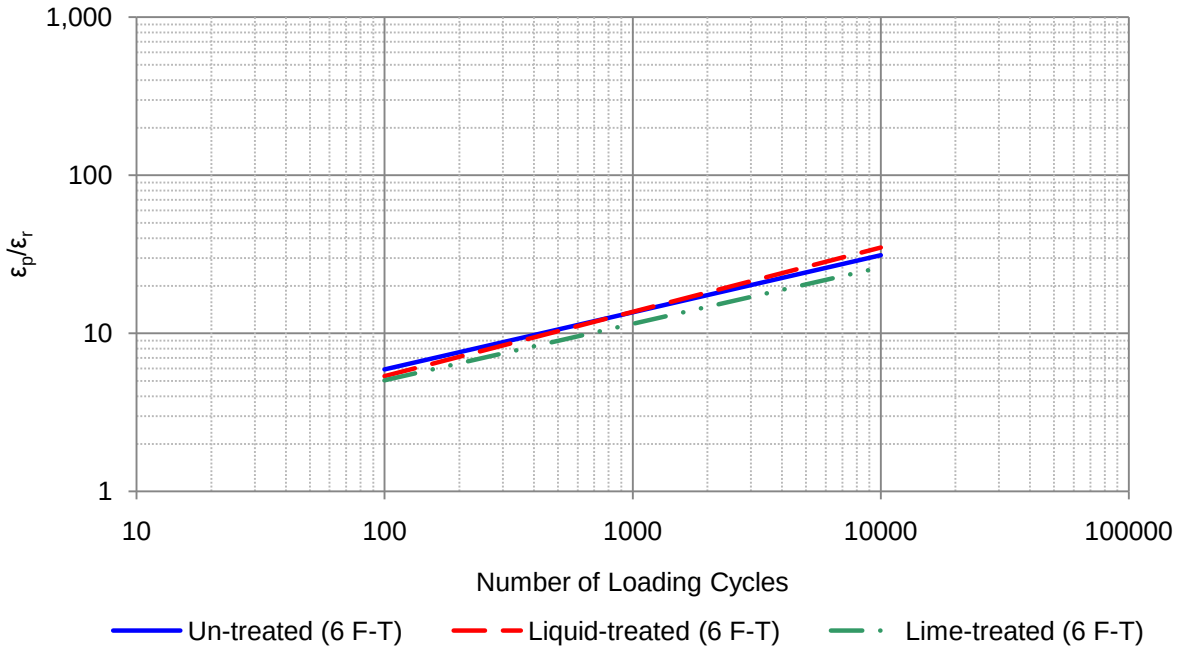

Figure 58. Permanent Deformation at 104°F for the South Carolina Mixes at 0 and 6 F-T Cycles.

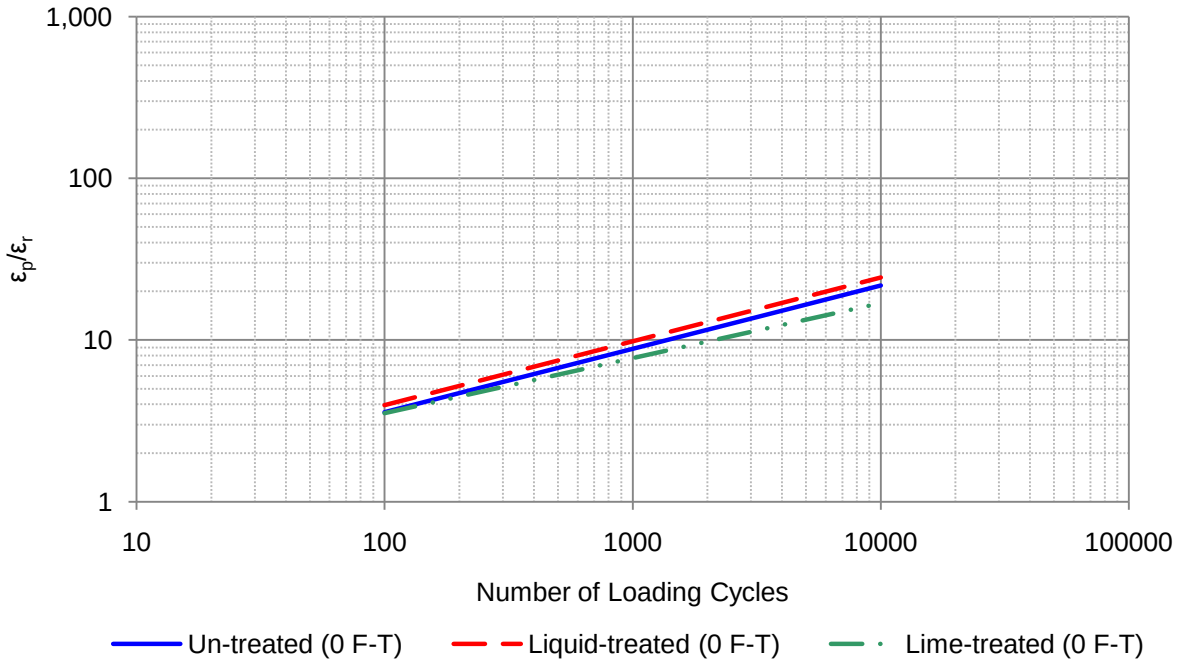

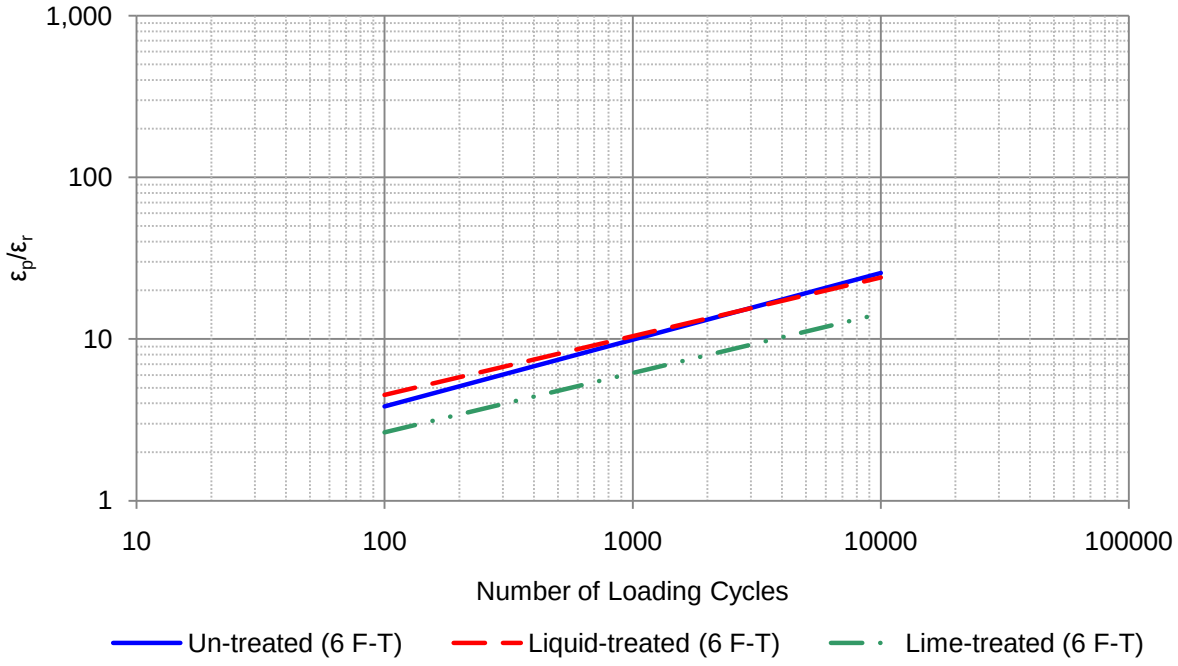

Figure 59. Permanent Deformation at 104°F for the Texas Mixes at 0 and 6 F-T Cycles.

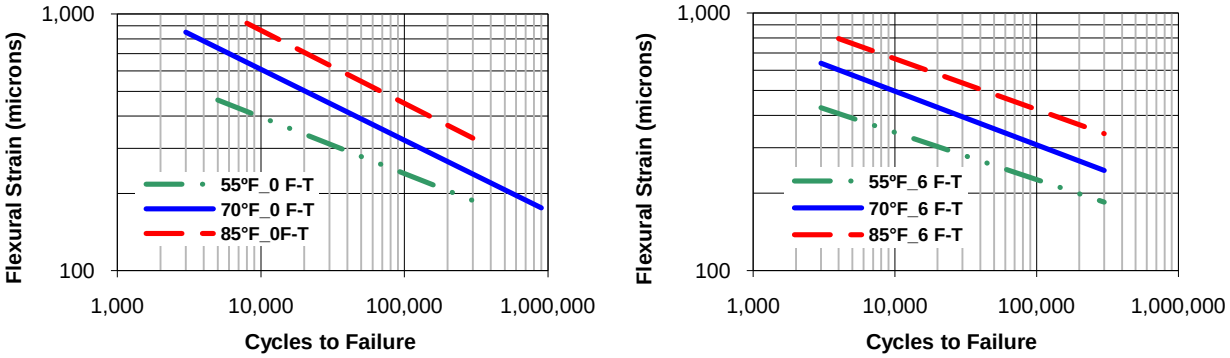

a. Alabama Un-treated Mixes at 0 and 6 F-T Cycles.

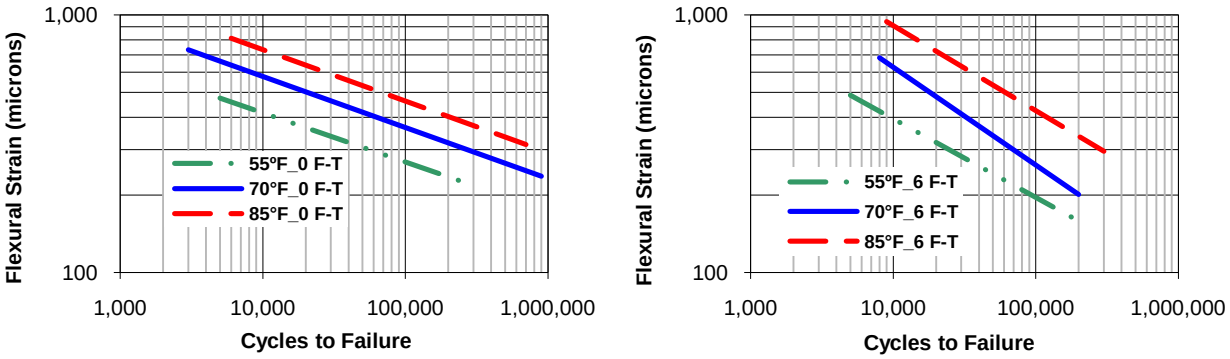

b. Alabama Liquid-treated Mixes at 0 and 6 F-T Cycles.

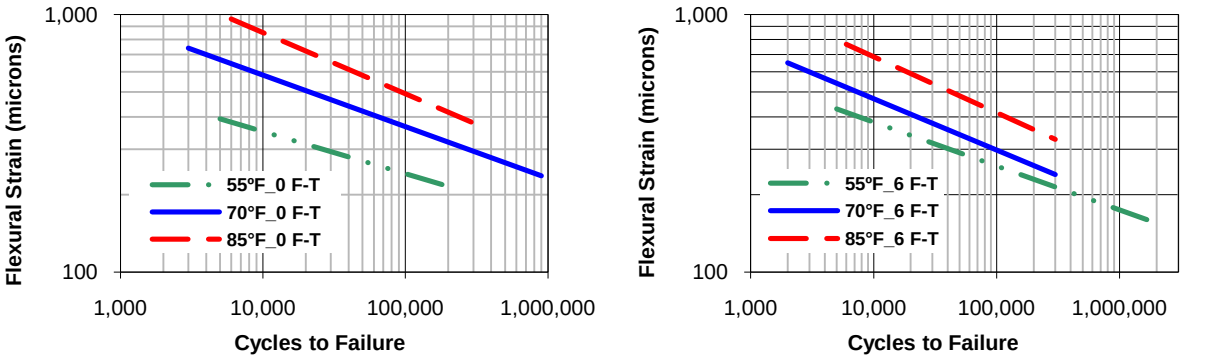

c. Alabama Lime-treated Mixes at 0 and 6 F-T Cycles.

Figure 60. Fatigue Characteristics of the Alabama Mixtures.

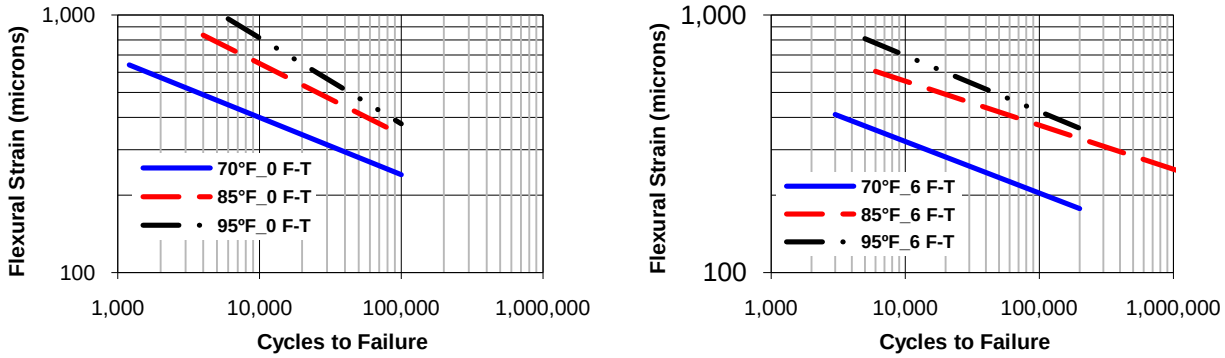

a. California Un-treated Mixes at 0 and 6 F-T Cycles.

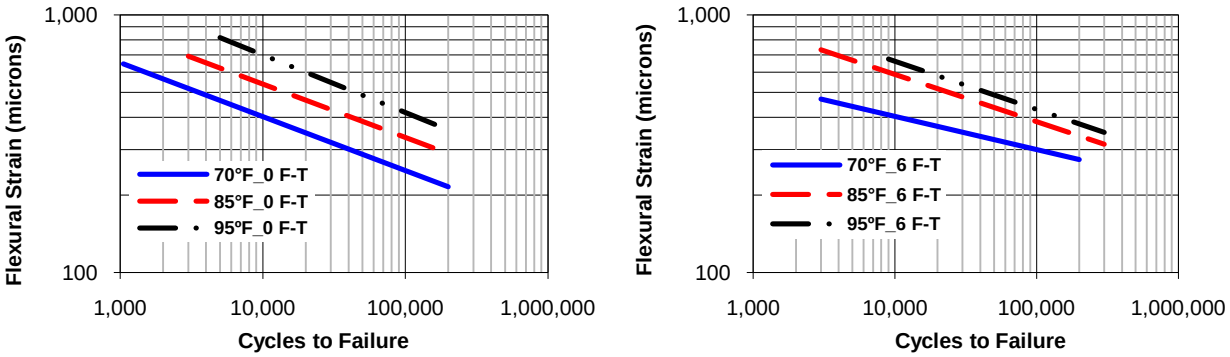

b. California Liquid-treated Mixes at 0 and 6 F-T Cycles.

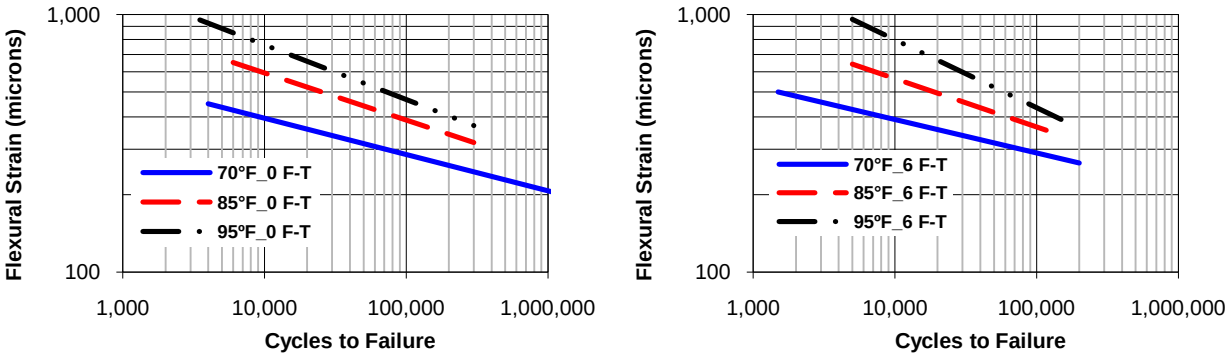

c. California Lime-treated Mixes at 0 and 6 F-T Cycles.

Figure 61. Fatigue Characteristics of the California Mixtures.

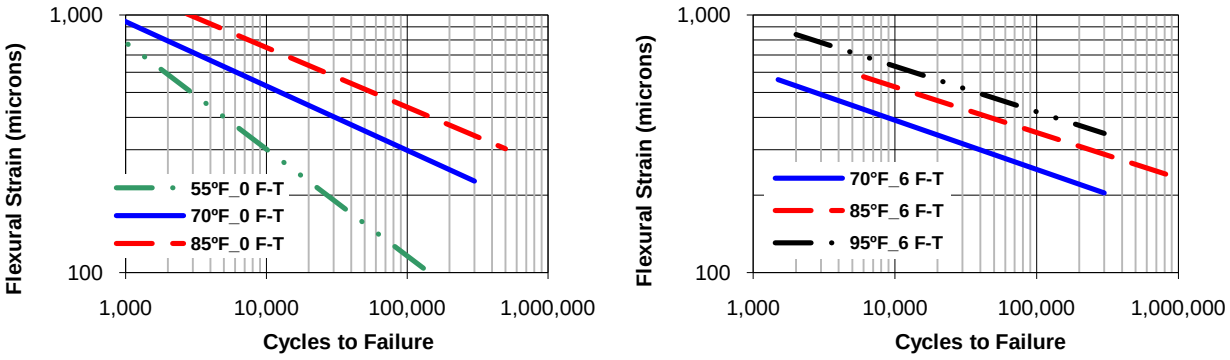

a. Illinois Un-treated Mixes at 0 and 6 F-T Cycles.

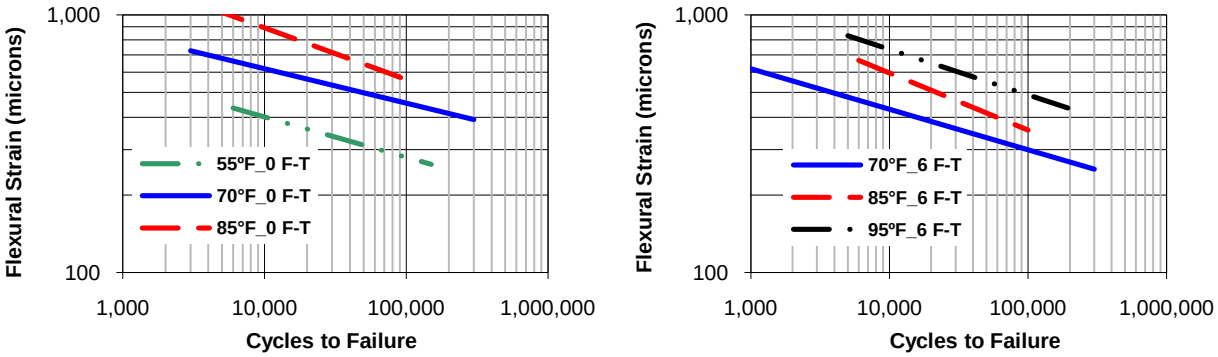

b. Illinois Liquid-treated Mixes at 0 and 6 F-T Cycles.

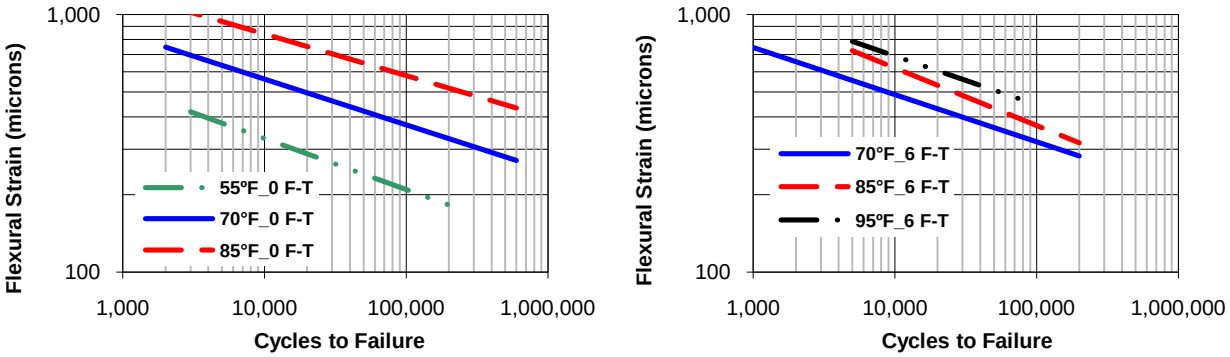

c. Illinois Lime-treated Mixes at 0 and 6 F-T Cycles.

Figure 62. Fatigue Characteristics of the Illinois Mixtures.

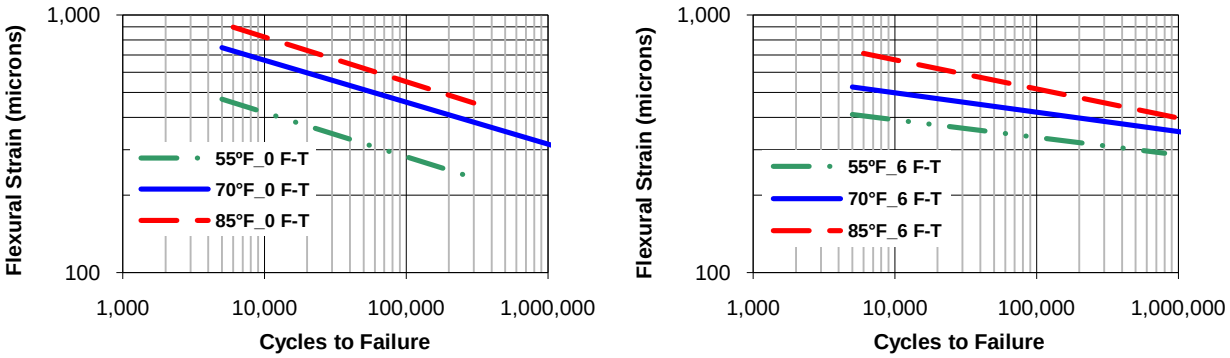

a. South Carolina Un-treated Mixes at 0 and 6 F-T Cycles.

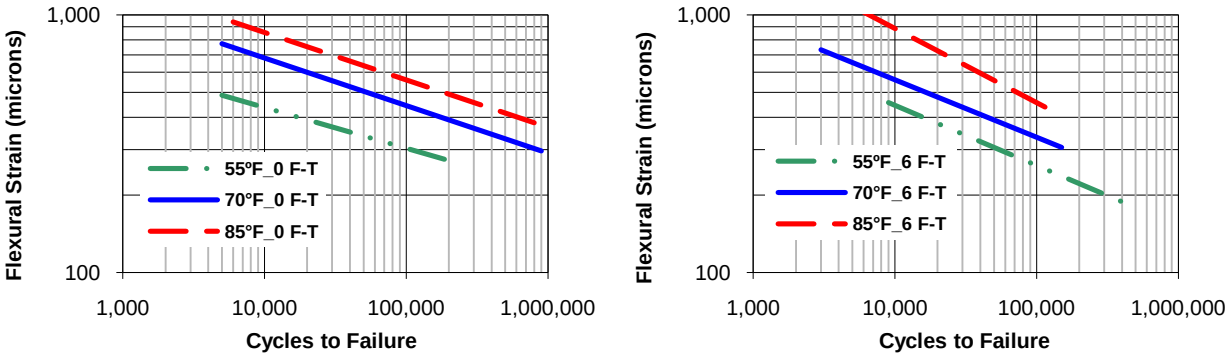

b. South Carolina Liquid-treated Mixes at 0 and 6 F-T Cycles.

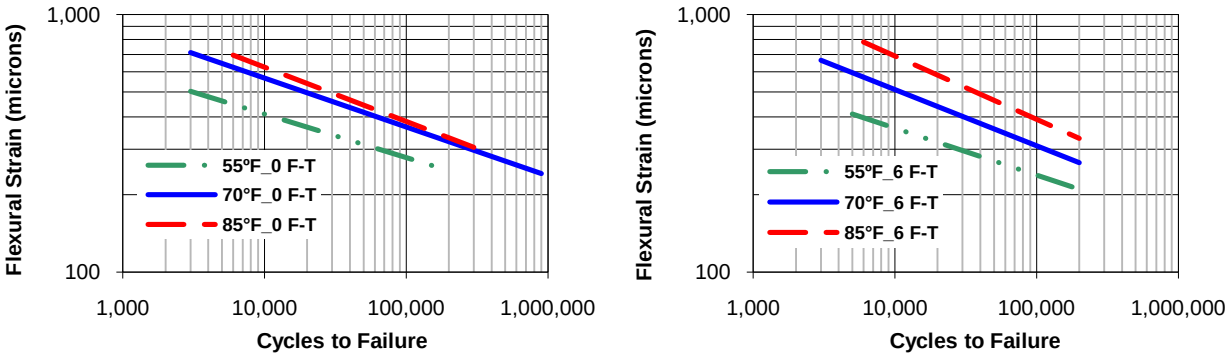

c. South Carolina Lime-treated Mixes at 0 and 6 F-T Cycles.

Figure 63. Fatigue Characteristics of the South Carolina Mixtures.

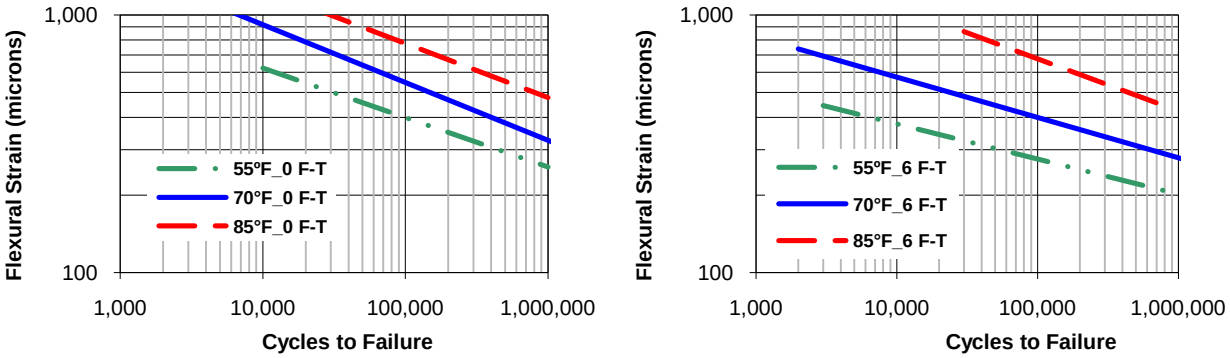

a. Texas Un-treated Mixes at 0 and 6 F-T Cycles.

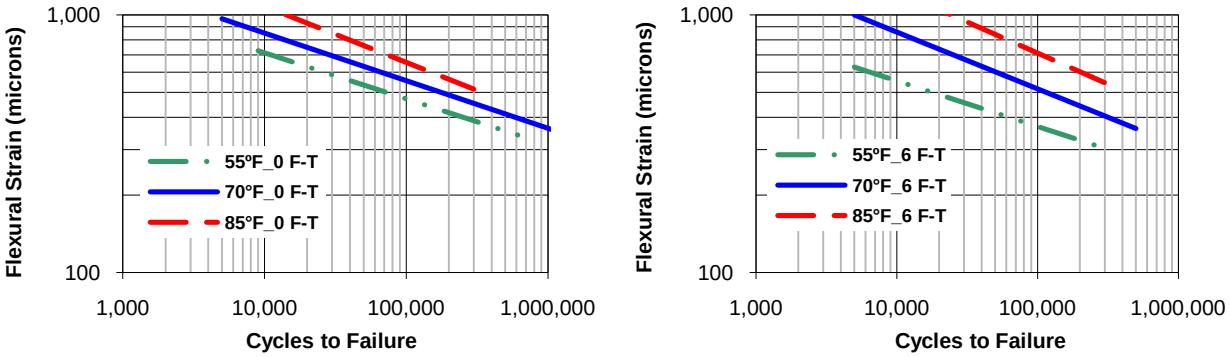

b. Texas Liquid-treated Mixes at 0 and 6 F-T Cycles.

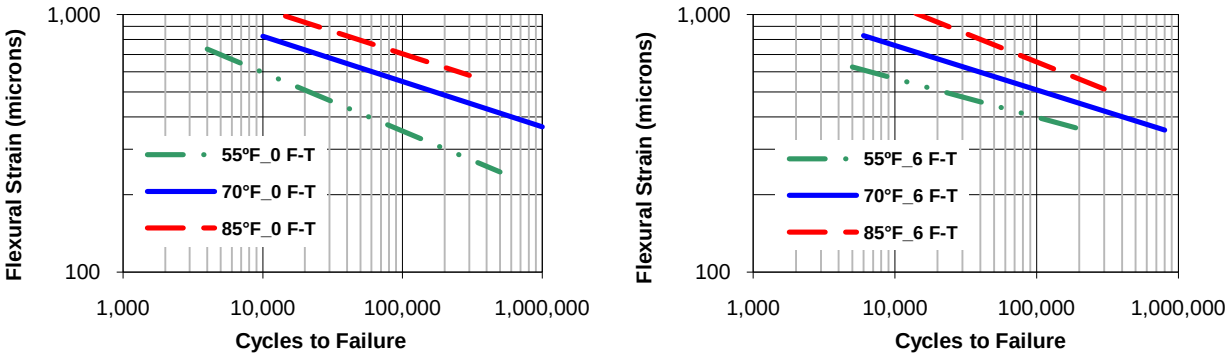

c. Texas Lime-treated Mixes at 0 and 6 F-T Cycles.

Figure 64. Fatigue Characteristics of the Texas Mixtures.

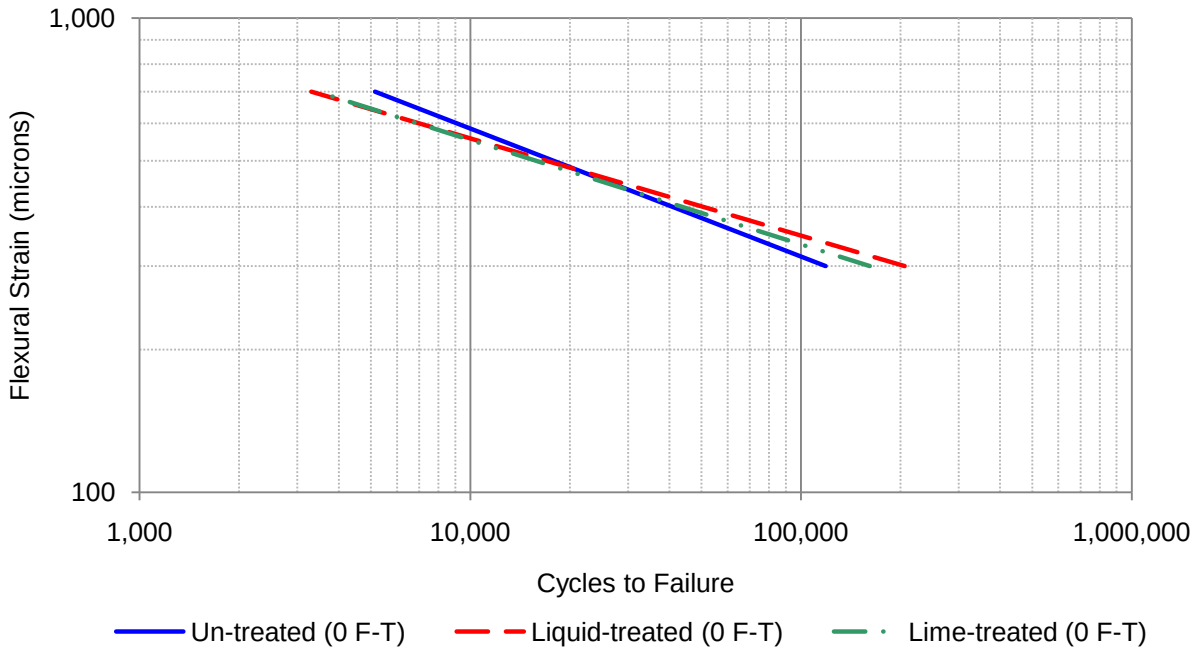

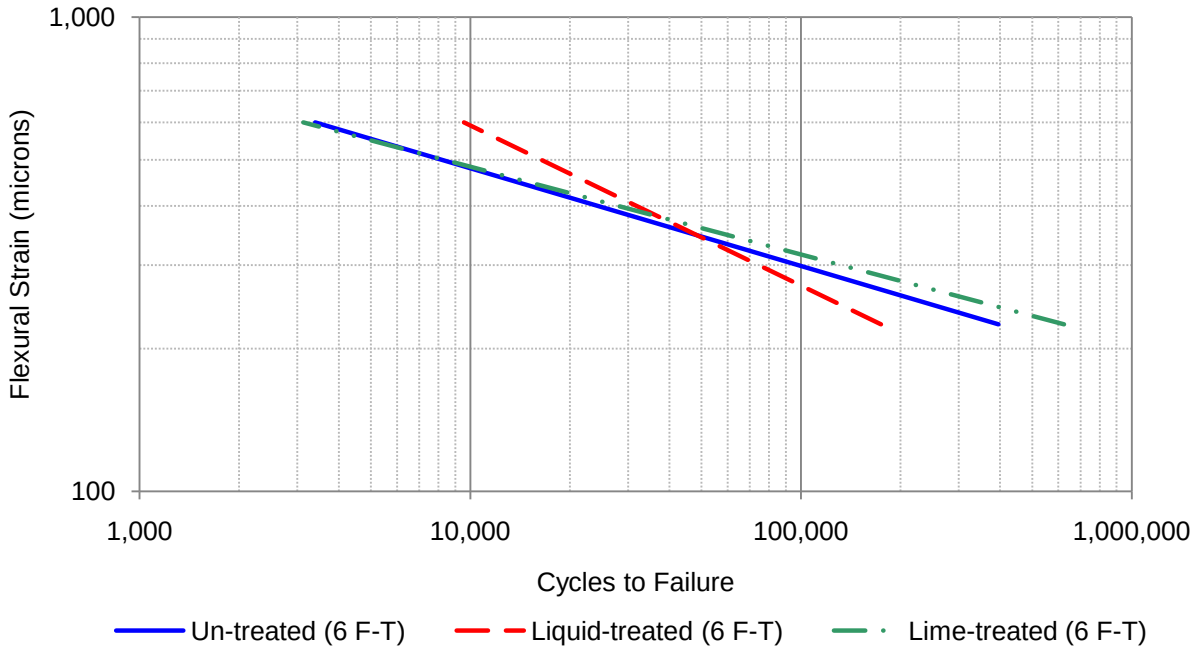

Figure 65. Flexural Beam Fatigue Relationships at 70°F for Alabama Mixes at 0 and 6 F-T Cycles.

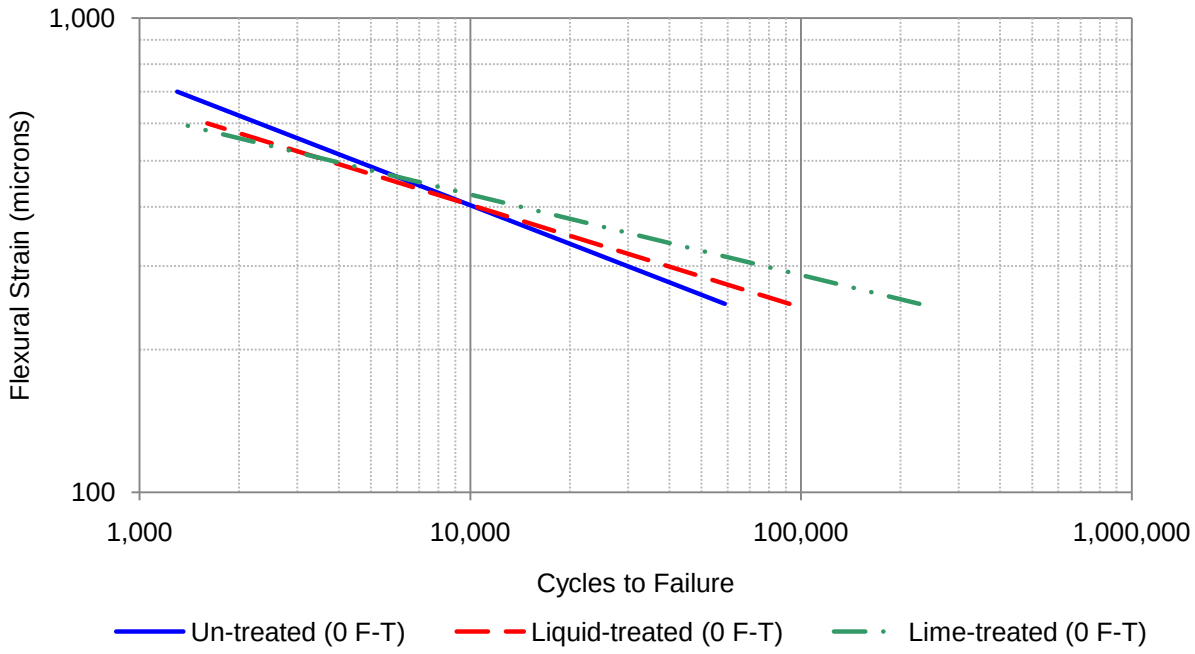

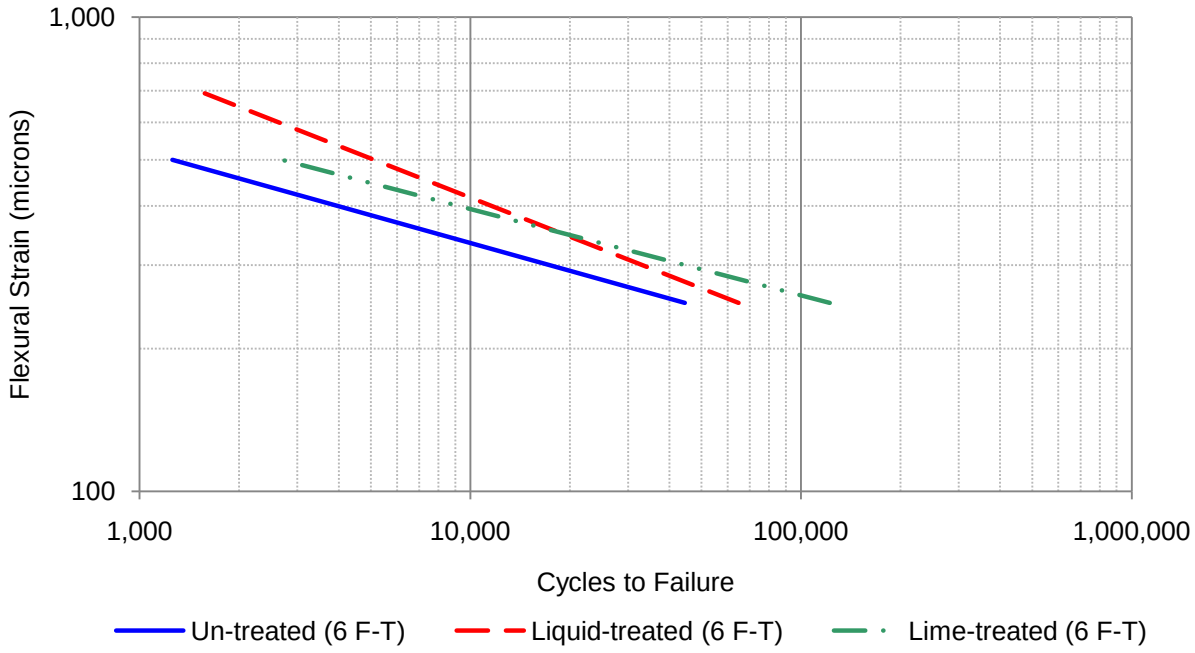

Figure 66. Flexural Beam Fatigue Relationships at 70°F for California Mixes at 0 and 6 F-T Cycles.

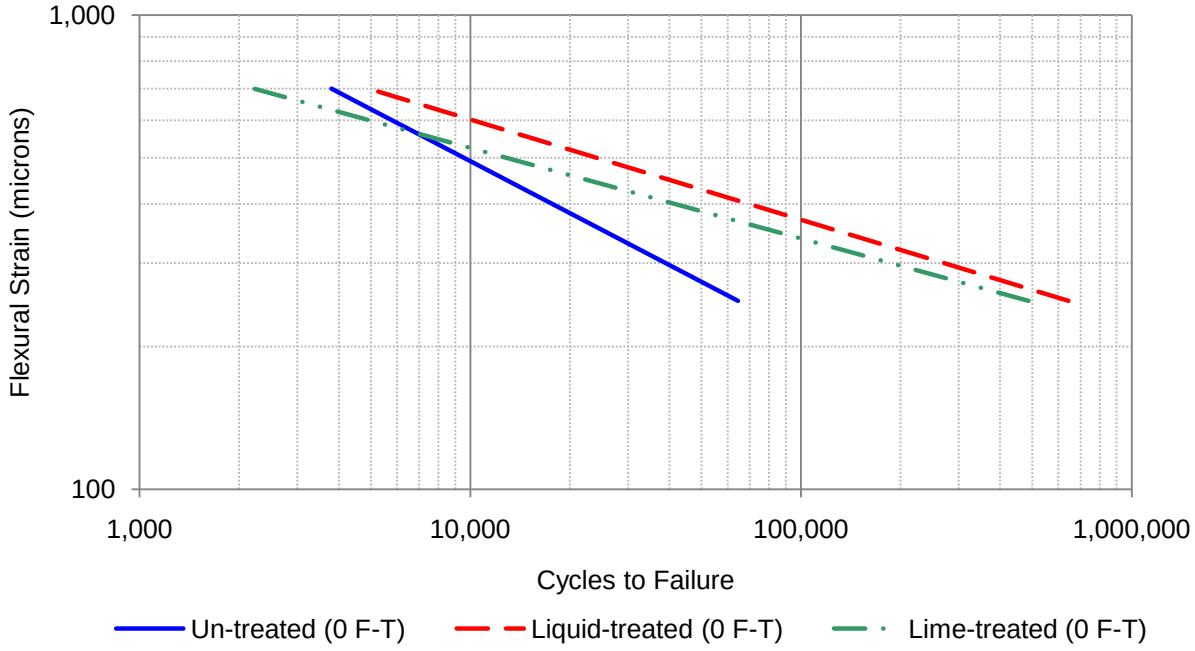

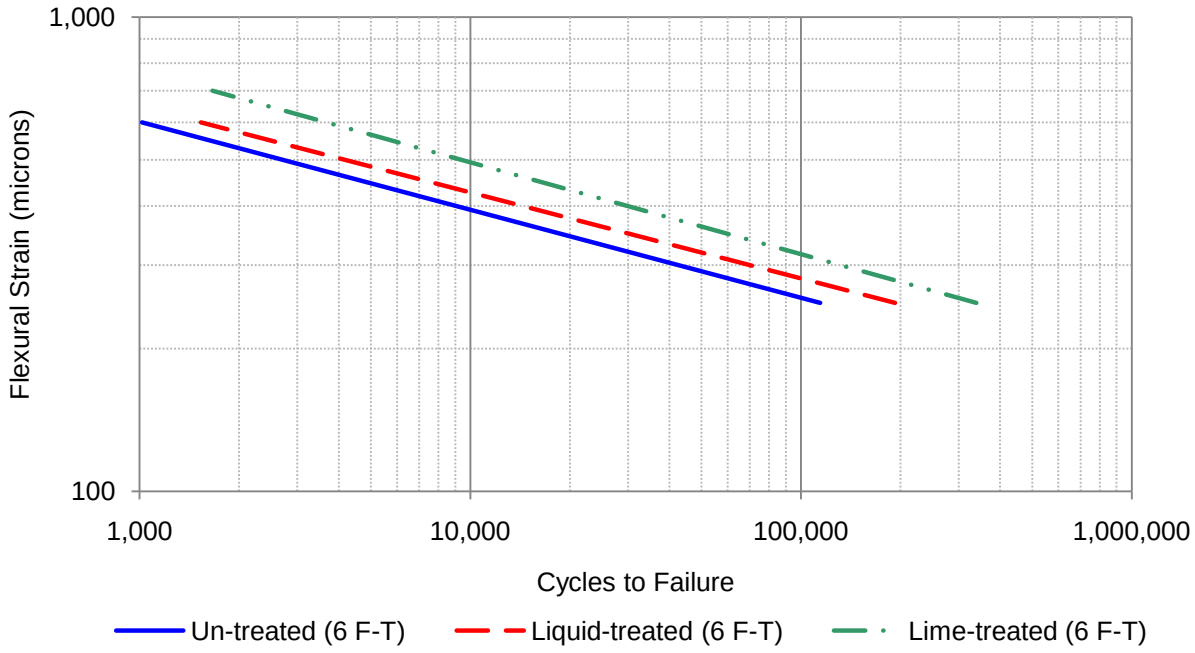

Figure 67. Flexural Beam Fatigue Relationships at 70°F for Illinois Mixes at 0 and 6 F-T Cycles.

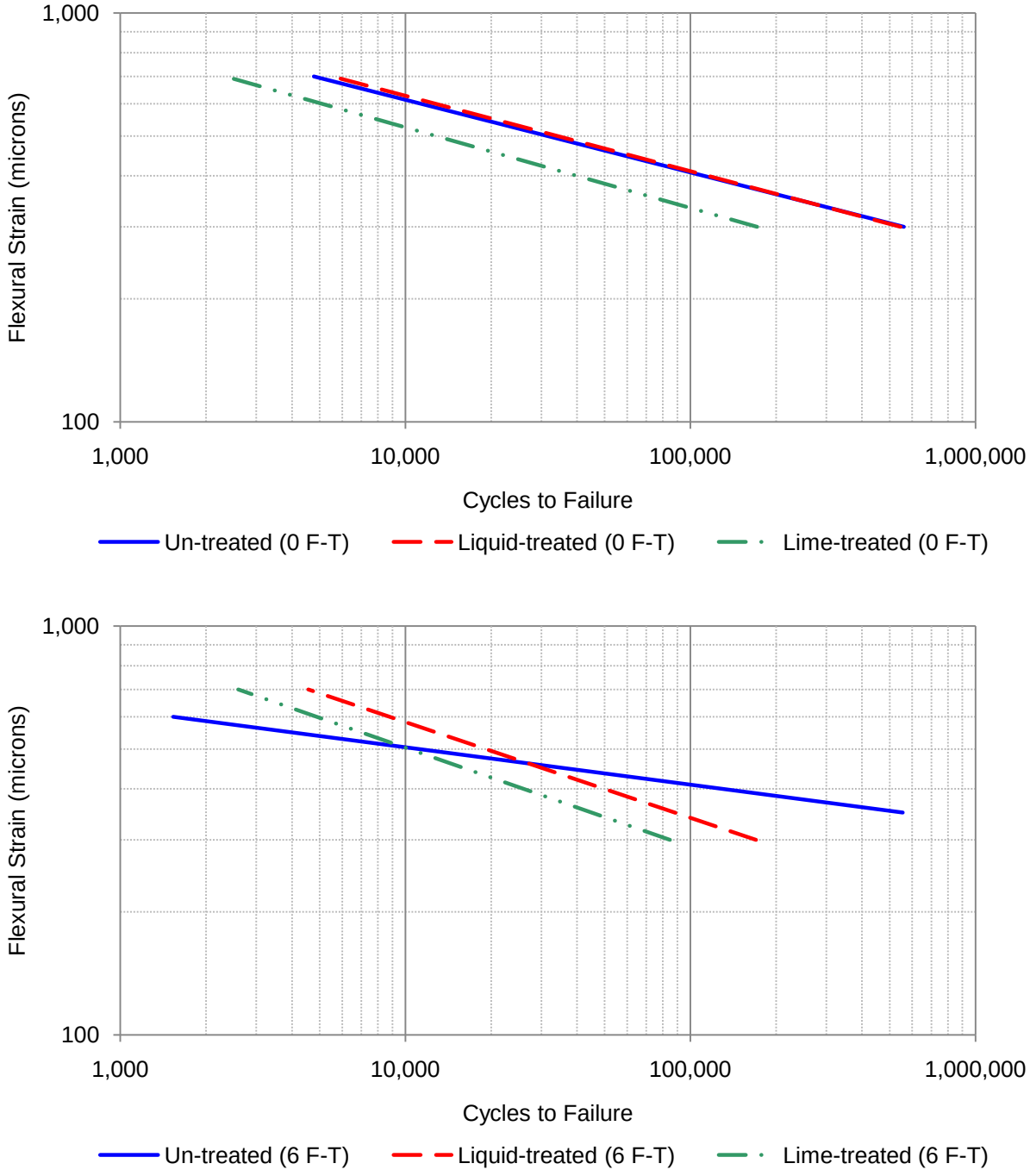

Figure 68. Flexural Beam Fatigue Relationships at 70°F for South Carolina Mixes at 0 and 6 F-T Cycles.

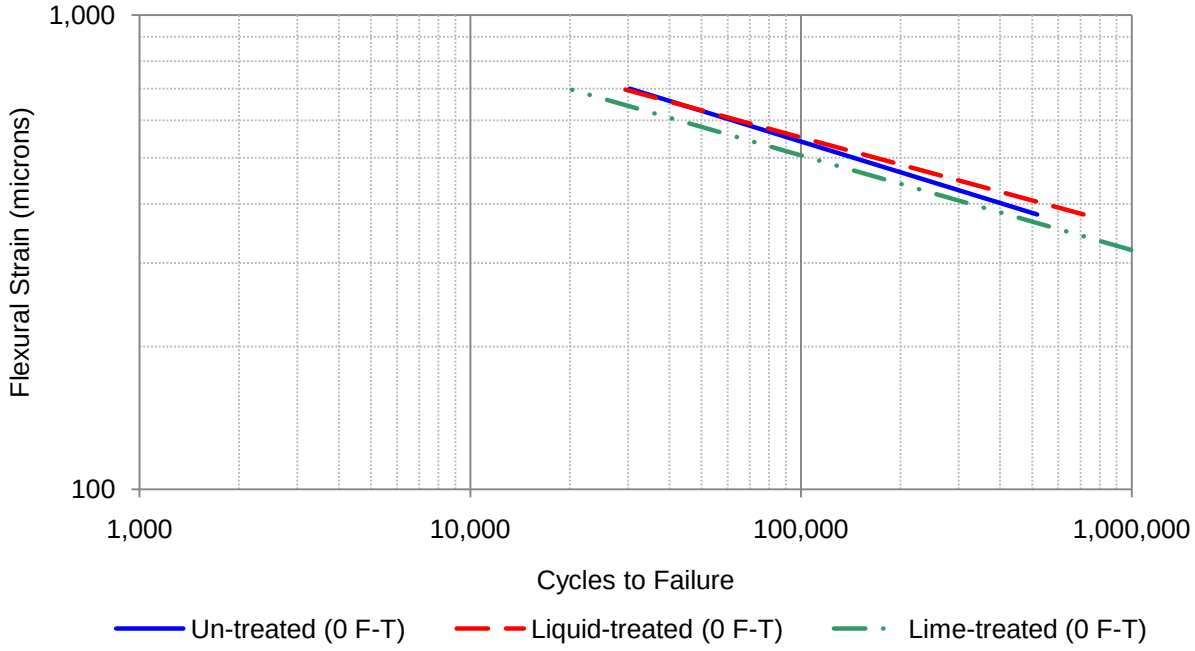

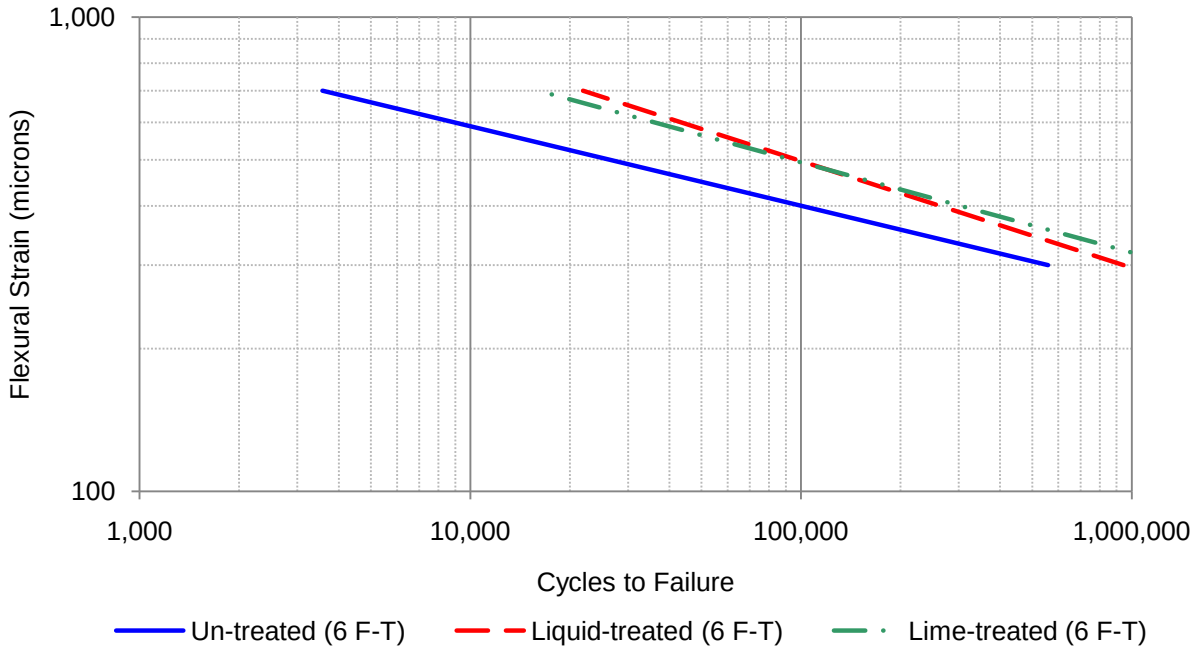

Figure 69. Flexural Beam Fatigue Relationships at 70°F for Texas Mixes at 0 and 6 F-T Cycles.

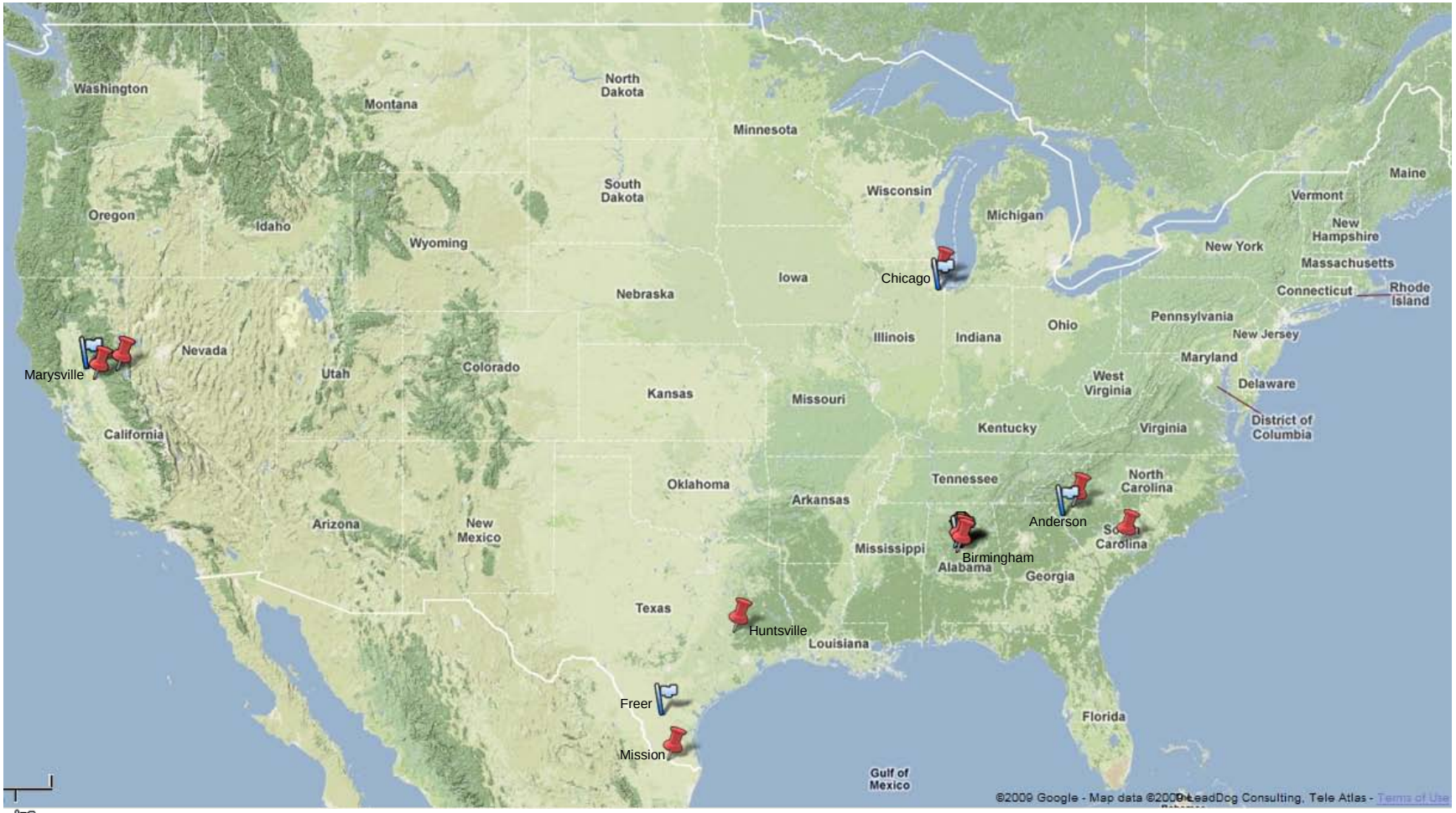

Aggregate Source Location

Project Location

Figure 70. Locations of Field Projects and Aggregate Sources.

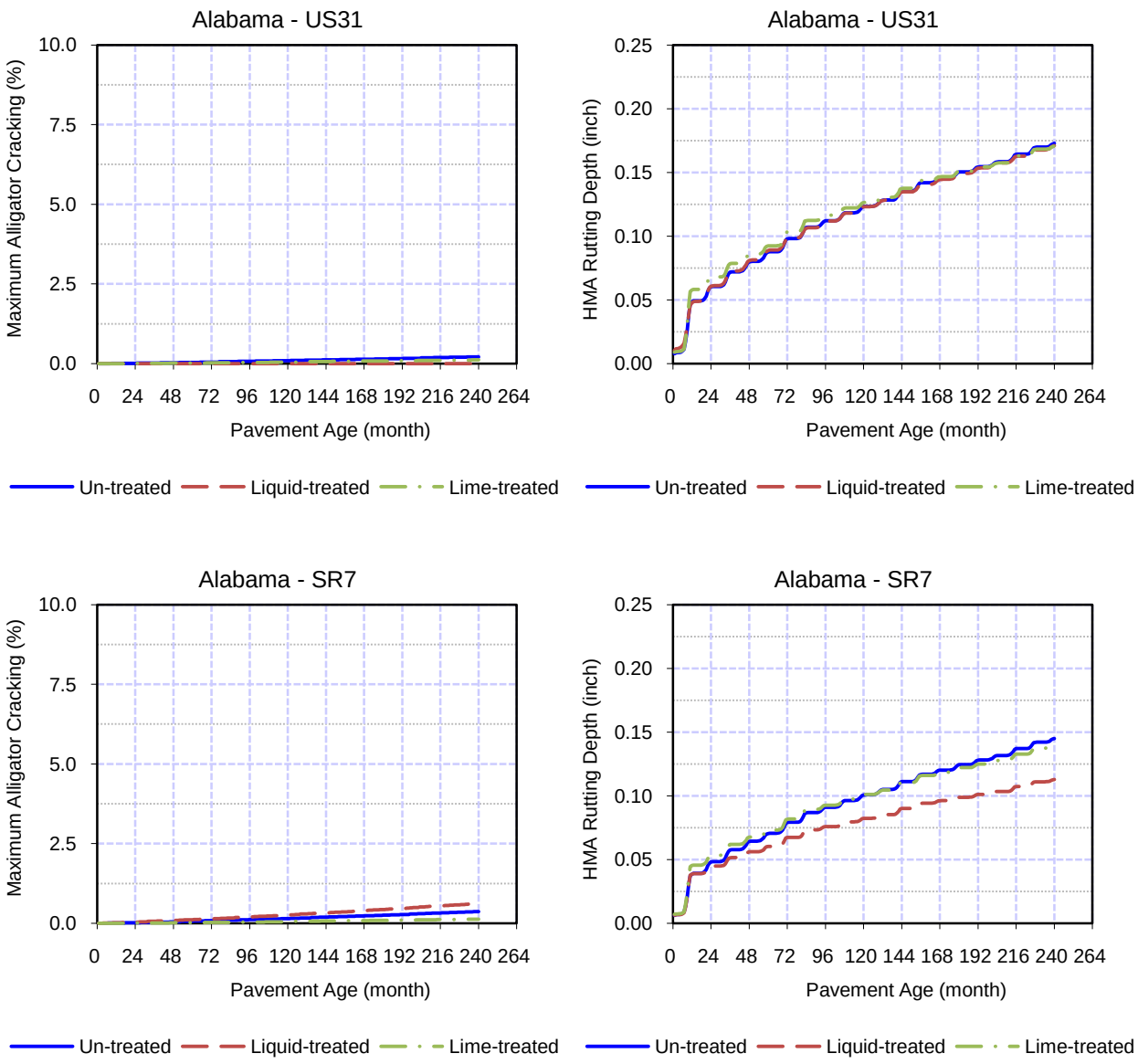

Figure 71. MEPDG 20 Years Design Fatigue and Asphalt Rutting Performance – Alabama.

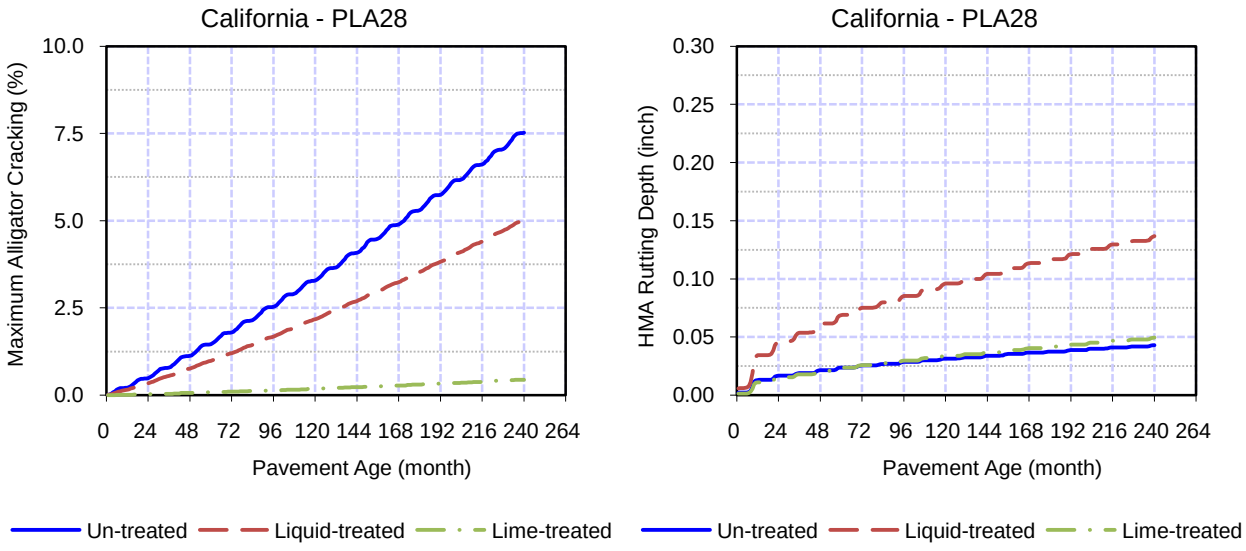

Figure 72. MEPDG 20 Years Design Fatigue and Asphalt Rutting Performance – California.

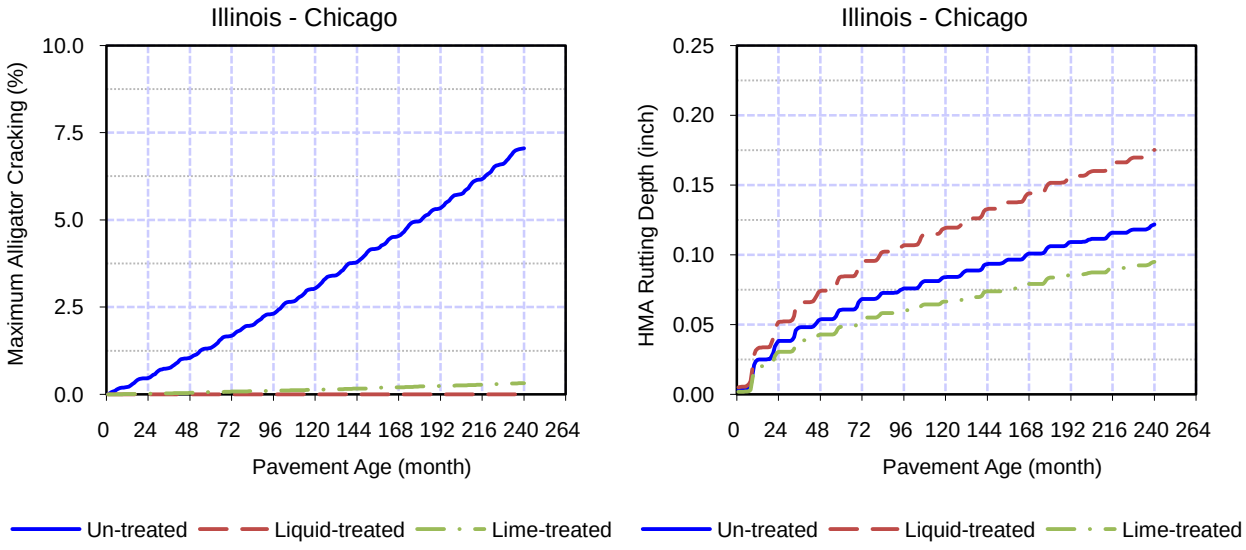

Figure 73. MEPDG 20 Years Design Fatigue and Asphalt Rutting Performance – Illinois.

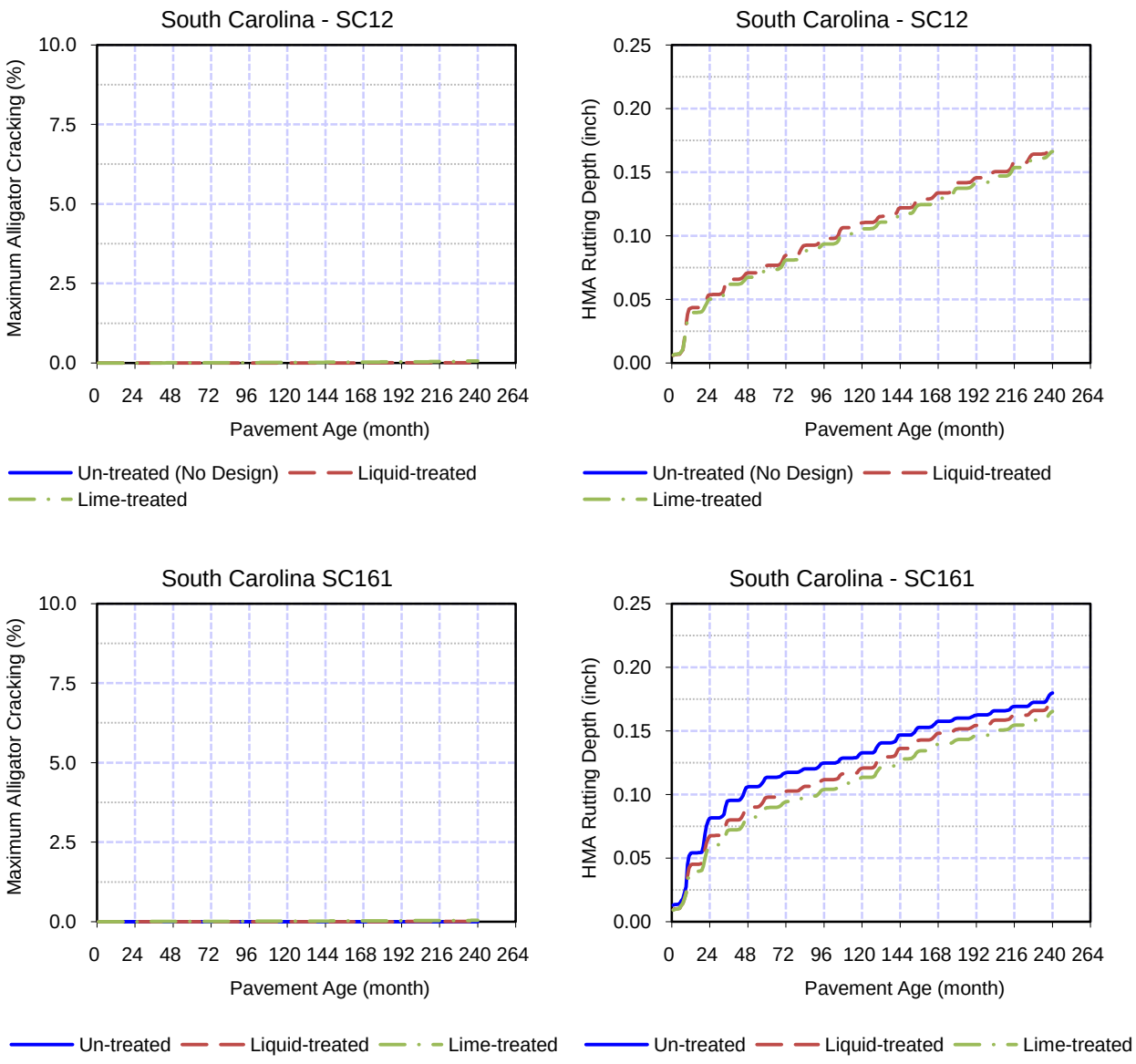

Figure 74. MEPDG 20 Years Design Fatigue and Asphalt Rutting Performance – South Carolina.

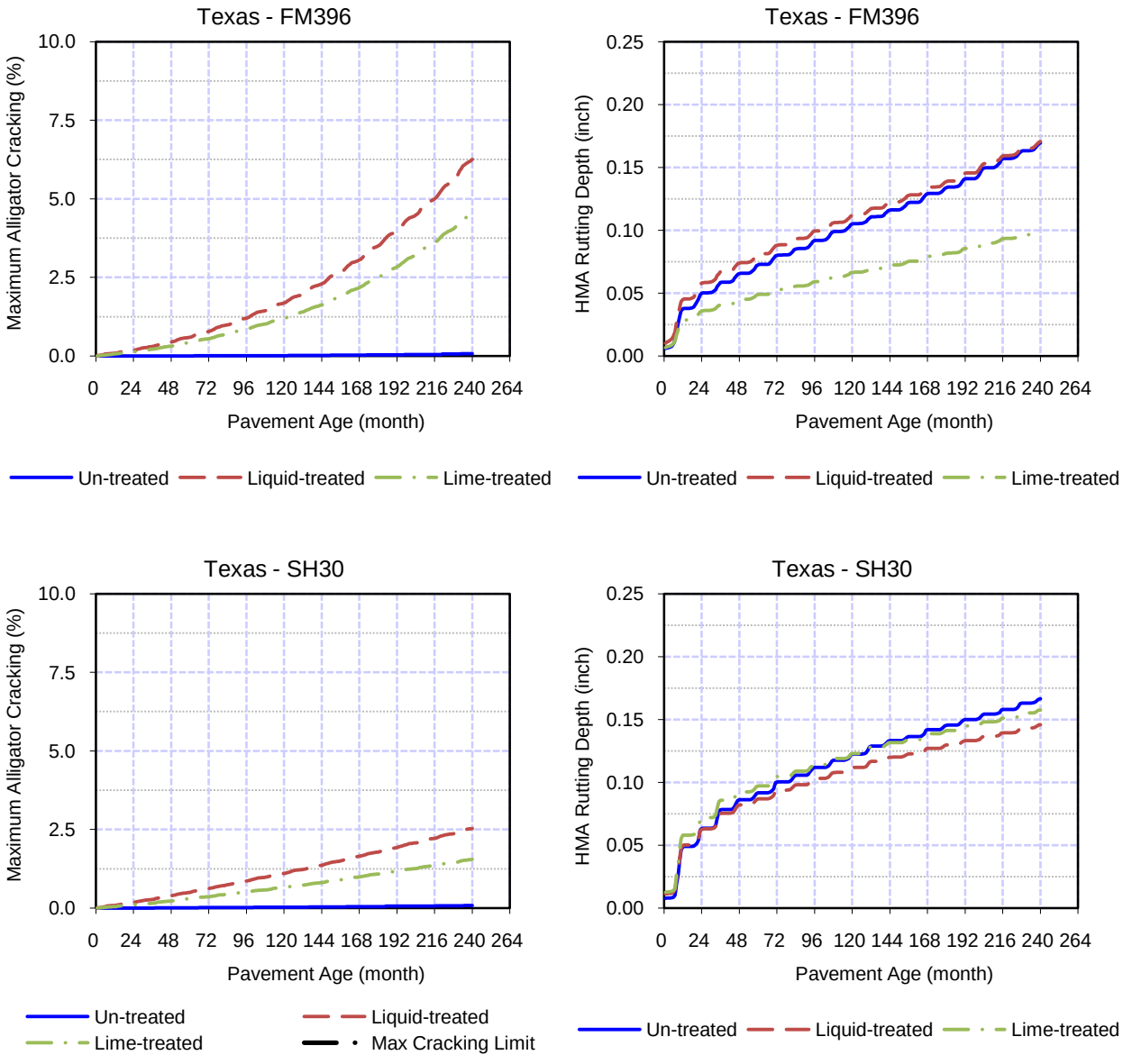

Figure 75. MEPDG 20 Years Design Fatigue and Asphalt Rutting Performance – Texas.

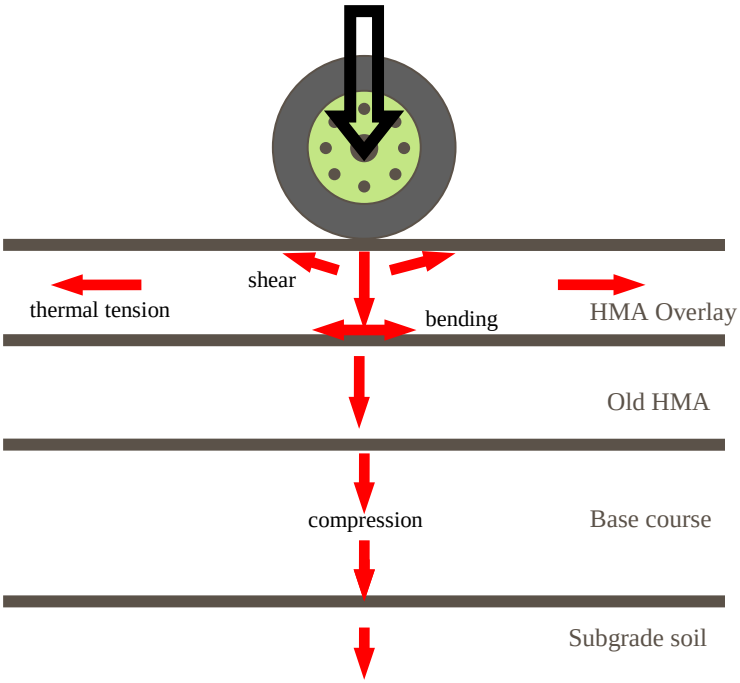

Figure 76. State of Stresses in Overlaid HMA Pavement without Cracking in the Old HMA.

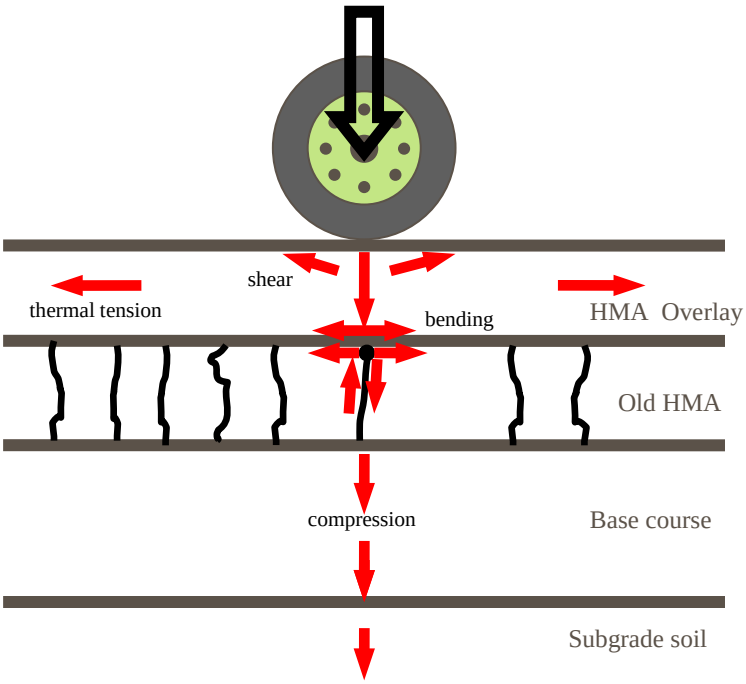

Figure 77. State of Stresses in Overlaid HMA Pavement with Cracking in the Old HMA.

APPENDIX A

GEOLOGICAL MAPS

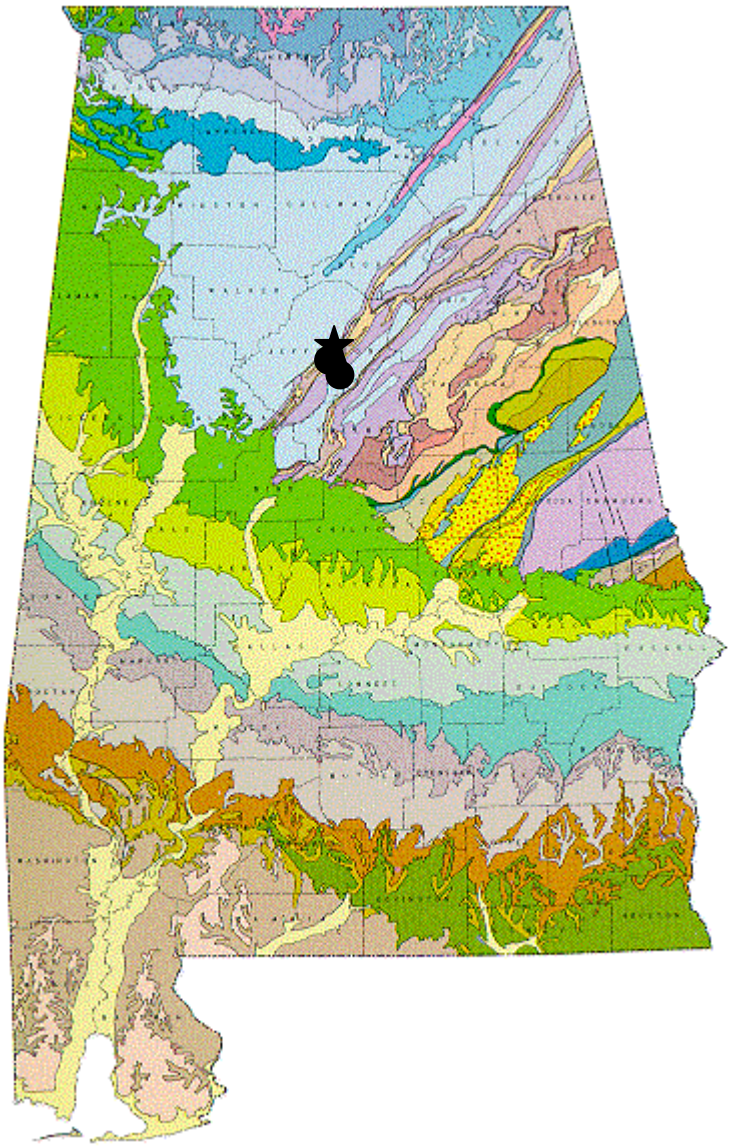

Image courtesy Alabama Geological Survey

★ Aggregate Source Location ● Project Location

Figure A1. Alabama Geological Map with Aggregate Source and Project Locations.

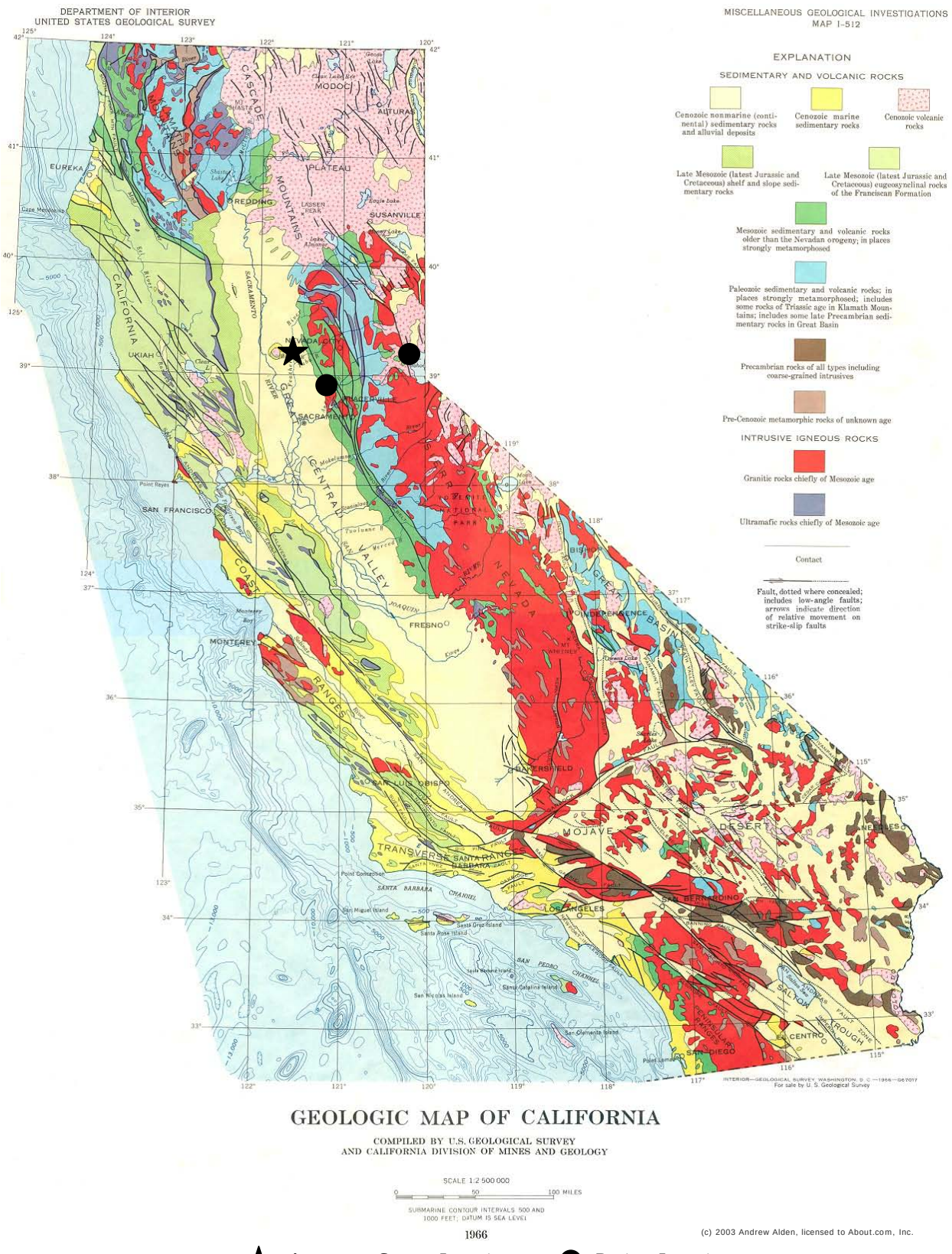

★ Aggregate Source Location ● Project Location

Figure A2. California Geological Map with Aggregate Source and Project Locations.

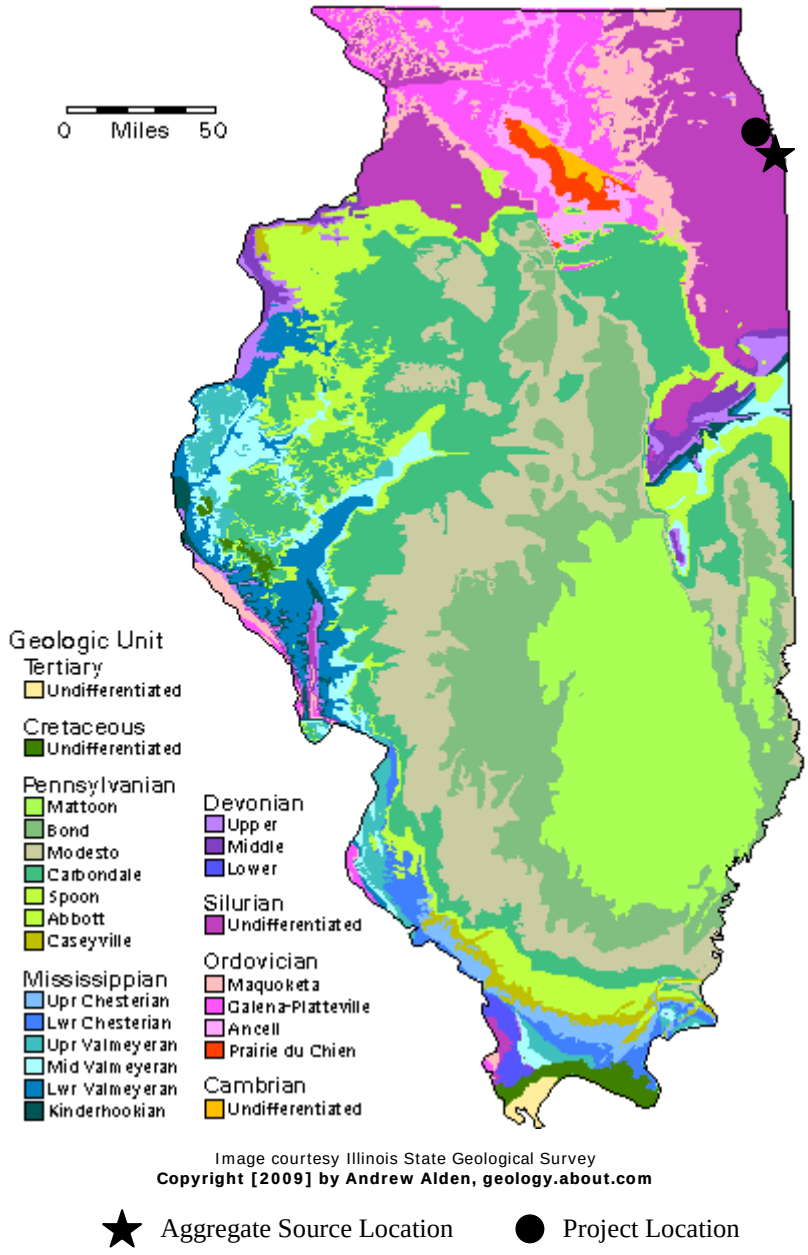

Figure A3. Illinois Geological Map with Aggregate Source and Project Locations.

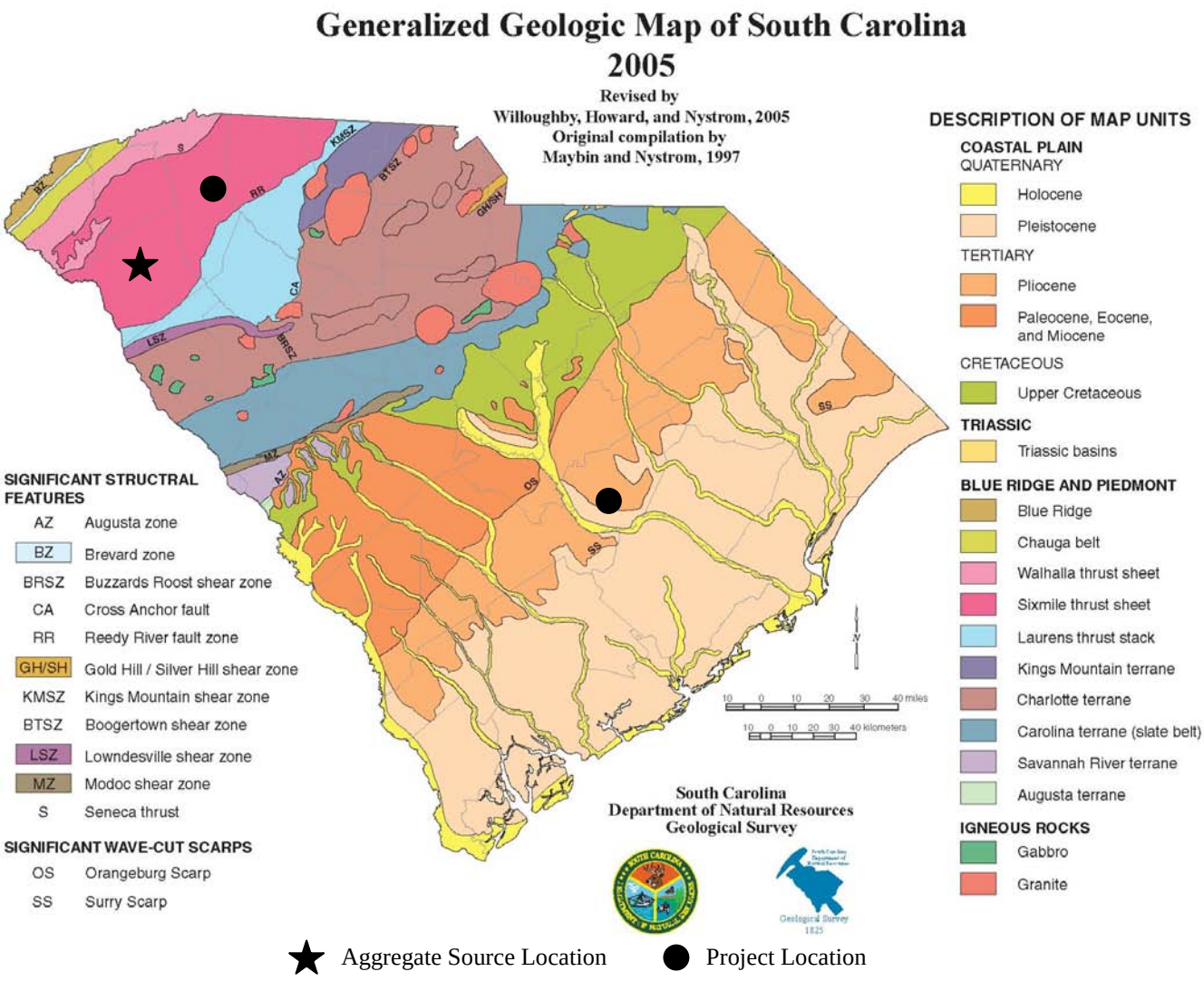

Figure A4. South Carolina Geological Map with Aggregate Source and Project Locations.

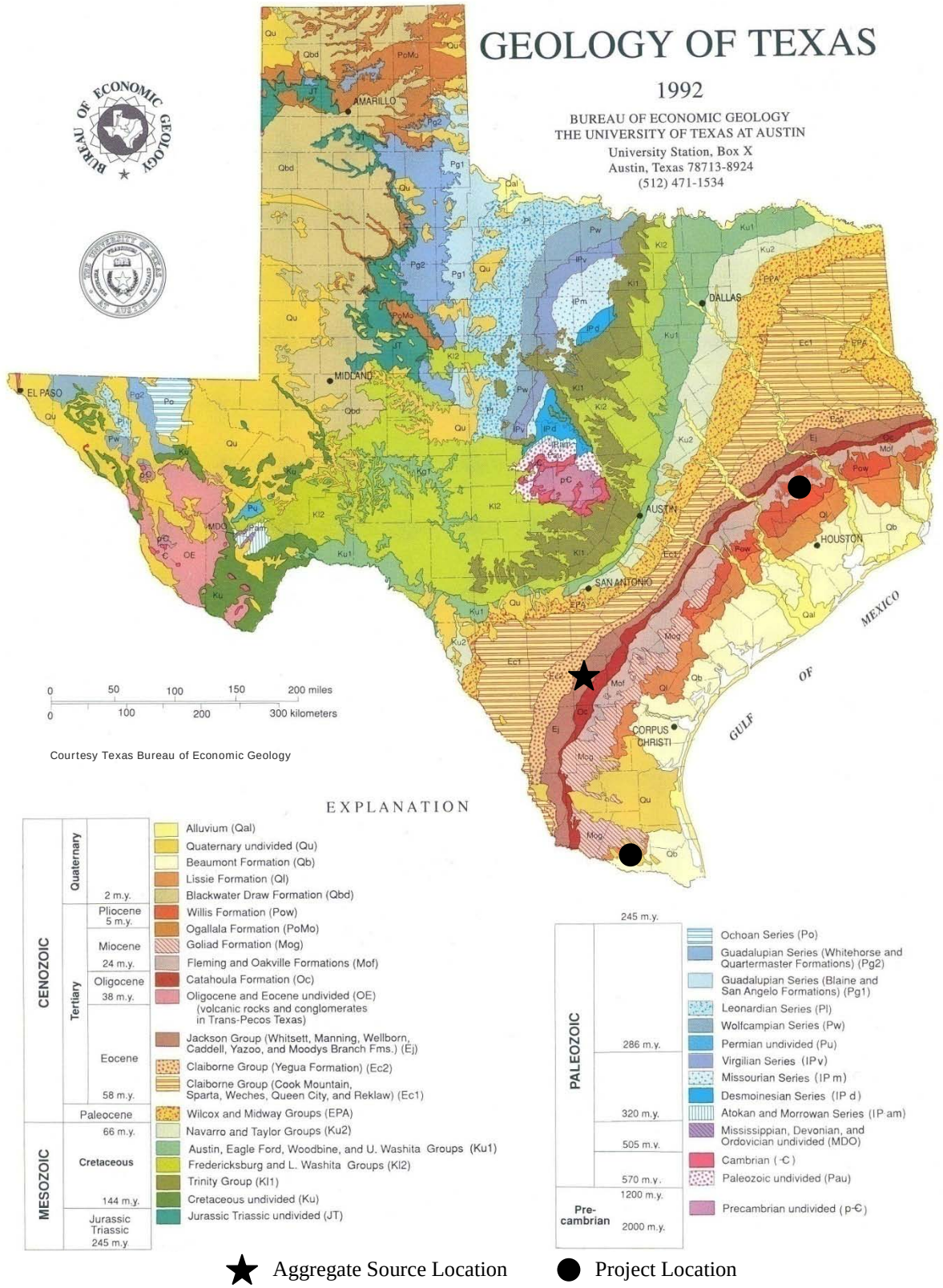

Figure A5. Texas Geological Map with Aggregate Source and Project Locations.

APPENDIX B

Dynamic Mechanical Analysis (DMA)

The DMA testing was conducted for exploratory purposes to assess the applicability of this technology to the evaluation of liquid and lime-treated HMA mixtures. The results of the DMA were used to compare with the findings of the traditional testing methods. None of the DMA results were used in the MEPDG designs and the LCCA.

The following procedure describes the process for preparing the fine graded asphalt mix (FAM) samples for DMA testing. The FAM samples are normally prepared by using the portion of the aggregate in the mixture smaller than 1.18 mm and the same asphalt binder content used for the mixture. Specific steps were as follows:

1. Select the HMA mix from which the FAM is to be developed and which the FAM will represent;
2. Obtain the following information for the HMA: (1) aggregates gradation, (2) percentage asphalt binder used. Essentially all aggregates larger than 1.18 mm are excluded and the FAM gradation includes sieves from the No. 16 (1.18 mm) through the No. 200 (0.074 mm);
3. Develop the fine asphalt mixture gradation curve keeping the same proportions for each aggregate passing the No. 16 sieve (1.18mm);
4. Establish the aggregates batch size (in grams) that will be used to compact the fine graded asphalt mixture sample according to the mold diameter and the desired sample height;
5. Calculate the weights of each size fraction of the aggregate required for one batch of the fine asphalt mixture. Use the gradation developed on step 3;
6. Calculate the amount of binder for the FMA using the aggregate batch size (step 4) and the percentage of binder used in the original HMA mix.

Binder(g) = [aggregate batch size x (%binder HMA - % binder absorbed by coarse aggregate)]

In this study, the amount of percent binder absorbed by the coarse aggregates was not known. Instead of using 100% of the binder content determined in step 6, only 70% were used in the initial trial batches. This adjustment was made because when 100% of the binder used in the full mix was used for the mixture from Illinois, the FAM was far too wet to compact.

The FAM mixture designs discussed above used to prepare representative Superpave Gyratory Compactor (SGC) samples. The mixing and compacting temperatures were provided by University of Nevada, Reno. Below are listed the steps followed:

1. Compact 4 inches specimens using the SGC.
2. Let samples cool for at least 3 hours.
3. Determine air void contents for DMA samples.

4. Saw the upper and lower part, approximately 1.0 inch from each end, of the cylindrical sample to obtain a new cylinder with the same diameter but only 2 inches high as shown in Figure B1a. X-ray tomography analysis has shown that the resulting 2.0 inches sample has relatively uniform air void content throughout the height of the sample.
5. Core DMA cylindrical of 2.0 inches height and 0.5 inch diameter DMA specimens as shown in Figure B1b.

Note: the aged samples were left in the oven for 5 days at 185°F before compaction.

In the DMA testing, the 2.0 inch (50 mm) high by 0.5 inch (12 mm) diameter cylindrical asphalt samples are subjected to cyclic torsional loading at two levels (Figure B2). During the first level, low strain, linear viscoelastic properties of the sample are determined. For this analysis, the most important is the shear modulus, a measure of stiffness. The second level of loading is high strain loading. This strain level causes continual damage to the specimen. The damage is monitored and related to a decrease in modulus and an increase in phase angle. These two parameters, together with viscoelastic parameters from the low strain testing, are used to calculate the dissipated pseudo strain energy (DPSE) between the time of initial cyclic loading in the high strain experiment and failure. A sample that can accumulate a higher level of DPSE will have longer fatigue life and is therefore desirable. DMA samples, are comprised of the fine aggregate mixture (FAM) portion of the total mixture, i.e., binder plus aggregate smaller than 0.05 inch (1.18 mm), and this is the portion of the mixture where damage is expected to predominately occur and where healing has the potential to occur. This underlies the importance of focusing on and testing the FAM. Approximately 25 DMA samples can be cored from a single Superpave Gyratory Compaction (SGC) sample. This is a substantial advantage in conveniently producing replicates. Before the DMA samples are cored the top and bottom inch of the SGC are sawed off leaving behind a sample base with a very uniform void structure. The uniformity of the air void content has been verified by non-destructive, computer assisted tomography.

The DMA testing evaluates the shear modulus (G*) and the DPSE of the mixtures. The G* property was used to evaluate the impact of the additives on the resistance of the mixtures to moisture damage. The combination of both the G* and the DSPE was used to evaluate the impact of additives on the fatigue resistance of the mixtures.

The DMA testing was conducted following the procedure described above. The DMA samples were tested under the unconditioned and moisture-conditioned stages. The moisture conditioning process for the DMA samples consisted of saturating the samples to 80% and testing them while the moisture is maintained inside the samples. The shear modulus of the various mixtures was measured at the unconditioned and moisture-conditioned stages.

The DMA testing was conducted on the mixtures from all five sources. The DMA testing on the Illinois source did not produce any repeatable results and only limited DMA data on the unconditioned stage were produced for the Texas source due to the limited amount of materials. Figures B3 and B4 summarize the impact of the additives on the G* property of the unconditioned and moisture-conditioned mixtures.

For the Alabama mixtures the addition of lime significantly increased the G* of the FAMs as compared to the un-treated mixture at both the unconditioned and moisture-conditioned stages. The addition of the liquid anti-strip did not have a statistically significant impact on G* as compared to the un-treated mixture. The finding of the DMA testing at the moisture-conditioned stage is consistent with the finding of the E* versus F-T cycles data shown in Figure 45.

The addition of lime to the California FAMs significantly increased the G* property at the unconditioned stage while maintained the same G* property at the moisture-conditioned stage. The addition of the liquid anti-strip to the California FAMs significantly increase the G* property at both the unconditioned and moisture-conditioned stages. The findings of the DMA testing on the lime-treated mixture is not consistent with the finding of the E* versus F-T cycles data shown in Figure 46. On the other hand the findings of the DMA testing on the liquid-treated mixture is consistent with the finding of the E* versus F-T cycles data shown in Figure 46.

The addition of lime to the South Carolina FAMs significantly increased the G* property at both the unconditioned and moisture-conditioned stages. The addition of the liquid anti-strip reduced the G* property at both the unconditioned and moisture-conditioned stages. The finding of the DMA testing at the unconditioned and moisture-conditioned stages is consistent with the finding of the E* versus F-T cycles data shown in Figure 48.

The addition of lime to the Texas FAMs maintained the G* property at the unconditioned stage while the addition of liquid anti-strip reduced the G* property of the mixture.

In general, the findings of the DMA testing for the resistance of mixtures to moisture damage were consistent with the E* versus F-T cycles evaluations.

When analyzing the DMA data for fatigue, it should be recognized that both the G* property and the DPSE play a role in defining the resistance of the mixtures to fatigue cracking. The higher the G* the lower the generated strain in the HMA layer and the higher the DPSE the more resistant the mix is to cumulative damage. Therefore, an increase in both the G* and DPSE would lead to an increase in the fatigue life of the HMA mix. Figures B5 and B6 show the DPSE of the various mixtures at the unconditioned and moisture-conditioned stages, respectively.

The addition of lime for the Alabama FAMs resulted in significant increases in the G* and DPSE while the addition of the liquid anti-strip did not significantly increase the magnitude of either G* or the DPSE. The net effect for the Alabama source was that the lime-treated mixture would have a better fatigue life than both the un-treated and liquid-treated mixtures. The finding of the DMA testing on the Alabama mixture is consistent with the finding of the flexural beam test shown in Figure 65.

The addition of lime to the California FAMs significantly increased both the G* and DPSE at the unconditioned stage only while the addition of the liquid anti-strip increased the G* and DPSE at both the unconditioned and moisture-conditioned stages as compared to the un-treated mixture. Therefore, at the unconditioned stage the lime-treated mix would experience superior fatigue performance while at the moisture-conditioned stage the liquid-treated mix would show an

improved fatigue performance. The finding of the DMA testing on the California mixture is inconsistent with the finding of the flexural beam test shown in Figure 66.

The addition of lime to the South Carolina FAMs significantly increased the G* and DPSE properties at both the unconditioned and moisture-conditioned stages. The addition of the liquid anti-strip significantly reduced the G* and DPSE at both the unconditioned and moisture-conditioned stages. The net impact was that superior fatigue life should be expected for the lime-treated mixtures as compared to both the un-treated and liquid-treated mixtures. The finding of the DMA testing on the South Carolina mixture is inconsistent with the finding of the flexural beam test shown in Figure 68.

Based on the available data for the Texas source at the unconditioned stage, it can be concluded that the addition of lime maintained the G* and DPSE properties while the addition of liquid anti-strip reduced both the G* and DPSE leading to a lower fatigue resistance. The finding of the DMA testing on the Texas mixture is consistent with the finding of the flexural beam test shown in Figure 69.

In general, the findings of the DMA testing for the resistance of mixtures to fatigue cracking were 50 percent consistent with the flexural beam test evaluations. It should be noted that the DMA evaluation combines the impact of both the G* and DPSE while the flexural beam test evaluates the direct resistance of the mixtures to flexural bending which is combined with the E* property to assess the overall resistance of the mix to fatigue cracking.

(a) (b)

Figure B1. SGC Sample with Ends Sawed off (a) Cored DMA Samples (b).

Dynamic Mechanical Analysis Set-Up

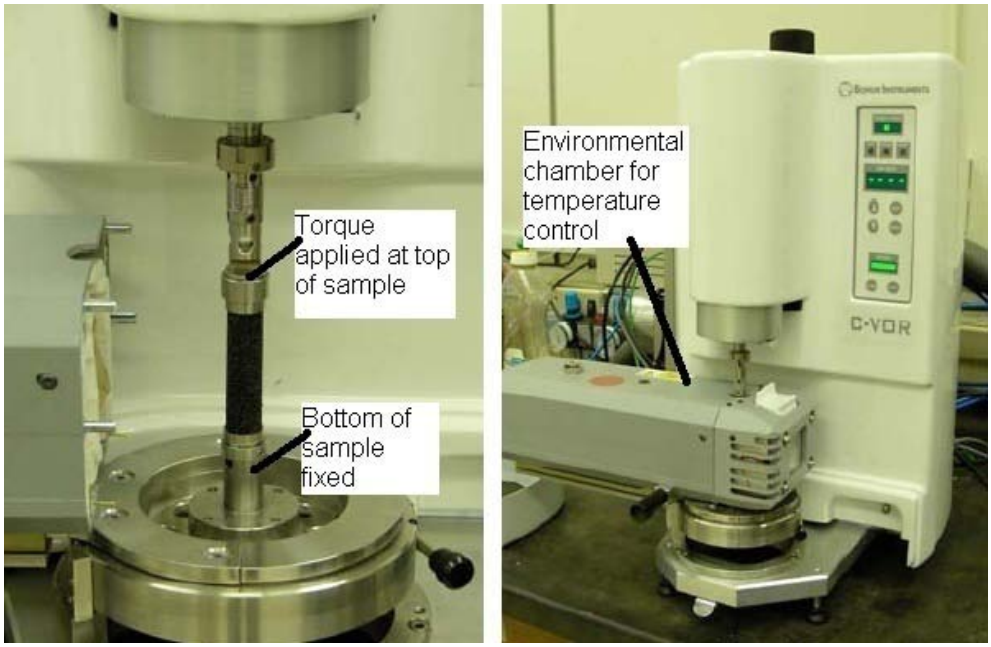

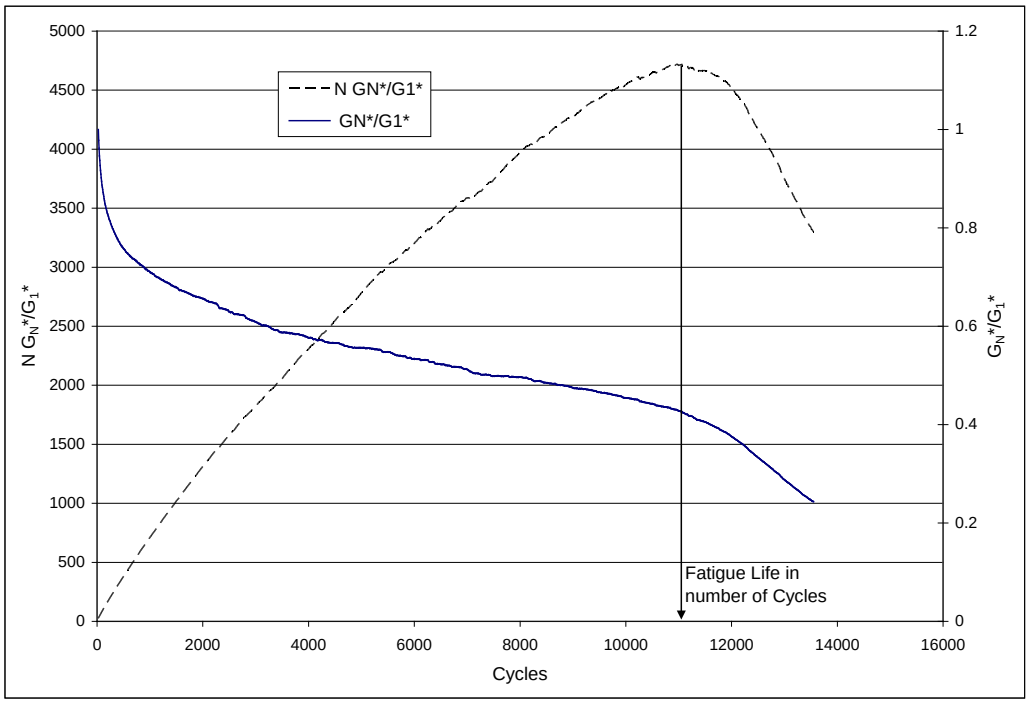

Figure B2. Components of the Dynamic Mechanical Analysis Test and a Typical Curve for an HMA Mix.

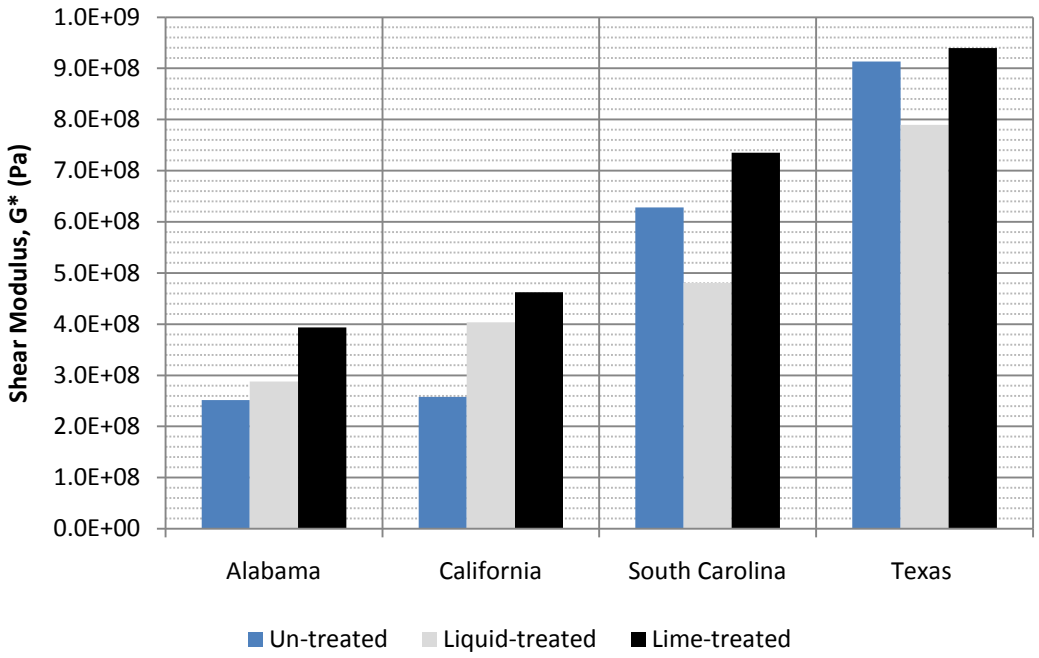

Figure B3. Shear Modulus (G*) at 70°F of FAM Samples without Moisture Conditioning.

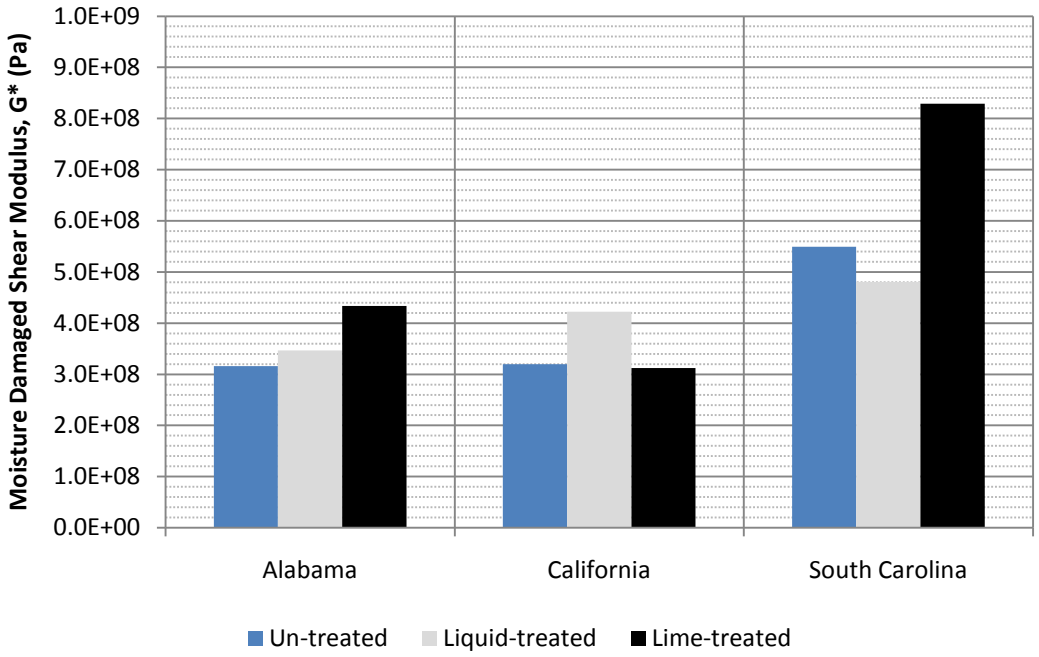

Figure B4. Shear Modulus (G*) at 70°F of FAM Samples with Moisture Conditioning.

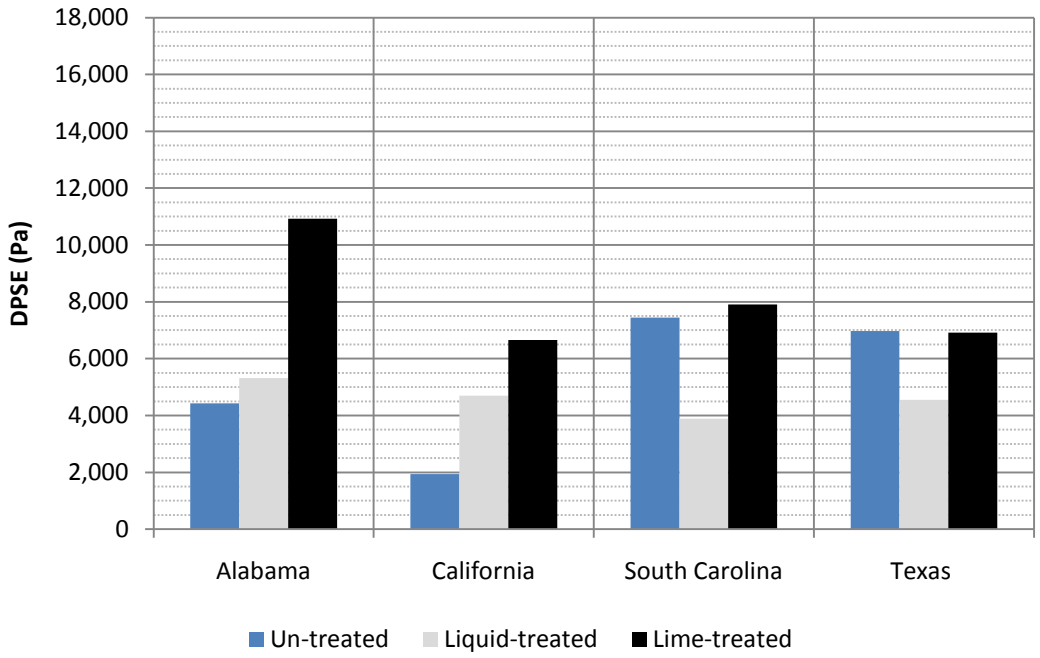

Figure B5. Dissipated Pseudo Strain Energy (DPSE) at 70°F used to assess Fatigue Damage in FAM Samples without Moisture Conditioning.

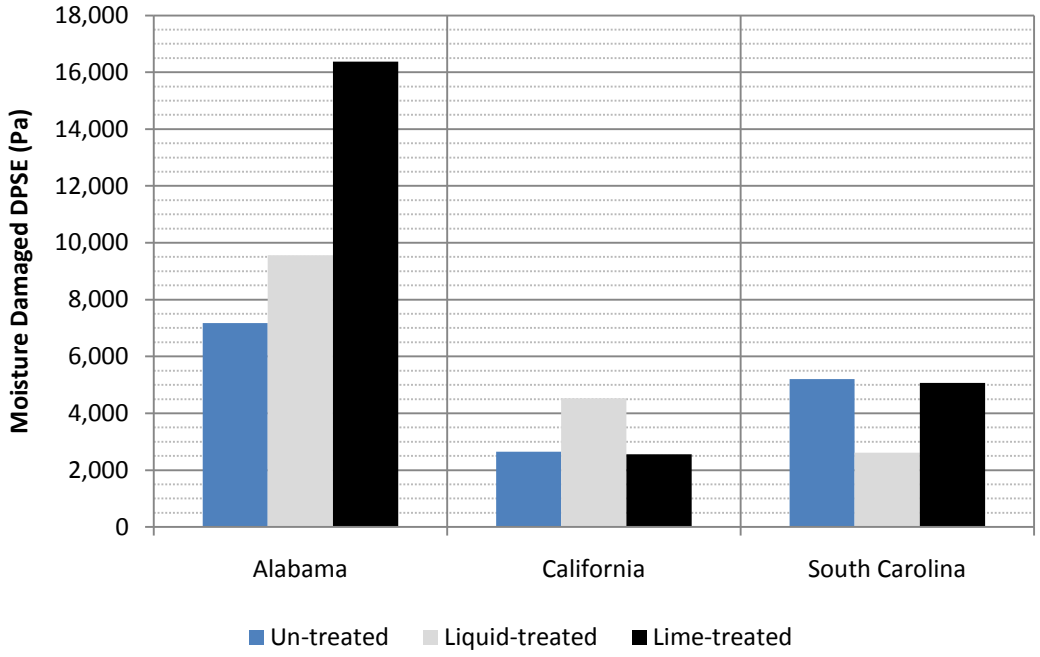

Figure B6. Dissipated Pseudo Strain Energy (DPSE) at 70°F used to assess Fatigue Damage in FAM Samples with Moisture Conditioning.